

MONTHLY NOTICES  
OF THE  
ROYAL ASTRONOMICAL SOCIETY

Vol. 113 No. 6 1953



*Published and Sold by the*  
**ROYAL ASTRONOMICAL SOCIETY**  
**BURLINGTON HOUSE**  
**LONDON, W.1**

*Price Thirteen Shillings and Sixpence*

## NOTICE TO AUTHORS

1. *Communications*.—Papers must be communicated to the Society by a Fellow. They should be accompanied by a summary at the beginning of the paper conveying briefly the content of the paper, and drawing attention to important new information and to the main conclusions. The summary should be intelligible in itself, without reference to the paper, to a reader with some knowledge of the subject; it should not normally exceed 200 words in length. Authors are requested to submit MSS. in duplicate. These should be typed using double spacing and leaving a margin of not less than one inch on the left-hand side. Corrections to the MSS. should be made in the text and not in the margin. Unless a paper reaches the Secretaries more than seven days before a Council meeting it will not normally be considered at that meeting. By Council decision, MSS. of accepted papers are retained by the Society for one year after publication; unless their return is then requested by the author, they are destroyed.

2. *Presentation*.—Authors are allowed considerable latitude, but they are requested to follow the general style and arrangement of *Monthly Notices*. References to literature should be given in the standard form, including a date, for printing either as footnotes or in a numbered list at the end of the paper. Each reference should give the name and initials of the author cited, irrespective of the occurrence of the name in the text (some latitude being permissible, however, in the case of an author referring to his own work). The following examples indicate the style of reference appropriate for a paper and a book, respectively :—

A. Corlin, *Zs. f. Astrophys.*, 15, 239, 1938.

H. Jeffreys, *Theory of Probability*, 2nd edn., section 5.45, p. 258, Oxford, 1948.

3. *Notation*.—For technical astronomical terms, authors should conform closely to the recommendations of Commission 3 of the International Astronomical Union (*Trans. I.A.U.*, Vol. VI, p. 345, 1938). Council has decided to adopt the I.A.U. 3-letter abbreviations for constellations where contraction is desirable (Vol. IV, p. 221, 1932). In general matters, authors should follow the recommendations in *Symbols, Signs and Abbreviations* (London : Royal Society, 1951) except where these conflict with I.A.U. practice.

4. *Diagrams*.—These should be designed to appear upright on the page, drawn about twice the size required in print and prepared for direct photographic reproduction except for the lettering, which should be inserted in pencil. Legends should be given in the manuscript indicating where in the text the figure should appear. Blocks are retained by the Society for 10 years; unless the author requires them before the end of this period they are then destroyed.

5. *Tables*.—These should be arranged so that they can be printed upright on the page.

6. *Proofs*.—Costs of alterations exceeding 5 per cent of composition must be borne by the author. Fellows are warned that such costs have risen sharply in recent years, and it is in their own and the Society's interests to seek the maximum conciseness and simplification of symbols and equations consistent with clarity.

7. *Revised Manuscripts*.—When papers are submitted in revised form it is especially requested that they be accompanied by the original MS.

### Reading of Papers at Meetings

8. When submitting papers authors are requested to indicate whether they will be willing and able to read the paper at the next or some subsequent meeting, and approximately how long they would like to be allotted for speaking.

9. Postcards giving the programme of each meeting are issued some days before the meeting concerned. Fellows wishing to receive such cards whether for Ordinary Meetings or for the Geophysical Discussions or both should notify the Assistant Secretary.

MONTHLY NOTICES  
OF THE  
ROYAL ASTRONOMICAL SOCIETY

Vol. 113      No. 6

---

MEETING OF 1953 NOVEMBER 13

Dr J. Jackson, President, in the Chair

The election by the Council of the following Fellows was duly confirmed :—

John Grant Davies, M.A., Ph.D., 140 Manchester Road, Wilmslow, Cheshire (proposed by A. C. B. Lovell);  
C. Gordon Little, Jodrell Bank Experimental Station, Lower Withington, Macclesfield, Cheshire (proposed by A. C. B. Lovell);  
Marjorie Elsie Pillow, B.Sc., Ph.D., A.Inst.P., 16 Redford Avenue, Wallington, Surrey (proposed by R. W. B. Pearse);  
Harold Bytham Ridley, 20 Boileau Road, Barnes, London, S.W.13 (proposed by J. P. M. Prentice);  
William Marshall Sutherland, 39 Auchinloch Road, Lenzie, Lanarkshire (proposed by T. R. Tannahill); and  
Albert William Vince, Wyeross, 17 Stanley Hill Avenue, Amersham, Buckinghamshire (proposed by N. J. Goodman).

The election by the Council of the following Junior Members was duly confirmed :—

Roger Derek Wade, 76 Stortford Road, Hoddesdon, Hertfordshire (proposed by R. M. Baum); and  
Derek Henry Wilson, M.Sc., 47 Parkfield Road, Ickenham, Uxbridge, Middlesex (proposed by F. Sheldrake).

One hundred and two presents were announced as having been received since the last Meeting, including :—

E. Guyot, *Reprints of astronomical articles* (presented by the author);  
The Earl Nelson, *Life and the Universe* (presented by the author);  
F. A. Paneth, *Reprints of articles relating to Thomas Wright* (presented by the author); and  
M. F. Soonawala, *Maharaja Sawai Jai Singh II of Jaipur and his observatories* (presented by Dr A. Armitage).

Professor Subrahmanyan Chandrasekhar delivered the George Darwin Lecture (see p. 667), taking as his subject "Problems of stability in hydrodynamics and hydromagnetics".

After the lecture, the President delivered a short address, and presented the Gold Medal of the Society to Professor Chandrasekhar, to whom it had been awarded for his contributions to mathematical astrophysics. The President said :—

Professor Chandrasekhar, if I were to follow precedent it would now be my privilege and pleasure to present to you the Gold Medal of the Society. You have mentioned that for some purposes  $10^8$  years is not a long time, but you might have thought that a Society which has existed for more than a hundred years would have reached stability in presenting its Gold Medal. However, the Chancellor of the Exchequer has introduced a disturbing influence on our proceedings by the introduction of purchase tax. The Treasurer of the Society is here and so I must be careful what I say or do. Although I am not going to hand over the medal to you I do not think there is any objection to your seeing it now, while I assure you that in due course it will be forwarded to you.

With the Gold Medal goes our best wishes for you in the future and on behalf of the Society I would like to express the hope that you may have the satisfaction of seeing the application of many of your theoretical results to the interpretation of the nature of the actual bodies of the Universe.

#### MEETING OF 1953 DECEMBER 11

Dr J. Jackson, President, in the Chair

The election by the Council of the following Fellows was duly confirmed :—  
 Sydney George Brewer, M.A., Fettes College, Edinburgh (proposed by D. W. Dewhirst);  
 Joseph W. Chamberlain, Ph.D., Yerkes Observatory, Williams Bay, Wisconsin, U.S.A. (proposed by S. Chandrasekhar);  
 George Herbert Avery Cole, B.Sc., Ph.D., 1a Alma Terrace, Allen Street, London, W.8 (proposed by H. S. W. Massey);  
 Amulya Narayan Datta, M.Sc., Bengal Engineering College, Howrah, India (proposed by K. E. Bullen);  
 John Edward Geake, B.Sc., M.Sc., A.Inst.P., The Physical Laboratories, The University, Manchester 13 (proposed by Z. Kopal);  
 Johann Wolfgang Goethe, Dr.rer.Nat., 77 Falkstrasse, Frankfurt-am-Main, Germany (proposed by A. Beer);  
 Richard Ingram, S.J., M.Sc., Seismological Observatory, Rathfarnham Castle, Co. Dublin, Eire (proposed by H. A. Brück);  
 Alan Hamer Jarrett, B.Sc., M.Sc., Ph.D., A.Inst.P., The University Observatory, St. Andrews, Fife (proposed by A. Beer);  
 David Nelson Limber, Princeton University Observatory, Princeton, New Jersey, U.S.A. (proposed by S. Chandrasekhar);  
 Robert J. Lockhart, B.A., University of Manitoba, Winnipeg, Manitoba, Canada (proposed by A. Vibert Douglas);

Hari Narain, M.Sc., D.Phil., The University, Sydney, Australia (proposed by K. E. Bullen);  
William Newsham, M.B.E., Brancepeth, 22 Sandbanks Road, Parkstone, Dorset (proposed by T. K. Metcalfe);  
James Ring, B.Sc., The Physical Laboratories, The University, Manchester 13 (proposed by Z. Kopal);  
Allan R. Sandage, Ph.D., Mount Wilson and Palomar Observatories, Pasadena 4, California, U.S.A. (proposed by E. M. Burbidge);  
Norman D. Sykes, 56 Springfields, Welwyn Garden City, Hertfordshire (proposed by H. Wildey);  
Waltham Vaughan, 8 New Dock Road, Llanelly, Carmarthenshire (proposed by B. E. Featherstone);  
Joan George Erardus Gysbertus Voûte, Daendelsstrasse 46, The Hague, Holland (proposed by W. S. van den Bos);  
William Leslie Wilcock, B.Sc., Ph.D., A.Inst.P., The Physical Laboratories, The University, Manchester 13 (proposed by Z. Kopal); and  
Robert I. Wolff, Ph.D., College of the City of New York, New York 31, U.S.A. (proposed by S. N. Milford).

The election by the Council of the following Junior Members was duly confirmed :—

Joyce Margaret Blackler, B.Sc., Royal Holloway College, Englefield Green, Surrey (proposed by W. H. McCrea); and  
Roderick Vernon Willstrop, Emmanuel College, Cambridge (proposed by B. G. Tunmore).

Seventy-seven presents were announced as having been received since the last Meeting, including :—

United States Hydrographic Office, *Sight reduction tables for air navigation* (presented by D. H. Sadler).

Mr R. H. Garstang and Mr H. C. King were appointed Honorary Auditors of the Treasurer's accounts for 1953.

## THE LAW OF RED-SHIFTS

*George Darwin Lecture\*, delivered by Dr Edwin Hubble on 1953 May 8*

I propose to discuss the law of red-shifts—the correlation between distances of nebulae and displacements in their spectra. It is one of the two known characteristics of the sample of the universe that can be explored and it seems to concern the behaviour of the universe as a whole. For this reason it is important that the law be formulated as an empirical relation between observed data out to the limits of the greatest telescope. Then, as precision increases, the array of possible interpretations permitted by uncertainties in the observations will be correspondingly reduced. Ultimately, when a definite formulation has been achieved, free from systematic errors and with reasonably small probable errors, the number of competing interpretations will be reduced to a minimum.

The path towards such a definitive formulation is now clear and the investigations are under way at Mount Wilson and Palomar. I shall discuss this programme in some detail after sketching the history of the law of red-shifts as a convenient background.

There are three phases in the history, namely, the discovery phase which ended with a crude formulation in 1928–29, the rapid extension and improved formulation out to the limit of the 100-inch in 1929–36, and the current attempts to reach the limit of the 200-inch with the definite formulation, which began about two years ago.

### I. THE FIRST PHASE (DISCOVERY)

#### A. Radial Velocities

The discovery emerged from a combination of radial velocities measured by Slipher at Flagstaff with distances derived at Mount Wilson. You will recall that the first velocity of a spiral nebula was measured by Slipher in 1912 ( $-300$  km/sec for M 31). I mention the incident because the first step in a new field is the great step. Once it is taken, the way is clear and all may follow. In this case, however, Slipher worked almost alone, and ten years later, when he turned to other problems, he had contributed 42 out of the 46 nebular velocities then available. The list was completely dominated by large positive velocities, ranging up to  $+1800$  km/sec for NGC 584.

Attempts were made, from 1916 onward, to derive the solar motion with respect to the nebulae; but the positive signs, indicating general recession, proved intractable. Then, in 1918, Wirtz attempted to "save the phenomena" by introducing a constant  $K$  term in the equations. The device improved the results somewhat but not enough to render them acceptable. Nevertheless,

\* Editorial Note.—This paper comprises the text of the George Darwin Lecture, which the late author had intended to revise before publication. His notes, together with the manuscript from which he spoke, made it clear what form he wished the published material to take. A reorganization of the original manuscript according to his marginal notes, with the addition of a few connecting sentences, was the extent of the editing required.—A. R. Sandage.

it did suggest that the next logical step would be to replace the constant  $K$  with  $rK$ , a term which varied with the distances of the individual nebulae. This procedure was suggested by the run of residuals in the earlier solutions but it was also encouraged by the rapidly developing studies of relativistic cosmology.

Various solutions were made in the early and middle twenties, using apparent luminosities and apparent diameters as measures of relative distance. They failed but, as later appeared, only because the distance criteria were not sufficiently accurate to give reliable individual distances over the relatively short range covered by the radial velocities. The uncertainties are evident in the triple system comprising M 31 and its two companions, M 32 and NGC 205, where luminosities ranged from 100 to 1, and diameters from 60 to 1.

#### B. Distances from Brightest Stars

The problem was finally solved when the brightest stars in late-type spirals and irregular nebulae were established as suitable distance indicators, and were calibrated by Cepheids in a few of the nearest nebulae.

This new development started in 1923-24 when Cepheids were found in M 31 and M 33. The variables indicated the distances of the spirals, confirmed their suspected resolution and identified them as extragalactic stellar systems. Following up the clue, stars were soon recognized in many of the more conspicuous spirals, and the upper limits of brightness of these stars appeared to be substantially constant. It was this upper limit for the three or four brightest stars in great stellar systems which was used as a measure of distance. When, in 1928, it was applied to the nebulae with measured velocities, the law of red-shifts, or, as it was then called, the velocity-distance relation, emerged at once in approximately its present form. The law was established out as far as the Virgo Cluster, or about 7 million light-years, as an approximately linear relation, according to which velocities of recession increased at a rate of the order of 500 km/sec per million parsecs of distance.

### II. THE SECOND PHASE (RECONNAISSANCE)

#### A. Humason's Adventures among the Clusters

The second phase was entirely a Mount Wilson project, and lasted from 1928 to 1936. Humason assembled spectra of nebulae and I attempted to estimate their distances. Attention was concentrated on clusters because their brightest members could be regarded as distance indicators, and, at the same time, offered maximum distances for a given apparent magnitude. Furthermore, the populations of great clusters are dominated by elliptical systems, which are the most highly concentrated of all nebulae, and hence the most easily observed with spectrographs. Faint elliptical nebulae give semi-stellar images and, therefore, they respond to the increased light-gathering power of great telescopes.

Humason's adventures were spectacular. He first observed some of Slipher's nebulae, and then, when he was sure of his techniques, and confident of his results, he set forth. From cluster to cluster he marched with giant strides right out to the limit of the 100-inch. Spectrographs were improved from time to time—the names of Rayton and Schmidt and others are associated with the cameras—and each improvement was followed by a new surge forward. The

limit was bracketed when apparent velocities of 40 000 km/sec were recorded in the Boötes Cluster and in Ursa Major No. 11, and readable spectra could not be obtained in the fainter Hydra Cluster (now known to have shifts half again as large). And always, throughout the march, the data fell in line with the relation as originally formulated.

When clusters could not be observed to advantage, spectra of field nebulae, isolated or members of small groups, were assembled in large numbers. These data furnished an account of red-shifts in the nearer, more conspicuous nebulae of all types.

### B. Results of the Second Phase

When the second phase ended, the following results could be listed.

(1) The law of red-shifts appeared to be linear (within the uncertainties of the distance estimates) out to approximately 250 million light-years, and the red-shifts, when expressed as velocities ( $c \cdot d\lambda/\lambda$ ), increased at the rate of about 530 km/sec per million parsecs.

(2) The solar motion is largely accounted for by galactic rotation, the residual representing the peculiar motion of the stellar system being small and uncertain (order of 100–150 km/sec towards galactic latitude about  $+30^\circ$  and longitude in the quadrant  $50^\circ$  to  $140^\circ$ ).

(3) The law of red-shifts does not operate within the Local Group.

(4) Magnitude-velocity relations, fitted to data for clusters, resolved nebulae and field nebulae, and, of course, displaced from one another by magnitude intervals indicating relative absolute luminosities, could be used to calibrate all the relations in terms of brightest stars. Assuming  $M_{pg} = -6.35$  for Brightest Stars, the corresponding values for Field Nebulae and Fifth Nebulae in Clusters were  $-15.20$  and  $-16.45$ , respectively.

## III. INTERIM BETWEEN SECOND AND THIRD PHASES

### A. Lists of Velocities Assembled by Humason and Mayall

Towards the end of the second phase, Mayall entered the field and began assembling spectra with a very fine ultra-violet spectrograph on the 36-inch Crossley at Mount Hamilton. He paid special attention to the later-type spirals and other systems of low surface brightness for which his reflector was fully as efficient as the larger telescopes on Mount Wilson. From 1935 onward, the data increased in volume until now he has a list of the order of 280 nebular velocities as compared with Humason's list of about 570. There are some 100 nebulae in common which ensure a reliable comparison of the two systems, and the two lists when published will include about 750 individual nebulae.

These data furnish a wealth of information concerning nebulae of all kinds. Although full discussions must await publication of the lists, it is permitted to say that the data confirm and refine the results previously mentioned and, in particular, establish the order of precision in the measures (probable errors of the order of 30 km/sec or less) and of the dispersions among nebulae of different categories. Thus, by making reasonable allowance for the spread of absolute luminosities, the dispersion among isolated nebulae and small groups appears to be less than 150 km/sec. The dispersion among 11 members of the Local Group is about 60 km/sec, and, in general, the dispersions within groups and clusters increase steadily with compactness of the clusters. For instance,

$\sigma$  is 140 km/sec for the small loose M 81 Group, 275 km/sec for the Large Ursa Major Cloud, 700 km/sec for the Virgo Cluster, 1050 km/sec for the compact Coma Cluster, and perhaps 1200 km/sec for the Corona Borealis Cluster (from velocities of eight nebulae by Humason).

These results are important for the present discussion because they indicate the reliability of the measured red-shifts for clusters used in the formulation of the law of red-shifts. The percentage errors are trivial except possibly for the nearby Virgo Cluster where it is about 5 per cent (in addition to the unknown peculiar motion of the cluster). With increasing distance the percentage errors diminish, and, beyond the Coma Cluster, they can safely be ignored. Evidently the uncertainties in the formulation of the law of red-shifts are entirely those in the distances. Furthermore, because distances are derived from the apparent faintness of objects of supposedly known luminosity, the difficulties seem to be largely those of photometry, except for uncertainties in the fundamental unit of distance.

#### IV. THE THIRD PHASE (ATTEMPTS AT A DEFINITIVE FORMULATION WITH THE 200-INCH REFLECTOR)

##### A. *Extension of the Observed Range*

This was the situation when the completion of the 200-inch, and its accessories, initiated the third and current phase of the development. Because this phase represents an attempt at the definitive formulation of the law, I will be a little more precise in the use of terms. Red-shifts, for instance, will be used for the fractions,  $d\lambda/\lambda$ , by which details in the spectra are shifted. The shifts cannot be distinguished from Doppler shifts; they are constant throughout any given spectrum within the errors of measurement, the most reliable tests being those made on emission lines in large-scale spectra from  $H\alpha$  to  $\lambda 3727$ . The term "apparent velocity" will be discarded, and replaced by "velocity" signifying  $c \cdot d\lambda/\lambda$ , or red-shifts expressed on a scale of velocities. The procedure is not formally correct but it is convenient.

The current programme has two parts: one is the extension of the observed range and the other is the revision of the distance scale. The first part is straightforward, once suitable clusters are found. During the first season that a nebular spectrograph could be used on the 200-inch (1950-51), Humason obtained spectra in three clusters beyond the limit reached with the 100-inch. They gave velocities of the order of 50 000, 54 000 and 61 000 km/sec, respectively, the last being the Hydra Cluster which had been tried unsuccessfully with the 100-inch. Out to these limits, clusters can be selected from plates with the 48-inch Schmidt reflector, and the programme calls for groups of clusters at successive intervals to furnish mean points for the correlation curve. Beyond 60 000 km/sec, clusters cannot be identified with certainty on the survey plates. Many possible cases suggested by the 48-inch are being checked with the larger reflectors, but otherwise we must depend upon purely chance finds with the 100-inch and 200-inch. Humason has now observed groups of three clusters each at 25 000 km/sec, at 40 000, at 50 000 (representing both galactic hemispheres), and two clusters at about 58 000 to group with Hydra. He is confident that larger velocities, at least up to one-quarter of the velocity of light, can be recorded when such clusters have been located.

### B. Distances of Clusters

The second part of the programme, namely, the revision of the distance scale, lags behind the measurement of red-shifts. There are several steps in the programme, namely, the revision of the unit of distance, the setting up of faint magnitude sequences in Selected Areas, the actual measurement of nebular magnitudes, corrections for effects of red-shift on apparent magnitudes, and, finally, the examination of the possibility of errors arising from inter-nebular obscuration and systematic evolutional changes in luminosities during the travel-time of the light from the nebulae. Let us consider these steps in their logical order, beginning with the revision of the unit of distance.

1. *The unit of distance.*—A review of the unit of distance has been pending for more than twenty years—ever since it was realized that the many novae and globular clusters in M 31 were fainter with respect to the Cepheids than was the case in our own system. The discrepancy was emphasized when Baade resolved the body of M 31 and recognized it as a Type II stellar population whose brightest stars were known to be comparable with those in globular clusters. Then, recently, Baade and his younger colleagues calibrated the cluster-type variables (and hence the brightest stars) in globular clusters by extending the colour-magnitude arrays in some clusters down to very faint limits on the main sequence, and comparing them with the corresponding arrays for stars in the vicinity of the Sun (stars so near that their distances were known from direct triangulation). Shapley's value for the cluster-type variables was confirmed within small uncertainties.\*

The results clearly indicated that the classical Cepheids in M 31 are nearly  $1^m.5$  brighter than previously supposed, and, consequently, all our current estimates of absolute distances must be nearly doubled. The revision does not affect the estimates of relative distances, of course, but it nearly doubles the so-called "age of the universe". Further study will be required to reach a definitive value for the revision but meanwhile the factor 2 can be used in discussions. At the moment it seems likely that the final value may be less rather than greater than the even number.

The revision was unexpected because Shapley made his primary calibration from parallactic motions of classical Cepheids in the galactic system (in 1918), and used it to derive his secondary calibration of cluster-type variables. It now appears that the latter is about correct while the former was in error by nearly  $1^m.5$ .

2. *Magnitude standards.*—The faint stellar magnitude standards and colours required for photometry near the limit of the 200-inch are being established in nine Selected Areas forming a convenient pattern around the sky. The first measures, reaching to about  $m_{pg}=18.5$ , were made by Stebbins and Whitford in three of the Areas, using their photo-cells on the Mount Wilson reflectors. The programme has been continued and expanded by Baum, who has reached the 19th magnitude in all nine Areas and had pushed experimental measures in one or two of them down beyond the 21st magnitude. He is now putting in operation a new instrument designed to reach the limit of the 200-inch. The standards already available are sufficient for the faintest

\* Since this was written, preliminary results by Baum in the globular cluster M 13 suggest that grave uncertainties exist in this method of calibration. The colour-magnitude diagrams of the globular clusters M 3 and M 13 appear to differ by two magnitudes in the region of the main sequence. However, Blaauw's direct calibration of the classical Cepheids and Savedoff's fit of pulsation theory to the observations leave little doubt that the order of the correction to the classical Cepheids is  $\Delta M = -1^m.5$ .—A.R.S.

clusters in which red-shifts have been measured, and Baum's new programme should soon reach the faintest clusters in which red-shifts can be measured.

3. *Measurement of nebular magnitudes.*—The measurement of total magnitudes of nebulae has been revolutionized since the war, both by the photo-cell in the hands of Stebbins and Whitford, Pettit, and others, and by the precise photographic techniques of Bigay and Holmberg. All these investigations tend to reach general agreement on magnitudes (and colours, where measured) for given diameters. However, they all agree on the necessity of increasing apertures until no further change in luminosity can be detected. The formulation of a practical definition of diameter, however arbitrary, remains a problem for the future. The subject is under investigation but, meanwhile, the application of uniform principles to apparently similar nebulae in different clusters, using apertures adjusted to red-shifts, is expected to control the relative errors within reasonable limits (possibly of the order of  $0^m.1$  either way).

The character of the energy-distribution curves for E nebulae shows that the corrections to observed magnitudes due to red-shifts are smallest in the wave-length region centred about  $\lambda 6300$  Å. With this circumstance, the definitive formulation of the law of red-shifts can be most accurately made in the red. Unfortunately, the most reliable method of measuring magnitudes—the photoelectric technique—does not yet reach the necessary limits in the red, although of course it does so easily in the blue and yellow. The compromise adopted at Mount Wilson and Palomar is to use a joggle-camera in all three colours, blue, yellow and red, and to use the photo-cell for the blue and yellow. This procedure furnishes valuable information on colours as a function of distance, and also permits the photo-cell calibrations in blue and yellow to be applied to the red as well. One additional safeguard has been added to the joggle-camera programme. Because these images must be large compared with the in-focus images, and the size of throw must be adjusted accordingly, it is found convenient to make images in all three colours with a uniform, medium size, and to repeat in one colour only (generally yellow) with double the throw. Corrections for size of in-focus images can then be transferred to the other colours on the plausible assumption that colour does not vary much throughout the images of elliptical nebulae.

A joggle-camera for the prime focus of the 200-inch, giving smooth, square images with throws of  $0.5$ ,  $1$ ,  $2$  and  $4$  mm on a side, was put into operation last autumn by my colleague, A. R. Sandage. Plates have now been assembled on half a dozen of the fainter clusters, although the delay in getting transfers of stellar magnitudes from Selected Areas, due to exceptionally poor winter weather, has seriously hampered the progress in final reductions. Baum proposes to join in the programme, now that his new photo-cell is ready for operation, and he has already contributed some data to the calibration problem. Meanwhile, Pettit has measured many of the nebulae in the nearer clusters with a photo-cell on the Mount Wilson reflectors in the course of his programme of getting magnitudes and colours of all nebulae for which radial velocities have been measured (except the very faint cluster nebulae observed with the 200-inch).

These remarks summarize the state of the programme. They indicate why the present discussion must necessarily be a progress report, with perhaps some indications of the direction in which any revisions of the earlier results are likely to fall.

4. *Effects of red-shifts on apparent magnitudes.*—The total effects of red-shifts on apparent luminosities depend upon their interpretation. The mere fact that we observe the shifts clearly indicates that each light-quantum from the nebulae reaches us with reduced energy. Regardless of the interpretation of red-shifts, we must accept the loss of energy by the individual quanta (or reject the fundamental relation  $E \cdot \lambda = \text{constant}$ ) and we must correct the apparent magnitudes accordingly. These corrections are routine and have the same kind of validity as those for atmospheric extinction or instrumental characteristics. The bolometric luminosities are evidently reduced by the factors  $(1 + d\lambda/\lambda)$ , but since the red-shifts change the wave-length scales of the energy-distribution curves, the effects are selective. If the true, unshifted energy curves are known, they can be distorted by the observed shifts, and the effects then traced through the atmosphere, the telescopes, and the measuring devices to give the desired corrections. This procedure has been possible only since Stebbins and Whitford in 1947 derived the energy curve for the elliptical nebula, M 32, reduced to no atmosphere. The curve is derived from 6-colour photo-cell measures, ranging from  $\lambda 10300$  to  $\lambda 3530$ .

Because elliptical nebulae, which dominate cluster populations, are remarkably homogeneous as to spectral types, colours and distribution of colour throughout their images, the energy curve for M 32 can be applied directly to the estimation of corrections for red-shifts to apparent magnitudes of all elliptical nebulae in any region of the observed range in the spectrum. Minor uncertainties may arise from the facts that M 32 is a dwarfish nebula, that it is superposed on an outer arm of M 31 and, finally, that it is in the low galactic latitude of  $-22^\circ$ . The curve will be redetermined eventually from giant elliptical nebulae in the Virgo Cluster, but the present formulation seems to be fairly reliable and it is all we have.

Luminosities of nebulae are measured through "windows" consisting of the atmosphere, telescope and plate-filter or other receiving devices. By means of the energy-curve for M 32, the energy getting through a window from a nebula with a known red-shift can be compared with the energy that would have got through in the absence of a red-shift. These ratios furnish the desired corrections required by the mere observed presence of the red-shifts. These corrections I once called the "energy effects" and, I repeat, they must be applied to the measured luminosities, regardless of the interpretation of red-shifts.

5. *Progress report.*—In eleven clusters blue and yellow magnitudes are available for a number of the brightest nebulae, and in two of the faint clusters red magnitudes also have been measured. Among these data, corrected for galactic obscuration and for red-shifts, the 1st, 3rd, 5th and 10th nebula in each cluster have been used as distance indicators, and the magnitudes plotted against logarithms of red-shifts. The curves suggest that the brightest nebulae in the different clusters are about equally luminous, but that the spread between 1st and 10th varies with the richness of the cluster or with the size of the sample. On this interpretation of the data, the most accurate results should be furnished by the 10th nebula in the great clusters only. This procedure represents a compromise, because a higher ordinal number, say the 25th nebula, would be expected to reduce accidental errors but at the price of introducing systematic errors due to variations in size of samples.

The yellow magnitudes offer the most reliable results, because corrections for red-shifts in the blue are large and uncertain while the red measures are not yet assembled in sufficient numbers. The favoured correlation, at the moment, is

$$\log_{10} v = 0.2 m_{pv} + 1.16 \text{ (10th nebula),}$$

where

$$v = c \cdot d\lambda/\lambda.$$

This correlation is shown in Fig. 1. Evidently the correlation is linear within the uncertainties of the data, and the residuals are surprisingly small. There are no indications of absorption in space in these particular directions. As the number of observed clusters increases, the residuals should offer a critical test of the presence of inter-nebular absorption. Meanwhile the colours offer an approximate criterion where spectra have not yet been recorded.

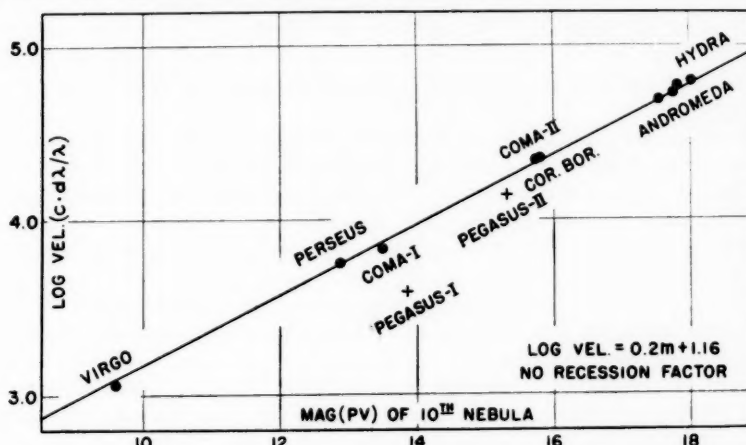


FIG. 1.—The relation between velocity and apparent magnitude. The new data obtained with the 200-inch are represented by the last four points on the regression line. Humason's red-shifts are expressed on a scale of velocities as  $c \cdot d\lambda/\lambda$  in km/sec. The photovisual magnitudes have been corrected for the energy effect only. They do not include the recession factor.

Similar correlations are readily derived for other distance indicators in clusters, for isolated field nebulae, for isolated pairs, and for brightest stars (blue supergiants) in late-type spirals and irregulars with Type I populations. The curves are all parallel, and are displaced by 0.2 times the difference in the absolute magnitudes of the distance indicators. In this way it is possible to calibrate all the correlations in terms of any one, the most accessible, of course, being the brightest stars in nearby nebulae. Thus, the  $M_{pv}$  of the 10th nebula seems to be of the order of  $-17.4$  on the old distance scale, and  $-18.9$  or somewhat less on the new.

Another method is offered by novae and globular clusters in Type II populations found in the Virgo Cluster. The rather meagre results now in hand appear to be consistent with those from brightest stars in Type I populations. When precise photometric data are available, the two methods together should furnish a reliable calibration for all the correlations.

Meanwhile, the relations between red-shift and apparent magnitude represent relative distances that should be reliable, and the slope of the curve,

$\log_{10} v = 0.2m + C$ , indicates a linear relation to a very close approximation. It should be emphasized that the magnitudes have not been corrected for recession of the nebulae.

Such corrections are closely represented by the term,  $\Delta m = d\lambda/\lambda$ , which must be subtracted from the measured magnitudes if the red-shifts are interpreted as Doppler shifts. The corrections range up to a maximum of  $0^{m}.2$  for the Hydra Cluster, and, if the uncorrected data define a linear relation, the corrected data would lead to a non-linear relation in the sense of an accelerated expansion. However, the data now available are not sufficient to furnish a critical test of the two interpretations; either one is permitted by the uncertainties, although it seems unlikely that a decelerated expansion can be represented.

In conclusion it should be repeated that the discussion necessarily ends with a progress report, and not with a definitive solution of the problems considered. Nevertheless, it can be stated with some confidence that a definitive formulation of the law of red-shifts will be available before long, in the form of a relation between red-shifts and apparent magnitudes, out to red-shifts of the order of  $0.25$ .

When no recession factors are included, the law will represent approximately a linear relation between red-shifts and distance. When recession factors are included, the distance relation is expected to be linear or non-linear in the sense of accelerated expansion. The "age of the universe" is likely to be between 3000 and 4000 million years, and thus comparable with the age of rock in the crust of the Earth.

The implications of the law established over this distance may be traced out to nearly double that distance by its effect on the apparent distribution of nebulae in depth,  $N_m = f(m)$ .

Thus, if red-shifts do measure the expansion of the universe, we may be able to gather reliable information over a quarter of its history since expansion began, and some information over nearly a half of the history.

As for the future, it is possible to penetrate still deeper into space—to follow the red-shifts still farther back in time—but we are already in the region of diminishing returns; instruments will be increasingly expensive, and progress increasingly slow. The most promising programmes for the immediate future accept the observable region as presently defined, hope for only modest extensions in space, but concentrate on increased precision and reliability in the recorded description. The reconnaissance is being followed by an accurate survey; the explorations are pushed towards the next decimal place instead of the next cipher. This procedure promises to reduce the array of possible worlds as surely as did the early rapid inspections of the new territory. And later perhaps, in a happier generation, when the cost of a battleship can safely be diverted from insurance of survival to the consolations of philosophy, the march outward may be resumed.

For I can end as I began. From our home on the Earth, we look out into the distances and strive to imagine the sort of world into which we are born. Today we have reached far out into space. Our immediate neighbourhood we know rather intimately. But with increasing distance our knowledge fades, and fades rapidly, until at the last dim horizon we search among ghostly errors of observations for landmarks that are scarcely more substantial. The search will continue. The urge is older than history. It is not satisfied and it will not be suppressed.

## PROBLEMS OF STABILITY IN HYDRODYNAMICS AND HYDROMAGNETICS

*George Darwin Lecture, delivered by Professor S. Chandrasekhar on  
1953 November 13*

### I

Most of what I shall say may be considered as properly belonging to applied mathematics; indeed, in large part they will be based on the works of the great applied mathematicians: Lord Rayleigh of the past and Sir Geoffrey Taylor and Sir Harold Jeffreys of the present. And applied mathematics though it be, I hope I can succeed in bringing some measure of conviction to you that the considerations I shall present have some bearing on and some relevance to the problems of astronomy.

Let me begin then by stating in general terms what we may expect to learn from studies on stability.

When we know that an object has existed in nearly the same state for a long time we generally infer that it is stable; and by this we mean that there is something in its construction and in its constitution which enables it to withstand small perturbations to which any system in Nature must be subject. More precisely, what we have in mind when we say that an object is stable is this: if the object experiences an external perturbation which produces small displacements among its component parts, then it reacts in such a way that it eventually restores itself to its original state. In practice this definition of the meaning of stability requires some amplification: for, though an object may be strictly unstable, it may still be that the time which an external perturbation needs to manifest itself is so long compared to the total duration of its existence that its potential instability has not had time to reveal itself. All that we can conclude, then, from the knowledge that an object has endured for a certain period of time is that its time of instability is long compared to that period. If this is the case, what, one may ask, can we learn from an investigation of the stability of an object? It appears that an investigation of the stability of an object can, under favourable conditions, provide information of two sorts. First, we can often infer some significant facts concerning the construction and the constitution of an object merely from the knowledge that it has successfully endured the effects of small perturbations for a known period of time; I shall presently give illustrations of this. Second, an investigation of stability may disclose the relative importance and sometimes the conflicting tendencies of the different forces and constraints which are kept dormant in the undisturbed state of the object. Thus, when we are confronted with a novel object—and most astronomical objects are novel—a study of its stability may provide a basis for a first comprehension. And I may confess that for an applied mathematician problems of stability present a particular attraction: by their very nature, these problems lead to linear equations and linear equations are always more pleasant to deal with than nonlinear ones. While to emphasize problems of stability for this last reason may appear as an undue concession to one's limitations, I think it will be admitted that an attempt to unravel the wide range of astronomical phenomena in which turbulence,

rotation and magnetism all play their parts, is not likely to meet with success if one started with the most general equations of hydrodynamics and electromagnetism without discrimination. In any event, I should like to illustrate by means of examples as to what we might learn about some of the newer problems of astronomy from studies of stability.

## II

I said that we can often infer some significant facts concerning the constitution of an object from the mere knowledge that it has existed for a long period of time. Let me illustrate this by a classical example from the theory of stellar structure and then by a more modern version of the same.

Consider a sphere of perfect gas—a “star” let us say—in equilibrium under its own gravitation. Then a simple calculation shows that its total energy,  $\mathfrak{E}$ , including its internal heat energy ( $\mathfrak{U}$ ) and its gravitational potential energy ( $\Omega$ ), is given by

$$\mathfrak{E} = -\frac{3\gamma-4}{3(\gamma-1)} |\Omega|, \quad (1)$$

where  $\gamma$  denotes the ratio of the specific heats. Now it is clearly necessary that  $\mathfrak{E}$  be negative; otherwise the star will expand to infinity releasing energy in a time measurable in days. The condition  $\mathfrak{E} < 0$  requires that  $\gamma > \frac{4}{3}$ . This conclusion regarding a physical parameter describing the star is clearly a significant piece of information.

The meaning of the condition  $\gamma > \frac{4}{3}$  becomes clearer when we examine the stability of the gas sphere to its own natural modes of oscillation. By considering adiabatic radial oscillations, Ledoux (1) showed by a very simple argument based on the virial theorem that the formula

$$\sigma^2 = (3\gamma-4) |\Omega| / I,$$

where  $I = \int_0^M r^2 dM(r) \quad (2)$

denotes the moment of inertia, gives  $\sigma$  the frequency of the oscillation to a sufficient degree of accuracy under most conditions. The meaning of the condition  $\gamma > \frac{4}{3}$  is apparent from this formula: if this condition is not met, the frequency of the oscillation will become imaginary and the star will be dynamically unstable, i.e. unstable with respect to one of its own natural modes of oscillation. All this, of course, is well known. But let us apply similar considerations to the magnetic variables discovered by Horace Babcock.

It can be shown that for a gas sphere of the dimensions of a star in which there is a prevalent magnetic field,  $\mathbf{H}$ , the total energy,  $\mathfrak{E}$ , including the heat ( $\mathfrak{U}$ ), the gravitational ( $\Omega$ ) and the magnetic ( $\mathfrak{M}$ ) energies is given by (cf. Chandrasekhar and Fermi (2))

$$\mathfrak{E} = -\frac{3\gamma-4}{3(\gamma-1)} (|\Omega| - \mathfrak{M}), \quad (3)$$

where  $\mathfrak{M} = \frac{I}{8\pi} \iiint |\mathbf{H}|^2 dx_1 dx_2 dx_3. \quad (4)$

From equation (3) it follows that one of the conditions for equilibrium is

$$\mathfrak{M} < |\Omega|. \quad (5)$$

This condition clearly sets an upper limit to the strength of a magnetic field which may prevail in a star. Since for a spherical configuration of uniform density  $\Omega = -3GM^2/5R$  (where  $G$  denotes the constant of gravitation,  $M$  the mass and  $R$  the radius of the configuration), we can estimate the limit on the magnetic field set by (5) by using this expression for  $\Omega$  in it. In this manner we find

$$\sqrt{|\mathbf{H}|^2_{\text{av}}} < 2.0 \times 10^8 M/R^2 \text{ gauss}, \quad (6)$$

where  $M$  and  $R$  are now expressed in solar units. While for most of the magnetic variables discovered by Babcock the surface fields measured are a hundred to a thousand times smaller than the limit for the root mean square field set by (6), there are a few stars—three to be exact—for which the surface fields already approach the limit set by (6) to within a factor ten.

Now the meaning of this upper limit to the magnetic field which may prevail in a star can be understood by considering the period of radial adiabatic pulsation. By following the method of Ledoux, we can show that in this case equation (2) is replaced by (*cf.* Chandrasekhar and Limber (3))

$$\sigma^2 = (3\gamma - 4)(|\Omega| - \mathfrak{M})/I; \quad (7)$$

the meaning of the condition  $\mathfrak{M} < |\Omega|$  is apparent. From formula (7) it would appear that we can make  $\sigma^2 \rightarrow 0$  (i.e. make the period tend to infinity) by letting  $\mathfrak{M} \rightarrow |\Omega|$ . It is possible that this is the explanation of the known relatively long periods of the magnetic variables. I am here referring to the fact that while the observed periods of the magnetic variables are of the order of 6 to 10 days, the period of radial pulsation which we should predict for these stars, were they normal, is of the order of  $\frac{1}{2}$  day. If the suggested explanation of the long periods is correct, then the peculiar A-stars for which surface fields of the order of  $10^4$  gauss have been measured must have internal fields which are a thousand times larger; and this is perhaps not impossible.

### III

I should like to consider next a problem in gravitational stability which may have a bearing on galactic structure (*cf.* Chandrasekhar and Fermi (2)).

Consider an infinite cylinder of an incompressible fluid of uniform circular cross-section of radius  $R_0$ . Is this gravitationally stable? We can answer this question by considering a perturbation of the cylinder which deforms the boundary into

$$r = R + a \cos kz \quad (8)$$

(where  $a \ll R$ ,  $z$  is measured along the axis of the cylinder and  $k$  is a constant) and asking whether the resulting change in the gravitational potential energy,  $\Delta\Omega$ , per unit length is positive or negative. The fact that the potential energy per unit length of an infinite cylinder is infinite requires that some care be exercised in the evaluation of  $\Delta\Omega$ .

When  $\Delta\Omega$  is evaluated it is found that

$$\Delta\Omega > 0 \text{ for } kR_0 > 1.067 \quad (9)$$

and

$$\Delta\Omega < 0 \text{ for } kR_0 < 1.067.$$

The cylinder is, therefore, gravitationally unstable for all symmetrical deformations of the boundary with wave-lengths exceeding  $\lambda_* = 2\pi R_0/1.07$ . This recalls to mind a well-known result of Rayleigh's (4) that a liquid jet is unstable, on

account of surface tension, for all symmetrical deformations with wave-lengths exceeding the circumference of the cylinder. And as in Rayleigh's discussion of the stability of the liquid jet, we may ask whether there is a mode of maximum instability. We find that there is one whose wave-length is approximately 1.84 times the minimum wave-length,  $\lambda_*$ , for instability; and the time of instability as judged by this most unstable mode is

$$\tau = 4.07(4\pi G\rho)^{-1/2}. \quad (10)$$

If we substitute for  $\rho$  in this formula the value of the mean density of the interstellar matter in the spiral arm in which we are located (namely  $2 \times 10^{-24} \text{ g/cm}^3$ ) we obtain  $\tau = 10^8$  years. This is so short a time that a structure like the spiral arm, if we can idealize it as an infinite cylinder, would have disintegrated a long time ago.

Now the spiral arms of a galaxy show every sign of instability; but we should be happier if the time of instability were of the order of  $5 \times 10^9$  years. It appears that we can make an infinite cylinder gravitationally stable for periods of this order by supposing that along the axis of the cylinder there is a magnetic field of the order of

$$H_s = 4\pi\rho R_0 V/G. \quad (11)$$

Thus a field  $H = H_s$  increases the wave-length of maximum instability by a factor ten and the time of instability by a factor nine. Table I gives more data relating to this problem. From this table we may conclude that if the spiral arms can be idealized in the manner we have done, the requirement that they be unstable but with times of instability of the order of  $5 \times 10^9$  years will imply that there are magnetic fields of the order of  $7 \times 10^{-6}$  gauss along the arms. It is gratifying that a number of other independent evidences lead one to postulate galactic magnetic fields of this same order.

TABLE I

*Wave-lengths  $\lambda_*$  and  $\lambda_m$  at which instability sets in and at which it is maximum, and characteristic time,  $\tau$ , needed for instability to manifest itself for case  $R_0 = 250$  parsecs and  $\rho = 2 \times 10^{-24} \text{ g/cm}^3$*

$H$ (gauss)	$\lambda_*$ (parsecs)	$\lambda_m$ (parsecs)	$\tau$ (years)
0	$1.5 \times 10^3$	$2.7 \times 10^3$	$1.0 \times 10^8$
$1.25 \times 10^{-6}$	$1.9 \times 10^3$	$3.3 \times 10^3$	$1.2 \times 10^8$
$2.5 \times 10^{-6}$	$3.3 \times 10^3$	$5.6 \times 10^3$	$1.8 \times 10^8$
$3.75 \times 10^{-6}$	$6.8 \times 10^3$	$1.1 \times 10^4$	$3.6 \times 10^8$
$5.0 \times 10^{-6}$	$1.7 \times 10^4$	$2.8 \times 10^4$	$8.7 \times 10^8$
$6.25 \times 10^{-6}$	$5.2 \times 10^4$	$8.6 \times 10^4$	$2.7 \times 10^9$
$7.5 \times 10^{-6}$	$2.1 \times 10^5$	$3.4 \times 10^5$	$1.1 \times 10^{10}$
$10.0 \times 10^{-6}$	$6.9 \times 10^6$	$1.1 \times 10^7$	$3.5 \times 10^{11}$

## IV

In a general way one may expect that a conducting fluid in the presence of a magnetic field and under the influence of Coriolis' force is subject to conflicting tendencies and that it may exhibit unexpected patterns of behaviour. I should like to illustrate this by considering a classical problem in the theory of thermal instability. The problem I have in mind is the instability of a layer of fluid heated below which has been investigated by Rayleigh (5), Jeffreys (6) and others.

When a horizontal layer of an incompressible fluid is heated below—"underside" as Rayleigh calls it—then on account of thermal expansion the liquid above, being colder, will be heavier. This is a top-heavy arrangement and is potentially unstable. Consequently, if the temperature gradient is made sufficiently adverse, we should expect the instability to manifest itself.

The manner of the onset of convection under these circumstances has been the subject of both experimental and theoretical investigations since Bénard's first experiments on the subject in 1900 and 1901. Those early experiments of Bénard established that instability sets in only when the temperature gradient exceeds a certain critical value and that when it does set in, it does so as a pattern of cellular convection. The correct interpretation of Bénard's experiments was given by Rayleigh in 1916. Rayleigh showed that what decides the stability of a layer of fluid heated below is the numerical value of the non-dimensional quantity

$$R = \frac{g\alpha\beta}{\kappa\nu} d^4, \quad (12)$$

where  $g$  denotes the value of gravity,  $d$  the depth of the layer,  $\beta = |dT/dz|$ , the constant adverse temperature gradient which is maintained, and  $\alpha$ ,  $\kappa$  and  $\nu$  are the coefficients of volume expansion, thermometric conductivity and kinematic viscosity respectively. We shall call  $R$  the Rayleigh number. Both experiments and theory show that instability must set in when the Rayleigh number exceeds a certain determinate critical value: for example, it is 1708 when it is confined between two rigid plane boundaries. Accordingly, higher temperature gradients can be maintained, before instability sets in, in a liquid of higher viscosity and/or higher thermal conductivity; and the reason for this is quite evident.

Before passing on to an examination of the effects of Coriolis' force and magnetic field on the onset of convection by thermal instability we may first consider very briefly the manner in which one determines the critical Rayleigh number, theoretically. One determines this by supposing that an initial constant state is slightly disturbed and asking whether there exists any type of disturbance which will not be damped. Since any disturbance in the horizontal plane can be expressed as a superposition of two-dimensional periodic waves, we can investigate this problem by asking what the lowest Rayleigh number,  $R(a)$ , is at which a mode of disturbance in the horizontal plane of a given wave number,  $a$ , when excited, does not get damped. On solving this problem one finds that the resulting function  $R(a)$  has in general a single minimum which it attains for a particular value of  $a$ . It is clear that this minimum of the function  $R(a)$  specifies the critical Rayleigh number at which instability will first set in; at the same time the value of  $a$  at which the minimum occurs determines the dimensions of the cell which will appear at marginal stability.

We shall now suppose that in addition to gravity the fluid is subject to the Coriolis acceleration  $2\mathbf{u} \times \boldsymbol{\Omega}$  resulting from the fluid partaking in a rotation with angular velocity  $\boldsymbol{\Omega}$ . The discussion of the stability of fluid heated below under these circumstances can be carried out and it is found (Chandrasekhar (7)) that the effect of the Coriolis acceleration is to inhibit the onset of convection, the extent of the inhibition depending on the value of the non-dimensional parameter

$$T = 4 \frac{\Omega^2 \cos^2 \theta}{\nu^2} d^4, \quad (13)$$

where  $\vartheta$  denotes the angle which the direction of  $\Omega$  makes with the vertical and  $\Omega = |\Omega|$ . The inhibition factors are of the order of ten for  $T$  of the order of  $10^6$  (see Fig. 1). It is further found that

$$R \rightarrow \text{constant } T^{2/3} \text{ and } a \rightarrow \text{constant } T^{1/6} \text{ as } T \rightarrow \infty; \quad (14)$$

here  $a$  denotes the wave number (in units of  $1/d$ ) of the cells which appear at marginal stability. I might mention here that experiments carried out by Dr D. Fultz at Chicago confirm the predicted dependence of  $R$  on  $T$ .

In a general way the reason for the inhibiting effect of  $\Omega$  is clear: according to a theorem of Kelvin and Helmholtz, the vortex lines have a tendency to be dragged with the fluid, the attachment of the fluid to the vortex lines being stronger the lower the viscosity and the higher the angular velocity; and in the limit of zero viscosity the attachment is a permanent one. Consequently as  $\Omega \cos \vartheta$  increases and/or  $\nu$  decreases, motions at right angles to the vertical will

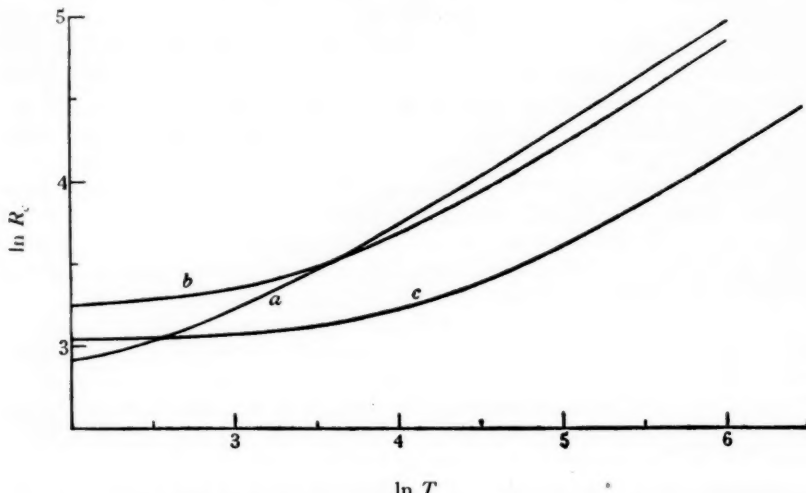


FIG. 1.—The variation of the critical Rayleigh number,  $R_c$ , for the onset of convection as a function of  $T (= 4\Omega^2 d^4 \cos^2 \vartheta / \nu^2)$  for the three cases: (a) both bounding surfaces free, (b) both bounding surfaces rigid and (c) one bounding surface free and the other rigid.

[Reproduced by courtesy of the Royal Society (*Proc. Roy. Soc. A*, **217**, 306, 1953)]

become increasingly difficult; and this prevents an easy closing-in of the stream lines required for convection. This also explains why instability, when it sets in, does so for a value of  $a$  which is increasingly large: for, a large value of  $a$  means that the cells are elongated in the direction of the vertical and motions in this direction are not hindered by the component of  $\Omega$  in this direction.

According to equations (13) and (14), in the limit  $T \rightarrow \infty$ , the relation giving the critical temperature gradient at which convection sets in changes from

$$g\alpha\beta_c = \text{constant } \kappa\nu d^{-4} \quad (15)$$

to

$$g\alpha\beta_c = \text{constant } \kappa(\Omega^4 \cos^4 \vartheta / d^4 \nu)^{1/3}. \quad (16)$$

This changed dependence of  $\beta_c$  on  $d$  from a  $d^{-4}$ -law to a  $d^{-4/3}$ -law is likely to be a decisive factor in determining the character of the convection when Coriolis'

force is acting. If the indications of this theory may be taken as a guide as to what may happen in reality, then we should conclude that the effects of Coriolis' force must control thermally induced convection in all atmospheric layers exceeding ten metres on the Earth and a hundred kilometres on the Sun.

We turn next to the effect of a magnetic field on the onset of convection. On general grounds, we may expect that the effect of a magnetic field will also be to inhibit convection and that this inhibiting effect will be greater the stronger the magnetic field (**H**) and the higher the electrical conductivity ( $\sigma$ ): for, when the field is strong (or the conductivity high), the lines of force tend to be glued to the material and this will make motions at right angles to the vertical increasingly difficult. Moreover, when cellular convection does set in, we should expect that the cells are elongated in the direction of the vertical, the elongation being greater the stronger the vertical component of the magnetic field. In the limit of infinite electrical conductivity, when the lines of force are permanently attached to the fluid, convection in the usual sense will become impossible. A detailed theoretical treatment of the problem (*cf.* Chandrasekhar (8)) confirms these anticipations. In particular, it is found that the critical Rayleigh number for the onset of instability in the presence of a magnetic field depends on the strength of the field and the electrical conductivity  $\sigma$  through the non-dimensional parameter

$$Q = \frac{\sigma H^2 \cos^2 \vartheta}{\rho v} d^2, \quad (17)$$

where  $\vartheta$  now denotes the inclination of the direction of the impressed magnetic field to the vertical. It is further found that we have inhibition factors of the order of ten for  $Q$  of the order of a thousand (see Fig. 2) and that in the limit  $Q \rightarrow \infty$ ,

$$R \rightarrow \text{constant } Q \text{ and } a \rightarrow \text{constant } Q^{1/6}. \quad (18)$$

All that I have said so far regarding the effect of  $\Omega$  and **H** on the onset of thermal instability might possibly have been predicted on general grounds. But let us now consider what happens when both  $\Omega$  and **H** are simultaneously present. The results I shall describe have been obtained for the case when **g**, **H** and  $\Omega$  are all co-planar and both the confining boundaries are free surfaces; however, the general character of the solution to be described does not depend on these latter restrictions.

The solution of the problem presents some unexpected features which result from the curve  $R(a)$  (which represents the lowest Rayleigh number at which a horizontal disturbance having a wave number  $a$  when excited is undamped) having two minima, the one occurring at the larger  $a$  giving the lower Rayleigh number when  $Q$  is small and the higher Rayleigh number when  $Q$  is large (see Figs. 3 and 4). Thus for  $T_1 (= T/\pi^4) = 100,000$  and  $Q_1 (= Q/\pi^2) = 50$  the two minima occur at  $a$  (the wave number measured in the unit  $1/d$ ) = 18.6 and 3.48 where  $R = 4.03 \times 10^5$  and  $7.26 \times 10^5$ , respectively. On the other hand for  $Q_1 = 100$  (and the same value of  $T_1$ ) the two minima occur at  $a_1 = 18.2$  and 3.37 where  $R = 3.98 \times 10^5$  and  $3.93 \times 10^5$ , respectively. Consequently, for a value of  $Q_1$  slightly less than 100 the wave number of the cells which appear at marginal stability will suddenly decrease from  $a = 18.2$  to  $a = 3.4$ . In other words, if we start with an initial situation in which  $T_1$  has the value  $10^5$  and no magnetic field is present and gradually increase the strength of the magnetic field, then at first the cells which appear at marginal stability will be elongated; but when the

magnetic field has increased to a value corresponding to  $Q_1 = 100$ , cells of two very different sizes will appear simultaneously: one set which will be highly elongated and another set which will be much less elongated. As the magnetic field increases beyond this value, the critical Rayleigh number will actually begin to decrease. However, for sufficiently large  $Q$  the inhibition due to the magnetic field will predominate and will take control of the situation. This is an unexpected sequence of events and I do not know if one could have predicted it.

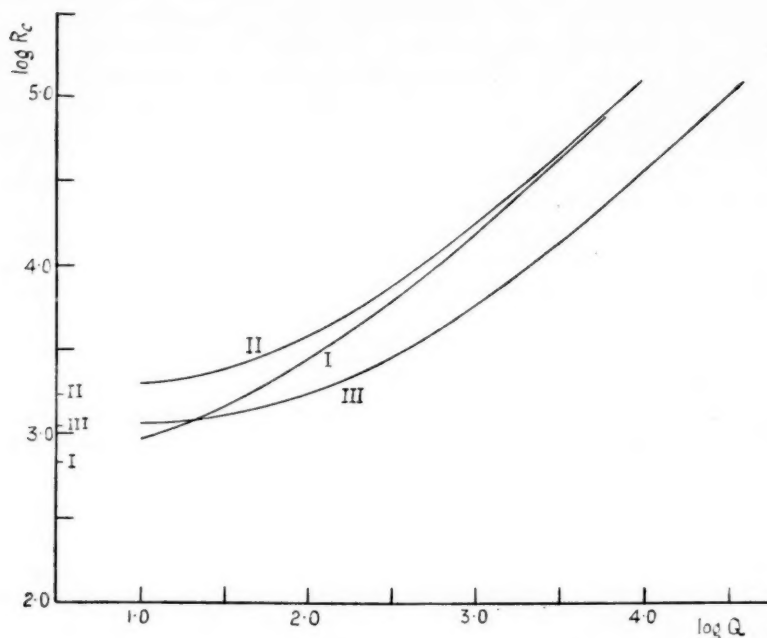


FIG. 2.—The variation of the critical Rayleigh number,  $R_c$ , for the onset of instability as a function of  $Q$  for the three cases (i) both bounding surfaces free (curve marked I), (ii) both bounding surfaces rigid (curve marked II) and (iii) one bounding surface free and the other rigid (curve marked III). The points marked I, II and III on the  $R_c$ -axis are the limiting values for the three cases considered in the absence of a field.

[Reproduced by courtesy of the Editors of the Philosophical Magazine (*Phil. Mag.* (7), **43**, 501, 1952)]

## V

I shall turn now from these problems in thermal instability to one of a somewhat different kind: the problem of the gravitational instability of an infinite homogeneous medium. This was first considered by Jeans (9) more than fifty years ago. In this problem we start from an initial state of homogeneity and rest and consider the velocity of propagation of a density fluctuation through the medium. If the gravitational effects of the density fluctuation are ignored, the problem is the classical one of the propagation of sound; and as is well known, the velocity of sound in a gaseous medium is independent of wave-length and is given by

$$c = \sqrt{(\gamma p/\rho)}, \quad (10)$$

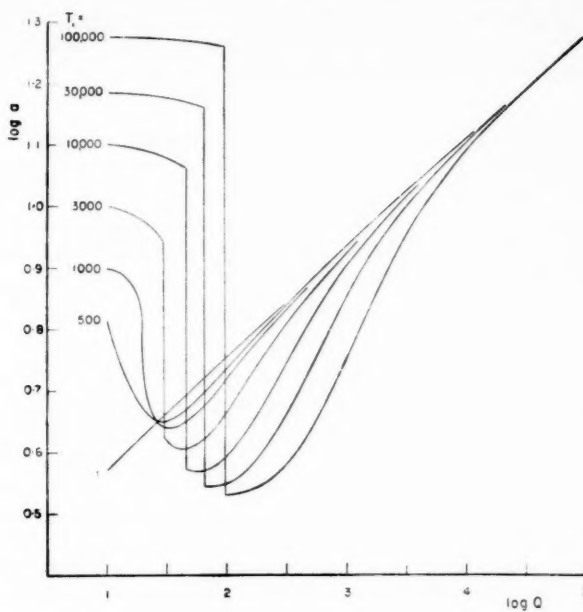


FIG. 3.—The dependence of the wave number  $a$  of the cells which appear at marginal stability under the simultaneous influence of a Coriolis acceleration and a magnetic field. The different curves refer to the various assigned values of  $T_1$  and varying values of  $Q_1$ .

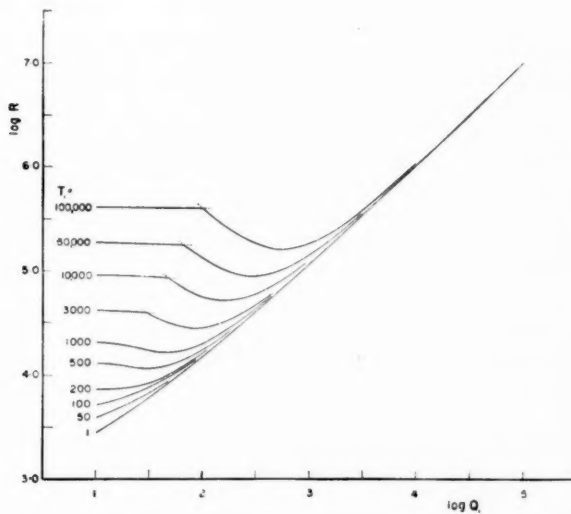


FIG. 4.—The variation of the critical Rayleigh number  $R$  for the onset of instability as a function of  $Q_1$  for various assigned values of  $T_1$ .

where  $p$  denotes the pressure,  $\rho$  the density and  $\gamma$  the ratio of the specific heats. On the other hand, if the change in the gravitational potential,  $\delta V$ , consequent on the density fluctuation,  $\delta\rho$ , is taken into account in the equation of motion, with  $\delta V$  related to  $\delta\rho$  through Poisson's equation

$$\nabla^2 \delta V = -4\pi G \delta\rho, \quad (20)$$

then, as Jeans showed, the velocity of wave propagation is no longer independent of the wave-length. It is given by

$$V_J^2 = c^2 - 4\pi G \rho / k^2, \quad (21)$$

where  $k (= 2\pi/\lambda)$  is the wave number. The velocity of wave propagation, therefore, becomes imaginary if

$$k^2 < \frac{4\pi G \rho}{c^2} \text{ or } \lambda^2 > \frac{\pi c^2}{G \rho} = \lambda_J^2 \text{ (say).} \quad (22)$$

But an imaginary velocity of wave propagation only means that the amplitude of the wave will increase exponentially with time. Accordingly, if an arbitrary initial perturbation in density is represented by a Fourier integral, then the amplitudes of those components in the Fourier representation which have wave-lengths exceeding  $\lambda_J$  will increase exponentially with time;  $\lambda_J$  is therefore a measure of the linear dimensions of the condensations which will form in the medium on account of this instability; this is Jeans's result.

Now suppose that the medium considered is partaking in rotation and that there is a term  $2\mathbf{u} \times \boldsymbol{\Omega}$  representing the Coriolis acceleration in the equation of motion. Then a reconsideration of Jeans's problem taking account of this additional term shows that there are now two modes of wave propagation. If  $V_1$  and  $V_2$  are the velocities of propagation of these two modes, then one finds that

$$V_1^2 V_2^2 = 4 \left( \frac{\Omega \cos \vartheta}{k} \right)^2 V_J^2, \quad (23)$$

where  $\vartheta$  denotes the angle between the direction of  $\boldsymbol{\Omega}$  and the direction of wave propagation considered. From this relation between  $V_1$  and  $V_2$  it follows that if  $V_J^2 < 0$  then either  $V_1^2$  or  $V_2^2$  must be negative. In other words if Jeans's condition for gravitational instability is satisfied, then the propagation by one of the two modes must be unstable. Jeans's condition is, therefore, unaffected by the inclusion of Coriolis' force. There is only one exception to this rule and this occurs when we consider a wave propagated in a direction at right angles to  $\boldsymbol{\Omega}$ . In this latter case, there is only one mode in which a wave can be propagated and its velocity is given by

$$V^2 = 4 \frac{\Omega^2}{k^2} + c^2 - \frac{4\pi G \rho}{k^2}. \quad (24)$$

Consequently, in this plane the propagation of a wave will always be stable provided

$$\Omega^2 > \pi G \rho. \quad (25)$$

But even when this last condition is satisfied the propagation of waves in other directions will exhibit gravitational instability.

Similarly, we find (*cf.* Chandrasekhar and Fermi (2)) that Jeans's condition is unaffected also when a uniform magnetic field is present. In this case it is found that there are three modes of wave propagation. One of these is

unaffected by gravity and compressibility and represents the usual hydromagnetic wave of Alfvén. But the other two modes are affected and their velocities are related by

$$V_1^2 V_2^2 = \frac{H^2 \cos^2 \vartheta}{4\pi\rho} V_J^2, \quad (26)$$

where  $\vartheta$  now denotes the angle between the direction of  $\mathbf{H}$  and the direction of wave propagation considered. From this relation it is apparent that if  $V_J^2 < 0$  then either  $V_1^2$  or  $V_2^2$  must be negative; and Jeans's condition follows.

Finally, if we consider the case when a magnetic field is present and Coriolis' force is also acting, we find that Jeans's condition is still unaffected. In this case there are three modes of wave propagation all coupled in such a way that their velocities  $V_1$ ,  $V_2$  and  $V_3$  are related by

$$V_1^2 V_2^2 V_3^2 = \left( \frac{H^2 \cos^2 \vartheta}{4\pi\rho} \right)^2 V_J^2, \quad (27)$$

where  $\vartheta$  has the same meaning as in (26). And again if  $V_J^2 < 0$ , one of these modes will be unstable and gravitational instability will ensue.

## VI

The foregoing discussion of the various problems of stability draws attention to an aspect of theoretical investigations in astronomy and geophysics which is not often recognized: it is that matter and motions in the large may exhibit patterns of behaviour which one might never suspect if one restricted oneself to matter and motions in the small. Several examples could be given to underline this. Thus, in most hydromagnetic problems which occur in astronomy one may treat the matter (be it in interstellar space, stellar atmospheres or stellar interiors) as an infinitely good electrical conductor with the lines of magnetic force permanently attached to it; and one may do this even though the electrical conductivity of stellar material judged by terrestrial standards is by no means extraordinary. And the reason why we may do this is simply the very large linear dimensions of the systems one deals with, the large dimensions leading to times of decay of a prevalent magnetic field which are very long compared to the times in which one is normally interested. This applies even to certain aspects of geomagnetism. For example, in considering the secular variation of the Earth's magnetic field we may treat the fluid core of the Earth as an infinitely good conductor; for, while the time of decay is of the order of 50 000 years, the periods in which the secular variations take place are of the order of a hundred to two hundred years. This reference to the Earth's magnetic field reminds us that its existence is the best illustration of what a large mass of electrically conducting fluid, in rotation, can exhibit. Indeed, rotation must influence fluid behaviour in the large in a manner which we are still very far from comprehending. Thus, all the evidence we have tends to support the view that solar rotation plays a decisive role in the entire complex of phenomena associated with the sunspots and the solar cycle; and yet the magnitude of the solar rotation is, by all conventional standards, very small.

It would appear then that the scope for applied mathematics in astronomy and geophysics is a very large one. But in order to make progress it may often be necessary to make the most severe idealizations, as will have been evident from

the examples I have considered. In defence I may quote from Sir George Darwin's address of welcome to the Fifteenth International Congress of Mathematicians when it met in Cambridge in 1909:

"I appeal, then, for mercy to the applied mathematician and would ask you to consider in a kindly spirit the difficulties under which he labours. . . . yet they are honest attempts to unravel the secrets of the Universe in which we live."

#### *References*

- (1) P. Ledoux, *Ap. J.*, **102**, 143, 1945.
- (2) S. Chandrasekhar and E. Fermi, *Ap. J.*, **118**, 116, 1953.
- (3) S. Chandrasekhar and D. Nelson Limber, *Ap. J.*, **119**, 10, 1954.
- (4) Lord Rayleigh, *Scientific Papers*, **2**, 361, Cambridge, 1900.
- (5) Lord Rayleigh, *Phil. Mag.* (6), **32**, 529, 1916; also *Scientific Papers*, **6**, 432, Cambridge, 1920.
- (6) H. Jeffreys, *Phil. Mag.* (7), **2**, 833, 1926.
- (7) S. Chandrasekhar, *Proc. Roy. Soc. A*, **217**, 306, 1953.
- (8) S. Chandrasekhar, *Phil. Mag.* (7), **43**, 501, 1952.
- (9) J. H. Jeans, *Phil. Trans. A*, **199**, 1, 1902.

## THE MOTION OF MAGNETIC FIELDS

J. W. Dungey

(Received 1953 July 20)

### Summary

The temporal change of a magnetic field cannot be described as a motion, if it involves interlinking of the lines of force. It is shown that the idea of motion can be retained, if the lines of force are regarded as being "disconnected" on a suitable surface. A process is described by which magnetic flux can be generated other than at a neutral line.

1. *Introduction.*—The idea of the motion of a magnetic field has been found to be useful in problems of cosmic electrodynamics, because the motion can often be taken to be the same as the motion of the material. Sweet (1) has extended this idea and has considered the motion of the field relative to the material. He does not point out, however, that in some cases the temporal change of a magnetic field cannot be described by a motion of the field. If it could, it would follow that the magnetic flux linked by any closed curve moving with the velocity of the field would be constant, and in particular the flux linked by a line of force would be constant. But the rate of change of the flux linked by a line of force is given by the e.m.f.  $\oint \mathbf{E} \cdot d\mathbf{s}$  round the line of force, and this need not be zero. It is shown here that the change in the magnetic field can still be represented as a motion except on some suitably chosen surface.

2. *Representations of the field.*—We denote the magnetic field by  $\mathbf{H}$ . Sweet (1) uses the representation

$$\mathbf{H} = F \nabla \phi \wedge \nabla \psi, \quad (1)$$

where  $\phi$  and  $\psi$  are functions of position and time and  $F$  is a function of  $\phi$  and  $\psi$ . The lines of force are the lines of intersection of the surfaces of constant  $\phi$  and  $\psi$ . Sweet shows that the motion of the field is equivalent to motion of the surfaces of constant  $\phi$  and  $\psi$ ,  $F$  remaining the same function of  $\phi$  and  $\psi$ . Corresponding to the difficulty concerning the motion of the field, there is a difficulty concerning the representation (1).

Lundquist (2) has pointed out that the problem is more complicated than appears from Sweet's paper. Lundquist uses a similar representation

$$\mathbf{A} = \nabla \alpha + \phi \nabla \psi$$

and

$$\mathbf{H} = \nabla \wedge \mathbf{A} = \nabla \phi \wedge \nabla \psi.$$

He then points out that the flux linked by a line of force is given by

$$\oint \mathbf{A} \cdot d\mathbf{s} = \oint \nabla \alpha \cdot d\mathbf{s},$$

since  $\nabla \psi$  is perpendicular to the line of force. He concludes that, if this flux does not vanish,  $\alpha$  is multivalued. We now show how the representation (1) can be modified, so that it can still be used when the flux linked by a line of force does not vanish.

In this case there must be linked lines of force. The simplest field of this type is the twisted toroidal field, in which each line of force lies on a toroidal surface and is linked with the lines of force inside this surface. In general each line of force is infinite in length and covers the whole of the toroidal surface; this is possible because the surface is not simply connected and so the line need not cross itself. Then the only surfaces containing lines of force are the toroidal surfaces. The representation (1) can still be used, however, if a cut is made, so that the surface covered by any line of force is made to be simply connected; on a toroidal surface the cut may be taken to be a closed curve linking the toroid. Then, supposing that  $\phi$  is constant on the surface,  $\psi$  may vary, but will be discontinuous at the cut;  $F$  can be chosen so as to make  $\psi$  single-valued.

3. *Motion of the field.*—The statement that a magnetic field moves with velocity  $\mathbf{u}$  means

$$-c \operatorname{curl} \mathbf{E} = \partial \mathbf{H} / \partial t = \operatorname{curl} (\mathbf{u} \wedge \mathbf{H}), \quad (2)$$

but, if the electric field  $\mathbf{E}$  is given,  $\mathbf{u}$  is not completely determined by (2); any velocity  $\mathbf{w}$  such that  $\mathbf{w} \wedge \mathbf{H}$  is irrotational can be added to  $\mathbf{u}$ . Thus the component of  $\mathbf{u}$  parallel to  $\mathbf{H}$  is arbitrary, and is conveniently taken to vanish. The component of  $\mathbf{w}$  perpendicular to  $\mathbf{H}$  must have the form  $H^{-2} \mathbf{H} \wedge \nabla W$ , where  $H = |\mathbf{H}|$  and  $W$  is constant on any line of force, but is otherwise arbitrary. Such a velocity  $\mathbf{w}$  does not change  $\mathbf{H}$ , but just permutes the lines of force.

The temporal change of a magnetic field cannot always be described as a motion of the field. By integrating (2) over a surface bounded by a line of force and using Stokes' theorem,

$$-c \oint \mathbf{E} \cdot d\mathbf{s} = \frac{\partial}{\partial t} \int \mathbf{H} \cdot dS = \oint (\mathbf{u} \wedge \mathbf{H}) \cdot d\mathbf{s}. \quad (3)$$

For a line of force the right-hand side vanishes and hence the magnetic flux linked by a line of force must be constant; this may also be seen by picturing the change in the field resulting from any motion. The left-hand side of (3), however, does not in general vanish, so that the concept of the motion of the field is not always valid.

This difficulty can be overcome by choosing a surface  $S$  which is crossed at least once by each line of force and by regarding the lines of force as being "disconnected" on  $S$ . The lines can be pictured as being cut at this surface, the two ends arising from the same cut being allowed to move on  $S$  with different velocities. Their motion must be such that  $\mathbf{H}$  remains continuous and hence their relative motion must just permute the ends of the lines of force; at any boundary of  $S$  their relative motion must be parallel to the boundary.  $S$  may consist of a set of separate surfaces and in general these must be given a motion such that  $S$  continues to intersect every line of force. This picture is of course just a mathematical device and  $S$  has no physical significance.

The motion of the field can be defined as follows. Let

$$V = \int \mathbf{E} \cdot d\mathbf{s}, \quad (4)$$

the integral being taken along a line of force in the direction of  $\mathbf{H}$ , starting from  $S$  and not crossing  $S$  again. Then, everywhere except on  $S$ ,  $\mathbf{E} - \nabla V$  is perpendicular to  $\mathbf{H}$  and (2) is satisfied with

$$\mathbf{u} = cH^{-2}(\mathbf{E} - \nabla V) \wedge \mathbf{H}. \quad (5)$$

At  $S$  both  $V$  and  $\mathbf{u}$  may be discontinuous, but, on both sides of  $S$ ,  $\partial \mathbf{H} / \partial t$  is equal to  $-c \operatorname{curl} \mathbf{E}$ , which is continuous.

If, as in the case of the twisted toroidal field, some lines of force cover a whole surface, they will cross the surface  $S$  an infinite number of times. A line of force which crosses  $S$  more than once is cut into sections, which could be labelled and followed through the motion. The connections at  $S$  between the sections are altered by the motion, so that two sections, which at one instant form part of the same line of force, may belong to different lines of force at another instant. Similarly a line of force, which at one instant crosses  $S$  only once, may at another instant be just a section of a line of force which crosses  $S$  more than once. Thus the lines of force do not generally retain their identity during the motion, though the sections do so.

The validity of the description of the change in the field as a motion has some useful implications. It is also rather convenient that the change in the field is separated into two parts represented by the continuous motion and the discontinuity, because the change in the linkages between lines of force depends only on the latter. The Hall electric field is perpendicular to  $\mathbf{H}$ , so that it does not contribute to  $V$  and it is usually the effect of the Ohmic electric field  $\mathbf{j}/\sigma$  that is required. The effect of the Ohmic field is well known, it causes a decay of field energy and generally tends to untwist the lines of force. This effect is usually very slow in astrophysical systems, but may be increased by turbulent motion in the gas.

Sweet (1) used the idea of the motion of the field to discuss the effective conductivity in a gas in turbulent motion. Due to the Ohmic field any surface generated by lines of force crosses material at a rate inversely proportional to  $\sigma$ . This rate may be expressed as a surface integral and is found to be increased by turbulence; the effect can then be expressed as a reduction in  $\sigma$ . Sweet's discussion is restricted to axially symmetric fields and turbulence, and, though this is sufficient for certain applications, an extension to three dimensions may be of interest. The results obtained here show that the motion of the field could still be used, but  $V$  would not vanish as it does in the two-dimensional problem, and, if the effect were to be represented as a reduction in conductivity, the untwisting of the field would also have to be considered.

4. *The generation of magnetic flux.*—Some time ago Cowling (3) used a formulation, very similar to that of Section 3, to discuss the possibility of a sunspot field being maintained by the mechanism of the self-excited dynamo. Alfvén (4) and Bondi and Gold (5) have also discussed this problem using the idea of the motion of the field. These discussions are concerned with the "creation" and "destruction" of magnetic flux. When the lines of force retain their identity, the significance of these terms is obvious and it is easily seen that they can occur only at neutral lines of the field. Flux flows into or out of a neutral line at a finite rate, since  $u \propto H^{-1}$ . If the limiting lines of force near a neutral line are circular, the Ohmic field always destroys flux there. At the other type of neutral line the lines of force have the form of an X. Here flux is created by the breaking of a line of force to form two lines or destroyed by the reverse process; this has been described in detail by the author (6).

In the general case, when the lines of force do not retain their identity, the term "creation of flux" is not so easily defined. It may be noted here that the flux through an unclosed surface such as a sunspot can in any case be much larger

than the "total flux" of the field, if the individual lines of force cross the surface many times. We now describe a process, not involving a neutral line, which clearly creates flux. An attractive mechanism, in which this occurs, has been suggested by Alfvén (4). Suppose that two parts of the surface of a tube of force come into contact over a finite area; in practice the field will be continuous at the interface. Now choose  $S$  to be a surface crossing both parts of the tube where they are in contact. It is evidently possible in principle for the ends of the lines of force to move, so that the ends which originally belonged to one part of the tube become connected to the ends which originally belonged to the other part; if this occurs, two separate tubes are obtained, each containing the same amount of flux as the original tube.

This example shows that care is sometimes needed in applying the picture developed here. If  $S$  had been taken to cross only one part of the tube, the correct result would not have been obtained. The reason is that the relative velocity of the ends of the lines of force at the boundary of  $S$  would not have been parallel to the boundary. Care is also needed in discussing any model containing finite regions of zero field, since magnetic flux can cross such a region at a finite rate.

I would like to thank Dr R. G. Giovanelli for the benefit of his comments.

This work was carried out during the tenure of a Senior Research Fellowship at the University of Sydney.

*School of Physics,  
University of Sydney:  
1953 June 4.*

#### *References*

- (1) P. A. Sweet, *M.N.*, **110**, 69, 1950.
- (2) S. Lundquist, *Ark. f. Phys.*, **5**, No. 15, 1952.
- (3) T. G. Cowling, *M.N.*, **94**, 39, 1934.
- (4) H. Alfvén, *Tellus*, **2**, 74, 1950.
- (5) H. Bondi and T. Gold, *M.N.*, **110**, 607, 1950.
- (6) J. W. Dungey, *Phil. Mag.*, **44**, 725, 1953.

# THE MAXIMUM EFFECT OF CONVECTION IN STELLAR ATMOSPHERES ON THE OBSERVED PROPERTIES OF STELLAR SPECTRA. I

*Antoni Przybylski*

(Communicated by the Commonwealth Astronomer)

(Received 1953 October 3)\*

## *Summary*

Computations have been made of model stellar atmospheres corresponding to spectral types from about G0 to A0. The atmospheres have been constructed with radiative temperature gradients and also with adiabatic gradients in those regions where they are less than radiative gradients.

The calculations have been carried so far as to give the monochromatic fluxes and colour temperatures of the stars. It is found that the difference of colour gradients between "radiative" and "adiabatic" models is easily accessible to observation (0.58 in the most extreme case).

**1. Introduction.**—In spite of many attempts to solve the problem of convection in stellar atmospheres, our present knowledge of its effects on the structure of the outer layers of stars is still inadequate. The observations of solar granulation and theoretical investigations show clearly that there is an unstable zone in stellar atmospheres, in which the transfer of energy is partly due to radiation and partly to convection and in which therefore the actual temperature gradient has a value intermediate between the two limiting values of the radiative and adiabatic gradients; but we have no sure basis on which to investigate theoretically the influence of convection on the temperature distribution in the convectively unstable zone. Since, however, the energy distribution in the stellar spectrum is a function of the temperature distribution in the outer layers of stellar atmospheres, it can be hoped that the analysis of stellar spectra may lead to an approximate evaluation of the influence of convection on the structure of the convective zone, if there are any properties of stellar spectra which are sensibly affected by convection and which can be easily measured. The present investigation shows that the colour gradient of a star satisfies both the above conditions and therefore may be used for that purpose. In subsequent papers it is intended to deal with other such properties.

The present investigations consist in the computation of colour gradient for a number of pairs of model stellar atmospheres, the models of every pair having the same surface temperature and the same value of surface gravity, but differing by disregarding convection in one model altogether, and by taking it at its highest amount, i.e. the adiabatic value, in the convective zone in the other; the colour gradients of real stellar atmospheres must then lie between the two values found in that way. Such pairs of model stellar atmospheres were computed ten years ago by Strömgren and his collaborators (1), but they soon became obsolete, when the investigation of Chandrasekhar and Breen (2) showed that the old

\* Received in original form 1953 June 22.

value of the absorption coefficient for the negative hydrogen ion used by Strömgren was only a rough approximation. Since they seemed to be inadequate for the study of the effect of convection in stellar atmospheres on the observable properties of stellar spectra, a new series of models based on recent values of absorption coefficients was computed.

2. *Mean absorption coefficient used.*—The natural constants  $c$  (velocity of light),  $e$  (electronic charge),  $m_e$  (electron mass),  $\hbar$  (Planck's constant),  $k$  (Boltzmann's constant),  $m_H$  (mass of the H atom) appearing in the formulae for absorption were taken from the critical work of Du Mond and Cohen (3), whose values differ slightly from those used by Strömgren. In order to achieve agreement between the adopted values of the natural constants and the observed limits of the spectroscopic series of hydrogen the value of 13.595 volts was assumed for the ionization potential of hydrogen; this seems to be confirmed by recent experiments (4).

As in the work of Strömgren (1), only the continuous absorption coefficients of the neutral atom and negative ion of hydrogen were taken into account, the effect of other sources of absorption being reserved for further investigations. The metal atoms were considered only as affording a supply of electrons, and they are very important at lower temperatures, where the amount of ionization of hydrogen is small on account of its relatively high ionization potential. The logarithm of the ratio  $A$  between the number of hydrogen particles and the number of metal particles is assumed to be 3.8, the composition of the metal mixture being the same as in the work of Strömgren (1); hence Strömgren's table of the average ionization degree of the metals  $X_M$  was used throughout in the present investigations.

The mean absorption coefficient has been computed simply by weighting the coefficients for various wave-lengths with Planck's function. The Planck mean has been chosen rather than Rosseland's mean or Chandrasekhar's mean for a number of reasons. In the first place, the weights for the Chandrasekhar mean are given only to optical depth 2, which is insufficient for our purposes; and again, while there was no special reason to use a mean based on the theory of radiative equilibrium in the convective zone, yet it was desired to use the same mean in both cases. Finally, theoretical arguments have been put forward by Michard (5) to show that the Planck mean gives a good approximation to the temperature distribution in the radiative case. Since the Planck mean has been chosen rather than the Rosseland mean, the tables of absorption coefficients published by Vitense (6) cannot be used.

2.1. *Mean absorption coefficient for neutral hydrogen.*—The continuous absorption coefficient for a neutral H atom corrected for stimulated emission is given by the formula

$$\kappa_\nu = \frac{64\pi^4 m_e e^{10}}{3\sqrt{3} c \hbar^6 \nu^3} (1 - e^{-h\nu/kT}) e^{-\chi_H/kT} \cdot D,$$

where

$$D = \sum_{n < \infty} \frac{g_n}{n^3} e^{\chi_H/n^2 kT},$$

$\chi_H$  being the ionization potential of hydrogen in the ground state and  $g_n$  the Gaunt factor for the  $n$ th quantum state. Defining the Planck mean by

$$a(H) = \int_0^\infty \kappa_\nu \frac{B_\nu}{B} d\nu,$$

where  $B_\nu = \frac{2hv^3}{c^2} \cdot \frac{I}{e^{hv/kT} - 1}$ ,  $B = \frac{\pi^4}{15} \cdot \frac{2k^4}{c^2 h^3} T^4$ ,

and letting  $u = hv/kT$ ,  $u_H = \chi_H/kT$ ,

we find  $a(H) = \frac{320}{\sqrt{3}} \cdot \frac{m_e e^{10}}{e^{u_H} c h^3 (kT)^3} \cdot \int_0^\infty D e^{-u} du$ . (1)

Introducing further the numerical values and the reciprocal temperature

$$\theta = \frac{5040}{T}$$

we obtain  $a(H) = 3.7429 \cdot 10^{-14} \theta^3 e^{-u_H} \int_0^\infty D e^{-u} du$ .

If  $D$  is constant in an interval, that is, if the Gaunt factors are put equal to 1, the contribution of this interval to the Planck mean can be found algebraically.

In the present investigations only the initial terms were summed in  $D$  and the remainder with  $n \geq 9$  were approximated by the corresponding integral, giving for all terms

$$D = \sum_{n=2}^8 \frac{g_n}{n^3} e^{u_H/n^2} + \frac{I}{2u_H} e^{u_H/81}.$$

The Gaunt factors computed by Menzel and Pekeris (7) were taken into account for  $n=2, 3, 4, 5$ . The Lyman continuum ( $n=1$ ) was omitted altogether, since it can be expected that the radiative flux in it is negligible. The contributions of the four next continua were evaluated numerically with the aid of Cotes' formulae, the corresponding intervals being divided according to need at five or more equidistant points; and those of further continua were found algebraically. In all, eight continua were computed and the effect of the rest was evaluated approximately by extrapolation. The contribution of the further continua to the Planck mean is generally higher than their contribution to the Rosseland mean.

The Planck mean  $a(H)$  was computed from  $\theta=0.18$  to  $\theta=0.72$  at intervals of 0.02 and from  $\theta=0.72$  to  $\theta=1.08$  at intervals of 0.04, and then interpolated for intermediate values of  $\theta$ . This interpolation was performed with the aid of the function  $\int D e^{-u} du$ , which varies only slowly in the whole interval of  $\theta$ . The results of the computations are given in Table I.

*2.2. Mean absorption coefficient for negative hydrogen ion.*—The absorption of the negative hydrogen ion is the main source of opacity in lower-temperature stars, especially in dwarfs. The numerical value of the coefficient  $\kappa_\nu$  of absorption of the negative hydrogen ion  $H^-$ , referred to one neutral hydrogen atom and unit electron pressure  $p_e$  (in  $\text{dyn cm}^{-2}$ ) and corrected for stimulated emission was tabulated by Chandrasekhar and Breen (2). Defining its mean again as

$$a(H^-) = \int_0^\infty \kappa_\nu \frac{B_\nu}{B} dv$$

and using equation (1) we find

$$a(H^-) = \frac{15}{\pi^4} \int_0^\infty \kappa_\nu \frac{u^3 e^{-u}}{1 - e^{-u}} du.$$

For the sake of convenience (easier interpolation for intermediate values) the computations were carried out with values of  $\kappa_\nu$  referred to one negative

hydrogen ion and then referred to one neutral hydrogen atom by multiplying by the factor

$$\phi(\theta) = 4.158 \times 10^{-10} \theta^{5.2} \cdot e^{1.726 \theta},$$

giving the number of negative ions present for one neutral atom. The numerical

TABLE I  
*Mean absorption coefficient of neutral hydrogen per atom*  
(The quantity tabulated is the common logarithm of  $a(H)$  in  $\text{cm}^2$ )

$\theta$	$\log_{10} a(H)$	$\theta$	$\log_{10} a(H)$	$\theta$	$\log_{10} a(H)$
0.18	19.334	0.49	22.319	0.80	26.712
0.19	.262	0.50	.208	0.81	.592
0.20	.186	0.51	.096	0.82	.471
0.21	.107	0.52	23.984	0.83	.351
0.22	.026	0.53	.871	0.84	.230
0.23	20.943	0.54	.758	0.85	.109
0.24	.857	0.55	.645	0.86	27.988
0.25	.769	0.56	.531	0.87	.866
0.26	.680	0.57	.417	0.88	.745
0.27	.589	0.58	.303	0.89	.623
0.28	.496	0.59	.188	0.90	.501
0.29	.402	0.60	.073	0.91	.379
0.30	.307	0.61	24.958	0.92	.257
0.31	.210	0.62	.842	0.93	.134
0.32	.113	0.63	.726	0.94	.012
0.33	.014	0.64	.609	0.95	28.889
0.34	21.914	0.65	.493	0.96	.766
0.35	.813	0.66	.376	0.97	.644
0.36	.711	0.67	.259	0.98	.521
0.37	.608	0.68	.141	0.99	.397
0.38	.504	0.69	.023	1.00	.274
0.39	.400	0.70	25.905	1.01	.151
0.40	.295	0.71	.787	1.02	.027
0.41	.189	0.72	.668	1.03	29.904
0.42	.082	0.73	.550	1.04	.780
0.43	22.975	0.74	.431	1.05	.656
0.44	.867	0.75	.312	1.06	.532
0.45	.758	0.76	.192	1.07	.408
0.46	.649	0.77	.072	1.08	.284
0.47	.540	0.78	26.953	1.09	.160
0.48	.430	0.79	.833	1.10	.035

evaluations between  $\lambda=912\text{\AA}$  and  $\lambda=22800\text{\AA}$  were made with the aid of Cotes' formulae, using the same points of division as for neutral hydrogen; five equidistant points were used between  $u=0$  ( $\lambda=\infty$ ) and the value of  $u$  corresponding to  $\lambda=22800\text{\AA}$ . Computations were made between  $\theta=0.50$  and  $\theta=0.72$  at intervals of 0.02 and for  $\theta>0.72$  at intervals of 0.04. The results are given in Table II.

3. *Construction of models.*—Models were computed for five dwarfs with  $\log_{10} g = 4.5$  and  $\theta_0 = 0.6, 0.7, 0.8, 0.9, 1.0$ , and for three giants with  $\log_{10} g = 3.5$  and  $\theta_0 = 0.6, 0.8, 1.0$ ,  $\theta_0$  being the reciprocal temperature of the stellar surface.

The tabulated results of the computations (Tables V to XII) give the values of  $\theta$ ,  $p$  and  $p_e$  for a certain number of suitably chosen values of the mean optical depth  $\tau$ .

Two models for  $\theta_0=0.6$  were computed in order to extend on a uniform basis the available data, though probably they do not correspond to real

TABLE II

*Mean absorption coefficient of negative hydrogen ion per neutral hydrogen atom and unit electron pressure, in  $10^{-26} \text{ cm}^4 \text{ dyn}^{-1}$*

$\theta$	$a(H^-)$	$\theta$	$a(H^-)$	$\theta$	$a(H^-)$
0.50	0.615	0.74	2.809	0.98	8.288
0.51	0.665	0.75	2.959	0.99	8.620
0.52	0.717	0.76	3.114	1.00	8.961
0.53	0.772	0.77	3.275	1.01	9.313
0.54	0.830	0.78	3.442	1.02	9.670
0.55	0.891	0.79	3.614	1.03	10.041
0.56	0.956	0.80	3.794	1.04	10.422
0.57	1.024	0.81	3.979	1.05	10.814
0.58	1.095	0.82	4.170	1.06	11.215
0.59	1.170	0.83	4.369	1.07	11.628
0.60	1.250	0.84	4.575	1.08	12.051
0.61	1.332	0.85	4.789	1.09	12.485
0.62	1.419	0.86	5.011	1.10	12.933
0.63	1.509	0.87	5.239	1.11	13.389
0.64	1.604	0.88	5.477	1.12	13.859
0.65	1.703	0.89	5.720	1.13	14.342
0.66	1.806	0.90	5.971	1.14	14.834
0.67	1.914	0.91	6.231	1.15	15.344
0.68	2.027	0.92	6.499	1.16	15.863
0.69	2.144	0.93	6.775	1.17	16.396
0.70	2.267	0.94	7.061	1.18	16.944
0.71	2.395	0.95	7.353	1.19	17.506
0.72	2.527	0.96	7.656	1.20	18.079
0.73	2.666	0.97	7.967		

stellar atmospheres, since at higher temperatures the electron scattering is not negligible. It is intended to include the effect of this source of opacity in further investigations.

3.1. *Radiative models.*—The computation of model stellar atmospheres in radiative equilibrium consists in the numerical integration of the equation

$$d\tau = \frac{I}{g} \bar{\kappa} dp, \quad (2)$$

where

$$\bar{\kappa} = \frac{I}{m_H} (1 - X_H) \{a(H) + a(H^-) p_e\} \quad (3)$$

is the absorption coefficient per unit stellar mass. The ionization degree  $X_H$  of hydrogen and the electron pressure  $p_e$  must be found in each step of integration from the value of  $\theta$  given by Milne's formula

$$\theta = \theta_0 (1 + \frac{3}{2}\tau)^{-1/4};$$

Milne's law of temperature distribution was used instead of Chandrasekhar's more recent "fourth approximation" (8) in order to have a common basis for comparison of our models with those of Strömgren, who also used Milne's formula. The values of  $X_H$  and  $p_e$  were computed with the aid of the formulae

$$\log_{10} s = -0.477 - 13.595 \theta + \frac{5}{2} \log_{10} T,$$

$$p_e = \frac{p}{2A} X_M - s + \left\{ \left( \frac{p}{2A} X_M - s \right)^2 + ps \left( 1 + \frac{X_M}{A} \right) \right\}^{1/2},$$

$$1 - X_H = p_e / (p_e + s),$$

the ionization degree of metals  $X_M$  being taken from the tables of Strömgren. No use was made of Strömgren's tables for  $X_H$  and  $p_e$  on account of the change of ionization potential from 13.53 to 13.595 volts.

The integration of equations (2) and (3) can be effected by choosing  $p$  as the independent variable and computing  $\tau$  from

$$\tau = \frac{1}{gm_H} \int_0^p (1 - X_H) \{a(H) + a(H^-)p_e\} dp, \quad (4)$$

where the integrand depends only on  $p$  and  $\theta$  (since  $p_e$ ,  $X_M$ ,  $a(H)$ ,  $a(H^-)$  are functions of  $p$  and  $\theta$ , or even  $\theta$  only). As  $\theta$  does not vary much for the first small values of  $\tau$  it is possible to assume  $\theta = \theta_0$ , to compute the values of the integrand for a number of equidistant values of  $p$  and then, using Cotes' integration formulae, to find  $\tau$ . When  $\theta$  begins to deviate from  $\theta_0$  its correct value at each step of the integration is found from Milne's equation, in which the extrapolated value of  $\tau$  is introduced, and then the corresponding value of the integrand in (4) is calculated. From this the integral  $\Delta\tau$ , and thus  $\tau$ , are found. Should the value of  $\tau$  found by the integration differ appreciably from the extrapolated one, the corresponding step of integration must be repeated; but by choosing the interval of integration reasonably small it is possible to extrapolate  $\tau$  correctly and thus avoid the repetition of computations.

The numerical integration of equation (4) was made with the aid of a Cotes formula extended over a number of steps including the new step and several previous steps. The integrated value of  $\tau$  added to its value at the beginning of the interval of integration gives the new value of  $\tau$  at the end of the interval. Generally each new value of  $\tau$  was found by using two different Cotes formulae applied to two different intervals of integration; the agreement between the values thus obtained is a check on the computations and indicates that the Cotes formulae used were sufficiently accurate. This method of integration seems to be more convenient than the use of other quadrature formulae, in which it is sometimes difficult to include the differences of higher orders. Moreover the use of a Cotes formula reduces the effect of summation of errors, which enters the other quadrature formulae more seriously.

The interval of integration, which was chosen small for the initial steps of integration, was increased for moderate values of  $\tau$ , at which it was possible to extrapolate with more confidence. Since, however, the increase of temperature with the increase of optical depth affects seriously the integrand in equation (4), it was finally necessary at larger values of  $\tau$  to reduce the interval of integration again, usually by halving it when necessary.

The method of integration described above gives the optical depth  $\tau$  as a function of total pressure  $p$ . For the sake of convenience the final tables of model stellar atmospheres are arranged so as to give  $\theta$ ,  $\log_{10} p$  and  $\log_{10} p_e$  as functions of  $\tau$ .

*3.2. Adiabatic models.*—The stellar atmosphere computed under the assumption that the temperature is controlled by radiative equilibrium becomes unstable at a certain depth  $\tau_e$ , at which the radiative temperature gradient

$$\left( \frac{d \log_{10} T}{d \log_{10} p} \right)_{\text{rad}} = \frac{3}{8} \cdot \frac{1}{g} p \bar{\kappa} \left( 1 + \frac{3}{2} \tau \right)^{-1} \quad (5)$$

becomes greater than the adiabatic gradient, defined with sufficient accuracy by Unsöld's formula

$$\left( \frac{d \log_{10} T}{d \log_{10} p} \right)_{\text{adiab}} = \frac{1 + X_H + \frac{1}{A} X_M + \frac{X_H(1 - X_H)}{X_H + (1/A)X_M} + X_H(1 - X_H) \left( \frac{5}{2} + \frac{X_H}{kT} \right)}{\frac{5}{2} \left\{ 1 + X_H + \frac{1}{A} X_M + \frac{X_H(1 - X_H)}{X_H + (1/A)X_M} \right\} + X_H(1 - X_H) \left( \frac{5}{2} + \frac{X_H}{kT} \right)^2}. \quad (6)$$

By computing both values of the gradient for several depths in the radiative model one easily finds the level  $p_e$  at which both gradients become equal. The stellar atmosphere below this level is convectively unstable and its real temperature gradient lies between the limiting values (5) and (6). Since the radiative value (5) is valid for the radiative model, in order to find the possible maximum effect of convection on the structure of stellar atmospheres, an additional "adiabatic" model was computed for every radiative one, assuming that the temperature gradient in the unstable zone is adiabatic, i.e. defined by equation (6). The computation of these adiabatic models consists in numerical integration of equation (6),  $\log_{10} p$  being the independent variable.

The process of integration was similar to that for radiative models, the intervals for  $\log_{10} p$  being chosen, according to circumstances, between 0.01 (for  $\theta_0 = 1.0$ ) and 0.10 (for  $\theta_0 = 0.6$ ). The optical depth in these models was computed additionally with the aid of the formula

$$\tau(\log_{10} p) = \tau_e + \frac{1}{gm_H \log_{10} e} \int_{\log_{10} p_e}^{\log_{10} p} (1 - X_H) \{a(H) + a(H')p_e\} p d \log_{10} p, \quad (7)$$

which can be derived from equations (2) and (3) and in which  $\tau_e$  and  $p_e$  signify the optical depth and the total pressure at the top of the convectively unstable zone. The use of equation (7) instead of equation (4) for the adiabatic models is due to the fact that the computations of adiabatic models give the values of  $T$  (or  $\theta$ ),  $p_e$  and  $X_H$  as functions of  $\log_{10} p$ , thus making the formula (7) more suitable in practice.

*4. Monochromatic fluxes.*—As a preparatory step for the evaluation of monochromatic fluxes\*  $F_\nu$ , necessary for computing colour gradients, the monochromatic depths  $\tau_\nu$  were found as functions of total pressure  $p$  for two wave-lengths,  $\lambda = 4235 \text{ \AA}$  and  $\lambda = 6252 \text{ \AA}$ . These particular wave-lengths were chosen because they are division points of the numerical integration for  $a(H)$  and  $a(H')$  in the visible part of the spectrum, and therefore their monochromatic coefficients of

\* The symbol  $F_\nu$  for monochromatic flux is as used by Woolley and Stibbs in *The Outer Layers of a Star* (Oxford, 1953). In his book *Radiative Transfer* (Oxford, 1950) Chandrasekhar uses  $\pi F_\nu$  for this quantity, and does not use the symbol  $F_\nu$ , which is employed by Woolley and Stibbs where Chandrasekhar uses  $F_\nu$ .

absorption  $\kappa_v(H)$  and  $\kappa_v(H^-)$  were immediately available without extensive computations. The monochromatic depths for the radiative models were found by integrating the equation (4) rewritten in the form

$$\tau_v = \frac{I}{gm_H} \int_0^P (1 - X_H) \{\kappa_v(H) + \kappa_v(H^-) p_e\} dp,$$

and those for adiabatic models with the aid of formula (7) rewritten as

$$\tau_v(\log_{10} p) = \tau_c(v) + \frac{I}{gm_H \log_{10} e} \int_{\log_{10} p_c}^{\log_{10} P} (1 - X_H) \{\kappa_v(H) + \kappa_v(H^-) p_e\} p d \log_{10} p,$$

in which  $\tau_c(v)$  and  $p_e$  signify the monochromatic depth and the total pressure at the top of the convectively unstable zone.

The monochromatic fluxes  $F(v)$  were found by numerical evaluation of the integral

$$F(v) = 2\pi \int_0^{8.4} B_\nu E_2(\tau_v) d\tau_v$$

with the aid of a Cotes eight-point formula applied to the intervals from  $\tau_v=0$  to  $\tau_v=2.8$  and from  $\tau_v=2.8$  to  $\tau_v=8.4$ . The contribution of deeper layers to the monochromatic fluxes was omitted since it is negligible. Special tables of  $B_\nu$  were constructed for both wave-lengths in question.

5. Colour gradients.—The colour gradient is defined by the equation

$$\phi = - \frac{d}{d(\lambda/\lambda)} \{\ln \lambda^5 F_\lambda\}.$$

From that equation we find as an approximation over a finite interval  $\lambda_1 < \lambda < \lambda_2$ :

$$\phi = - \frac{\ln(\lambda_2^5 F(\lambda_2)) - \ln(\lambda_1^5 F(\lambda_1))}{1/\lambda_2 - 1/\lambda_1}$$

or, introducing  $F_\lambda = (c/\lambda^2) F_\nu$ ,

$$\phi = - \frac{3 \ln(\lambda_2/\lambda_1) + \ln(F(\nu_2)/F(\nu_1))}{1/\lambda_2 - 1/\lambda_1}.$$

Introducing further the numerical values  $\lambda_1 = 4235 \text{ \AA}$  and  $\lambda_2 = 6252 \text{ \AA}$  used in computation of monochromatic fluxes we find

$$\phi = 3.0231(0.5074 + \log_{10} F(\nu_2)/F(\nu_1)).$$

6. Results.—The model stellar atmospheres are given in Tables V–XII. The upper part of each table gives the reciprocal temperature  $\theta$ , the total pressure  $p$  and the electron pressure  $p_e$  as functions of the optical depth  $\tau$  above the top of the convectively unstable zone; the last entries in this part give the critical values  $\tau_c$ ,  $\theta_c$ ,  $\log_{10} p_c$  and  $\log_{10} p_{e,c}$ . The lower part gives, side by side, the structures of the radiative model and of the adiabatic model. The actual computations of models were made to one or two places more than are given in the tables.

The monochromatic fluxes for  $\lambda = 4235 \text{ \AA}$  and  $\lambda = 6252 \text{ \AA}$  are given in Table III.

The colour gradients of the computed models are listed in Table IV.

For adiabatic models the increase of gradient with the reciprocal temperature is quite uniform; they show also only slight differences in colour gradient between dwarfs and giants.

These regularities do not exist for radiative models. The change of gradient with the reciprocal temperature is less regular than in the adiabatic series of

models, though the interpolation of gradients for intermediate values of  $\theta_0$ , which will be necessary for further investigations, is quite possible. The giants have lower gradients than the dwarfs, with the exception of the models with  $\theta_0 = 0.6$ , when the dwarfs and the giants have the same gradient, corresponding to an atmosphere in which neutral hydrogen is practically the only source of opacity.

The differences in colour gradients between the corresponding radiative and adiabatic models are easily accessible to observation, especially in hotter stars, in which the unstable zone begins at low optical depths; in giants, for

TABLE III  
*Monochromatic fluxes  $F_\nu$  in units of  $10^{-5} \text{ erg cm}^{-2} \text{ sec}^{-1}$*

$\theta_0$	$\log_{10} g$	Radiative model		Adiabatic model	
		$\lambda = 4235 \text{ \AA}$	$\lambda = 6252 \text{ \AA}$	$\lambda = 4235 \text{ \AA}$	$\lambda = 6252 \text{ \AA}$
0.6	3.5	97.62	60.98	50.00	47.42
0.6	4.5	96.56	60.32	49.69	47.50
0.7	4.5	55.75	42.01	28.98	32.26
0.8	3.5	31.02	25.98	16.64	21.63
0.8	4.5	26.42	24.75	16.99	21.61
0.9	4.5	13.37	16.00	10.11	14.73
1.0	3.5	7.75	10.70	5.94	9.97
1.0	4.5	7.44	10.63	6.22	10.16

TABLE IV  
*Colour gradients*

Dwarfs ( $\log_{10} g = 4.5$ )				Giants ( $\log_{10} g = 3.5$ )			
$\theta_0$	Radiative model	Adiabatic model	Difference	$\theta_0$	Radiative model	Adiabatic model	Difference
1.0	2.00	2.18	0.18	1.0	1.96	2.21	0.25
0.9	1.77	2.03	0.26				
0.8	1.44	1.85	0.41	0.8	1.30	1.88	0.58
0.7	1.10	1.67	0.57				
0.6	0.92	1.48	0.56	0.6	0.92	1.46	0.54

the same reason, these differences are higher than in dwarfs, with the exception of the hottest stars, in which they seem to reach an asymptotic value (about 0.56) corresponding to an atmosphere in which the contribution of negative hydrogen absorption to the opacity is negligible.

The calculations shown here would go some way towards deciding the amount of convection in actual stars, by referring to measures of their colour gradients, if the connection between  $\theta_0$  and spectral type were well established. Unfortunately this connection is not well enough known at present to enable us to make a decisive comparison with the observations. It is therefore proposed to calculate

the strength of the calcium lines in the present models, in order to provide a criterion of spectral type. It is intended to construct in this way a diagram connecting two observable quantities, spectral type and colour gradient, for the two cases maximum convection and zero convection. Comparison with observation will then, it is hoped, give a good indication of the amounts of convection present in actual stars.

7. *Comparison with the models of Strömgren.*—Comparison of our radiative models with Strömgren's work (1) shows that both kinds of models have a similar structure. The increase of total pressure and electron pressure with optical depth in Strömgren's models is however steeper, since his values of the mean absorption coefficient are lower; for models with  $\theta_0$  between 0·8 and 1·0 the values of  $p$  and  $p_e$  are higher by a factor of roughly 1·3 than in our models, this factor being almost constant throughout the whole atmosphere; for  $\theta_0 = 0\cdot7$  this factor is higher and its constancy is less striking. Another feature in common between Strömgren's models and ours, resulting from their similar structure, is that the unstable zones begin at almost exactly the same optical depth in both kinds of model; the differences in  $\tau_c$  between our models and Strömgren's do not exceed 0·03. Further, in our giants as well as in Strömgren's the top of the convective zone lies at lower optical depth than in dwarfs.

8. *Acknowledgment.*—The present investigations are due to the initiative and were made under the supervision of Professor R. v. d. R. Woolley, to whom the author is grateful for many valuable discussions and much advice.

*Commonwealth Observatory,  
Mount Stromlo,  
Canberra, A.C.T.,  
Australia :  
1953 June 15.*

#### References

- (1) B. Strömgren, K. Gyldenkaerne, M. Rudkjøbing and K. A. Thernoe, *Publ. Medd. Københavns Obs.*, Nr. 138, 1944.
- (2) S. Chandrasekhar and F. H. Breen, *Ap. J.*, **104**, 430, 1946.
- (3) Jesse W. H. Du Mond and E. Richard Cohen, *Rev. Mod. Physics*, **20**, 82, 1948.
- (4) Charlotte E. Moore, *Atomic Energy Levels*, *Circ. Nat. Bur. Stand.*, 467, 1949.
- (5) Raymond Michard, *Ann. d'Ap.*, **12**, 291, 1949.
- (6) E. Vitense, *Zs. f. Astrophysik*, **28**, 81, 1951.
- (7) Donald H. Menzel and Chaim L. Pekeris, *M.N.*, **96**, 77, 1936.
- (8) S. Chandrasekhar, *Ap. J.*, **100**, 76, 1944.

TABLE V  
Model stellar atmosphere:  $\theta_0 = 0.6$ ,  $\log_{10} g = 3.5$

$\tau$	$\theta$	$\log_{10} p$	$\log_{10} p_e$
0.00	0.600		
0.01	0.598	1.32	0.92
0.02	0.596	1.50	1.07
0.03	0.593	1.61	1.17
0.04	0.591	1.69	1.24
0.05	0.589	1.75	1.29
0.06	0.587	1.80	1.34
0.07	0.585	1.84	1.38
0.08	0.583	1.88	1.41
0.09	0.581	1.91	1.44
0.10	0.579	1.94	1.47
0.12	0.576	1.99	1.52
0.122	0.575	1.99	1.52

$\tau$	Radiative model			Adiabatic model		
	$\theta$	$\log_{10} p$	$\log_{10} p_e$	$\theta$	$\log_{10} p$	$\log_{10} p_e$
0.14	0.572	2.03	1.56	0.572	2.02	1.56
0.16	0.569	2.06	1.60	0.569	2.06	1.60
0.18	0.565	2.09	1.64	0.567	2.09	1.63
0.20	0.562	2.11	1.67	0.565	2.12	1.66
0.25	0.554	2.17	1.74	0.560	2.17	1.72
0.30	0.547	2.21	1.79	0.556	2.22	1.77
0.35	0.540	2.25	1.84	0.553	2.25	1.81
0.40	0.533	2.27	1.88	0.550	2.28	1.84
0.45	0.527	2.30	1.92	0.547	2.31	1.87
0.50	0.522	2.32	1.95	0.545	2.34	1.90
0.60	0.511	2.36	2.01	0.541	2.38	1.95
0.70	0.501	2.40	2.05	0.538	2.42	1.99
0.80	0.493	2.43	2.09	0.535	2.45	2.02
0.90	0.485	2.46	2.13	0.533	2.48	2.05
1.0	0.477	2.48	2.16	0.531	2.51	2.08
1.2	0.464	2.53	2.21	0.527	2.55	2.13
1.4	0.452	2.57	2.26	0.524	2.59	2.17
1.6	0.442	2.61	2.30	0.521	2.62	2.20
1.8	0.433	2.65	2.34	0.518	2.65	2.23
2.0	0.424	2.68	2.38	0.516	2.67	2.26
2.5	0.406	2.76	2.46	0.512	2.73	2.32
3.0	0.392	2.83	2.52	0.508	2.77	2.36
3.5	0.379	2.89	2.58	0.504	2.81	2.40
4.0	0.369	2.94	2.64	0.502	2.84	2.44
4.5	0.360	2.99	2.69	0.499	2.87	2.47
5.0	0.351	3.04	2.73	0.497	2.90	2.50
6.0	0.337	3.11	2.81	0.493	2.94	2.54
7.0	0.326	3.18	2.88	0.489	2.98	2.58
8.0	0.316	3.24	2.94	0.486	3.01	2.62
9.0	0.307	3.30	3.00	0.484	3.04	2.65
10.0	0.300	3.35	3.05	0.482	3.07	2.68

TABLE VI  
Model stellar atmosphere:  $\theta_0 = 0.6$ ,  $\log_{10} g = 4.5$

$\tau$	$\theta$	$\log_{10} p$	$\log_{10} p_e$
0.00	0.600		
0.01	0.598	1.98	1.42
0.02	0.596	2.21	1.59
0.03	0.593	2.34	1.68
0.04	0.591	2.43	1.75
0.05	0.589	2.49	1.80
0.06	0.587	2.55	1.85
0.07	0.585	2.59	1.89
0.08	0.583	2.63	1.93
0.09	0.581	2.67	1.96
0.10	0.579	2.70	2.00
0.12	0.576	2.76	2.05
0.137	0.573	2.79	2.09

$\tau$	Radiative model			Adiabatic model		
	$\theta$	$\log_{10} p$	$\log_{10} p_e$	$\theta$	$\log_{10} p$	$\log_{10} p_e$
0.14	0.572	2.80	2.10	0.572	2.80	2.09
0.16	0.569	2.83	2.14	0.569	2.82	2.13
0.18	0.565	2.86	2.18	0.566	2.86	2.17
0.20	0.562	2.89	2.21	0.564	2.89	2.20
0.25	0.554	2.94	2.28	0.559	2.94	2.26
0.30	0.547	2.98	2.35	0.555	2.99	2.31
0.35	0.540	3.01	2.41	0.551	3.02	2.35
0.40	0.533	3.03	2.46	0.549	3.05	2.39
0.45	0.527	3.05	2.50	0.546	3.08	2.42
0.50	0.522	3.07	2.54	0.544	3.11	2.45
0.60	0.511	3.11	2.61	0.540	3.15	2.50
0.70	0.501	3.13	2.67	0.537	3.18	2.54
0.80	0.493	3.15	2.71	0.534	3.21	2.57
0.90	0.485	3.17	2.75	0.532	3.24	2.60
1.0	0.477	3.19	2.79	0.530	3.27	2.63
1.2	0.464	3.21	2.85	0.526	3.31	2.68
1.4	0.452	3.24	2.89	0.523	3.34	2.72
1.6	0.442	3.26	2.93	0.520	3.37	2.75
1.8	0.433	3.29	2.96	0.518	3.40	2.78
2.0	0.424	3.31	2.98	0.515	3.42	2.81
2.5	0.406	3.36	3.04	0.511	3.47	2.87
3.0	0.392	3.41	3.10	0.507	3.52	2.92
3.5	0.379	3.45	3.14	0.504	3.55	2.96
4.0	0.369	3.49	3.19	0.501	3.58	2.99
4.5	0.360	3.53	3.23	0.499	3.61	3.02
5.0	0.351	3.57	3.27	0.497	3.63	3.05
6.0	0.337	3.64	3.34	0.493	3.67	3.09
7.0	0.326	3.70	3.40	0.490	3.71	3.13
8.0	0.316	3.76	3.46	0.488	3.74	3.17
9.0	0.307	3.81	3.51	0.485	3.77	3.20
10.0	0.300	3.86	3.56	0.483	3.79	3.23

TABLE VII  
Model stellar atmosphere:  $\theta_0 = 0.7$ ,  $\log_{10} g = 4.5$

$\tau$	$\theta$	$\log_{10} p$	$\log_{10} p_e$
0.00	0.700		
0.01	0.697	2.74	1.16
0.02	0.695	2.99	1.34
0.03	0.692	3.12	1.43
0.04	0.690	3.22	1.50
0.05	0.688	3.29	1.56
0.06	0.685	3.34	1.61
0.07	0.683	3.39	1.65
0.08	0.680	3.43	1.68
0.09	0.678	3.47	1.72
0.10	0.676	3.50	1.75
0.12	0.672	3.55	1.81
0.14	0.667	3.59	1.86
0.16	0.663	3.62	1.91
0.18	0.659	3.65	1.95
0.20	0.656	3.67	1.99
0.25	0.646	3.72	2.08
0.256	0.646	3.73	2.09

$\tau$	Radiative model			Adiabatic model		
	$\theta$	$\log_{10} p$	$\log_{10} p_e$	$\theta$	$\log_{10} p$	$\log_{10} p_e$
0.30	0.638	3.76	2.17	0.639	3.76	2.16
0.35	0.630	3.78	2.24	0.633	3.79	2.22
0.40	0.622	3.81	2.31	0.628	3.81	2.27
0.45	0.615	3.82	2.37	0.624	3.83	2.31
0.50	0.609	3.84	2.43	0.620	3.85	2.34
0.60	0.596	3.86	2.53	0.615	3.88	2.40
0.70	0.585	3.88	2.62	0.610	3.90	2.45
0.80	0.575	3.89	2.70	0.606	3.93	2.49
0.90	0.565	3.90	2.77	0.603	3.94	2.52
1.0	0.557	3.91	2.84	0.600	3.96	2.55
1.2	0.541	3.92	2.96	0.595	3.99	2.61
1.4	0.528	3.93	3.05	0.591	4.02	2.65
1.6	0.516	3.94	3.14	0.587	4.04	2.69
1.8	0.505	3.94	3.20	0.584	4.06	2.72
2.0	0.495	3.94	3.25	0.582	4.07	2.75
2.5	0.474	3.95	3.35	0.576	4.11	2.81
3.0	0.457	3.96	3.44	0.571	4.14	2.86
3.5	0.443	3.96	3.51	0.568	4.16	2.90
4.0	0.430	3.97	3.56	0.564	4.19	2.93
4.5	0.420	3.97	3.60	0.562	4.20	2.96
5.0	0.410	3.97	3.62	0.559	4.22	2.99
6.0	0.394	3.98	3.65	0.555	4.25	3.04
7.0	0.380	3.99	3.67	0.551	4.28	3.08
8.0	0.369	4.00	3.68	0.548	4.30	3.11
9.0	0.359	4.01	3.70	0.545	4.32	3.14
10.0	0.350	4.02	3.71	0.543	4.34	3.17

TABLE VIII  
Model stellar atmosphere:  $\theta_0 = 0.8$ ,  $\log_{10} g = 3.5$

$\tau$	$\theta$	$\log_{10} p$	$\log_{10} p_e$
0.00	0.800		
0.01	0.797	2.66	0.43
0.02	0.794	2.88	0.56
0.03	0.791	3.01	0.65
0.04	0.788	3.09	0.71
0.05	0.786	3.16	0.76
0.06	0.783	3.21	0.81
0.07	0.780	3.25	0.85
0.08	0.778	3.29	0.89
0.09	0.775	3.32	0.92
0.10	0.773	3.34	0.96
0.12	0.768	3.39	1.02
0.14	0.763	3.43	1.07
0.16	0.758	3.46	1.12
0.18	0.754	3.48	1.17
0.20	0.749	3.51	1.21
0.25	0.739	3.55	1.31
0.30	0.729	3.58	1.40
0.346	0.721	3.61	1.48

$\tau$	Radiative model			Adiabatic model		
	$\theta$	$\log_{10} p$	$\log_{10} p_e$	$\theta$	$\log_{10} p$	$\log_{10} p_e$
0.35	0.720	3.61	1.48	0.720	3.61	1.48
0.40	0.711	3.63	1.55	0.712	3.63	1.55
0.45	0.703	3.65	1.62	0.706	3.65	1.60
0.50	0.696	3.66	1.69	0.701	3.66	1.65
0.60	0.681	3.68	1.80	0.693	3.69	1.72
0.70	0.669	3.70	1.91	0.686	3.71	1.78
0.80	0.657	3.71	2.00	0.681	3.73	1.83
0.90	0.646	3.72	2.09	0.677	3.74	1.87
1.0	0.636	3.73	2.16	0.673	3.75	1.90
1.2	0.618	3.74	2.30	0.667	3.78	1.96
1.4	0.603	3.74	2.42	0.661	3.80	2.01
1.6	0.589	3.75	2.52	0.657	3.81	2.05
1.8	0.577	3.75	2.61	0.653	3.83	2.09
2.0	0.566	3.76	2.69	0.650	3.84	2.12
2.5	0.542	3.76	2.86	0.643	3.87	2.18
3.0	0.522	3.77	2.99	0.638	3.89	2.24
3.5	0.506	3.77	3.09	0.633	3.91	2.28
4.0	0.492	3.77	3.17	0.629	3.93	2.32
4.5	0.479	3.77	3.23	0.626	3.95	2.35
5.0	0.469	3.77	3.28	0.623	3.96	2.38
6.0	0.450	3.77	3.35	0.618	3.98	2.43
7.0	0.434	3.77	3.39	0.614	4.00	2.47
8.0	0.421	3.78	3.42	0.610	4.02	2.51
9.0	0.410	3.78	3.44	0.607	4.04	2.54
10.0	0.400	3.78	3.45	0.605	4.05	2.57

TABLE IX  
Model stellar atmosphere:  $\theta_0 = 0.8$ ,  $\log_{10} g = 4.5$

$\tau$	$\theta$	$\log_{10} p$	$\log_{10} p_e$
0.00	0.800		
0.01	0.797	3.41	0.82
0.02	0.794	3.62	0.94
0.03	0.791	3.73	1.02
0.04	0.788	3.81	1.08
0.05	0.786	3.87	1.14
0.06	0.783	3.92	1.18
0.07	0.780	3.97	1.22
0.08	0.778	4.00	1.26
0.09	0.775	4.03	1.29
0.10	0.773	4.06	1.33
0.12	0.768	4.10	1.38
0.14	0.763	4.14	1.44
0.16	0.758	4.17	1.49
0.18	0.754	4.19	1.53
0.20	0.749	4.22	1.58
0.25	0.739	4.26	1.68
0.30	0.729	4.30	1.77
0.35	0.720	4.32	1.85
0.40	0.711	4.35	1.92
0.439	0.705	4.36	1.98

$\tau$	Radiative model			Adiabatic model		
	$\theta$	$\log_{10} p$	$\log_{10} p_e$	$\theta$	$\log_{10} p$	$\log_{10} p_e$
0.45	0.703	4.36	1.99	0.703	4.36	1.99
0.50	0.696	4.38	2.05	0.696	4.38	2.05
0.60	0.681	4.40	2.17	0.686	4.41	2.14
0.70	0.669	4.42	2.28	0.677	4.43	2.21
0.80	0.657	4.44	2.37	0.671	4.44	2.27
0.90	0.646	4.45	2.46	0.665	4.46	2.32
1.0	0.636	4.46	2.54	0.660	4.47	2.36
1.2	0.618	4.47	2.68	0.653	4.49	2.43
1.4	0.603	4.48	2.80	0.646	4.51	2.49
1.6	0.589	4.49	2.91	0.641	4.53	2.53
1.8	0.577	4.49	3.00	0.637	4.54	2.57
2.0	0.566	4.50	3.09	0.633	4.55	2.61
2.5	0.542	4.50	3.26	0.625	4.58	2.68
3.0	0.522	4.51	3.41	0.619	4.60	2.74
3.5	0.506	4.51	3.53	0.614	4.62	2.79
4.0	0.492	4.51	3.62	0.610	4.63	2.83
4.5	0.479	4.52	3.71	0.606	4.65	2.86
5.0	0.469	4.52	3.78	0.602	4.66	2.90
6.0	0.450	4.52	3.89	0.597	4.68	2.95
7.0	0.434	4.52	3.97	0.592	4.70	2.99
8.0	0.421	4.52	4.03	0.588	4.72	3.03
9.0	0.410	4.52	4.08	0.585	4.73	3.07
10.0	0.400	4.52	4.11	0.582	4.75	3.10

TABLE X  
Model stellar atmosphere:  $\theta_0 = 0.9$ ,  $\log_{10} g = 4.5$

$\tau$	$\theta$	$\log_{10} p$	$\log_{10} p_e$
0.00	0.900		
0.01	0.897	3.79	0.36
0.02	0.893	3.97	0.50
0.03	0.890	4.08	0.58
0.04	0.887	4.15	0.65
0.05	0.884	4.21	0.70
0.06	0.881	4.25	0.75
0.07	0.878	4.29	0.79
0.08	0.875	4.32	0.82
0.09	0.872	4.35	0.85
0.10	0.869	4.38	0.89
0.12	0.864	4.42	0.94
0.14	0.858	4.45	0.99
0.16	0.853	4.48	1.04
0.18	0.848	4.51	1.09
0.20	0.843	4.53	1.13
0.25	0.831	4.58	1.23
0.30	0.820	4.61	1.31
0.35	0.810	4.64	1.39
0.40	0.800	4.67	1.46
0.45	0.791	4.69	1.53
0.50	0.782	4.70	1.60
0.589	0.768	4.73	1.71

$\tau$	Radiative model			Adiabatic model		
	$\theta$	$\log_{10} p$	$\log_{10} p_e$	$\theta$	$\log_{10} p$	$\log_{10} p_e$
0.60	0.767	4.73	1.73	0.767	4.73	1.73
0.70	0.752	4.75	1.84	0.754	4.75	1.83
0.80	0.739	4.77	1.94	0.743	4.77	1.91
0.90	0.727	4.78	2.03	0.735	4.78	1.97
1.0	0.716	4.79	2.12	0.728	4.79	2.03
1.2	0.696	4.81	2.27	0.717	4.81	2.12
1.4	0.678	4.82	2.41	0.708	4.83	2.20
1.6	0.663	4.83	2.53	0.700	4.85	2.26
1.8	0.649	4.84	2.63	0.694	4.86	2.31
2.0	0.636	4.84	2.73	0.688	4.87	2.36
2.5	0.610	4.85	2.94	0.677	4.89	2.45
3.0	0.588	4.86	3.11	0.669	4.91	2.53
3.5	0.569	4.86	3.25	0.662	4.93	2.59
4.0	0.553	4.87	3.37	0.656	4.94	2.64
4.5	0.539	4.87	3.47	0.651	4.95	2.68
5.0	0.527	4.87	3.57	0.646	4.96	2.72
6.0	0.506	4.87	3.72	0.639	4.98	2.78
7.0	0.489	4.87	3.85	0.633	5.00	2.84
8.0	0.474	4.88	3.95	0.628	5.01	2.88
9.0	0.461	4.88	4.03	0.623	5.03	2.92
10.0	0.450	4.88	4.10	0.619	5.04	2.96

TABLE XI  
Model stellar atmosphere :  $\theta_0 = 1.0$ ,  $\log_{10} g = 3.5$

$\tau$	$\theta$	$\log_{10} p$	$\log_{10} p_e$
0.00	1.000		
0.01	0.996	3.37	1.66
0.02	0.993	3.54	1.80
0.03	0.989	3.64	1.88
0.04	0.986	3.70	1.95
0.05	0.982	3.76	0.01
0.06	0.979	3.80	0.05
0.07	0.975	3.84	0.09
0.08	0.972	3.87	0.12
0.09	0.969	3.90	0.15
0.10	0.966	3.92	0.18
0.12	0.959	3.96	0.23
0.14	0.953	4.00	0.27
0.16	0.948	4.03	0.31
0.18	0.942	4.05	0.35
0.20	0.937	4.08	0.39
0.25	0.923	4.13	0.47
0.30	0.911	4.17	0.55
0.35	0.900	4.20	0.62
0.40	0.889	4.22	0.69
0.45	0.879	4.25	0.75
0.50	0.869	4.27	0.81
0.60	0.852	4.30	0.93
0.70	0.836	4.32	1.04
0.702	0.835	4.32	1.05

$\tau$	Radiative model			Adiabatic model		
	$\theta$	$\log_{10} p$	$\log_{10} p_e$	$\theta$	$\log_{10} p$	$\log_{10} p_e$
0.80	0.821	4.34	1.14	0.822	4.34	1.14
0.90	0.808	4.36	1.24	0.811	4.36	1.22
1.0	0.795	4.37	1.33	0.802	4.37	1.29
1.2	0.773	4.39	1.50	0.788	4.39	1.40
1.4	0.754	4.40	1.64	0.777	4.41	1.48
1.6	0.736	4.41	1.77	0.768	4.42	1.55
1.8	0.721	4.42	1.89	0.760	4.44	1.61
2.0	0.707	4.43	2.00	0.754	4.45	1.67
2.5	0.677	4.44	2.22	0.741	4.47	1.77
3.0	0.653	4.45	2.40	0.731	4.49	1.85
3.5	0.632	4.45	2.56	0.722	4.50	1.92
4.0	0.615	4.45	2.70	0.716	4.52	1.98
4.5	0.599	4.46	2.81	0.710	4.53	2.02
5.0	0.586	4.46	2.92	0.705	4.54	2.07
6.0	0.562	4.46	3.09	0.696	4.56	2.14
7.0	0.543	4.46	3.24	0.690	4.57	2.20
8.0	0.527	4.46	3.35	0.684	4.59	2.25
9.0	0.512	4.46	3.45	0.679	4.60	2.29
10.0	0.500	4.46	3.54	0.674	4.61	2.33

TABLE XII  
Model stellar atmosphere :  $\theta_0 = 1.0$ ,  $\log_{10} g = 4.5$

$\tau$	$\theta$	$\log_{10} p$	$\log_{10} p_e$
0.00	1.000		
0.01	0.996	3.92	0.12
0.02	0.993	4.08	0.27
0.03	0.989	4.18	0.35
0.04	0.986	4.25	0.42
0.05	0.982	4.30	0.47
0.06	0.979	4.34	0.51
0.07	0.975	4.38	0.55
0.08	0.972	4.41	0.58
0.09	0.969	4.44	0.61
0.10	0.966	4.46	0.64
0.12	0.959	4.50	0.68
0.14	0.953	4.54	0.72
0.16	0.948	4.57	0.76
0.18	0.942	4.60	0.80
0.20	0.937	4.62	0.83
0.25	0.923	4.67	0.90
0.30	0.911	4.72	0.97
0.35	0.900	4.75	1.03
0.40	0.889	4.78	1.08
0.45	0.879	4.81	1.14
0.50	0.869	4.83	1.19
0.60	0.852	4.86	1.30
0.70	0.836	4.89	1.39
0.80	0.821	4.92	1.49
0.877	0.811	4.93	1.56

$\tau$	Radiative model			Adiabatic model		
	$\theta$	$\log_{10} p$	$\log_{10} p_e$	$\theta$	$\log_{10} p$	$\log_{10} p_e$
0.9	0.808	4.94	1.58	0.808	4.94	1.58
1.0	0.795	4.95	1.66	0.797	4.95	1.65
1.2	0.773	4.98	1.82	0.779	4.98	1.78
1.4	0.754	5.00	1.96	0.766	5.00	1.88
1.6	0.736	5.01	2.08	0.755	5.02	1.96
1.8	0.721	5.02	2.20	0.746	5.03	2.02
2.0	0.707	5.03	2.30	0.739	5.04	2.08
2.5	0.677	5.05	2.53	0.724	5.07	2.20
3.0	0.653	5.06	2.72	0.713	5.09	2.29
3.5	0.632	5.06	2.87	0.704	5.10	2.37
4.0	0.615	5.07	3.01	0.696	5.12	2.43
4.5	0.599	5.07	3.13	0.690	5.13	2.48
5.0	0.586	5.08	3.24	0.685	5.14	2.53
6.0	0.562	5.08	3.44	0.675	5.16	2.60
7.0	0.543	5.08	3.56	0.668	5.17	2.67
8.0	0.527	5.08	3.68	0.661	5.19	2.72
9.0	0.512	5.09	3.79	0.656	5.20	2.77
10.0	0.500	5.09	3.88	0.651	5.21	2.81

# THE STRUCTURE OF ROTATING STARS. I

P. A. Sweet and A. E. Roy

(Communicated by the Director, University Observatory, Glasgow)

(Received 1953 July 6)

## Summary

A successive perturbation theory is established for the structure of stars in uniform rotation with a known law of energy generation. The first-order structure is computed for a rotating Cowling model with a law of energy generation  $\epsilon \propto \rho T^{17}$ .

The results from a first-order model indicate that with the distribution of rotation velocities observed, rotation can produce a spread in luminosity of order half a magnitude in a mass-luminosity diagram, and of order half a magnitude for a given spectral type in a colour-magnitude array, this figure being for the most rapidly rotating Be stars.

**1. Introduction.**—The effect of rotation on a star of given mass is not known completely, even to the first order in the ratio of centrifugal force to gravity. The rotating polytropes of Chandrasekhar (1) give some idea of the redistribution of the mass of the star, together with the distortion of the equipotential surfaces; the work of Slettebak (2) on O, B and Be stars includes a discussion of the relative variation of effective temperature over the surface using von Zeipel's theorem, while recently (5) he has investigated the dependence of axial rotation on spectral type and luminosity among early-type stars and found a difference in axial rotation between the main-sequence stars and the giants and sub-giants. The distribution of observed values of  $v \sin i$  for these two groups appears to be quite different, the more luminous stars having generally smaller rotational velocities. G. R. and E. M. Burbidge (12) have constructed models of rotating Be stars with surrounding electron-scattering atmospheres; Öpik (3) and Sweet (4) have considered the circulation currents which would be produced by rotation in a star of uniform composition.

One effect outstanding at present is the change in luminosity and mean effective temperature of a star of given mass due to its rotation. For this purpose a knowledge is required of the absolute changes in temperature and density at given points in a star of given mass, rather than the relative distributions. It is well known that the central temperature and density of any model of known chemical composition cannot be computed from the mass until the source of energy is known. Normally the central conditions can be assessed if the radius of the star is known, but this procedure is not available when considering the effect of rotation, since the change of radius is itself one of the unknown quantities. For this reason the changes in central conditions due to rotation cannot be found without knowing the law of energy generation. The changes in central density of Chandrasekhar's rotating polytropes (1) are derived from an arbitrary polytropic relation, and cannot be used for a real star.

The object of the present paper is to provide a model of reasonable accuracy from which these changes can be derived. The effect of rotation on a given star depends on the ratio  $\alpha = \text{equatorial centrifugal force}/\text{surface gravity}$ . An analysis of  $\alpha$  for the various spectral types is given in Table I.

TABLE I

*Ratio  $\alpha = \text{equatorial centrifugal force}/\text{surface gravity}$*

Spectral type	$\alpha_{\text{average}}$	$\alpha_{\text{max}}$
O <sub>5-9</sub>	0.06	0.36
B <sub>2e-5e</sub>	0.32	0.89
B <sub>2-5</sub>	0.23	0.42
B8-A <sub>2</sub> { V III-IV	0.12	0.53
	0.04	0.31
A <sub>2-5</sub>	0.05	0.27
F <sub>0-2</sub>	0.01	0.15

The values given apply to the equatorial region of the surface of the rotating star; thus  $\alpha = \chi v_0^2/Rg_s(0)$ , where  $v_0$  is the equatorial rotation velocity,  $R$  and  $g_s(0)$  are the radius and surface gravity of a non-rotating star of the same mass, while  $\chi$  is a correction factor derived later in the paper, included to allow for the changes in equatorial radius and surface gravity due to rotation. The values of  $v_0$  are derived from the values given by Slettebak (2, 5) and Miss Westgate (6), and the masses and radii involved are based on the work of Kuiper and of Stebbins and Whitford (7). It appears later that the first-order model breaks down when  $\alpha > 0.29$ ; the table therefore shows that a first-order perturbation theory is likely to be sufficient to describe the average O, A and F types but that the theory should be extended to the second order for B stars and the most rapidly rotating O and A types. Such an extension is needed to investigate limb darkening in these stars, since von Zeipel's relation  $H \propto g$  does not hold in the second order; the analysis made by Slettebak (2) would therefore not be valid. It is also required in order to examine more carefully the question of possible circulation currents due to rotation. Öpik (3), for example, appears to find a singularity at the surface in the second-order term in the radial component of the circulation velocity, while Mestel (8), using a first-order theory, has shown that the forces which were previously regarded as producing circulation currents are insufficient to overcome the choking effects of the non-uniformity of molecular weight produced by hydrogen consumption in the core.

The second-order theory is rather complex; a method will therefore be established for the first-order structure in such a way as to facilitate the passage to the second order. For this purpose the initial zero-order model must be as self-consistent as possible; a Cowling model of high accuracy is available from Miss Gardiner's integration (9), and this is the one adopted.

2. *The structure equations.*—The equations of state, hydrostatic equilibrium and Poisson's equation in a uniformly rotating star are:

$$P = \rho \mathcal{R} T / m, \quad (2.1)^*$$

$$\text{grad } P = \rho \text{ grad } \psi, \quad (2.2)\dagger$$

$$\nabla^2 \psi = -4\pi G\rho + 2\Omega^2, \quad (2.3)$$

\* Radiation pressure is neglected.

† From the results of an earlier paper (4) it appears that the meridian-plane component of the circulation velocity would have a negligible effect on hydrostatic equilibrium as compared with that of rotation.

where  $P$ ,  $\rho$  and  $T$  are the pressure, density and temperature,  $m$  is the mean molecular weight in units of the mass of the hydrogen atom and  $\Omega$  is the angular velocity, while  $R$  and  $G$  are, respectively, the gas constant and the constant of gravitation.  $\psi$  is the total effective potential and is given by

$$\psi = \phi + \frac{1}{2}r^2\Omega^2[1 - P_2(\mu)], \quad (2.4)$$

where  $\phi$  is the gravitational potential,  $r$  and  $\theta$  are the radial distance and angular distance from the axis of the star and  $P_2(\mu)$  is the Legendre coefficient,  $\mu$  denoting  $\cos \theta$ .

In the convective core the adiabatic equation

$$\rho \propto T^{3/2} \quad (2.5)$$

holds, while in the envelope the equation of radiative transfer

$$\frac{4}{3}aT^3 \operatorname{grad} T = -\kappa\rho\mathbf{H}/c \quad (2.6)$$

is satisfied, where  $a$  is the coefficient of Stefan's law,  $\kappa$  is the opacity,  $c$  is the velocity of light and  $\mathbf{H}$  is the radiative flux.  $\mathbf{H}$  must also satisfy an equation of thermal equilibrium. In a non-rotating star this is simply  $L = 4\pi r^2 H$ , where  $L$  is the luminosity. When the star is rotating, convection currents may be set up and some of the energy transferred by these. If  $\mathbf{v}$  is the meridian-plane velocity of these currents, the modified thermal equilibrium condition can be written

$$L = \int_S [\mathbf{H} + \{\frac{1}{2}\mathbf{v}^2 + \frac{1}{2}r^2\Omega^2(1 - P_2) + \phi + c_v R T / m\} \rho \mathbf{v}] \cdot d\mathbf{s}, \quad (2.7)$$

where  $S$  is an equipotential surface,  $\psi = \text{constant}$  in the envelope. This expresses the fact that the total rate of outflow of energy from an equipotential surface is contributed by the radiative flux  $\mathbf{H}$  and the kinetic, potential and thermal energies  $\frac{1}{2}\mathbf{v}^2 + \frac{1}{2}r^2\Omega^2(1 - P_2)$ ,  $\phi$  and  $c_v R T / m$  respectively, where  $c_v$  is the specific heat at constant volume. The contribution  $\frac{1}{2}\mathbf{v}^2$  is neglected for reasons similar to the neglect of the effect of the meridian-plane circulation velocity on hydrostatic equilibrium. By using the relation in (2.4) equation (2.7) can be expressed in the form

$$L = \int_S [\mathbf{H} + (\psi + c_v R T / m) \rho \mathbf{v}] \cdot d\mathbf{s}. \quad (2.8)$$

The total rate of outflow of material from  $S$  must vanish, hence

$$\int_S \rho \mathbf{v} \cdot d\mathbf{s} = 0. \quad (2.9)$$

Remembering, moreover, that  $\psi$  is constant over  $S$ , (2.8) can be further reduced to

$$L = \int_S [\mathbf{H} + c_v R T \rho \mathbf{v} / m] \cdot d\mathbf{s}. \quad (2.10)$$

Equations (2.9) and (2.10) hold for all equipotential surfaces in the radiative envelope, and, together with (2.1), (2.2), (2.3), (2.5) and (2.6), constitute the structure equations of the star.

Finally, an energy equation is required; in a point-convective model this is

$$L = \int_{\text{core}} \rho \epsilon d\tau, \quad (2.11)$$

where  $\epsilon$  is the rate of generation of nuclear energy per gram. In the present paper the power law  $\epsilon \propto \rho T^{17}$  is adopted. Hence

$$L = \int_{\text{core}} \rho^2 T^{17} d\tau. \quad (2.12)$$

3. *The successive perturbation theory.*—In what follows a star of fixed mass  $M$  and uniform molecular weight  $m$  is considered. At any given point the structure quantities are therefore functions of  $\Omega$ . In order to work with a dimensionless quantity a parameter  $\lambda$  is introduced in place of  $\Omega$  and given by

$$\lambda = \Omega^2/2\pi G\rho_c(0), \quad (3.1)$$

where  $\rho_c(0)$  is the central density in the non-rotating star. The method adopted consists of expanding the structure variables as power series in  $\lambda$ ; equations for the coefficients are then derived from the structure equations and their derivatives with respect to  $\lambda$ . This procedure is equivalent to successive perturbations; it is, however, more straightforward than the direct method, particularly when deriving the boundary conditions at the core surface and at the surface of the star.

Thus, if  $Q$  is any quantity depending on  $\lambda$ ,  $Q$  is expressed in the form

$$Q(r, \theta; \lambda) = \sum_{n=0}^{\infty} Q_n(r, \theta) \frac{\lambda^n}{n!}, \quad (3.2)$$

where

$$Q_n = [\partial^n Q / \partial \lambda^n]_{\lambda=0}. \quad (3.3)$$

The functions  $Q_0$  are determined by taking  $\lambda=0$  in the structure equations, and are, of course, the quantities arising in the ordinary Cowling model. Having determined these,  $Q_1$  can be derived by differentiating the structure equations with respect to  $\lambda$  and putting  $\lambda=0$ . The boundary conditions for the  $Q_1$  at the centre, at the core surface and at the surface of the star are derived by differentiating the general boundary conditions with respect to  $\lambda$  and putting  $\lambda=0$ . Thus, conditions of the type  $Q=0$  at the surface of the star are written  $Q(r_s, \theta; \lambda)=0$ , where  $r=r_s(\theta, \lambda)$  defines the surface. On differentiation this leads to the condition  $Q_1 + (dQ_0/dr)r_{1s}=0$  at  $r=r_{0s}$ , where  $r_{0s}=R$  the radius of the non-rotating star and  $r_{1s}=[\partial r_s / \partial \lambda]_{\lambda=0}$ . Similarly, the type of condition where  $Q$  is continuous at the core surface  $r=r_c(\theta, \lambda)$  makes  $Q_1 + (dQ_0/dr)r_{1c}$  continuous at  $r=r_{0c}$ , where  $r_{0c}$  is the radius of the core in the non-rotating star. In this way the first-order model tabled in this paper was derived. The higher-order models may be derived similarly by continuing the process.

Dimensionless variables are introduced by the following substitutions:

$$\left. \begin{aligned} r &= r_a x, \text{ where } r_a^2 = 5\mathcal{R}T_c(0)/8\pi m G\rho_c(0), \\ P &= P_c(\lambda)p, \\ \rho &= \rho_c(\lambda)\sigma, \\ T &= T_c(\lambda)t, \\ \psi &= 5\mathcal{R}T_c(\lambda)(q-1)/2m + \psi_c(\lambda), \end{aligned} \right\} \quad (3.4)$$

where  $P_c(\lambda)$ ,  $\rho_c(\lambda)$ ,  $T_c(\lambda)$  and  $\psi_c(\lambda)$  are the central pressure, density, temperature and total potential in the rotating star, and  $p$ ,  $\sigma$ ,  $t$  and  $q$  are the new dimensionless variables.

The structure equations (2.1), (2.2), (2.3) and (2.5) then reduce successively to

$$p = \sigma t, \quad (3.5)$$

$$\operatorname{grad}_{(x, \theta)} p = \frac{5}{2}\sigma \operatorname{grad}_{(x, \theta)} q, \quad (3.6)$$

$$\frac{T_c(\lambda)}{T_c(0)} \nabla^2_{(x, \theta)} q + \frac{\rho_c(\lambda)}{\rho_c(0)} \sigma = \lambda, \quad (3.7)$$

$$\sigma = t^{3/2} \text{ in the core.} \quad (3.8)$$

Equations (2.9) and (2.10) can be written

$$\int_0^1 \rho r_v \left( r_v v_r - \frac{\partial r_v}{\partial \theta} v_\theta \right) d\mu = 0, \quad (3.9)$$

$$L(\lambda) = 4\pi \int_0^1 r_v \left[ r_v H_r - \frac{\partial r_v}{\partial \theta} H_\theta + \left( r_v v_r - \frac{\partial r_v}{\partial \theta} v_\theta \right) \rho c_v \mathcal{R} T / m \right] d\mu, \quad (3.10)$$

where  $r = r_v(\theta, \lambda)$  defines an equipotential surface and  $(H_r, H_\theta)$  and  $(v_r, v_\theta)$  are the components of  $\mathbf{H}$  and  $\mathbf{v}$  evaluated on  $r = r_v$ .

The boundary conditions are:

$$\sigma = t = q = 1; \text{grad } \sigma = \text{grad } t = \text{grad } q = 0 \text{ at } x = 0, \quad (3.11)$$

$$\sigma, t, q; \text{grad } \sigma, \text{grad } t, \text{grad } q \text{ continuous on } x = x_c, \quad (3.12)$$

$$\sigma = t = 0 \text{ on } x = x_s, \quad (3.13)$$

where  $x = x_c(\theta, \lambda)$  defines the interface between the core and the envelope and  $x = x_s(\theta, \lambda)$  defines the surface of the star. The boundary conditions for  $q$  at the surface are derived from the condition that  $\phi$  and its derivatives are continuous with the gravitational potential outside the star for a star of the same mass.

4. *The zero-order model.*—On putting  $\lambda = 0$  the structure equations, with Kramers' opacity, reduce to

$$\frac{d(\sigma_0 t_0)}{dx} = \frac{5}{2} \sigma_0 \frac{dq_0}{dx},$$

$$\frac{1}{x^2} \frac{d}{dx} \left[ x^2 \frac{dq_0}{dx} \right] = -\sigma_0,$$

$$\frac{dt_0}{dx} = -\frac{k \sigma_0^2}{t_0^{13/2} x^2},$$

where  $k$  is a constant. These are the equations for the normal Cowling model, and it is convenient to rename  $\sigma_0$ ,  $t_0$  and  $dq_0/dx$  in order to conform with the notation used in Miss Gardiner's numerical solution (9). Thus, take  $t_0 = y$ ,  $\sigma_0 = z$  and  $-x^2 dq_0/dx = w$ .

5. *The first-order model.*—On differentiating with respect to  $\lambda$  and putting  $\lambda = 0$  the structure equations become

$$p_1 = z t_1 + y \sigma_1, \quad (5.1)$$

$$\dot{p}_1 / \partial x = -5 \sigma_1 w / 2x^2 + \frac{5}{2} z \partial q_1 / \partial x, \quad (5.2)$$

$$\partial p_1 / \partial \theta = \frac{5}{2} z \partial q_1 / \partial \theta, \quad (5.3)$$

$$\nabla^2 q_1 + \sigma_1 = 1 - Xz, \quad (5.4)$$

where

$$X = \rho_c'(0) / \rho_c(0) - T_c'(0) / T_c(0). \quad (5.5)$$

The suffix fig. 1 denotes the operation  $[\partial/\partial\lambda]_{\lambda=0}$  as in (3.3). The above equations hold throughout the star. In the core (3.8) yields the further equation

$$\sigma_1 = \frac{3}{2} y^{1/2} t_1 \text{ in the core.} \quad (5.6)$$

In the envelope (2.6) gives

$$\mathbf{H}_1 = \mathbf{H}_0 \left[ \frac{15}{2} \frac{T_c'(0)}{T_c(0)} - 2 \frac{\rho_c'(0)}{\rho_c(0)} + \frac{13}{2} \frac{t_1}{y} - 2 \frac{\sigma_1}{z} \right] + \frac{H_{0r}}{dy/dx} \text{grad } t, \quad (5.7)$$

where Kramers' law is taken for the opacity. Again, from (2.9) and (2.10) the relation

$$L'(0) = 4\pi r^2 \int_0^1 H_{1r} d\mu \quad (5.8)^*$$

can be derived. By substituting for  $H_{1r}$  from (5.7), noting that  $\mathbf{H}_0 = [L(0)/4\pi r^2, 0]$ , the above equation reduces to

$$\int_0^1 \left( \frac{\frac{13}{2}}{y} t_1 - 2 \frac{\sigma_1}{z} + \frac{\partial t_1 / \partial x}{dy/dx} \right) d\mu = Y, \quad (5.9)$$

where

$$Y = \frac{L'(0)}{L(0)} - \frac{15}{2} \frac{T_c'(0)}{T_c(0)} + 2 \frac{\rho_c'(0)}{\rho_c(0)}. \quad (5.10)$$

(5.9) is the counterpart of the equation of radiative transfer in the Cowling model.

The boundary conditions, derived from (3.11), (3.12) and (3.13), are:

$$\sigma_1 = t_1 = q_1 = 0; \quad \partial \sigma_1 / \partial x = \partial t_1 / \partial x = \partial q_1 / \partial x = 0 \text{ at } x = 0, \quad (5.11)$$

$$\left. \begin{aligned} & \sigma_1 + \frac{dz}{dx} x_{1c}, \quad t_1 + \frac{dy}{dx} x_{1c}, \quad q_1 \frac{w}{x^2} x_{1c}; \\ & \partial \sigma_1 / \partial x + \frac{d^2 z}{dx^2} x_{1c}, \quad \partial t_1 / \partial x + \frac{d^2 y}{dx^2} x_{1c}, \quad \partial q_1 / \partial x + (2w/x^3 - z)x_{1c}; \\ & \partial \sigma_1 / \partial \theta, \quad \partial t_1 / \partial \theta, \quad \partial q_1 / \partial \theta, \end{aligned} \right\} \begin{array}{l} \text{continuous} \\ \text{at} \\ x = x_{0c} \end{array} \quad (5.12)$$

where  $x_{0c}$  is the core radius in the normal Cowling model and  $x_{1c}(\theta, \lambda) = [\partial x_c / \partial \lambda]_{\lambda=0}$ ; and

$$\sigma_1 + (dz/dx)x_{1s} = 0; \quad t_1 + (dy/dx)x_{1s} = 0 \text{ at } x = x_{0s}, \quad (5.13)$$

where  $x_{0s}$  is the radius of the star in the Cowling model and  $x_{1s} = [\partial x_s / \partial \lambda]_{\lambda=0}$ . From the Cowling model it is seen that  $dz/dx$ ,  $dy/dx$  and  $w$  are continuous at the interface; (5.12) therefore shows that

$$\sigma_1, t_1, q_1, \partial q_1 / \partial x \text{ are continuous at } x = x_{0c}. \quad (5.14)$$

$d^2z/dx^2$  and  $d^2y/dx^2$  are not continuous in the Cowling model, hence the fourth and fifth members of (5.12) only serve to derive  $x_{1c}$  at the end of the problem. Similarly,  $dz/dx = 0$  and  $dy/dx \neq 0$  at the surface of the Cowling model, hence the first member of (5.13) gives

$$\sigma_1 = 0 \text{ at } x = x_{0s}, \quad (5.15)$$

while the second member will be used to determine  $x_{1s}$  at the end of the problem.

The boundary conditions for  $q_1$  are derived from the boundary conditions for  $q$  referred to at the end of Section 3, and are found to be

$$q_1 = Z - \frac{T_c'(0)}{T_c(0)} \frac{w}{x} + \frac{1}{3} x^2 (1 - P_2) + \frac{AP_2}{x^3}, \quad (5.16)$$

$$x \frac{\partial q_1}{\partial x} = \frac{T_c'(0)}{T_c(0)} \frac{w}{x} + \frac{1}{3} x^2 (1 - P_2) - \frac{3AP_2}{x^3}, \quad (5.17)$$

at  $x = x_{0s}$ , where

$$Z = \frac{2m\psi_e(0)}{5\mathcal{R}T_c(0)} \left[ \frac{T_c'(0)}{T_c(0)} - \frac{\psi_e'(0)}{\psi_e(0)} \right],$$

and  $A$  is an unknown constant.

\* If the integrand on the R.H.S. of (2.10) is denoted by  $I$ , then  $dL/d\lambda = 4\pi \int_0^1 dI/d\lambda \cdot d\mu$ . Now  $I = I(r_\psi, \theta; \lambda)$ , hence  $dI/d\lambda = \partial I/\partial \lambda + \partial I/\partial r_\psi \cdot \partial r_\psi/\partial \lambda$ . (5.8) follows on noting that  $H_{0\theta} = 0$ ,  $r^2 H_{0\gamma} = \text{constant}$ ,  $v_0 = 0$  and  $\int_0^1 v_{1\theta} d\mu = 0$ .

The solution of the first-order structure equations can now be undertaken. (5.16), in conjunction with the structure equations, shows that  $q_1$  can be expressed in the form  $q_1 = a(x) + b(x)P_2$ , with similar expressions for  $p_1$ ,  $\sigma_1$  and  $t_1$ . It is found convenient to write  $a(x)$  and  $b(x)$  in the forms

$$a(x) = -\frac{1}{2}Xw/x + \frac{1}{6}x^2 + \frac{1}{6}\Lambda(x), \quad b(x) = -\frac{1}{6}x^2k(x),$$

thus

$$q_1 = -\frac{1}{2}Xw/x + \frac{1}{6}x^2 + \frac{1}{6}\Lambda - \frac{1}{6}x^2kP_2. \quad (5.18)$$

By substituting these expressions in (5.1) to (5.4) it follows, after some elementary algebra, that

$$p_1 = \frac{5}{2}z(q_1 - \frac{1}{6}\Gamma(x)), \quad (5.19)$$

$$\sigma_1 = -\frac{x^2z'}{w}(q_1 - \frac{1}{6}\Gamma(x)) + \frac{1}{6}\frac{x^2z}{w}\Gamma'(x), \quad (5.20)$$

$$t_1 = -\frac{x^2y'}{w}(q_1 - \frac{1}{6}\Gamma(x)) - \frac{1}{6}\frac{x^2y}{w}\Gamma'(x), \quad (5.21)$$

where  $\Lambda$ ,  $\Gamma$  and  $k$  satisfy

$$\Lambda'' + \frac{2}{x}\Lambda' - \frac{x^2z'}{w}\Lambda = \frac{x^4z'}{w} - \frac{x^2z'}{w}\Gamma - \frac{x^2z}{w}\Gamma', \quad (5.22)$$

$$k'' + \frac{6}{x}k' - \frac{x^2z'}{w}k = 0, \quad (5.23)$$

dashes denoting differentiation with respect to  $x$ . These last two equations are satisfied throughout the star, hence  $k$ , which occurs on its own, can be determined immediately the appropriate boundary conditions are known. (5.18) in conjunction with (5.11) shows that  $kx^2 \rightarrow 0$  as  $x \rightarrow 0$ . The two solutions of (5.23) near the origin are  $k = \text{constant}$  and  $k \propto x^{-5}$ ; at the origin the appropriate boundary condition is therefore that  $k$  should be finite. The second boundary condition necessary is obtained from (5.16) and (5.17). By equating coefficients of  $P_2$  and eliminating the unknown  $A$  these give

$$5(k-1) + xk' = 0 \text{ at } x = x_0, \quad (5.24)$$

The solution was then evaluated numerically. One further equation is necessary in order to determine  $\Lambda$  and  $\Gamma$ . In the core this is provided by (5.6) which reduces to

$$\Gamma' = 0 \text{ in the core}; \quad (5.25)$$

thus  $\Gamma = \text{constant}$  in the core. Noting that  $q_1 = p_1 = 0$  at the origin, (5.18) and (5.19) show that  $\Gamma = \Lambda = 0$  at  $x = 0$ ; therefore  $\Gamma = 0$  throughout the core. (5.22) thus reduces to

$$\Lambda'' + \frac{2}{x}\Lambda' - \frac{x^2z'}{w}\Lambda = \frac{x^4z'}{w} \text{ in the core}. \quad (5.26)$$

Since  $x^2z'/w$  is finite at the origin the two complementary functions behave as  $\Lambda = \text{constant}$  and  $\Lambda \propto x^{-1}$  at the origin. The second of these is unsuitable since  $\Lambda = 0$  at  $x = 0$ ; the solution required is therefore the particular integral commencing with  $\Lambda = 0$  at  $x = 0$ . This solution was derived numerically. In the envelope  $\Lambda$  and  $\Gamma$  are governed by (5.9), which, after a little reduction, gives the relation

$$\begin{aligned} \Gamma'' + \left(\frac{2}{x} - \frac{x^2z}{w} + \frac{17}{2}\frac{y'}{y}\right)\Gamma' + \frac{y'}{y}\Lambda' + \frac{x^2zy'}{wy}(\Gamma - \Lambda) + \frac{xy'}{y}\left(2 - \frac{x^3z}{w}\right) \\ = -\frac{6wy'}{x^2y}(\frac{1}{2}X + Y). \end{aligned} \quad (5.27)$$

The conditions (5.12) show that  $\Lambda$ ,  $\Lambda'$ ,  $\Gamma$  and  $\Gamma'$  are continuous at  $x=x_{0c}$ . The required boundary conditions at the core surface are therefore given directly by the core solution at  $x=x_{0c}$ . (5.22) and (5.27) cannot however be integrated directly from the core surface because the constant  $(\frac{1}{2}X+Y)$  in (5.27) is as yet unknown. By substituting  $\Lambda=(\frac{1}{2}X+Y)\frac{6}{5}w/x+l$  and  $\Gamma=(\frac{1}{2}X+Y)\frac{24}{25}y+h$ , (5.22) and (5.27) reduce to

$$l'' + \frac{2}{x} l' + \frac{x^2 z'}{w} (h-l) + \frac{x^2 z}{w} h' = \frac{x^4 z'}{w}, \quad (5.28)$$

$$h'' + \left( \frac{2}{x} - \frac{x^2 z}{w} + \frac{17}{2} \frac{y'}{y} \right) h' + \frac{y'}{y} l' + \frac{x^2 z y'}{w y} (h-l) = \frac{x y'}{y} \left( \frac{x^3 z}{w} - 2 \right). \quad (5.29)$$

The above equations have a singular point at the surface, where the four complementary functions behave as  $l \sim [(1/z), 1, y, yz]$ ;  $h \sim [(1/yz^2), 1, y, y^2 z]$ . The boundary conditions (5.13) and (5.16) show that  $l$  and  $h$  are finite at the surface, thus the solutions  $l \sim (1/z)$ ,  $h \sim (1/yz^2)$  are rejected. An inspection of the equations shows that one solution is  $(l=1, h=1)$ ; the two remaining linearly independent complementary functions  $(l_1, h_1)$  and  $(l_2, h_2)$  were computed by inward integration from the surface, using suitable starting series in the variable  $\xi=x_s/x-1$ . For this purpose the Cowling variables ( $w, y, z$ ) were also expanded in series. A particular integral  $(l_p, h_p)$  was computed in a similar manner.  $\Lambda$  and  $\Gamma$  can then be expressed in the forms

$$\left. \begin{aligned} \Lambda &= (\frac{1}{2}X+Y)\frac{6}{5}(w/x) + l_p + \alpha l_1 + \beta l_2 + \gamma, \\ \Gamma &= (\frac{1}{2}X+Y)\frac{24}{25}y + h_p + \alpha h_1 + \beta h_2 + \gamma. \end{aligned} \right\} \quad (5.30)$$

The constants  $[(\frac{1}{2}X+Y), \alpha, \beta, \gamma]$  are then determined from the four boundary conditions at the core surface. In particular it is found that

$$(\frac{1}{2}X+Y) = +0.312. \quad (5.31)$$

The solution  $(\Lambda, \Gamma)$  is then determined in the envelope.

The constants  $[X, Y, L'(0)/L(0), T_c'(0)/T_c(0), \rho_c'(0)/\rho_c(0)]$  may now be found in the following manner. The substitution of  $q_1$  from (5.18) into the boundary condition (5.17) shows that

$$\Lambda'_s = \frac{6w_s}{x_{0s}^2} \left[ \frac{T_c'(0)}{T_c(0)} - \frac{1}{2}X \right], \quad (5.32)$$

where  $\Lambda'_s$  is known from the envelope solution  $(\Lambda, \Gamma)$ . Thus (5.5), (5.10), (5.31) and (5.32) are four equations in the five unknowns required. The additional relation necessary is derived from the energy equation (2.12). By differentiating this logarithmically with respect to  $\lambda$  and putting  $\lambda=0$  it can be shown, after a little reduction, that

$$\frac{L'(0)}{L(0)} - 2 \frac{\rho_c'(0)}{\rho_c(0)} - 17 \frac{T_c'(0)}{T_c(0)} = \frac{\int_0^{x_{0c}} \int_0^{x_{0c}} z^2 y^{17} \left( \frac{2\sigma_1}{z} + \frac{17t_1}{y} \right) x^2 dx dy}{\int_0^{x_{0c}} z^2 y^{17} x^2 dx}. \quad (5.33)^*$$

By substituting for  $\sigma_1$  and  $t_1$  from (5.20) and (5.21), and using the core relations  $z'/z = 3y'/2y = -3w/2x^2y$ , (5.33) can be reduced to

$$\frac{L'(0)}{L(0)} - 2 \frac{\rho_c'(0)}{\rho_c(0)} - 17 \frac{T_c'(0)}{T_c(0)} = \frac{20 \int_0^{x_{0c}} y^{19} (-\frac{1}{2}Xxw + \frac{1}{6}x^2\Lambda + \frac{1}{3}x^4) dx}{\int_0^{x_{0c}} y^{20} x^2 dx}. \quad (5.34)$$

\* It has been assumed here that the energy production at the core surface in the non-rotating star is negligible.

With the aid of the core solutions for  $\Lambda$  and the Cowling variables, the necessary integrals on the right-hand side of this equation may be computed numerically. The resulting relation is

$$\frac{L'(0)}{L(0)} - 2 \frac{\rho_c'(0)}{\rho_c(0)} - 17 \frac{T_c'(0)}{T_c(0)} = -1.402X + 1.472. \quad (5.35)$$

Equations (5.5), (5.10), (5.31), (5.32) and (5.35), when solved, give

$$\left. \begin{aligned} X &= 5.842 & L'(0)/L(0) &= -22.14, \\ Y &= -2.609 & T_c'(0)/T_c(0) &= -1.427, \\ \rho_c'(0)/\rho_c(0) &= +4.415. \end{aligned} \right\} \quad (5.36)$$

The functions  $q_1$ ,  $t_1$  and  $\sigma_1$  may then be computed; the resulting model is tabulated in the Appendix.

The figure of the star is governed by  $x_{1s}$ ; the second member of the boundary conditions (5.13) gives

$$x_{1s} = -\frac{t_{1s}}{y_s}. \quad (5.37)$$

Here  $t_{1s}$  can be obtained from (5.21), thereby showing that

$$\begin{aligned} \frac{x_{1s}}{x_{0s}} &= \frac{r_{1s}}{R} = -\frac{1}{2}X + \frac{1}{6}\frac{x_{0s}^3}{w_s} + \frac{1}{6}\frac{x_{0s}}{w_s}(\Lambda_s - \Gamma_s) + \frac{1}{6}\frac{y_s}{y_s'}\frac{x_{0s}}{w_s}\Gamma_s' - \frac{1}{6}\frac{x_{0s}^3}{w_s}k_sP_2 \\ &= +11.80 - 18.91P_2. \end{aligned} \quad (5.38)$$

The surface gravity due to the material of the star is given by

$$g_s^2 = \text{grad } \phi_s \cdot \text{grad } \phi_s,$$

On differentiation with respect to  $\lambda$  this relation shows that

$$\begin{aligned} g_{0s}^1 \left[ \frac{dg_s}{d\lambda} \right]_{\lambda=0} &= X - \frac{1}{3}\frac{x_{0s}^3}{w_s} + \frac{1}{3}\frac{x_{0s}}{w_s}(\Gamma_s - \Lambda_s) + \frac{1}{3}\frac{x_{0s}^3}{w_s}(2k_s + \frac{1}{2}x_{0s}k_s' - 1)P_2 \\ &= -29.44 + 41.57P_2, \end{aligned} \quad (5.39)$$

where the chain of relations (2.4), (3.4) (last member) and (5.18) was used to find the derivatives of  $\phi_s$  and (5.38) provided the expression for  $x_{1s}$ . Similarly,

$$\begin{aligned} g_{0s}^1 \left[ \frac{dg_s^{\text{eff}}}{d\lambda} \right]_{\lambda=0} &= g_{0s}^1 \left[ \frac{dg_s}{d\lambda} \right]_{\lambda=0} - \frac{1}{3}\frac{x_{0s}^3}{w_s}(1 - P_2) \\ &= -66.20 + 78.33P_2, \end{aligned} \quad (5.40)$$

where  $g_s^{\text{eff}}$  is the effective surface gravity.

A similar procedure adopted for  $H_s$  the surface flux of radiation shows that

$$\begin{aligned} H_{0s}^1 \left[ \frac{dH_s}{d\lambda} \right]_{\lambda=0} &= \frac{L'(0)}{L(0)} + X - \frac{1}{3}\frac{x_{0s}^3}{w_s} + \frac{1}{3}\frac{x_{0s}}{w_s}(\Gamma_s - \Lambda_s) + \frac{1}{3}\frac{x_{0s}^3}{w_s}(2k_s + \frac{1}{2}x_{0s}k_s')P_2 \\ &= -45.74 + 78.33P_2, \end{aligned} \quad (5.41)$$

equations (5.7), (5.8) and (5.21) being used for the derivatives of  $H_s$ .

6. *The interpretation of the model.*—In order to apply the model to stars as observed, a parameter  $\alpha_1$ , defined by

$$\alpha_1 = \frac{R^3\Omega^2}{GM} = \frac{3}{2} \frac{\rho_c(0)}{\rho_m(0)} \lambda, \quad (6.1)$$

is introduced, where  $\rho_m(0)$  is the mean density of the non-rotating star;  $\alpha_1$  is therefore the ratio of centrifugal force at a distance equal to the radius of the

non-rotating star, to the surface gravity of the non-rotating star. In the Cowling model  $\rho_m/\rho_c = 0.0272$ , thus

$$\lambda = 0.0181\alpha_1. \quad (6.2)$$

A summary of the results of the previous section, in terms of  $\alpha_1$ , is given in Table II below.

TABLE II

*Summary of results to first order in  $\alpha_1$* 

$L = L(o) [1 - 0.401\alpha_1]$
$M_{\text{bol}} = M_{\text{bol}}(o) \begin{cases} + 0.569\alpha_1 & (\text{rotation axis } \perp \text{line of sight}) \\ - 0.427\alpha_1 & (\text{pole-on view}) \end{cases}$
$\rho_c = \rho_c(o) [1 + 0.0799\alpha_1]$
$T_c = T_c(o) [1 - 0.0259\alpha_1]$
$H_s = H_s(o) [1 - 0.828\alpha_1 + 1.420\alpha_1 P_2]$
$g_s = g_s(o) [1 - 0.533\alpha_1 + 0.754\alpha_1 P_2]$
$g_s^{\text{eff}} = g_s^{\text{eff}}(o) [1 - 1.200\alpha_1 + 1.420\alpha_1 P_2]$
$r_s = R [1 + 0.214\alpha_1 - 0.343\alpha_1 P_2]$
$\log_{10} \bar{T}_e = \log_{10} T_e(o) \begin{cases} - 0.065\alpha_1 & (\text{rotation axis } \perp \text{line of sight}) \\ - 0.040\alpha_1 & (\text{pole-on view}) \end{cases}$

The values for  $M_{\text{bol}}$  and  $\log \bar{T}_e$  require some comment; owing to the temperature variation over the surface the star will appear brighter and hotter when viewed pole-on than when viewed at right angles to the rotation axis. The results were obtained by integrating the emergent intensity in the appropriate directions over the appropriate parts of the surface, assuming a normal coefficient of limb darkening 0.6.

The parameter  $\alpha$  tabled in Section I from observations of stars is given by

$$\frac{\alpha}{\alpha_1} = \frac{r_s(\pi/2, \lambda)/R}{g_s(\pi/2, \lambda)/g_{0s}} = 1 + 1.295\alpha_1 \quad (6.3)$$

to the first order in  $\alpha_1$ , where  $r_s/R$  and  $g_s/g_{0s}$  are obtained from Table II. Further, remembering that  $r_0 = r_s(\pi/2, \lambda)\Omega$ , the correction factor  $\chi$  used in calculating  $\alpha$  from observation is therefore given by

$$\chi = 1 + 0.523\alpha_1 \quad (6.4)$$

to the first order in  $\alpha_1$ . Thus  $\alpha$  and  $\alpha_1$  may be expressed in terms of the observable quantity  $\alpha' = r_0^2/Rg_{0s}$  by

$$\alpha = \alpha'(1 + 0.523\alpha'), \quad (6.5)$$

$$\alpha_1 = \alpha'(1 + 0.772\alpha') \quad (6.6)$$

to the first order in  $\alpha'$ .

The relative displacements in a H-R diagram for the limiting case  $\alpha = 1$  as derived from Table II are shown in Fig. 1.\* The mean effective temperature of a star is reduced as seen from both pole-on and axis perpendicular viewpoints. The apparent luminosity is reduced when the star is viewed perpendicular to the rotation axis and, although the total light output is reduced, the apparent luminosity is increased when the star is viewed pole-on. It can be seen that the main sequence is brightened by about 0<sup>m</sup>.5 for a set of stars viewed pole-on, with a smaller increase for stars viewed at right angles to the rotation axis. Since a

\* The diagram indicates only the order of magnitude of these displacements.

"pole-on" star would show no apparent rotation as judged from line broadening, no definite separation of stars according to rotation would be expected. On the observational side there seems to be no conclusive correlation between luminosity and rotation velocity. Eggen (10) appeared to find a brightening with rotation for the late A and early F types in the Hyades and Pleiades, with the reverse effect, however, for early A types. The limiting spread of half a magnitude is approached only by the most rapidly rotating Be stars. The observed spread for B-type stars

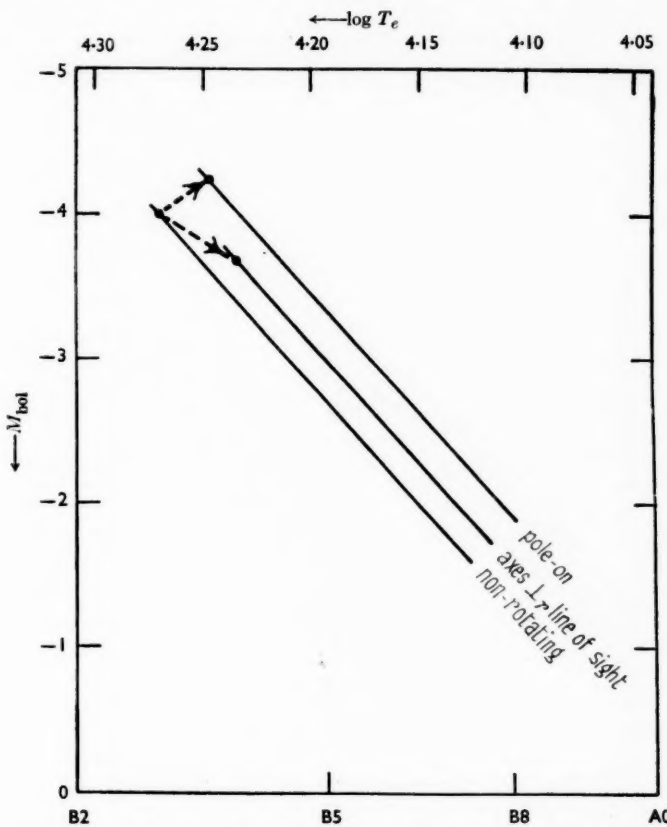


FIG. 1.—*Limiting displacements of star of given mass and resulting spread in H-R diagram.*

of luminosity class V in clusters, as illustrated for example in Roman and Morgan's work (11) on the Perseus cluster, appears to be of the order of a magnitude. It seems unlikely that rotation can account directly for the whole of this, unless rotation were more rapid in the interiors of stars than in their outer regions.

Table II also shows (a) that the surface oblateness for small angular velocities is  $0.514z_1$ , which is close to the figure  $0.5z_1$  for the Roche model, and to the figures obtained by Chandrasekhar (1) for rotating polytropes, and (b)  $H_s \propto g_s^{\text{eff}}$  to the first order in  $z_1$ , as expected from von Zeipel's theorem.

The distribution of  $\rho$  and  $T$  within the star can be computed to the first order in  $\alpha_1$ . Working in terms of  $(\nu, \theta)$ , where  $\nu$  is the proportion of the total radius  $x_s(\theta, \lambda)$  of the star at an angle  $\theta$  to the rotation axis, the substitutions (3.4), expanded in the forms defined by (3.2) and (3.3), give the first-order expressions

$$\rho(\nu, \theta; \lambda) = \rho_0(x) \left[ 1 + \frac{2}{3} \frac{\rho_m(0)}{\rho_c(0)} \alpha_1 \left\{ \frac{\rho_c'(0)}{\rho_c(0)} + \frac{z'x}{z} \frac{x_{1s}}{x_{0s}} + \frac{\alpha_1}{z} \right\} \right], \quad (6.7)$$

$$T(\nu, \theta; \lambda) = T_0(x) \left[ 1 + \frac{2}{3} \frac{\rho_m(0)}{\rho_c(0)} \alpha_1 \left\{ \frac{T_c'(0)}{T_c(0)} + \frac{y'x}{y} \frac{x_{1s}}{x_{0s}} + \frac{\alpha_1}{y} \right\} \right], \quad (6.8)$$

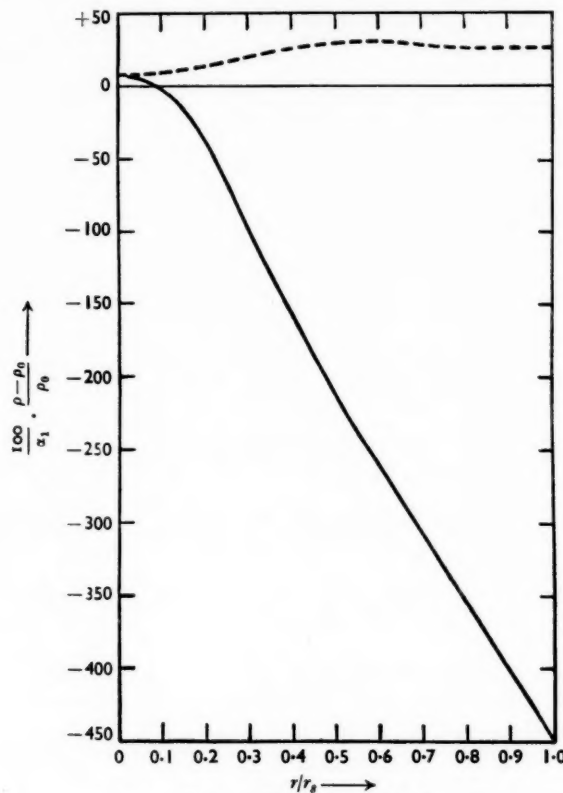


FIG. 2.—First-order density changes.  
 —— polar axis.  
 —— equatorial plane.

where the right-hand sides are evaluated at  $x = \nu x_{0s}$ . The results are presented graphically in Figs. 2 and 3 in the form of the percentage changes per unit  $\alpha_1$  in the corresponding values at the same  $\nu$  in the non-rotating star. It can be seen from the figure that the surface density at the equator becomes negative for  $\alpha_1 > 0.22$ , corresponding to  $\alpha > 0.29$ ; the model formally breaks down at this value of  $\alpha$ . A first-order model will therefore not give accurate results for surface phenomena such as figure of surface, variation of effective temperature over the surface and surface gravity in the more rapidly rotating stars. In discussing these stars

von Zeipel's relation  $H_s \propto g_s^{\text{eff}}$  therefore cannot be used as in Slettebak's discussion (2) of limb darkening in O and B stars, since it only holds to the first order in  $\alpha$ .

It can be stated in conclusion that (i) the direct effect of rotation, apart from questions of mixing, may account for part of the observed spread in luminosity for a given spectral type in the case of B and A stars in clusters, and (ii) a theoretical study of limb darkening and also of circulation currents in rapidly rotating stars requires a second-order model.

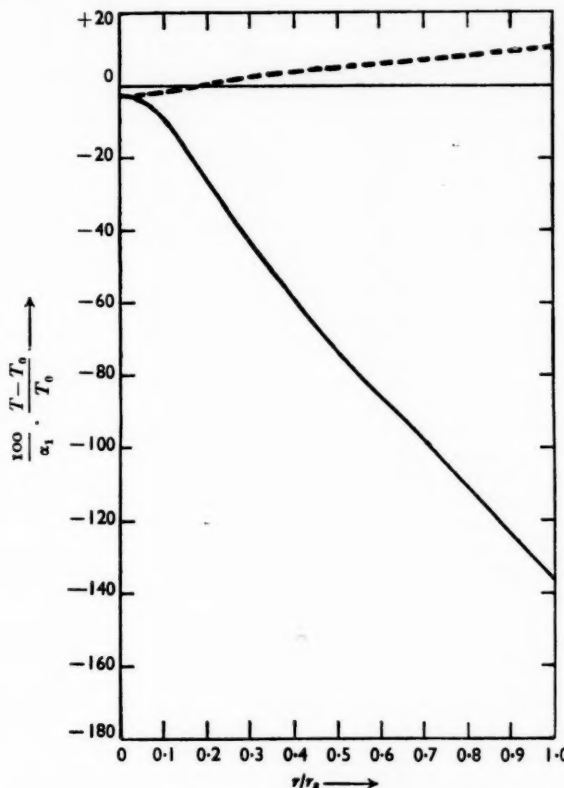


FIG. 3.—First-order temperature changes.

— polar axis.  
— equatorial plane.

## APPENDIX

The following table gives the quantities  $q_1$ ,  $t_1$  and  $\sigma_1$  associated with the effective potential, temperature and density, respectively, from which the first-order model illustrated in Figs. 2 and 3 was derived.

$x$	$q_1$	$t_1$	$\sigma_1$
0	0	0	0
0.2	-0.032 - 0.026 $P_2$	-0.032 - 0.026 $P_2$	-0.048 - 0.038 $P_2$
0.4	-0.126 - 0.102 $P_2$	-0.126 - 0.102 $P_2$	-0.186 - 0.150 $P_2$
0.6	-0.274 - 0.224 $P_2$	-0.274 - 0.224 $P_2$	-0.398 - 0.326 $P_2$
0.8	-0.465 - 0.386 $P_2$	-0.465 - 0.386 $P_2$	-0.660 - 0.549 $P_2$
1.0	-0.684 - 0.582 $P_2$	-0.684 - 0.582 $P_2$	-0.943 - 0.802 $P_2$
$x_{0e} = 1.1923$	-0.907 - 0.792 $P_2$	-0.907 - 0.792 $P_2$	-1.207 - 1.054 $P_2$
1.2	-0.916 - 0.801 $P_2$	-0.910 - 0.796 $P_2$	-1.221 - 1.068 $P_2$
1.4	-1.143 - 1.034 $P_2$	-0.999 - 0.907 $P_2$	-1.554 - 1.403 $P_2$
1.6	-1.347 - 1.271 $P_2$	-1.068 - 1.016 $P_2$	-1.764 - 1.658 $P_2$
1.8	-1.513 - 1.502 $P_2$	-1.104 - 1.119 $P_2$	-1.831 - 1.808 $P_2$
2.0	-1.631 - 1.722 $P_2$	-1.122 - 1.216 $P_2$	-1.764 - 1.852 $P_2$
2.2	-1.698 - 1.928 $P_2$	-1.192 - 1.308 $P_2$	-1.599 - 1.866 $P_2$
2.4	-1.714 - 2.122 $P_2$	-1.078 - 1.394 $P_2$	-1.377 - 1.696 $P_2$
2.6	-1.683 - 2.305 $P_2$	-1.019 - 1.478 $P_2$	-1.132 - 1.545 $P_2$
2.8	-1.609 - 2.481 $P_2$	-0.938 - 1.560 $P_2$	-0.894 - 1.376 $P_2$
3.0	-1.498 - 2.653 $P_2$	-0.840 - 1.643 $P_2$	-0.679 - 1.203 $P_2$
3.2	-1.356 - 2.824 $P_2$	-0.724 - 1.729 $P_2$	-0.495 - 1.037 $P_2$
3.4	-1.188 - 2.990 $P_2$	-0.597 - 1.818 $P_2$	-0.345 - 0.884 $P_2$
3.6	-0.991 - 3.180 $P_2$	-0.454 - 1.914 $P_2$	-0.226 - 0.747 $P_2$
3.8	-0.786 - 3.369 $P_2$	-0.308 - 2.016 $P_2$	-0.138 - 0.625 $P_2$
4.0	-0.557 - 3.560 $P_2$	-0.149 - 2.126 $P_2$	-0.073 - 0.519 $P_2$
4.2	-0.312 - 3.780 $P_2$	+0.017 - 2.244 $P_2$	-0.027 - 0.427 $P_2$
4.4	-0.054 - 4.006 $P_2$	+0.192 - 2.372 $P_2$	+0.004 - 0.349 $P_2$
4.6	+0.219 - 4.246 $P_2$	+0.374 - 2.509 $P_2$	+0.022 - 0.281 $P_2$
4.8	+0.505 - 4.501 $P_2$	+0.561 - 2.656 $P_2$	+0.033 - 0.224 $P_2$
5.0	+0.806 - 4.772 $P_2$	+0.755 - 2.813 $P_2$	+0.036 - 0.176 $P_2$
5.2	+1.119 - 5.060 $P_2$	+0.959 - 2.980 $P_2$	+0.036 - 0.135 $P_2$
5.4	+1.446 - 5.364 $P_2$	+1.168 - 3.156 $P_2$	+0.032 - 0.101 $P_2$
5.6	+1.788 - 5.686 $P_2$	+1.385 - 3.345 $P_2$	+0.027 - 0.073 $P_2$
5.8	+2.143 - 6.024 $P_2$	+1.608 - 3.544 $P_2$	+0.021 - 0.051 $P_2$
6.0	+2.511 - 6.380 $P_2$	+1.837 - 3.753 $P_2$	+0.015 - 0.033 $P_2$
6.2	+2.895 - 6.752 $P_2$	+2.073 - 3.972 $P_2$	+0.010 - 0.020 $P_2$
6.4	+3.293 - 7.141 $P_2$	+2.315 - 4.200 $P_2$	+0.006 - 0.010 $P_2$
6.6	+3.705 - 7.547 $P_2$	+2.563 - 4.439 $P_2$	+0.002 - 0.004 $P_2$
6.8	+4.132 - 7.969 $P_2$	+2.818 - 4.687 $P_2$	... - 0.001 $P_2$
7.0	+4.574 - 8.406 $P_2$	+3.079 - 4.945 $P_2$	...
$x_{0e} = 7.01168$	+4.600 - 8.432 $P_2$	+3.094 - 4.960 $P_2$	0

London University Observatory,  
Mill Hill Park,  
London, N.W.7 :  
1953 June 15.

The University Observatory,  
Glasgow, W.2.

*References*

- (1) S. Chandrasekhar, *M.N.*, **93**, 390, 1933.
- (2) A. Slettebak, *Ap. J.*, **110**, 498, 1949.
- (3) E. J. Öpik, *M.N.*, **111**, 278, 1951.
- (4) P. A. Sweet, *M.N.*, **110**, 548, 1950.
- (5) A. Slettebak, *A. J.*, **58**, 47, 1953.
- (6) C. Westgate, *Ap. J.*, **78**, 46, 1933.
- (7) G. P. Kuiper, *Ap. J.*, **88**, 429, 1938; *Ap. J.*, **88**, 472, 1938. J. A. Hynek, *Astrophysics*, pp. 20, 23, McGraw-Hill, 1951.
- (8) L. Mestel, *M.N.*, **113**, 716, 1953.
- (9) J. G. Gardiner, *M.N.*, **111**, 94, 1951.
- (10) O. J. Eggen, *Ap. J.*, **111**, 81, 1950; *Ap. J.*, **111**, 65, 1950.
- (11) N. G. Roman and W. W. Morgan, *Ap. J.*, **111**, 426, 1950.
- (12) G. R. and E. M. Burbidge, *Ap. J.*, **117**, 407, 1953.

## ROTATION AND STELLAR EVOLUTION

*L. Mestel*

(Received 1953 September 2)

### *Summary*

Sweet's discussion (1) of rotational currents in a Cowling model star is reviewed. It is shown that the non-spherical distribution of matter set up by the currents themselves tends to choke back the motion, so that no rotationally stable star can suffer any considerable mixing between core and envelope, if the angular velocity is nearly constant throughout the star. If, however, the rotation rate increases substantially inwards, enough mixing can occur to influence seriously the evolution of the star.

---

**1. Introduction.**—Recent research on stellar structure has shown that the observable parameters of a star depend strongly on the composition of the stellar material, and on inhomogeneities in its distribution. Thus the mass-luminosity and mass-radius relations for homogeneous stars (2) show that the luminosity increases strongly and the radius moderately as the mean molecular weight increases, leading to a slight increase in effective temperature. Further, it is found that the radii of some models with inner zones of high molecular weight are large enough to account for the most diffuse giant stars observed (3, 4, 5). It is also known that certain non-homogeneous stellar models depart from the static state (4, 6); the evolution of such stars is likely to differ profoundly from that of static stars.

Many theorists believe that it is impossible to explain the evolution of the stars without invoking some interaction between the stars themselves and the interstellar medium. Thus Hoyle and Lyttleton (7, 8) believe in accretion of interstellar matter, both on observational and theoretical grounds; on the other hand, Struve (9), Fessenkov, Ambartsumian (10) and others propose equally strongly that stars emit "corpuscular radiation", so losing substantial quantities of their mass at a rate comparable with their rate of evolution by consumption of hydrogen. Whatever the arguments for or against either of these mechanisms, it seems desirable to work out carefully the course of evolution of a star when left to itself. When this has been done, appeal to observation may be able to decide unambiguously what further hypotheses are necessary to avoid discrepancies between theory and observation.

A star of mass well above that of the Sun generates its energy by means of the Bethe cycle; as shown by Cowling (11), the high temperature-sensitivity of the cycle causes the innermost regions to be in convective equilibrium. Such a star has had sufficient time since the birth of the Galaxy to undergo considerable evolution through the conversion of hydrogen into helium in the convective core. The convection currents are sufficiently rapid to keep the core uniform in composition, but the radiative zone is highly stable against turbulence, and

other causes of mixing must be sought if material of high molecular weight is to penetrate into the radiative zone.

In a recent paper (1) Sweet has discussed the suggestion that Eddington's meridional currents, due to stellar rotation, will provide the necessary stirring in a short enough time. Sweet's corrections reduce Eddington's value for the vertical velocity of the currents by a large factor; in particular, he shows that mixing between core and envelope in the Sun (assumed to rotate throughout with its surface angular velocity) must be negligible. Early-type stars, however, tend to have much higher surface angular velocities, and Sweet's figures lead him to conclude that such stars, rotating as rigid bodies, will remain homogeneous in structure, except for the effect of accretion.

Except for one detail, discussed in Section 2 and the Appendix, this paper does not criticize Sweet's analysis as far as it goes, but it will be shown that the conclusions he draws as regards stellar evolution need considerable revision. The Eddington currents are due fundamentally to the departure from spherical symmetry caused by centrifugal force. It is impossible, in a uniformly rotating star, to satisfy both the hydrostatic condition and the equation of radiative equilibrium; heating occurs at the poles and cooling at the equator of each level surface, and a system of meridional currents is set up, with velocities just sufficient to preserve thermal equilibrium through the energy they transport. Similar results hold for a star with a more general angular velocity field.

The inadequacy of Sweet's analysis arises from the neglect of the departure from spherical symmetry brought about by the currents themselves. Material is transported out of the core at different epochs, and the value, at time  $t$ , of the mean molecular weight  $\mu$  at a particular point of the radiative envelope is the value of  $\mu$  in the core at an earlier time  $(t - \bar{t})$ , where  $\bar{t}$  is the time of flow from the core to the point in question. As  $\bar{t}$  is a function of position, in general a non-spherical  $\mu$ -distribution will be set up, which will react back strongly on the thermal equation, and hence on the forces driving the circulation. It is the object of this paper to combine with Sweet's theory a discussion of this "feed-back" process.

The mechanism of mixing by rotational currents is very delicate, and the detailed theory discussed below is relevant only on the assumption that the radiative envelope does not suffer any local turbulent mixing, tending to smooth out the distribution of matter set up by the currents. The strongly subadiabatic temperature gradient in the envelope is stable even in a star with considerable non-uniformities of angular velocity (12), and most workers assume that no convection occurs within the radiative zone. An exception is Alfvén (13), who suggests that magneto-hydrodynamic waves emanating from the core may bring about local convection even in the stable envelope. However, he brings forward no quantitative arguments, and the possibility will be disregarded in this paper.

In Section 2, Sweet's theory, in which centrifugal force is the only perturbation, is summarized, and in the Appendix it is extended so as to avoid the singularities that appear at the surface of the star, near surfaces of discontinuity within it, and near convective regions. In Sections 3, 4 and 5, the effect on the radiative equation of a non-spherical distribution of matter is determined, and the results applied to a rotating star possessing initially a gravitationally stable  $\mu$ -gradient. The rest of the paper is devoted to an analysis of the evolution of a rotating Cowling model star.

2. *Summary of Sweet's theory.*—We consider a Cowling model star rotating as a rigid body with angular velocity  $\Omega$ ; the theory is easily extensible to other cases. The equations of mechanical equilibrium, and Poisson's equation, are

$$\frac{\partial P}{\partial r} = \rho \frac{\partial \phi}{\partial r} + \rho r \Omega^2 \sin^2 \theta, \quad (1)$$

$$\frac{\partial P}{\partial \theta} = \rho \frac{\partial \phi}{\partial \theta} + \rho r^2 \Omega^2 \sin \theta \cos \theta, \quad (2)$$

$$\nabla^2 \phi = -4\pi G\rho, \quad (3)$$

where  $P$ ,  $\rho$  and  $\phi$  are the perturbed pressure, density and gravitational potential, and  $r$ ,  $\theta$  are respectively central distance and colatitude. Each function is expanded as a series in the perturbing parameter; to the first order,

$$\begin{aligned} P &= P_0(r) + P_1(r, \theta) \cdot \Omega^2, \\ \rho &= \rho_0(r) + \rho_1(r, \theta) \cdot \Omega^2, \\ \phi &= \phi_0(r) + \phi_1(r, \theta) \cdot \Omega^2. \end{aligned} \quad (4)$$

Similarly, the temperature  $T$  is written as

$$T = T_0(r) + T_1(r, \theta) \cdot \Omega^2. \quad (5)$$

$P$  is eliminated from (1) and (2), and  $\partial \rho_1 / \partial \theta$  is substituted from (3).  $\chi \equiv \partial \phi_1 / \partial \theta$  is then given by

$$\chi = r^2(h-1) \sin \theta \cos \theta, \quad (6)$$

where  $h$  satisfies a homogeneous second-order linear equation.  $\chi$  must vanish both at the star's centre and at infinity, while both  $\chi$  and  $\partial \chi / \partial r$  are continuous at the surface. In the present problem,  $\partial^2 \chi / \partial r^2$  is also continuous there because of the continuity of density, in contrast to the problem of a gravitating liquid.

From (3) and (2), and the equation of state,  $\partial \rho_1 / \partial \theta$  and  $\partial T_1 / \partial \theta$  are now found, and substituted in the thermal equation

$$\rho_0 T_0 \frac{v_r}{\mu} \frac{dS_0}{dr} = -\operatorname{div} \mathbf{H}. \quad (7)$$

Here  $S_0$  is the entropy per gram-mole in the unperturbed state,  $v_r$  the vertical component of the circulation velocity and  $\mathbf{H}$  the radiation flux; only first-order terms have been retained. This equation asserts that the rotation causes at each point a net influx of energy of amount  $(-\operatorname{div} \mathbf{H})$ , and that the rate of circulation must be such that just this amount of energy is convected away.

Together with the condition of zero outflow over a sphere,

$$\int_0^\pi v_r \sin \theta d\theta = 0, \quad (8)$$

$v_r$  is given by (6) as

$$v_r = f(r) P_2(\cos \theta) \Omega^2 (LR^5/M^3), \quad (9)$$

where  $f(r)$  is a complicated function that must be tabulated\*, and  $L$ ,  $R$ ,  $M$  are luminosity, radius and mass respectively. The horizontal component velocity is given by the equation of continuity.

The perturbing terms  $\phi_1$ ,  $\rho_1$ , etc., contain also parts independent of  $\theta$ . Thus, for example,

$$\phi_1 = -\frac{1}{3}r^2(h-1)P_2 + k_1(r). \quad (10)$$

\* I am indebted to Dr Sweet for informing me that the "3" in equation 3.8 of his paper (1) should be a "4".

The function  $k_1$  must vanish at infinity, and again, together with its first two derivatives, is continuous at the edge of the star. Also,  $k_1'$  and hence  $k_1$  are zero outside the star; this follows from the constancy of the stellar mass under the perturbation. The parts in (1) and (3) independent of  $\theta$  give equations to the perturbed mean state. In the radiative zone, the part of  $(\text{div } \mathbf{H})$  dependent on  $\theta$  causes the circulation; when this is averaged out, as in (8), we are left with the perturbed mean state energy equation. Together with the perturbed adiabatic condition for the convective core, these equations suffice to determine the change in the mean state brought about by the rotation. To the first order, the equations giving circulation can be separated from those giving the perturbed mean state; in a higher-order theory, however, coupling necessarily arises.

Sweet points out that the difficulties found by previous workers on the problem result from demanding the too stringent condition that the vertical circulation velocity should vanish at the star's surface. He argues that it is sufficient that it be finite at the surface, as the zero density implies that the vertical transport of matter vanishes. But this cannot be the final answer, for the equation of continuity then demands an infinite horizontal component at the surface; in order that the horizontal component be finite, the vertical component must vanish as least as rapidly as the depth beneath the surface. A theory which gives an infinity must be incomplete in some detail.

A similar difficulty arises in a star with a discontinuity in  $\mu$ , such as is assumed to exist in current giant models, with the conditions of continuity of pressure and temperature being preserved by a jump in density. Such a surface cannot be distorted without violating the hydrostatic equation, and so bringing into play restoring gravitational forces. Thus meridional currents cannot cross from one zone into the other, but are deflected horizontally. But the heating and cooling due to rotation must still occur, and at an infinitesimal distance from the discontinuity a finite vertical velocity field exists. The only way of fitting into Sweet's quasi-static theory a zero vertical velocity at the barrier is to let the horizontal component become infinite as the barrier is approached from either side. Physically, this means that the energy available to drive the circulation is not used up, as the motion is constrained by the barrier to be horizontal. There is, to the first order, no horizontal entropy gradient, and so this energy accelerates the material. The only steady state allowed by Sweet's theory unmodified is one with an infinite horizontal component along the barrier.

In fact, the material cannot be accelerated indefinitely; the viscosity of stellar material is finite, and sooner or later the velocity will tend to a finite limit. In the ultimate steady state, the viscosity terms in the equations of motion so modify the temperature field that heating and cooling over the barrier is eliminated. The theory of this process is given in the Appendix. It should be noted that this effect is due to viscous force, which depends linearly on the velocity components, and not on the effect of viscous dissipation on the energy equation, which is quadratic in the perturbation, and can therefore contribute only in a second-order theory. For the same reason, the non-linear inertial terms in the equations of motion are of no help; in the expansion of the circulation velocity in powers of  $\Omega^2$ , each coefficient of the vertical component must vanish at the barrier.

Viscosity is small enough to have negligible effect on the circulation at non-singular points; it is only when the velocity gradient becomes large that it

plays a decisive role. Near a convective zone the polytropic index  $n$  approaches the adiabatic value  $\frac{5}{3}$ . In Sweet's theory the vertical component  $\propto 1/(n - \frac{2}{3})$  and the horizontal component  $\propto 1/(n - \frac{2}{3})^2$ , and so again a large horizontal shearing motion is set up, and the viscosity prevents the velocities from becoming infinite. In all cases the layer in which viscosity acts is very narrow, and, as in hydrodynamic flow theory, will be termed a "boundary layer".

3. *The effect of a non-spherical  $\mu$ -distribution on the radiative equation.*— Consider now the modification of the rotational currents brought about by the unsymmetric nature of the  $\mu$ -distribution to which the rotational currents themselves lead. The distribution in  $\mu = \mu(r, \theta)$  may be regarded as a perturbation from a spherically symmetric distribution  $\mu_0(r)$ . A convenient parameter measuring the perturbation is

$$\frac{\mu(r, \theta) - \mu_0(r)}{\mu_0(r)} \equiv \lambda(r, \theta). \quad (11)$$

Here  $\mu_0(r)$  can be defined simply as the average of  $\mu(r, \theta)$  over a sphere  $r = \text{const.}$ ; or it could be an original spherical distribution perturbed by rotational currents to  $\mu(r, \theta)$ . The only condition imposed is that  $\lambda$  should be small, so that first-order perturbation theory is applicable. Then to the functions  $\rho_0, P_0, \phi_0, T_0$ , there will be added perturbing terms due both to rotation and to the perturbation in  $\mu$ . Since only first-order terms in the two perturbations are retained, the two effects may be simply superposed. Hence, in considering the immediate effects of the perturbation  $\lambda(r, \theta)$ , we shall regard the star as non-rotating.

Let  $\rho_1, P_1, \phi_1$  and  $T_1$  respectively be the perturbing effects of  $\lambda$ . Then the equation of hydrostatic support and Poisson's equation

$$\text{grad } P = (\text{grad } \phi)/\rho, \quad (12)$$

$$\nabla^2 \phi = -4\pi G\rho \quad (13)$$

show that  $\rho_1, P_1, \phi_1$  are spherically symmetric. From the equation of state

$$P = \frac{\mathfrak{R}}{\mu} \rho T \quad (14)$$

it follows that  $T/\mu$  can be written as

$$\{T_0(r) + \bar{T}(r)\}/\mu_0(r), \quad (15)$$

leading to

$$T_1(r, \theta) = \lambda(r, \theta) T_0(r) + \bar{T}(r). \quad (16)$$

The function  $\bar{T}$  is the mean of  $T_1(r, \theta)$  over a sphere only in the case when the mean of  $\lambda$  vanishes.

The first-order effect of the perturbation on the thermal equation is now required. We have

$$-\frac{\text{div } \mathbf{H}}{\frac{4}{3}ac} = \frac{1}{r^2} \frac{\partial}{\partial r} \left( \frac{r^2 T^3}{\kappa \rho} \frac{\partial T}{\partial r} \right) + \frac{1}{r^2 \sin \theta} \frac{\partial}{\partial \theta} \left( \frac{T^3}{\kappa \rho} \sin \theta \frac{\partial T}{\partial \theta} \right), \quad (17)$$

where  $\kappa$  is the opacity. It is supposed that all the energy liberation occurs within the convective core, where the present theory does not apply; then the unperturbed equation of heat flow is

$$T_0' \equiv \frac{dT_0}{dr} = -\frac{\kappa_0 \rho_0 L}{4\pi r^2} \cdot \frac{1}{\frac{4}{3}ac T_0^3}, \quad (18)$$

where  $L$  is the luminosity. Also,  $\kappa$  is taken as a function of  $\rho$  and  $T$  independent of  $\mu$ , as is approximately the case. Thus substitution of the perturbed functions in (17) yields, after simplifying by (18),

$$\frac{\text{div } \mathbf{H}}{L} = \frac{1}{4\pi r^2} \left[ \frac{\partial}{\partial r} \left\{ \frac{\partial}{\partial T_0} \left( \ln \frac{T_0^3}{\kappa_0 \rho_0} \right) (\bar{T} + \lambda T_0) + \frac{\partial}{\partial \rho_0} \left( \ln \frac{T_0^3}{\kappa_0 \rho_0} \right) (\rho_1) \right. \right. \\ \left. \left. + \frac{1}{T_0'} \left( \bar{T} + \lambda T_0' + \frac{\partial \lambda}{\partial r} T_0 \right) \right\} + \frac{T_0}{T_0'} \frac{1}{r^2} \frac{1}{\sin \theta} \frac{\partial}{\partial \theta} \left( \sin \theta \frac{\partial \lambda}{\partial \theta} \right) \right]. \quad (19)$$

The spherically symmetric part of this expression corresponds to an expansion or contraction as a whole of the sphere considered, and is of no interest for the problem of meridional circulation. To the present order of working, the spherical part of a perturbation alters the structure of the star, while the rest gives rise to circulation, as discussed in the rotational case. Thus (*cf.* Sweet's equation (3.6)) the perturbation in  $\mu$  leads to a motion with a vertical component  $v_r^\mu$ , where

$$v_r^\mu \frac{(n - \frac{3}{2})}{(n+1)} \cdot \rho_0 g_0 = - \frac{L}{4\pi r^2} \left[ \frac{\partial}{\partial r} \left\{ \frac{\partial}{\partial T_0} \left( \ln \frac{T_0^3}{\kappa_0 \rho_0} \right) \lambda T_0 + \left( \lambda + \frac{T_0}{T_0'} \frac{\partial \lambda}{\partial r} \right) \right\} \right. \\ \left. + \frac{T_0}{T_0'} \frac{1}{r^2} \frac{1}{\sin \theta} \frac{\partial}{\partial \theta} \left( \sin \theta \frac{\partial \lambda}{\partial \theta} \right) \right], \quad (20)$$

$g_0 = -\phi_0'$  is the local value of gravity in the unperturbed star and  $n$  is the local value of the polytropic index. The horizontal component  $v_\theta^\mu$  is then found from the equation of continuity

$$v_\theta^\mu = - \frac{1}{\rho r \sin \theta} \frac{\partial}{\partial r} \left[ \rho r^2 \int_0^\theta v_r^\mu \sin \theta d\theta \right]. \quad (21)$$

The term  $\partial \rho / \partial t$  should strictly appear in the equation of continuity; however, if the changes in  $\rho$  are due ultimately to transport of matter by currents, this term will involve  $\mathbf{v} \cdot \text{grad } \mu$ , where  $\mathbf{v}$  is the current velocity. As  $\mathbf{v}$  is of order  $\lambda$ , this term is of second order, and so is neglected.

In the general case currents arise both from the non-spherical  $\mu$ -distribution and from the rotation. The total circulation is found by adding vectorially the velocity  $\mathbf{v}^\mu$  just found to Eddington's velocity  $\mathbf{v}^\Omega$ .

4. *Variation of  $\mu$  with time.*—The equation of convection in the radiative zone is

$$\frac{d\mu}{dt} = \frac{\partial \mu}{\partial t} + (\mathbf{v}^\Omega + \mathbf{v}^\mu) \cdot \text{grad } \mu = 0. \quad (22)$$

It is to be noted that the theory ceases to be linear at this point, for the changes in  $\mu$  are brought about by the transport of variations in  $\mu$  by currents which themselves depend on the variations in  $\mu$ .

$\lambda$  is now expanded in a series of Legendre functions:

$$\lambda = a_0 + a_2 P_2 + a_4 P_4 + \dots, \quad (23)$$

the odd terms being omitted, as we are mainly interested in perturbations symmetric about the equator as well as about the axis of rotation.

If, as is assumed,  $\Omega$  is uniform throughout the star, the vertical component of  $\mathbf{v}^\Omega$  contains only a  $P_2$  term. However,  $v_r^\mu$  in general involves an infinite

number of Legendre functions. In a star with opacity obeying the unmodified Kramers law,  $v_r^\mu$  is given by

$$\begin{aligned} v_r^\mu = & \frac{(n+1)}{(n-\frac{3}{2})} \cdot \frac{1}{\rho_0 g_0} \cdot \frac{L}{4\pi r^2} \left[ P_2 \left\{ \frac{6a_2}{r^2} \frac{T_0}{T_0'} - \left( \frac{15}{2} + \left( \frac{T_0}{T_0'} \right)' \right) a_2' - \frac{T_0}{T_0'} a_2'' \right\} \right. \\ & \left. + P_4 \left\{ \frac{20a_4}{r^2} \frac{T_0}{T_0'} - \left( \frac{15}{2} + \left( \frac{T_0}{T_0'} \right)' \right) a_4' - \frac{T_0}{T_0'} a_4'' \right\} \dots \right], \quad (24) \end{aligned}$$

with corresponding terms in  $v_\theta^\mu$  involving  $(P_{2n-1} - P_{2n+1})/\sin \theta$ .

The resultant vertical velocity function is written as

$$v_r = f_2 P_2 + f_4 P_4 + \dots \quad (25)$$

In the present case  $f_2(r)$  is the sum of an  $\Omega$ -velocity and a  $\mu$ -velocity, while the other terms are just the respective parts of (24). Then, from (22), the rate of change of the  $P_0$  component of  $\lambda$  is given by

$$(\rho r^2) \mu_0 \dot{a}_0 = - \left\{ \sum_{s=1}^{\infty} (\rho r^2 \mu_0 a_{2s} f_{2s})' / (4s+1) \right\}. \quad (26)$$

The equations for  $\dot{a}_2$ ,  $\dot{a}_4$ , etc. are much more complicated. It is reasonable, as a first attempt, to neglect all components but  $a_0$  and  $a_2$ . The equations governing the variation in  $\lambda$  throughout the motion are then

$$5\mu_0 \dot{a}_0 (\rho r^2) = - \{ (\rho r^2) f_2 \mu_0 a_2 \}', \quad (27)$$

$$\mu_0 \dot{a}_2 = - \left\{ f_2 \left[ (\mu_0 (1+a_0))' + \frac{2}{7} (\mu_0 a_2)' \right] + \frac{1}{7} \frac{(a_2 \mu_0)}{\rho r^2} (\rho r^2 f_2)' \right\}. \quad (28)$$

However, whereas (27) may be expected to give results qualitatively correct and of the right order of magnitude, use of (28) may in some cases lead to misleading results. The last term in the brackets in this equation is proportional to  $-v_\theta$ , and indicates that a positive horizontal component of velocity tends to increase  $a_2$ , i.e. to increase the variation of  $\mu$  over a sphere  $r=\text{const}$ . Simple physical considerations show, however, that a sufficiently great horizontal velocity, whatever its sign, tends to reduce  $a_2$ . This indicates the importance of the terms neglected in (28); in fact, in Section 10, this equation is shown to imply an incorrect sign for  $a_0'$  in part of the star. However, the principal results may be obtained by use of (27) alone.

*5. Direction and magnitude of the  $\mu$ -currents.*—The first question of interest is whether the  $\mu$ -currents choke back or augment the Eddington circulation. The function  $f_2$  giving the vertical motion can, by (24), be written as

$$f_2(r) = p(r) + \frac{L}{4\pi r^2} \frac{(n+1)}{(n-\frac{3}{2})} \cdot \frac{1}{\rho_0 g_0} \left\{ \frac{6}{r^2} \frac{T_0}{T_0'} a_2 - \frac{d}{dr} \left( \frac{T_0}{T_0'} a_2' \right) - \frac{15}{2} a_2' \right\}, \quad (29)$$

where  $p(r)$ , proportional to  $\Omega^2$ , is given by Sweet's theory, and the remaining terms give the  $\mu$ -currents. We have to determine the sign of the  $a_2$ -term in this.

Now  $\mu_0' < 0$ , since the  $\mu_0$ -gradient is due to the progressive transmutation of hydrogen into helium; a positive  $\mu_0$ -gradient is in any case unstable, as follows from a simple application of Archimedes' Principle to a small vertical disturbance. The  $a_2$ -distribution is due to the distortion of the surfaces of constant  $\mu_0$  by the circulation, bringing heavy material up near the axis of rotation; thus  $a_2 > 0$ . Accordingly, since  $T_0' < 0$ , the first term in the brackets in (29) is negative, and its effect is to choke back the rotational currents. The other terms in the brackets involve  $a_2'$ ; thus, if  $a_2$  does not vary too greatly from point to point, the effect of

the  $\mu$ -currents is to reduce the circulation. The term  $-\frac{15}{2}a_2'$  increases the choke-back effect if  $a_2$  increases outwards; the remaining term is smaller unless  $a_2'$  alters very rapidly.

These conclusions can be put in another way. Suppose that locally  $a_2 \sim T_0^\eta$ ; then the  $a_2$ -terms in (29) produce a reduction in the circulation if

$$\eta(\eta + \frac{15}{2}) \leq \frac{6}{r^2} \left( \frac{T_0}{T_0'} \right)^2. \quad (30)$$

The expression on the right has been calculated for a Cowling model star, using Miss Gardiner's tables for the model (14). The range within which  $\eta$  must lie for a reduction in the circulation is shown in Table I.

TABLE I

$z$	Range of $\eta$
2	$-8.32 \leq \eta \leq 0.82$
3	$-7.82 \leq \eta \leq 0.32$
4	$-7.65 \leq \eta \leq 0.153$
5	$-7.57 \leq \eta \leq 0.066$
7 (edge of star)	$-7.50 \leq \eta \leq 0$

Thus a reduction in circulation is secured if  $a_2$  increases at any reasonable rate, or decreases fairly slowly, as  $r$  increases.

As an example, consider a star which possesses initially a negative  $\mu_0$ -gradient (without inquiring as to how the gradient has been built up). Then except near a convective or other singular region both vertical and horizontal components of velocity are of the same order; hence if  $|\mu_0'|$  is not too small, equation (28) reduces to

$$\mu_0 \dot{a}_2 = -\mu_0' f_2, \quad (31)$$

where  $f_2(r)$  is given by (29). Hence, after time  $t$ ,

$$a_2 = -(\mu_0'/\mu_0) \cdot p(r) \cdot t \quad (32)$$

approximately. The function  $p(r)$  is slowly varying, and so if  $\mu_0'$  does not change too rapidly with distance, the distortion of the surfaces of constant  $\mu_0$  by the  $\Omega$ -currents induces  $\mu$ -currents which oppose further distortion; if  $|\mu_0'|$  is large enough, the motion may be damped out altogether. Equation (29) shows that the  $\mu$ -currents reduce the circulation very considerably if

$$a_2 \sim p(r) \cdot \frac{4\pi r^4}{6L} \cdot \frac{(n - \frac{3}{2})}{(n + 1)} \cdot \frac{1}{\rho_0 g_0} \cdot \left( -\frac{T_0'}{T_0} \right). \quad (33)$$

On substituting numerical values, this gives  $a_2 \sim 1.5 \times 10^{-6} (\bar{\Omega})^2$ , where  $\bar{\Omega}$  is the angular velocity in solar units. (The solar angular velocity is taken as  $2.85 \times 10^{-6}$  radians/sec.) With normal angular velocities this is quite small; it corresponds to a distortion of the surfaces  $\mu_0 = \text{constant}$  through a distance  $a_2 P_{2\mu_0} |\mu_0'|$ , which is also small if  $|\mu_0'|$  is at all appreciable. This is sufficient to show how profound is the effect of asymmetries in  $\mu$  on the thermal equation.

The  $\mu_0$ -distribution through the star may be such as to damp out the rotational currents through a part of the star only. Thus, for example, consider a star with a  $\mu_0$ -gradient which is both large and slowly varying throughout a large zone, but which gradually tapers off to zero on both sides. The circulation in the zone of varying  $\mu_0$  rapidly distorts the surfaces of constant  $\mu_0$ , and leads to an  $a_2$ -distribution which, like the  $\mu_0$ -gradient, is large and slowly varying.

Such an  $a_2$ -distribution will be able effectively to stop the circulation in the zone of varying  $\mu_0$ ; but away from this zone the  $\mu$ -velocities become progressively weaker, until the  $\Omega$ -currents cease to be inhibited at all and Sweet's theory applies. Hence there must be critical radii between which the circulation effectively stops, while outside them the  $\Omega$ -currents sweep away the material with small initial  $\mu_0$ -gradient. Material brought along by the  $\Omega$ -currents in the zones outside cannot flow past the barriers at the critical radii, and so must be deflected horizontally. Thus outside the barriers Sweet's currents circulate, with boundary layers reducing the vertical velocities to zero at the barriers; the star settles down into a quasi-static state, with the region of high  $\mu_0$ -gradient separating the two zones of circulation.

The discussion based on (31) breaks down near the convective core, where the horizontal component of velocity is large compared with the vertical, and where material of high  $\mu$  is flowing in from the core. However, some information as to the  $a_2$ -distribution set up near the core may be gained by integrating (27) from a radius  $r$  to the surface  $R$ :

$$\rho r^2 f_2 \mu_0 a_2 = 5 \int_r^R \mu_0 \dot{a}_0 \rho r^2 dr. \quad (34)$$

This equation may be interpreted as indicating that the time-variation of  $\mu$  outside the sphere of radius  $r$  is due to the radial flow, proportional to  $f_2$ , carrying heavy material across this sphere. Near the convective core the Sweet velocity is large, and  $f_2$  can be expected also to be large; thus  $a_2=0$  at the boundary of the core, and increases outwards. Thus unless  $a_2''$  is very large and positive, the  $\mu$ -currents set up by the material flowing out of the core may be expected to impede the flow near the core.

The results of this section and of the Appendix show how powerful is the influence of previously existing non-uniformities of  $\mu$  on the meridional circulation; a naïve application of the results found by Sweet and Öpik is liable to be misleading. Thus, for example, in a recent paper (15) the present writer has considered the distribution of accreted matter through a white dwarf. It was shown that the simple Eddington currents are negligibly slow, and it was concluded, correctly, that mixing is therefore negligible; but, in fact, it is now seen that the circulation must be divided into two separate zones by the discontinuity in composition.

*6. Rotational currents in a Cowling model star; the equations of circulation.*—The most important application of the theory of this paper is to the  $\mu$ -distribution set up by rotational currents within a Cowling model star. In the convective core  $\mu$  increases with time; the rotational currents drag material of high  $\mu$  into the radiative zone, and also slow down the increase of  $\mu$  within the core by replenishing it with hydrogen-rich material. But as explained above, the inevitable asymmetry of the  $\mu$ -distribution must affect the driving velocity, so that both qualitatively and quantitatively the resulting circulation will differ from that predicted by Sweet.

In this paper the star is at first taken as rotating uniformly; later, the possibility is mentioned that the star may consist of a uniformly rotating bulk, with outer layers rotating considerably slower. In either case the angular velocity field is taken as constant in time, so that the rotational current velocities also remain constant in time. The conditions for this to hold are discussed in Section II.

The equations to the circulation are (27) and (28), with the unperturbed mean molecular weight  $\mu_0$  a constant. These equations then become

$$5\dot{a}_0 = - \frac{I}{\rho r^2} \frac{d}{dr} (\rho r^2 f_2(r) a_2), \quad (35)$$

$$\dot{a}_2 = - \left\{ f_2(r)(a_0' + \frac{2}{7}a_2') + \frac{1}{7} \frac{a_2}{\rho r^2} \frac{d}{dr} (\rho r^2 f_2(r)) \right\}, \quad (36)$$

where  $f_2(r)$  is defined in (29). Equations (35) and (36) can be combined to give, as an alternative to (36),

$$\dot{a}_2 - \frac{5}{7}\dot{a}_0 = -f_2(r)(a_0' + \frac{1}{7}a_2'). \quad (37)$$

In order to isolate the driving parameter  $\Omega^2$ , and to simplify the analysis, the following transformations are made. The non-dimensional radial coordinate used by Cowling (11) is introduced by the substitution

$$r = \epsilon z, \quad (38)$$

where

$$\epsilon^2 = (5\pi T_c / 8\pi\mu G\rho_c). \quad (39)$$

$\rho_c$  and  $T_c$  are the unperturbed central density and temperature respectively. The quantities  $y$ ,  $w$  and  $m$  are defined by

$$\rho = \rho_c y, \quad (40)$$

$$T = T_c w, \quad (40)$$

$$M(r) = 4\pi\rho_c\epsilon^3 m.$$

The driving velocity  $p(r)$  is then written as

$$p(z) \cdot (\bar{L} \bar{\Omega}^2 \bar{R}^5 / \bar{M}^3), \quad (41)$$

where quantities with bars have been expressed in solar units, and  $p(z)$  is a tabulated function of order  $10^{-10}$  cm/sec through most of the star. In addition,  $a_0$  and  $a_2$  are put equal to  $\gamma A_0$  and  $\gamma A_2$  respectively, where

$$\gamma = \left( \frac{16\pi^2 \rho_c^2 G \epsilon^4}{10^{10} L} \right) \cdot \left( \frac{\bar{L} \bar{\Omega}^2 \bar{R}^5}{\bar{M}^3} \right) = 7.27 \times 10^{-6} \left( \frac{\bar{\Omega}^2 \bar{R}^3}{\bar{M}} \right). \quad (42)$$

Then (35) and (37) reduce to

$$5\dot{A}_0 \lambda = - \frac{1}{yz^2} \{ \beta (F + CA_2 + DA_2' + EA_2'') \}', \quad (43)$$

$$(\dot{A}_2 - \frac{5}{7}\dot{A}_0) \lambda = - \frac{\beta}{yz^2} (F + CA_2 + DA_2' + EA_2'')(A_0' + \frac{1}{7}A_2'), \quad (44)$$

where

$$\beta = \frac{(n+1)}{(n-\frac{3}{2})} \cdot \frac{z^2}{m}, \quad (45)$$

$$5\lambda = 5\epsilon \frac{\bar{M}^3 \cdot 10^{10}}{\bar{L} \bar{R}^5 \bar{\Omega}^2} = 4.96 \times 10^{20} \bar{M}^3 / \bar{R}^4 \bar{L} \bar{\Omega}^2, \quad (46)$$

and

$$F = 10^{10} p(z) \cdot (n - \frac{3}{2})ym/(n+1),$$

$$C = -6 \left( -\frac{w}{w'} \right) / z^2,$$

$$D = - \left( 7.5 - \left( -\frac{w}{w'} \right)' \right), \quad (47)$$

$$E = \left( -\frac{w}{w'} \right).$$

The factor  $10^{10}$  in  $F$ ,  $\gamma$  and  $\lambda$  is chosen so that  $F$ ,  $C$ ,  $D$ ,  $E$  are all of order unity through the bulk of the star. The expression  $(F + CA_2 + DA_2' + EA_2'')$  is proportional to the radial part of the vertical component of the velocity.

It is assumed explicitly through the following work that the stellar functions  $y$ ,  $m$ , etc., and hence also the circulation functions  $F$ ,  $C$ ,  $D$ ,  $E$ , remain unchanged functions of  $z$  as changes in  $\mu$  are brought about by the circulation. This is certainly only an approximation, as the altered structure of the star will react back on the driving velocity. However, it is shown below that if circulation is able to persist at all it will tend to bring the star into the Hoyle-Lyttleton giant state, which can be looked upon as effectively a Cowling model star with a highly distended envelope superimposed. Hence the circulation in the inner zone, which is our main concern, will not alter sensibly on account of changes in the structure of the star.

*7. Quasi-static circulation.*—The  $\Omega$ -current streamlines calculated by Sweet traverse the whole star from the convective core to the surface. If the feed-back terms are neglected, the variations in  $\mu$  through the star are due simply to the different times of flow from the core along the  $\Omega$ -current streamlines:

$$\mu(z, \theta) = \mu_c(t - \bar{t}(z, \theta)) \quad (48)$$

for  $t \geq \bar{t}$ . Here the suffix  $c$  refers to the core and  $\bar{t}(z, \theta)$  is the time for matter to reach  $(z, \theta)$  from the core along the relevant streamline. The luminosity changes only slowly with time, so  $d\mu_c/dt$  is a constant. Provided, then, that  $\bar{t}$  is finite for all  $(z, \theta)$ , once matter has had time to circulate once round the star,  $d\mu/dt$  will be constant everywhere. This implies that  $\dot{A}_0$  is a constant, and  $\dot{A}_2$  etc., are zero. Such a circulation will be called "quasi-static".

On Sweet's theory, a star will remain "homogeneous" if the variations in  $\mu$  brought about by flow along the  $\Omega$ -current streamlines are not large enough to have any sensible effect on the structure of the star; otherwise it will become "non-homogeneous". The present theory shows, however, that the streamlines themselves may be profoundly modified by the distribution of matter, and it may not be assumed *a priori* that matter from the core will reach the edge of the star even if sufficient time be allowed. It is the principal aim of the rest of this paper to estimate as a function of  $\Omega$  the proportion of the stellar mass through which currents from the core may circulate continuously.

Consider now the flow due to the joint effect of  $\Omega$ -currents and  $\mu$ -currents. Equation (48) still holds, but  $\bar{t}(z, \theta)$  must be measured along the joint streamlines; and as  $\mu(z, \theta)$  changes, so will  $\bar{t}$  in general. We are interested, however, not in the details of the initial motion but in the ultimate state to which the circulation approximates. One possible assumption is that the flow settles down into a quasi-static state as defined above, except that the zone of circulation is not assumed to extend throughout the star, but only up to a radius  $z'$ . This implies again that within this zone  $\dot{A}_0$  is a constant, and  $\dot{A}_2$ ,  $\dot{A}_4$ , etc., zero; as the driving velocity depends only on  $A_2$ , etc., such assumptions are self-consistent. The interior of the sphere of radius  $z'$  is called the "mixing zone". The further assumption is made implicitly that  $\bar{t}$  is everywhere finite within the mixing zone; this will be reviewed later.

Since we are interested less in the details of the circulation than in the effect of the currents on the structure of the star, the quasi-static case is the one best worth considering. For suppose that after a certain radius  $\bar{z}$ ,  $\dot{A}_0$  drops off

sensibly from a uniform value. Relation (48) must still hold for a region connected with the core within a finite time, and so it follows that the average of  $d\bar{t}/dt$  over a sphere must be positive after  $\bar{z}$ . Thus the time taken by matter to reach points beyond  $\bar{z}$  increases steadily, and this can only mean that the currents themselves build up such a  $\mu$ -distribution as to cause them to decay after the radius  $\bar{z}$ . The value of  $\dot{A}_0$  beyond  $\bar{z}$  will therefore decrease still further with time, so that the decay progressively increases. Hence it is only in regions of quasi-static circulation that rotational currents can be expected to have an important influence on the evolution of the star.

Equations (43) and (44), with  $\dot{A}_0$  constant and  $\dot{A}_2$  zero, give

$$\beta A_2 [F + CA_2 + DA_2' + EA_2''] = (5\dot{A}_0\lambda)(m' - m), \quad (49)$$

$$A_0' = -\frac{1}{7} \left( A_2' - \frac{A_2yz^2}{(m' - m)} \right). \quad (50)$$

The constant of integration  $m'$  is the non-dimensional mass of the mixing zone; the equation of mixing (49) states that across any sphere of radius  $z$  within the zone the net flow of molecular weight is sufficient to increase  $A_0$  at the rate  $\dot{A}_0$  within a mass  $(m' - m)$ .

The first problem is to determine the relation between  $m'$  and  $(5\dot{A}_0\lambda)$ , i.e. to find for what values of the spin quasi-static flow is possible within a sphere of mass  $m'$ . Before (49) can be solved, however, the boundary conditions must be determined. At the surface of the core  $A_2$  must vanish, as the horizontal component of the velocity becomes large there compared with the vertical. This condition is consistent with (49), as the term  $1/\beta \propto (n - \frac{3}{2})$  and so vanishes at the core surface. The condition at  $z'$ , however, requires more thought.

Consider first values of  $m'$  less than the stellar mass. Then at  $z'$  either  $A_2 = 0$  or  $(F + CA_2 + DA_2' + EA_2'') = 0$ . (It is easy to verify that solutions behaving near  $z'$  like  $(z' - z)^\eta$  with  $0 < \eta < 1$ , do not exist.) Now imagine a barrier placed at  $z'$  so as to prevent flow beyond this sphere—either a discontinuity in  $\mu$  at  $z'$ , or a region beyond  $z'$  in which an  $A_2$ -distribution cancels out the  $\Omega$ -currents. In a star with infinite spin the  $\mu$ -current terms disappear, and there is no question of any choking of the circulation; the currents flow up to the barrier and are deflected there. The vertical velocity component remains finite at the barrier, and so from (49)  $A_2$  vanishes there.

Now let the spin of the star be gradually reduced, so that the parameter  $(5\dot{A}_0\lambda)$  increases. The feed-back terms begin to modify the circulation, but initially there will be solutions of (49) satisfying the conditions of vanishing  $A_2$  at each end of the range. Sooner or later, however, the equation will cease to have a solution satisfying these conditions, implying that  $\dot{A}_0$  cannot remain constant throughout the zone. It is this limiting solution in which we are particularly interested. The physically relevant solutions of (49), for given  $m'$ , must form a continuous sequence in  $(5\dot{A}_0\lambda)$ , and so the condition  $A_2 = 0$  is the correct one to use. Near  $z = z'$ ,  $A_2$  behaves as  $k(z' - z)$ , and it is possible, *a priori*, that the constant of proportionality  $k$  may tend to infinity as the limiting value of  $(5\dot{A}_0\lambda)$  is approached, so that it is in fact the vertical velocity and not  $A_2$  that vanishes at  $z'$  in the limiting solution; but if this is so, the solution of the equations will produce this result, and no *a priori* assumptions about the velocity at  $z'$  are needed.

However, it must be remembered that the problem just summarized is a problem with a constraint, namely a barrier at  $z'$ . A Cowling model star has no barriers except those built up by the circulation itself, and so interpretation of the results will need care. This is further discussed in Section 9.

If  $m'$  is the mass of the whole star, the same argument applies, and  $A_2=0$  is again the correct boundary condition to use. In this case, of course, there is no need to introduce an artificial barrier. From (47) and (49), it follows that  $A_2=k(z'-z)^{21/8}$  near the edge of the star—the feed-back currents completely dominate the  $\Omega$ -currents, and give rise to an infinite positive vertical component of velocity. The constant  $k$  remains finite for all finite values of  $(5\dot{A}_0\lambda)$ , and so in this case we may anticipate that as the limiting value of  $(5\dot{A}_0\lambda)$  is approached, the velocity remains non-zero (and, in fact, infinite).

It has already been remarked in Section 2 that any infinities given by the theory can and must be eliminated by the action of viscosity within a boundary layer. However, the zone in which the simple theory breaks down is very narrow, and this correction is negligible when considering the properties of the circulation as a whole (*cf.* Section 10).

The parameter characterizing the particular quasi-static circulation is  $(5\dot{A}_0\lambda)$ , which by (42) and (46) can be expressed as

$$10^{-2} \left( \frac{\bar{M}}{\bar{R}} \right) / m' q^2, \quad (51)$$

where  $\bar{M}$  and  $\bar{R}$  are mass and radius in solar units and  $q$  is the ratio of centrifugal to gravitational force at the equator on the surface. Use has been made here of the fact that in the conversion of hydrogen to helium,  $\frac{1}{125}$  of the mass is available for liberation as energy. The quantity  $m'$  appears explicitly because the rate of increase of  $\mu$  in the core depends on the mass of material circulating, that is, on the mass of the mixing zone, and not just on the mass of the convective core. The angular velocity appears raised to the fourth power. This is due to the non-linearity of the problem; for if  $\Omega^2$  is doubled, for example, not only is the driving velocity doubled, but the feed-back terms are halved, as only half the time has been available for changes in  $\mu$  to take place in the core.

It is seen from (51) that the theory is not quite homology-invariant, in that the value of  $q$  giving the same amount of mixing varies slightly with mass: with  $\bar{R} \propto \bar{M}^{0.7}$ ,  $q$  varies as  $\bar{M}^{0.15}$ . This is because the driving velocity, which is proportional (16) to  $\Omega^2 r^3/GM(r)$ , is not itself homology-invariant.

According to the theory without  $\mu$ -currents, the efficiency of mixing between core and envelope is measured simply by the velocity of the  $\Omega$ -currents, which by (41) is proportional to  $\bar{\Omega}^2 \bar{R}^8 \bar{L}/\bar{M}^3$ . From this it follows that if a star in the course of its evolution changes its dimensions at all, the mixing efficiency remains effectively the same; for  $\bar{\Omega}^2 \bar{R}^4$  must remain nearly constant, by conservation of angular momentum, and so the velocity is proportional to the radius, implying that the time of flow of the  $\Omega$ -currents is unaltered. On the present theory, however, the efficiency of mixing is measured by the size of the parameter  $(5\dot{A}_0\lambda)$ , each value of which is shown to define a mixing zone. This parameter varies as  $\bar{R}\bar{M}^3/\bar{\Omega}^4\bar{R}^8$ , which in a star of given angular momentum varies as  $\bar{R}$ . Thus if the star contracts during the course of its evolution,  $(5\dot{A}_0\lambda)$  drops, and the mixing efficiency of the currents increases. The physical reason is that, from (24),

$v_r'' \propto \bar{R}^2$ , whereas  $v_r^\Omega \propto \bar{R}$ ; thus as the star contracts, the feed-back terms decrease more rapidly than the driving velocity, so that mixing becomes easier.

8. *Solutions of the equation of mixing.*—The simplest case to discuss is the limiting one with the mixing zone coinciding with the convective core, and so containing 0·15 of the stellar mass. It is found convenient to introduce here the function  $x$  defined by

$$xF = F + CA_2 + DA_2' + EA_2''. \quad (52)$$

$x$  is just  $(v_r^\Omega + v_r'')/v_r^\Omega$ , and so measures the effect of the  $\mu$ -current terms on the current velocity.

Then from (49) and the two boundary conditions,

$$A_2 = \frac{(5\dot{A}_0\lambda)}{x} \cdot (z' - z)(z - z') \cdot \left( \frac{dn}{dz} \cdot \frac{m}{(n+1)z^2} \cdot \frac{yz^2}{F} \right), \quad (53)$$

where  $z'$  coincides with  $z_c$ , the radius of the core. Then  $A_2$  and  $A_2'$  both vanish, and

$$A_2'' = -2 \frac{dn}{dz} \cdot \frac{m}{(n+1)} \cdot \frac{y}{F} \cdot \frac{(5\dot{A}_0\lambda)}{x}. \quad (54)$$

From (52),

$$xF = F + EA_2'' = F - \frac{2En'my}{(n+1)F} \cdot \frac{(5\dot{A}_0\lambda)}{x}, \quad (55)$$

and so

$$x = \frac{1}{2} \left[ 1 + \left\{ 1 - \left( \frac{8En'my}{(n+1)F} \right) (5\dot{A}_0\lambda) \right\}^{1/2} \right], \quad (56)$$

where values at  $z_c$  are used for the quantities in parentheses. There is no ambiguity of sign in the solution, for as  $\Omega^2 \rightarrow \infty$ ,  $x$  must approach unity, as the  $\mu$ -currents then become negligible; to ensure this, the positive sign must be taken in (56). Thus (56) provides an immediate discriminant for material to be able to escape from the core. It is to be noted that in the limiting case the vertical component of velocity is reduced not to zero but to just half its rotational value.

Inserting numerical values in (56), it is found that  $(5\dot{A}_0\lambda) = 0\cdot05733$ . Taking as a typical case a star with  $\bar{M} = 5$ , (51) gives that  $q = 0\cdot96$ , implying that on the surface the equatorial value of centrifugal force nearly equals gravity.

This rather startling result merits some comment. The velocity of the rotational currents at any point of the star is proportional (16) to  $\Omega^2 r^3/GM(r)$ , and with  $\Omega^2$  constant this decreases by a factor of about 30 from the surface to the core. But at the surface  $\Omega^2 R^3/GM(R) = q$  is limited to be  $\ll 1$  by the condition that the star be rotationally stable, so that the  $\Omega$ -current velocities near the core are correspondingly limited, and just at the region where the choking effect of the  $\mu$ -currents is strongest. The result just found means that no uniformly rotating star can be rotationally stable and also suffer any mixing between core and envelope.

In this paper attention is confined to Sweet's driving velocity function, which assumes  $\Omega$  constant; it is quite permissible, however, to imagine the inner portions of a star to be rotating uniformly at a high enough rate for some mixing to occur, while the outer regions rotate slowly enough to ensure stability at the surface. In the following work the parameter  $q$ , representing conditions at the surface of a uniformly rotating star, will still be used, but it must be borne in

mind that if the theory is to be physically relevant, the high value of the angular velocity must be confined to the inner regions. The conditions for this to be possible will be discussed in Section 11; meanwhile, this first result shows very strikingly the difficulties that are encountered by the theory of rotational mixing between core and envelope.

The next cases considered were those with  $z' = 1.3$  and  $1.5$ ; the mixing zones then contain respectively 0.18 and 0.26 of the stellar mass. For each value of  $z'$ , different values of  $(5\dot{A}_0\lambda)$  were assumed and the equation of mixing (49) was integrated from both ends of the range simultaneously, using various values for  $x$  at  $z_e$  and  $z'$ . At a convenient point within the range two graphs of  $A_2$  against  $A_2'$  were plotted, the variable parameters being the two values of  $x$ .

For  $z' = 1.3$ , the two graphs were found for small enough  $(5\dot{A}_0\lambda)$  to intersect at two points (corresponding roughly to the positive and negative signs in (56)). The critical value of  $(5\dot{A}_0\lambda)$  is given by the coincidence of the two solutions. One sequence of solutions is again rejected, as it gives  $x$  tending to zero instead of to unity as  $(5\dot{A}_0\lambda)$  tends to zero. In each member of the physically relevant sequence,  $x$  decreases monotonically from  $z_e$  to  $z'$ . The remarkable result is found that the critical value of  $(5\dot{A}_0\lambda)$  gives from (51) a value of  $q$  smaller by a factor of about 0.96 than the limiting value of  $q$  found above for  $z' = z_e$ .

In the case  $z' = 1.5$  the details have changed somewhat. The two graphs now have three intersections for small enough  $(5\dot{A}_0\lambda)$ , but two of them may be rejected, again because of their behaviour as  $q$  varies. The third is the physical solution; it merges into one of the others at the critical value of  $(5\dot{A}_0\lambda)$ , which this time gives for  $q$  a value slightly greater—by a factor of about 1.025—than that found for  $z' = z_e$ . The function  $x$  now behaves differently; in the critical case it begins by decreasing from about 0.65 at  $z_e$  and then increases to about 2.5 at  $z'$ .

For larger values of  $z'$  results hold that are similar to those for  $z' = 1.5$ . In each case there exists a critical value of  $(5\dot{A}_0\lambda)$  which is considerably smaller than the value 0.05733 found for  $z' = z_e$ , but when the larger mass of the mixing zone is taken into account, as in (51), the critical value of  $q$  is found to be only very slightly larger than 0.96. The minimum value of  $q$  increases monotonically with  $m'$ ; for  $m' = m_s$  (the non-dimensional stellar mass), Cowling estimated that the minimum value exceeds 0.96 by a factor of about 1.2. In all cases the variation in  $x$  follows the same pattern—a drop from  $x_e$  to a minimum value near  $x = 1.4$ , and then an increase outwards.

Further integrations for  $z'$  near 1.4 show that the critical value of  $q$  reaches again the value 0.96 for  $z' \approx 1.46$ . Also, it is for a value of  $z'$  in this neighbourhood that the function  $x$  ceases to decrease monotonically outwards from the core, but acquires a minimum in the neighbourhood of  $z = 1.46$ .

The general behaviour of the solutions is due to the form of the driving function  $p(r)$ . This is effectively the product of  $1/(n - \frac{3}{2})$  and  $\Omega^2 r^3/GM(r)$ , the first of which falls off rapidly near the core from infinity to a nearly constant value, while the second increases monotonically outwards. Together these functions account for the minimum in  $p(r)$ , which in turn produces the minimum in  $x$ . The extreme sensitivity of the mass of the mixing zone to values of  $q$  greater than 0.96 is again due ultimately to the functional form of  $p(r)$ , in that the  $\mu$ -currents induced by  $p(r)$  lead to an enhancement of the velocity on the other side of the minimum.

9. *Interpretation of the results.*—Consider first a star with the parameter  $q$  smaller than 0.96, the critical value found above for the case  $m' = m_c$ . From the form of the solution (56) it is seen that the value of  $(5\dot{A}_0\lambda)$  must begin to decrease a small distance away from the core, and, as pointed out in Section 7, such a decrease corresponds to a decay of current velocities which becomes progressively more pronounced with time. Thus for  $q$  less than the critical value 0.96, the  $\Omega$ -currents are checked as soon as they emerge from the core: the induced  $\mu$ -currents are strong enough to choke the circulation, and a barrier is built up which prevents any further exchange of matter between core and envelope. The circulation in the envelope remains of Sweet's type except near the core, where the barrier diverts the descending flow horizontally. Hence the only hydrogen available for energy liberation in this stage of the star's evolution is that contained in the core.

Now imagine  $q$  at the critical value 0.96. It was found above that with this value quasi-static circulation can occur in any zone between  $z' = z_c$  and  $z' = 1.46$ . Thus matter will be able to stream out of the core and reach  $z' = 1.46$ . The feed-back terms cut down the velocity, but are not strong enough in this range to choke the flow; the numerical results mean physically that the  $\mu$ -currents, which depend, roughly speaking, on differences between  $\mu$  at pole and equator, do not for this value of  $q$  become too powerful anywhere, *provided the motion is restricted to a sphere with  $z' \leq 1.46$* . A previously existing barrier at  $z' = 1.46$  would divert the flow horizontally, and so prevent the  $\mu$ -currents from becoming too strong. But a Cowling model star contains no barriers initially, and the flow can be constrained only by barriers that it builds up for itself. Also, at  $z' = 1.46$  the matter has a non-vanishing vertical component of velocity, and so in the absence of a barrier the initial matter from the core will try to flow further out. But it is known that for  $q = 0.96$ , no quasi-static circulation can occur in a zone of mass greater than  $m(1.46)$ , and so it is concluded that the condition  $\dot{A}_0 = \text{constant}$  must break down somewhere in the range, leading to the decay of the motion, and the formation of a barrier region.

It is difficult to determine rigorously where exactly this decay sets in, but it is certainly plausible that it should occur near the radius where the  $\mu$ -currents are already exerting their maximum choking effect, i.e. where the function  $x$ , defined by (52), attains its minimum value. For  $q = 0.96$ , it was found that  $x$  decreases monotonically outwards, and so is smallest at  $z = 1.46$ . The flow for this value of  $q$  is therefore pictured as follows: the initial flow from the core is able to reach  $z = 1.46$  without the  $\mu$ -currents becoming strong enough to choke the motion, but after this radius the motion decays, leading to the building of a barrier region. Further material coming up from the core is able to reach this barrier without being choked, but is diverted at the barrier, so that quasi-static circulation proceeds within the radius  $z = 1.46$ . About one-quarter of the star's mass is therefore available for energy liberation at this stage in its evolution.

With  $q$  slightly larger, but less than about 1.15, quasi-static circulation is able to proceed within a larger mass, but not through the whole star. The mass of the largest mixing zone allowed increases monotonically with  $q$ . The argument of the last paragraph applies again; in the absence of an already existing barrier the initial currents will attempt to flow towards the edge of the star, but as quasi-static circulation through all the star is impossible, choking of the motion must set in somewhere in the range. For these values of  $q$ , however, the

function  $x$  behaves differently: it decreases monotonically from the core to  $z \approx 1.46$ , and then increases monotonically. Again we expect the choking of the circulation to take place at the minimum of  $x$ , so this time the barrier is built up by the flow not at the edge of the maximum mixing zone allowed, for the given value of  $q$ , by the equation of mixing (49), but at the "bottle-neck" near  $z = 1.46$ . Thus again only about one-quarter of the star is mixed, as the barrier at the "bottle-neck" separates the part of the circulation linked with the core from the part in the rest of the envelope, which has no influence on the evolution of the star. The solution of the equation of mixing describing the asymptotic state is that with  $m' = m_s/4$ , and with  $(5\dot{A}_0\lambda)$  found from (51) with this value of  $m'$  and the given value of  $q$ .

In the absence of an equation to replace (44), it is difficult to estimate accurately the time taken by the currents to decay once quasi-static circulation is no longer possible. However, it is plausible that when choking of the motion starts,  $A_2$  should approach its asymptotic value at roughly the same rate as  $A_0$ , in which case it follows that the currents decay, and the barrier is built up, in a time comparable with the time for the matter to make one circulation, which is about  $\frac{1}{100}$  of the time required for all the hydrogen in the mixing zone to be used up.

With  $q = 1.15$ , the equation of mixing was found to have a solution with  $m' = m_s$ , so that it appears that the whole star can be mixed by rotational currents. But a rotationally stable star cannot rotate in its outer regions with the high value of the angular velocity given by  $q \approx 1$ , and so the driving velocity function  $p(r)$ , which is proportional to  $\Omega^2 r^3/GM(r)$ , must stop increasing well before the surface. The function  $F$  of Section 8 will therefore decrease more rapidly than that calculated using Sweet's function, and this will have some effect on the solutions of the mixing equation. However, it is found that with  $q \approx 1$ , and  $\Omega^2$  a constant, the function  $\Omega^2 r^3/GM(r)$  remains less than  $\frac{1}{10}$  up to  $z \approx 3$ , which contains 80 per cent of the mass, so that the bulk of the star can rotate with the high angular velocity corresponding to  $q \approx 1$  without  $\Omega^2 r^3/GM(r)$  becoming dangerously large anywhere. The integrations of the equation of mixing show that the extent of the mixing zone is controlled mainly by conditions near the "bottle-neck" at  $z = 1.46$ ; it is therefore unlikely that a decrease in  $\Omega$  after  $z = 3$  will do more than increase very slightly the value of  $q$  required for complete mixing.

The present work has been based on Sweet's first-order  $\Omega$ -current theory. In Öpik's treatment of the rotational problem (16), one term of the second order in  $\Omega^2$  has been retained, as it involves the factor  $1/p$ . Öpik's expression for  $v_r^\Omega$  is

$$v_r^\Omega = p(r) P_2 \left[ 1 - \frac{3}{8} \left( \frac{\Omega^2 r^3}{GM(r)} \right) \left( \frac{M(r)}{\frac{4}{3}\pi\rho r^3} - 1 \right) \right]. \quad (57)$$

The singularities given by this formula at the edge of the star are of no significance, as they can be eliminated by a technique similar to that developed in the Appendix. What is important is that for high enough  $\Omega^2$  the vertical component is reduced to zero and then reversed before the edge of the star is reached. With the parameter  $q \approx 1$ ,  $v_r^\Omega$  from (57) vanishes when  $M(r) \approx 0.9M$ . With this formula used in computing  $F$  of Section 8, and the new function  $F$  used in the solution of (49), it is probable that the maximum allowed mixing zone

will contain less still of the star's mass. This result will have considerable effect on the position of the star in the Hertzsprung-Russell diagram in the course of its evolution; but it is desirable that the formula (57) be verified by an extension of Sweet's analysis to include second-order terms.

To sum up, there exist two critical values of the parameter  $q$ . In order that the material may be able to escape from the core at all,  $q$  must exceed the very high value 0.96. With  $q$  at this value, the mixing zone has a mass of about  $M/4$ , and it retains this value as  $q$  is increased until the second critical value, which is only very slightly greater, is reached. According to the first-order theory, the whole star will be mixed once  $q \approx 1.15$ ; while if Öpik's second-order term is accepted, the maximum fraction of the star that will be mixed by any value of the angular velocity is about  $\frac{9}{10}$ .

Quite apart from the physical assumptions explicitly made, such as the form of the angular velocity field, the present results do depend on the validity of certain mathematical approximations. First, all but the  $P_2$  terms have been neglected in the treatment. By considering a quasi-static solution of (26) for  $z' = z_c$ , it is easy to show that the higher Legendre coefficients will choke the circulation even more near the core, so that the minimum value of  $q$  found above cannot be reduced by such refinements. A more serious criticism can be made of the step from the results of Section 8 to those of Section 9. In Section 8 it is shown that for a given value of  $q$  there exists a series of mixing zones with masses up to a limit. Thus, for example, the value  $q = 0.96$  was shown to allow quasi-static flow through a zone of mass up to  $m_s/4$ , and the conclusion was drawn that a star containing just so much angular momentum will develop a mixing zone of mass  $m_s/4$ , the best possible case. But the initial  $\mu$ -distribution set up by the first currents from the core will be highly asymmetric, and it is possible that the  $\mu$ -currents in the early stages of the flow will exert a stronger choking influence on the  $\Omega$ -currents than the symmetrical  $\mu$ -distributions discussed in Section 8, so that the barrier is built at a radius nearer the core than  $z' = 1.46$ . This doubt can be settled only by tackling the formidable problem of following the motion from the first flow of matter from the core. However, with the assumed angular velocity field, the results are so sensitive to slight changes of  $q$  above the critical value 0.96, that errors arising from this cause are of little consequence. The main results hold: a high angular velocity is needed in the inner regions for matter to be able to escape from the core, and a star with a spin slightly greater will possess a mixing zone containing a substantial fraction of the star's mass.

10. *Flow near the edge of the mixing zone.*—The condition  $A_2 = 0$  at the edge of the mixing zone implies a finite vertical velocity field there, and so an infinite horizontal component. According to the picture so far, the matter reaches the barrier with a finite vertical velocity, moves with infinite horizontal velocity to the other point where its streamline intersects the barrier, and then descends again. The way the material in fact avoids this unphysical behaviour near the barrier has already been pointed out in Section 2: the viscosity of the stellar material prevents the matter from being accelerated horizontally beyond a certain high velocity, and the flow settles down into a state with the vertical component reduced to zero in a distance of order one kilometre, and the horizontal component reaching a value about  $10^5$  times the normal speed of the currents. Thus  $A_2$  does not become exactly zero, but certainly small enough for the condition  $A_2 = 0$  to be adequate for a discussion of the large-scale properties of the circulation.

The  $A_2$ -distribution in the boundary layer may be determined as follows. As in (52), we write

$$xF = F + CA_2 + DA_2' + EA_2''. \quad (58)$$

Just outside the boundary layer  $x$  must take on the value at the edge of the mixing zone, written as  $x_0$ , found from the integration of (49); but within the layer the changed conditions will cause it to vary rapidly. The vertical velocity due to both  $\Omega$ - and  $\mu$ -currents will have multiplying it a further factor  $g$ , this being due to the action of viscosity in reducing the velocity to zero. Thus the theory of the Appendix must be applied to the function  $(xg)F$ ; as  $F$  is slowly varying, the product  $(xg)$  is given by

$$x_0(1 - e^{k(z'-z)}), \quad (59)$$

where  $|k|$  is of order  $10^5$ . The equation of quasi-static mixing then becomes

$$A_2 x_0 \beta F (1 - e^{k(z'-z)}) = (5\dot{A}_0 \lambda)(m' - m), \quad (60)$$

so that  $A_2$  is given by

$$A_2 = \frac{(5\dot{A}_0 \lambda) \cdot yz^2}{\beta x_0 F} \cdot \frac{(z' - z)}{(1 - e^{k(z'-z)})} = \eta \frac{(z' - z)}{(1 - e^{k(z'-z)})} \quad (61)$$

say. The feed-back terms are then determined; the first differs from zero by a term of order  $\eta/|k|$ , while the other terms make large positive contributions to  $x$  of order  $\eta$  and  $\eta/|k|$  respectively. The functions  $x$  and  $g$ , giving respectively the influence of the feed-back terms and the viscosity on the flow, can then be found from (58) and (59).

In a similar way, if the mixing zone should extend to the edge of the star, the positive infinite vertical component of velocity given by the solution of (49) must be reduced to zero by the effect of the stellar viscosity on the thermal equation, so that the horizontal component is finite. A modification of the theory in the Appendix will be required, and the  $A_2$ -distribution may then be found as above.

It is to be noted that strictly speaking, quasi-static flow in the boundary layer is an asymptotic state, requiring an infinite time to be reached; for with the velocity behaving like  $(z' - z)$  near  $z'$ , the time function  $\bar{t}(z, \theta)$  becomes infinite at  $z'$  like  $-\ln(z' - z)$ . This result is in fact a simple consequence of demanding that the horizontal component at the barrier should be finite: for this to be the case, the vertical component must decrease at least as rapidly as  $(z' - z)$ , so that  $\bar{t}$  must become infinite at the barrier. A similar result holds for flow near the edge of the star.

It is in this connection that the dubious nature of equations (28) and (50) appears. With the quasi-static assumptions,  $A_0'$  is given by (50). If the vertical component is made to vanish at  $z'$ , then  $A_2$  and  $A_2'$  must remain finite, leading to a positive infinity for  $A_0'$ , whereas the positive infinity in the time function  $\bar{t}$  should produce a negative infinity in  $A_0'$ . Thus (50), and hence also the equation (28) from which it is derived, are quite unreliable near the edge of the mixing zone. Equation (28) has therefore not been used above except in the form (31), where the doubtful terms are omitted.

**11. The angular velocity field.**—It has been assumed above that the mixing zone continues to rotate uniformly throughout the star's lifetime, so that the field of the driving velocity, and hence the function  $F$ , is also constant in time. For this to be the case, some azimuthal force must act on the fluid elements so as

to nullify the changes in angular velocity brought about by the transport of angular momentum by the circulation. Stellar viscosity is much too small to exert much influence, but rough uniformity of angular velocity is preserved if the mixing zone possesses a meridional magnetic field with lines of force threading the whole zone, including the convective core. The high conductivity of stellar material causes the lines of force to be effectively frozen into the matter (17), so that a meridional magnetic field will have its lines of force distorted and stretched by non-uniform rotation. The resulting azimuthal component of the ponderomotive force reacts back on the star, and sooner or later the non-uniformity of angular velocity along a line of force is reversed. Thus angular momentum is propagated to and fro along the lines of force; if the lines pass through the convective core, which necessarily rotates as a rigid body, then the angular velocity of the whole mixing zone will oscillate about a constant mean. The period of the oscillation is roughly the period of a magneto-hydrodynamic wave along the lines of force, i.e.  $R/H(\mu/4\pi\bar{\rho})^{1/2}$ , where  $H$  is the magnitude of the magnetic field,  $\mu$  the permeability, and  $\bar{\rho}$  the mean density. This is small compared with the time of circulation of the currents if  $H$  is larger than  $10^{-4}$  gauss. Thus quite a small magnetic field is both adequate and necessary to stiffen the angular velocity field of the mixing zone, so that the theory of this paper is relevant.

However, it must be noted that a general magnetic field of this magnitude threading the *whole* of the star will destroy any chance of rotational mixing, not because of the very slight resistance it offers to flow across the lines of force (1), but simply because of the action of the field on the rotation of the star. Consider a star which begins by rotating rapidly enough in its inner regions for mixing to occur, but with the spin decreasing outwards so that rotational stability is preserved near the surface. Any meridional magnetic field present will redistribute the angular velocity by transporting angular momentum outwards. The effect will be to bring about rotational instability at the surface, so that the star must lose mass and angular momentum until the centrifugal force at the surface ceases to be of the same order as gravity. Thus the star must reach a state with the magnetic field preserving a mean uniformity of rotation throughout, with the value of the angular velocity well below the limit found earlier for mixing to occur. A magnetic field greater than  $10^{-6}$  gauss will suffice to produce this effect within the time-scale for consumption of the hydrogen within the mixing zone.

If any magnetic fields present are too small to influence the angular velocity, and if the inner regions of the star rotate rapidly enough, then circulation will take place, but the currents themselves will tend to set up a state of uniformity of angular momentum within the mixing zone. Also, equalization of angular momentum tends to be brought about by the braking effect of the radiative flux, as discovered by Jeans (18). The viscosity is negligible except near the axis of rotation, where strict conservation of angular momentum by the circulation would lead to infinities in the azimuthal velocity and in its gradient normal to the axis. Turbulent viscosity will ensure that the core rotates as a rigid body.

It is known (16) that rotational currents flow vertically upwards when the change of gravity due to rotation is positive; hence in a star in which  $\Omega r^2 \sin^2 \theta$  is constant throughout most of the mixing zone, currents will flow out of the core at the equator, and in at the poles. This ensures that matter leaving the core has a finite quantity of angular momentum to distribute through the mixing zone.

The details of the  $\Omega$ -currents for this case may be obtained by Sweet's general method, and then the feed-back currents determined by methods similar to those of this paper. The treatment is likely to be much more complicated because of the necessity of introducing more than one Legendre component to describe the field adequately. A more tractable problem would be the circulation in a star obeying the law  $\Omega r^2 = \text{constant}$ ; the  $\Omega$ -currents in this case again have a  $P_2$ -distribution, so that the theory of this paper is immediately applicable once the function  $F$  of (47) has been recomputed. Such a law of angular velocity would give some idea of the effect of the uniform distribution of angular momentum,  $\Omega r^2 \sin^2 \theta = \text{constant}$ , without introducing too great complication.

Some qualitative results may be predicted. First, the driving velocity will decrease outwards, instead of having a minimum, because of the monotonic decrease of the ratio of centrifugal to gravitational force. This will probably lead to a stronger choking effect by the  $\mu$ -currents, so that the results will not show the striking sensitivity of the mass of the mixing zone to small changes in angular momentum which was found for the case with  $\Omega = \text{constant}$ . The extent of the mixing zone will probably be limited by the amount of centrifugal force the inner region can safely bear. There will again exist a "bottle-neck", but it must be much further out than that found above, for the total vertical component of velocity will not begin to increase until the large positive feed-back terms  $DA'_2$  and  $EA'_2$  come into play at low densities far out into the envelope of the star.

*12. Evolutionary consequences.*—The applications of the work of this paper to stellar structure and evolution inevitably depend on what assumptions are made initially as to the properties of massive stars at the time of their birth. Thus it follows, for example, that a star rotating with roughly the same angular velocity throughout, or possessing a general magnetic field threading the whole volume, must begin its evolution by transmuting just the hydrogen in the convective core.

The results show that a star with its *inner* regions constrained by a magnetic field to rotate uniformly, and possessing enough internal angular momentum, will suffer some mixing; the zone will contain either one-quarter of the stellar mass, or, if the angular momentum be very slightly greater, the bulk of the star will be mixed. However, it seems unlikely that any general magnetic field possessed by the star will be restricted to just the inner regions, while if it threads the whole star, no mixing is possible. We shall therefore assume that if a star is able to mix at all, it is effectively free from magnetic fields. This implies, as discussed in Section 11, that the  $\Omega$ -currents due to the new angular velocity field within the mixing zone will have different properties, and, in particular, the mass of the mixing zone is likely to be far less sensitive to increases of angular momentum. Thus it is probable that we cannot expect more than one-half of the star to be mixed, even under the most favourable conditions; although further numerical results are desirable, for the moment we shall assume this to be the case.

The general conclusion to be drawn is that rotational mixing is far more unlikely than has been supposed in much recent work on stellar evolution, and in the absence of any alternative mechanism of mixing, it is seen that the present results will tend to eliminate some stellar models as being inaccessible in the normal course of evolution. Thus it is known from the mass-radius-composition and the mass-luminosity-composition relations for a homogeneous star that as  $\mu$  increases,

such a star describes in the Hertzsprung-Russell diagram an ascending path which diverges considerably to the left from the main sequence. Doubt has been felt recently by observers as to whether any such stars exist, and it is satisfactory that there should be strong theoretical objections to a star's remaining homogeneous.

Consider now the evolution of a star with a mixing zone extending into the envelope. Then within the zone  $\mu$  gradually increases, while the rest of the star is unaffected by the consumption of hydrogen in the core, so that the star will approximate very closely to the Hoyle-Lyttleton giant model (3, 4, 5). From the Bondis' detailed integrations and graphs, it is possible to follow the track of the star in the Hertzsprung-Russell diagram, once the mass of the mixing zone is given. As  $\mu$  in the mixing zone increases, at first the luminosity increases strongly, while the radius increases only moderately; but when the mixing zone contains already a high proportion of helium, the radius increases spectacularly for small increases in  $\mu$ , especially if the mass of the mixing zone is about half the total mass. Thus in the Hertzsprung-Russell diagram the star will at first ascend along a path diverging slightly to the right from the main sequence, but later will swing sharply to the right and move along an almost horizontal path, giving a large drop in surface temperature, accompanied by a slight rise in luminosity, as demanded by the integrations. Such a path is strongly suggestive of the main Type I giant sequence (9).

The way suggested by Hoyle and Lyttleton for the origin of red giants built on their model was the accretion of a hydrogen envelope by a completely mixed star which has had sufficient time to burn a large fraction of its hydrogen, and so has become a homogeneous star of high  $\mu$ . The present work shows at once that accretion is not necessary, as a star will almost certainly evolve towards a non-homogeneous state of its own accord. The Bondis' graphs show that the most extended giant models are obtained if the masses of the zones of high and low  $\mu$  are roughly equal; if, therefore, not more than half of the star can be mixed, accretion of extra hydrogen will diminish the extension of the envelope. Thus accretion will certainly tend to blur the evolutionary tracks in the Hertzsprung-Russell diagram, but it will not make any qualitative changes in the structure of the star.

It is known that some Hoyle-Lyttleton giant models, obeying a Kramers-type opacity law, are unable to remain in the static state—it is impossible to satisfy the conditions of continuity of energy flux everywhere, so that the star begins to gain energy (4). It is difficult to determine rigorously the future behaviour of such a star, but it is possible that it may get rid of surplus energy by performing non-linear oscillations (19), and so provide an explanation of some of the observed long-period red variables. If nearly one-half of the star is mixed, and if the opacity law obeyed is of the right sort, such a non-static star must necessarily arise in the normal course of evolution of a main-sequence star.

We turn now to stars which suffer no mixing in their Cowling model stage, and so simply burn out their cores. As  $\mu$  in the core increases, the luminosity increases slightly, and the radius increases gradually up to ten times its original value (20). When the core is completely burnt out, the convection currents die out, and the star contracts until the temperature in the shell surrounding the core reaches about 15 million degrees, when the Bethe cycle can start up there. A small convective zone will surround the shell, so that the barrier built up by the  $\mu$ -currents in the Cowling model stage, which prevented mixing between core and envelope, will be swept away.

It is well known that unless the mass of the core is a small fraction of the stellar mass, this "shell-source" stellar model cannot exist in the static state (6)—again, the star cannot transmit to the surface the energy liberated within it, and so must begin to gain energy. A plausible path for the first stages of the star's evolution has been put forward by Sandage and Schwarzschild (21), with the core slowly contracting and the envelope slowly expanding, giving in the Hertzsprung–Russell diagram a nearly horizontal curve in the direction of decreasing surface temperature. This line of evolution must ultimately be modified, however, by the onset of electron degeneracy at the centre, together with the possible liberation of energy by the synthesis of heavy elements from helium, which starts at about  $2 \times 10^8$  deg. K (22). The authors estimate that if helium burning starts, the rapid envelope expansion will cease, and the star's luminosity will increase sufficiently to account for the bright stars in Type II systems. However, they are not certain that the central temperature reached in the first stage of contraction will be high enough for helium burning to start, and suggest as an alternative that some rotational mixing may start at some point on the star's track. It is at this point that the present work may be relevant. It was noted in Section 7 that whereas the simple  $\Omega$ -current theory predicts the same efficiency whatever the star's dimensions, the theory with  $\mu$ -currents results in greater mixing efficiency after contraction. Thus a star which in its Cowling model state suffers no mixing may, after contraction to a shell-source state, possess a mixing zone extending beyond the convective zone surrounding the burnt-out core. Such a zone would probably slow up the envelope expansion, because of the gradual decrease in the discontinuity between core and mixing zone, and at the same time would increase the luminosity. Further integrations of composite shell-source models are needed to compare the theory with observation.

Once the mixing zone has consumed all its hydrogen, the mass of the burnt-out core effectively increases, so that the star will contract further. Electron degeneracy will probably play an increasingly important part in the central regions of the core, and we should expect both radius and luminosity to decrease quite sharply. It remains to be seen whether the theory can account in this way for the horizontal portion of the Type II giant sequence. It is in this part of the Hertzsprung–Russell diagram that the cluster-type Cepheids are found; it may be possible to find a criterion determining when a non-static star, which is continually gaining energy, prefers to start pulsating so as to get rid of the excess energy (19), and in this way account for the Type II short-period variables.

It may be remarked that Type II systems seem to be completely free of interstellar gas and dust. Any massive stars that condensed when these old systems were formed should have burnt themselves out, and there is no matter available to form new massive stars, either directly, or through accretion by moderate masses. Hence it is not possible that the very luminous red stars should be of large mass; the high luminosity must be due to composition rather than mass, and a fair-sized mixing zone of high  $\mu$  surrounding the core is one possible explanation.

If, as suggested above, a Type I giant is built on the Hoyle–Lyttleton model, implying that a fair degree of mixing takes place in the first stages of evolution, while a Type II star begins by consuming only its convective core, then there should exist a systematic difference in angular momentum between the two

populations. It is perhaps suggestive that Type I systems are confined to the galactic plane, and so have condensed from matter with comparatively high vorticity, while the typical Type II systems, the globular clusters, form a roughly spherical system around the galactic centre. Also, the theoretical differences that must exist between the evolutionary tracks of stars which do and do not mix, respectively, offer attractive possibilities for explaining the two population types. If, however, the conditions found above for rotational mixing to be possible are too stringent for stars of either type, then we are faced with the problem of explaining both types as being due to the evolution of stars which initially burn out just their convective cores. The differences between the two types would then presumably be due to the differences in composition reported by Greenstein and Schwarzschild (23). It seems worth while working out the consequences of all the different assumptions—mixing or no mixing in early or late stages of evolution—to see if the observations definitely rule out all but one set of possibilities. In particular, if evolutionary theory is found to demand mixing at some stage or other, then the conditions found in this paper will need to be satisfied; in this way we may gain some information about the distribution of angular momentum in initial condensations, or the presence or absence of stellar magnetic fields. This information could conceivably act as a censor on some theories of stellar origins.

So far we have discussed evolutionary problems in terms of the positions of stars in the Hertzsprung-Russell diagram. The mass-luminosity diagram is in general not so useful, because of the difficulties in estimating stellar masses accurately, but is of equal theoretical importance. Recently some Soviet astronomers, in particular Fessenkov (10), have drawn attention to discrepancies between the close fit of most stars observed to the mass-luminosity curve, and theoretical predictions from the mass-luminosity relation for homogeneous stars. It is well known that a high value of  $\mu$  throughout a star leads to a high internal temperature, and to a consequently high flux from core to surface. Thus in a star obeying the simple Kramers opacity law, the relation is  $L \propto \mu^{7.5} M^{5.5}$  (2), and so a homogeneous star containing a high proportion of helium will be of far higher luminosity than one of the same mass consisting of hydrogen. To avoid this difficulty, Fessenkov proposes that the stars emit corpuscular radiation at a rate proportional to their luminosity, so as to preserve the closeness of fit with the observed mass-luminosity curve. Other writers, notably Struve (9), also support the idea of corpuscular radiation, so that the initial stellar condensations, which they believe to be of high mass, may be able to lose enough mass so as to move down the main sequence into the dwarf regions. However, whatever the arguments in favour of or against this last line of evolution, it is seen at once that if the natural tendency of a star is to develop into a non-homogeneous state, and burn out initially only a fraction of its mass, then Fessenkov's argument is no longer valid. The mass-luminosity relation depends on assuming that energy is flowing from the core to the surface, and that the perfect-gas equation of state holds throughout the star. But if a star begins by burning out less than half its mass, as seems likely, there will not be any serious divergence from the mass-luminosity curve while the star still possesses a convective core; and when the mixing zone is completely burnt out, and the star contracts to a shell-source state, it is likely that degeneracy will set in over a large part of the core, and so there is no reason to expect the ordinary mass-luminosity relation to hold. What

relation replaces it cannot be decided until more theoretical work has been done but there is no reason to demand corpuscular radiation (by a mechanism as yet undetermined) so as to avoid theoretical difficulties.

13. *Conclusions.*—(1) Very slight departures of the distribution of matter from spherical symmetry lead to strong thermal currents within stars (" $\mu$ -currents").

(2) No continuous mixing between core and envelope can take place in a uniformly rotating Cowling model star; the  $\mu$ -currents induced by the rotational currents choke the flow near the core, unless the angular velocity of the star is so great that it is past the limit for rotational stability at the surface.

(3) A star rotating rapidly enough near the core will build up for itself a mixing zone of definite mass. If the inner regions of the star are constrained by a magnetic field to rotate uniformly, then the mass of the mixing zone is very sensitive to increases of the angular velocity above a certain limit. In a star in which the angular velocity decreases outwards, however, the mass of the mixing zone is likely to increase slowly with increasing angular momentum.

(4) The mass of the mixing zone is determined by a parameter which varies as the star's dimensions change. Thus the efficiency of mixing increases as the star contracts; in particular, a star which is unable to mix in its initial state with a convective core may possess a mixing zone after contraction into a shell-source state.

(5) The effects on the Hertzsprung-Russell diagram and on the mass-luminosity curve depend to a great extent on the assumptions made about the initial angular velocity distribution of the star, and the existence and strength of stellar magnetic fields. The general tendency of the work is to make rotational mixing much less probable than has been thought. The solution of the shell-source problem is urgently needed, to see whether both Type I and Type II giant sequences can be explained without use of the Hoyle-Lyttleton giant model and rotational mixing. The arguments of Fessenkov and others for corpuscular radiation, based on discrepancies between the observed mass-luminosity relation and the theoretical predictions for homogeneous stars, become much less compelling when it is recognized that it is very unlikely that stars remain homogeneous.

14. *Acknowledgments.*—The writer wishes to thank Professor T. G. Cowling for many discussions during the course of the work, and helpful criticisms of the manuscript. He is also indebted to the University of Leeds for the award of an I.C.I. Research Fellowship.

## APPENDIX

It was pointed out in Section 2 that at the edge of a star, near surfaces of discontinuity in composition, and at the interface between convective and radiative regions, the theory of meridional circulation so far developed gives infinities for the circulation velocities. It is concluded that the assumptions of negligible viscous force and inertial force, underlying the theory, must be invalid near certain singular surfaces. If the circulation velocity is expanded in powers of the perturbing parameter  $\Omega^2$ , then in a first-order treatment only the viscous force is retained, as the steady-state inertial terms are non-linear in the circulation velocity. The theory of flow near the singular points will now be given for the different cases.

1. *Motion near discontinuities and near the surface.*—To the first order in  $\Omega^2$ , the steady-state equations of motion are

$$\rho \frac{\partial \phi}{\partial r} + \rho_0 r \Omega^2 \sin^2 \theta - \frac{\partial P}{\partial r} + \eta \left( \nabla^2 v_r - \frac{2v_r}{r^2} - \frac{2 \cot \theta}{r^2} v_\theta - \frac{2}{r^2} \frac{\partial v_\theta}{\partial \theta} \right) = 0. \quad (1)$$

$$\rho_0 \frac{\partial \phi}{\partial \theta} + \rho_0 r^2 \Omega^2 \sin \theta \cos \theta - \frac{\partial P}{\partial \theta} + \eta r \left( \nabla^2 v_\theta - \frac{v_\theta}{r^2 \sin^2 \theta} + \frac{2}{r^2} \frac{\partial v_r}{\partial \theta} \right) = 0, \quad (2)$$

where  $\phi$  is the gravitational potential and  $\eta$  the coefficient of viscosity. These equations are cross-differentiated and subtracted one from the other, leading to

$$\begin{aligned} \frac{\partial \rho}{\partial \theta} \frac{d\phi_0}{dr} + \eta \frac{\partial}{\partial \theta} \left( \nabla^2 v_r - \frac{2v_r}{r^2} - \frac{2 \cot \theta}{r^2} v_\theta - \frac{2}{r^2} \frac{\partial v_\theta}{\partial \theta} \right) \\ = \frac{\partial \phi}{\partial \theta} \frac{dp_0}{dr} + \frac{dp_0}{dr} r^2 \Omega^2 \sin \theta \cos \theta + \eta \frac{\partial}{\partial r} \left\{ r \left( \nabla^2 v_\theta - \frac{v_\theta}{r^2 \sin^2 \theta} + \frac{2}{r^2} \frac{\partial v_r}{\partial \theta} \right) \right\}. \end{aligned} \quad (3)$$

We consider first the motion near a surface of discontinuity of  $\mu$  within the star. The type of solution sought is one in which the effect of viscosity is felt only within a thin layer near the discontinuity. The vertical velocity at the barrier must be zero; provisionally, therefore, we adopt for  $v$ , an expression of the form

$$v_r = pP_2(1 - e^{k(r-\bar{r})}) = \alpha(r)P_2, \quad (4)$$

where  $k$  is a constant,  $\bar{r}$  the radius of the sphere containing the barrier and  $pP_2$  is Sweet's vertical velocity component, proportional to  $\Omega^2$ . The constant  $k$  is positive below the barrier, negative above. It is shown in the analysis that  $|k|$  is so large that  $|r - \bar{r}|$  need be only a small fraction of the radius for (4) to reduce to Sweet's expressions; hence variations in  $p$ ,  $\phi_0'$ ,  $\rho_0'$ , etc. over distances comparable with  $|1/k|$  are negligible.

By the equation of continuity,

$$v_\theta = -\frac{1}{2\rho_0 r} \frac{d}{dr} (\rho_0 r^2 \alpha) \sin \theta \cos \theta. \quad (5)$$

Then the terms involving the viscosity in (3) are respectively

$$3 \sin \theta \cos \theta \eta \frac{d}{dr} \left\{ -\frac{2\alpha}{r} + \frac{1}{\rho_0 r} (\rho_0 r^2 \alpha)' - \frac{1}{6r} \frac{d}{dr} \left[ r^2 \left( \frac{(\rho_0 r^2 \alpha)'}{\rho_0 r} \right)' \right] \right\} \quad (6)$$

and

$$-3 \sin \theta \cos \theta \eta \left\{ \frac{1}{r^2} \frac{d}{dr} (r^2 \alpha') - \frac{8\alpha}{r^2} + \frac{2}{\rho_0 r^3} (\rho_0 r^2 \alpha)' \right\}. \quad (7)$$

The dominant term in these two expressions is the one with the highest derivative in  $r$ , as this has the highest number of  $k$  factors. With this term alone retained, (3) reduces to

$$\frac{\partial \rho}{\partial \theta} \frac{d\phi_0}{dr} = \frac{\partial \phi}{\partial \theta} \frac{dp_0}{dr} + \frac{dp_0}{dr} r^2 \Omega^2 \sin \theta \cos \theta + \frac{1}{2} \eta r^2 k^4 p e^{k(r-\bar{r})} \sin \theta \cos \theta. \quad (8)$$

The viscous term modifies  $\partial \phi / \partial \theta$  and  $\partial \rho / \partial \theta$ . Let  $\chi \equiv \partial \phi / \partial \theta$  have added to it a new term  $\chi_2$ . Then  $\partial \rho / \partial \theta$  has a new term given by Poisson's equation

$$\nabla^2 \chi_2 = -4\pi G \frac{\partial \rho_2}{\partial \theta}. \quad (9)$$

Hence  $\chi_2$  satisfies

$$\frac{\phi_0'}{4\pi G} (\nabla^2 \chi_2) + \chi_2 \rho_0' = -\frac{1}{2} \eta r^2 k^4 p e^{k(r-\bar{r})} \sin \theta \cos \theta. \quad (10)$$

$\chi_2$  must become negligible as soon as  $|r-\bar{r}| \gg |1/k|$ ; a solution of (10) satisfying this condition is

$$\lambda e^{k(r-\bar{r})} \sin \theta \cos \theta. \quad (11)$$

Again dropping all but the dominant terms,  $\lambda$  is seen to be

$$\lambda = -\frac{2\pi G}{\phi_0'} \eta r^2 k^2 p. \quad (12)$$

We now require the new terms that must be added to  $(\text{div } \mathbf{H})$ . From the expression given by Sweet (1) for  $\partial(\text{div } \mathbf{H})/\partial\theta$ , it follows that the largest contribution comes from the term

$$\frac{L}{4\pi r^2} \cdot \frac{1}{T_0'} \frac{\partial^2}{\partial r^2} \left( \frac{\partial T_2}{\partial \theta} \right), \quad (13)$$

where  $T_2$  is the modification in  $T$  due to the viscous terms. From (1) and (9) the dominant term in  $\partial T_2/\partial\theta$  is

$$-\frac{T_0}{\rho_0} \cdot \eta \frac{pk^4 r^2}{2\phi_0'} \cdot e^{k(r-\bar{r})} \sin \theta \cos \theta. \quad (14)$$

This gives for  $\partial(\text{div } \mathbf{H})/\partial\theta$

$$-\sin \theta \cos \theta \cdot \frac{L}{4\pi r^2} \cdot \frac{1}{\rho_0 T_0'} \cdot \frac{k^6 \eta p r^2 T_0}{2\phi_0'} e^{k(r-\bar{r})}. \quad (15)$$

The viscous heating terms in the energy equation are of the second order in the circulation velocities, and so are dropped. Hence we have

$$\rho_0 (-\phi_0') \frac{(n-\frac{3}{2})}{(n+1)} \cdot v_r = -\text{div } \mathbf{H}, \quad (16)$$

so that (15) must be put equal to

$$-\rho_0 (-\phi_0') \frac{(n-\frac{3}{2})}{(n+1)} \cdot e^{k(r-\bar{r})} p \cdot 3 \sin \theta \cos \theta, \quad (17)$$

for the change in the vertical component,  $-p e^{k(r-\bar{r})}$ , is due to the modification in  $(-\text{div } \mathbf{H})$  which in turn is caused ultimately by the viscous terms in the hydrodynamic equations.

Finally,  $k$  is given by (15) and (17) :

$$k^6 = -\frac{8\pi\rho_0}{v} \cdot \frac{(\phi_0')^2 \cdot T_0'}{LT_0} \cdot \frac{3(n-\frac{3}{2})}{(n+1)}, \quad (18)$$

where  $v$  is the kinematic viscosity  $\eta/\rho_0$ . In most stars the radiative kinematic viscosity  $2aT^4/15\kappa c\rho^2$  ( $\kappa$  here being the opacity) is somewhat greater than the molecular viscosity (18); both are of order unity (in c.g.s. units), except near the surface of the star. Hence (18) gives  $|k| \sim 10^{-5}$ , provided  $\bar{r}$  is not too near the surface, so that the thickness of the boundary layer is only about a kilometre, fully justifying the approximations made in determining (18).

In fact, the velocity function near the barrier will not be as simple as (4). As presented, the theory satisfies the condition of zero flow across the barrier, but in addition there are conditions of continuity of  $\chi_2$ ,  $\chi_2'$  and  $T_2$  across the distorted discontinuity, while the jump in  $\rho_2$  is fixed by the jump in  $\mu$ . These conditions themselves imply a restriction on the viscous terms in (2). In order

to satisfy all these conditions it is necessary to assume a generalized form of (4), involving several exponential terms, and to take explicit account of conditions on the other side of the barrier. This greatly complicates the theory; we are concerned merely to illustrate what happens near the discontinuity, and to obtain an order-of-magnitude estimate for the thickness of the boundary layer, and so the accurate analysis is not attempted.

Before the steady state is reached, material is accelerated up to the limiting velocity, so that both viscosity and first-order inertial terms should be included in equations (1) and (2). However, it is easy to see that the time for the system to reach the steady state is very small. The energy per unit mass that would be convected away per second by vertical motion in the absence of a barrier is of order  $(L/M) \cdot (\Omega^2 r^3/GM)$ . The presence of a barrier causes horizontal motion, and this energy is used to accelerate the material until the velocity gradient is large enough for viscosity to be important and to stop the acceleration. Hence the time to reach this state is given roughly by

$$v^2 \sim t \cdot \left( \frac{L}{M(r)} \cdot \frac{\Omega^2 r^3}{GM(r)} \right); \quad (19)$$

$v$  is here the horizontal component, which from (5) is  $\sim |k|\bar{r}p$ . Taking  $\bar{r} = 5 \times 10^{10}$  cm, and  $p$  to be  $\sim 10^{-10}(\bar{\Omega})^2$  cm/sec,  $t$  is found to be a small fraction of a second.

It is pointed out in the text that a finite vertical velocity at the surface implies an infinite horizontal component there, which again is physically impossible. The difficulty is resolved in a similar way: material is initially accelerated horizontally until the viscous forces come into play. The radiative viscosity, which far outweighs the molecular at the surface, is proportional to the temperature; also, as density and temperature vanish at the surface, a slightly more complex theory than that above is required. For a star obeying Kramers' opacity law, it is found that the velocity vanishes as

$$v_r = p P_2 \{1 - \exp(-h/\bar{h})^{21/2}\}, \quad (20)$$

where  $h$  is the distance from the surface. Thus both vertical and horizontal components vanish at the surface. The thickness of the boundary layer is of order  $\bar{h}$ , which for the Sun is about  $2.5 \times 10^8$  cm and is not much larger for more massive stars. This is again small enough to justify the approximations made in arriving at (20).

2. *Motion near a convective zone.*—In fact, the velocity distribution (20) will not hold near the surface of stars of solar order, because of the existence of the Unsöld convective zone, extending in the Sun from a depth of about  $10^9$  cm up to the photosphere; within a convective zone meridional circulation is irrelevant. However, as the polytropic index approaches the adiabatic value  $\frac{4}{3}$ , the vertical and horizontal components of velocity are by (16) and (5) proportional to  $1/(n - \frac{4}{3})$  and  $1/(n - \frac{4}{3})^2$  respectively. Similar infinities arise at the surface of the convective core, and must be eliminated by a technique similar to that used above.

The velocity function assumed is

$$v_r = l \cdot s \cdot P_2 = p(n - \frac{4}{3}) \cdot s \cdot P_2, \quad (21)$$

where  $p$  is Sweet's function. As a convective zone is approached  $l$  remains finite and of the same order as  $p$  at points far from the convective zone;  $s$  is a rapidly

varying function of  $r$  which becomes large but finite at the convective zone, and behaves like  $1/(n-\frac{3}{2})$  far from the singularity.

It is sufficiently accurate to assume that  $(n-\frac{3}{2})$  varies linearly with  $(r-r_c)$ , where  $r_c$  is the radius of the convective zone. Thus for  $(n-\frac{3}{2})$  we write  $(dn/dr)_e \cdot (r-r_c)$ , and assume for  $s$  the functional form

$$s = \frac{1}{(dn/dr)_e \cdot (r-r_c)} \cdot \left\{ 1 - \alpha_1 e^{k(r-r_c)} - \alpha_2 e^{2k(r-r_c)} - \dots - \alpha_t e^{tk(r-r_c)} \right\} \quad (22)$$

with the condition

$$\sum_{t=1}^{\infty} \alpha_t = 1. \quad (23)$$

Then as above,  $\partial\rho_2/\partial\theta$  is given by

$$\begin{aligned} \frac{\partial\rho_2}{\partial\theta} = & -\frac{\nabla^2\chi_2}{4\pi G} = -\frac{1}{(-\phi_0')} \cdot \frac{r^2\eta}{2} \cdot \frac{l \cdot \sin\theta \cos\theta}{(dn/dr)_e} \\ & \times \left\{ \sum_{t=1}^{\infty} \alpha_t \sum_{n=5}^{\infty} \frac{t^n k^n}{n(n-5)!} (r-r_c)^{n-5} \right\} \end{aligned} \quad (24)$$

and  $\partial T_2/\partial\theta$  by

$$\frac{\partial T_2}{\partial\theta} = -\frac{T_0}{\rho_0} \frac{\partial\rho_2}{\partial\theta}, \quad (25)$$

where only dominant terms have been retained.

The energy equation (16) reduces to

$$\left\{ \sum_{t=1}^{\infty} \alpha_t \sum_{n=1}^{\infty} \frac{t^n k^n (r-r_c)^n}{n!} \right\} = \gamma \cdot \left\{ \sum_{t=1}^{\infty} \alpha_t \sum_{n=7}^{\infty} \frac{t^n k^n}{n(n-7)!} \cdot (r-r_c)^{n-7} \right\}, \quad (26)$$

where  $\gamma$  is written for

$$\frac{L}{4\pi} \cdot \left( -\frac{T_0}{T_0'} \right) \cdot \frac{1}{(-\phi_0')^2} \cdot \frac{\eta}{6\rho_0^2} \cdot \frac{(n+1)}{(dn/dr)_e}. \quad (27)$$

On equating coefficients, we obtain an infinite homogeneous set of linear equations which, together with the non-homogeneous condition (23), yield an infinite determinantal equation for  $\gamma k^7 = u$ :

$$0 = \begin{vmatrix} 1 & 2^7 & 3^7 & 4^7 & \dots \\ \left(1 - \frac{u}{8}\right) & 2\left(1 - \frac{2^7 u}{8}\right) & 3\left(1 - \frac{3^7 u}{8}\right) & 4\left(1 - \frac{4^7 u}{8}\right) & \dots \\ \left(1 - \frac{u}{9}\right) & 2^2\left(1 - \frac{2^7 u}{9}\right) & 3^2\left(1 - \frac{3^7 u}{9}\right) & 4^2\left(1 - \frac{4^7 u}{9}\right) & \dots \\ \dots & \dots & \dots & \dots & \dots \end{vmatrix} \quad (28)$$

In a rigorous treatment it would be necessary to show the existence of only one physically relevant root of this determinantal equation as the number of  $\alpha$ -terms taken increases to infinity. This will not be attempted. Inspection of the first few members of the sequence of determinants, however, shows that there is a root of order  $-10$ . Near the convective core  $\gamma$  is roughly  $10^{-30}$  c.g.s. units, so that  $|k| \sim 3 \times 10^{-5}$  c.g.s. units. The thickness of the layer is then about  $\frac{1}{3}$  km, and the vertical and horizontal components of velocity are  $3 \times 10^{-5} (\bar{\Omega})^2$  and  $9 \times (\bar{\Omega})^2$  cm/sec respectively. Near the Unsöld convective zone  $|k|$  is about  $10^{-6}$  c.g.s. units, giving 10 km for the thickness of the layer, and  $10^{-4} (\bar{\Omega})^2$  and

$3(\bar{\Omega})^2$  cm/sec for vertical and horizontal components respectively. It is remarkable that even in a slowly rotating body like the Sun the very slight thermal disequilibrium set up by the rotation can lead, near an unstable region, to velocities of an observable magnitude.

Department of Mathematics,  
The University,  
Leeds, 2 :  
1953 September 1.

#### References

- (1) P. A. Sweet, *M.N.*, **110**, 548, 1950.
- (2) C. M. and H. Bondi, *M.N.*, **109**, 62, 1949.
- (3) F. Hoyle and R. A. Lyttleton, *M.N.*, **109**, 614, 1949.
- (4) C. M. and H. Bondi, *M.N.*, **110**, 287, 1950.
- (5) C. M. and H. Bondi, *M.N.*, **111**, 397, 1951.
- (6) S. Chandrasekhar and M. Schoenberg, *Ap. J.*, **96**, 161, 1942.
- (7) F. Hoyle and R. A. Lyttleton, *Proc. Camb. Phil. Soc.*, **81**, 277, 1939.
- (8) F. Hoyle, *M.N.*, **105**, 287, 1945.
- (9) O. Struve, *Stellar Evolution*, Princeton Univ. Press, 1950.
- (10) V. Fessenkov, V. A. Ambartsumian, papers submitted to the VIIIth General Assembly, I.A.U., Rome, 1952.
- (11) T. G. Cowling, *M.N.*, **96**, 42, 1936.
- (12) L. Biermann, *Zs. f. Astrophys.*, **5**, 117, 1932.
- (13) H. Alfvén, *Cosmical Electrodynamics*, Oxford, 1950.
- (14) J. G. Gardiner, *M.N.*, **111**, 94, 1951.
- (15) L. Mestel, *M.N.*, **112**, 598, 1952.
- (16) E. J. Öpik, *M.N.*, **111**, 278, 1951.
- (17) V. C. A. Ferraro, *M.N.*, **97**, 458, 1937.
- (18) J. H. Jeans, *M.N.*, **86**, 444, 1926.
- (19) L. Mestel, Ph.D. dissertation, Cambridge, 1952.
- (20) A. E. Roy, *M.N.*, **112**, 484, 1952.
- (21) A. R. Sandage and M. Schwarzschild, *Ap. J.*, **116**, 463, 1952.
- (22) E. Salpeter, *Ap. J.*, **115**, 326, 1952.
- (23) J. L. Greenstein and M. Schwarzschild, paper submitted to the VIIIth General Assembly, I.A.U., Rome, 1952.

## PHOTOMETRY OF THE GALACTIC CLUSTER NGC 6025

A. R. Hogg

(Communicated by the Commonwealth Astronomer)

(Received 1953 November 3)\*

### Summary

The southern galactic cluster NGC 6025 has been examined photoelectrically in two colours. A catalogue of magnitudes and colours of 84 stars in the region has been obtained. The colour-magnitude array is examined and compared with curves obtained for the Pleiades by Binnendijk and by Eggen.

These comparisons give distance moduli of  $9^m\cdot4$  and  $9^m\cdot6$  respectively (neglecting absorption). Owing to a lack of independent identification of cluster members the results do not provide a positive test of the fine structure suggested by Eggen, but an examination of the stars in the central region yields nothing against the fine-structure interpretation.

1. *Introduction.*—The galactic cluster NGC 6025 is included in the catalogues by Trumpler (1) and by Collinder (2), in both of which the position, taken from Franklin Adams charts, is given as  $\alpha(1900)=15^h 55^m\cdot2$  and  $\delta(1900)=-60^\circ 13' \dagger$ . Collinder describes the cluster as "a loose aggregation of stars of the Pleiades type"; Trumpler places it in class 113p, i.e. a detached cluster with but little central condensation, composed of moderately bright and faint stars numbering less than 50. Trumpler estimates the modulus  $m-M=9^m\cdot5$ , but considers this to be less satisfactory than most of his results as it is derived from the spectra of only five dwarf stars classified as B3 to B8 in the *Henry Draper Catalogue*. The giant branch is completely missing. Mrs C. A. Riecke (3) obtained a modulus of  $m-M=8^m\cdot4$  using absolute magnitudes derived from an estimate of hydrogen line intensities. The estimated dimensions of the cluster, as summarized by Collinder (2), range from  $10'$  (Melotte) to  $19'$  (Raab). No detailed investigations of the spectra or radial velocities have been located nor does the cluster appear to have been the subject of photometric study.

In the present work the cluster has been examined in two colours photoelectrically, with the object of obtaining a colour-luminosity array from which a distance might be derived and a classification of members according to the system of Eggen (4) obtained.

2. *Photometric technique.*—The observations were made with an 11-stage EMI photomultiplier tube attached to the Newtonian focus of the Reynolds 30-inch reflector of the Commonwealth Observatory. The photomultiplier fed into an amplifier designed by Kron (5). Records were obtained with a 0-1 milliamp recording meter. Blue and yellow filters were used and the star light was admitted through a focal-plane diaphragm subtending usually  $50''$  of sky. The transmissions of the filters were measured by the National Standards

\* Received in original form 1953 May 19.

† Values of  $15^h 54^m\cdot6$  and  $-60^\circ 10'$  have been derived by plotting positions of CPD stars and reducing to the equinox of 1900.

Laboratory, Sydney, and, together with the makers' data for the response of the cell, are shown in Table I.

TABLE I  
Percentage transmission of filters and cell response

$\lambda$ (A)	F 3653	F 4937	Cell	$\lambda$ (A)	F 3653	F 4937	Cell
4000	77.8	3.1	54.5	5400	0.0	91.5	58.1
4200	66.2	4.2	59.5	5600	0.0	91.7	42.6
4400	45.6	7.0	63.8	5800	0.0	91.7	30.8
4600	22.4	15.6	65.2	6000	0.0	91.5	16.5
4800	4.2	65.4	64.8	6200	0.0	91.4	7.9
5000	0.4	89.6	62.7	6800	0.0	90.7	1.0
5200	0.0	91.2	61.8	7000	0.0	90.4	0.0

Generally the method used was to expose the cell to a star for 1 minute through the blue filter, close the photometer for  $\frac{1}{2}$  minute, open through the yellow for 1 minute, close for  $\frac{1}{2}$  minute and finally open for 1 minute through the blue filter. The performance of the photometer was controlled by a radioactive luminous source and sky corrections were applied. Absorption corrections for colours were applied with an average coefficient throughout, based on results obtained by Woolley and Gascoigne (6) in the course of a spectrophotometric programme. The adopted values were  $k$  (blue) =  $0^m.34$ (sec  $z$ ) and

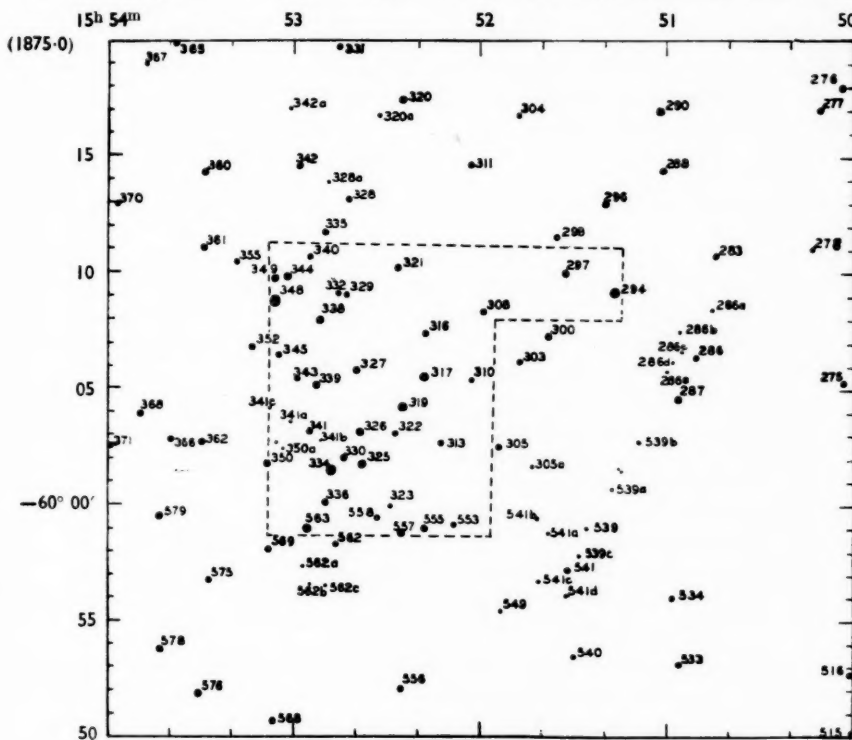


FIG. 1.—Chart of NGC 6025 region. Stars are marked with the last three numbers of the CPD designation. The broken line encloses the "central region" as defined by "star counts".

$k$  (yellow) =  $0^m\cdot2\Delta(\sec z)$ , the difference  $0^m\cdot1\Delta(\sec z)$  being used to correct the observed colours to a standard zenith distance such that  $\sec z = 1\cdot1$ , corresponding to that of the cluster at culmination. The use of such averaged coefficients may not be entirely satisfactory but as the measures were conducted during a spell of unusually cloudy weather it was decided to omit special measures of absorption on each, more especially as the corrections to be applied were usually less than  $0^m\cdot03$ .

3. *Programme and results.*—The observational programme aimed at determining colours and magnitudes of all CPD stars between the limits  $\alpha(1875) = 15^h 51^m$  to  $15^h 54^m$  and  $\delta(1875) = -59^\circ 50'$  to  $-60^\circ 15'$ . Certain regions were examined more closely to obtain measures of fainter stars. The stars are noted on the chart shown in Fig. 1. Four stars in the cluster were standardized by connection to working scales termed  $b$  and  $y$  which had been derived in the course of unpublished photoelectric measures of the Harvard F1 region. The  $b$  scale was related to the Harvard Photographic Scale (HPg, with the correction given in *Harvard Bulletin* 718) by the expression

$$pPg = b + 0\cdot13 - 0\cdot37Cpe = HPg \pm 0\cdot11 \text{ s.d.}, \quad (1)$$

using the results from 24 stars. In this expression the photoelectric colour  $Cpe$  is measured as the magnitude difference of the yellow and blue readings and is related to the difference  $b - y$  by the equation

$$Cpe = b - y - 0\cdot43.$$

Photovisual magnitudes were obtained by the comparison of 25 stars in the F1 region which were available from the Woolley, Gottlieb and Przybylski measures (7) and gave the result

$$pIPv = y + 0\cdot35 - 0\cdot12Cpe = IPv \pm 0\cdot05 \text{ s.d.} \quad (2)$$

The colours were obtained as the difference between (1) and (2), which reduces to

$$pCi = 0\cdot75Cpe + 0\cdot207.$$

The results are shown in Table II, which gives the following particulars:—

- Col. (1) CPD designation of star. (Stars not listed in CPD have been lettered and referred to an adjoining CPD star. The lettered stars are not in order of right ascension.)
- (2) Magnitudes in the  $b$  system used for the F1 region.
- (3) Dispersions (standard deviations) of  $b$  in hundredths of a magnitude.
- (4) Colours,  $Cpe$ , measured directly in thousandths of a magnitude.
- (5) Standard deviations of  $Cpe$ .
- (6, 7) Number of observations,  $r$ , on  $n$  nights.
- (8) Magnitudes  $pPg$ .
- (9) Colours reduced to International scale  $pCi$ .
- (10) Position in cluster,  $c$  = central,  $o$  = outer.
- (11, 12) HD spectral type and number when available.

4. *Colour-magnitude relations.*—The colour-magnitude relation is shown in Fig. 2 where the coordinates are  $pPg$  and  $pCi$ . Two alternatives present themselves in interpreting these results. The generally accepted method is to regard the cluster members as possessing an inherent scatter in the colour-magnitude relation, a scatter which is sometimes referred to as the "cosmic dispersion".

TABLE II  
Colours and magnitudes in the NGC 6025 region

CPD No.	<i>b</i>	Mean	s.d.	1000 Cpe	Obsns	<i>pPg</i>	<i>pCi</i> $\times 1000$	Posn	Sp	HD	
-60°				Mean	<i>r</i>	<i>n</i>					
6286a	12·86	2	+	309	13	6	12·90	+	439	o	
6286b	12·77	3	+	325	85	4	12·78	+	451	o	
6286c	12·60	2	-	105	24	6	12·77	+	128	o	
6286e	13·27	5	+	017	28	3	13·39	+	219	o	
6294	8·89	1	-	555	17	4	9·23	-	209	c	
6296	10·61	1	-	360	30	3	10·87	-	063	o	
6297	11·54	1	-	247	24	3	11·76	+	022	c	
6298	10·60	2	-	343	34	3	10·86	-	050	o	
6300	11·16	5	+	080	25	3	11·26	+	267	o	
6303	11·28	...	-	362	...	1	11·54	-	065	o	
6305	10·03	1	-	240	11	6	10·25	+	027	o	
6305a	12·53	3	-	093	32	3	12·69	+	137		
6308	10·88	4	-	560	35	3	11·22	-	213	c	
6310	12·36	11	-	040	72	3	12·51	+	177	c	
6311	10·37	4	-	400	52	3	10·65	-	093	o	
6313	10·49	4	-	510	13	3	10·81	-	175	c	
6316	9·92	4	-	440	32	3	10·21	-	123	c	
6317	8·49	1	-	560	20	2	8·83	-	213	c	
6319	9·61	...	-	510	...	1	9·93	-	175	c	
6320	11·21	1	-	180	24	5	11·41	+	072	o	
6320a	13·55	2	+	230	20	2	13·60	+	379	o	
6321	10·63	2	-	370	40	2	10·90	-	070	c	
6322	9·41	3	-	573	14	3	9·75	-	223	c	
6323	8·76	...	-	605	...	1	9·11	-	247	c	
6325	8·43	2	-	573	14	3	8·77	-	223	c	
6326	7·58	1	-	606	17	5	7·93	-	248	c	
6327	9·68	1	-	117	12	3	9·85	+	119	c	
6328	12·19	14	-	255	25	2	12·41	+	014	o	
6328a	12·95	2	+	1140	17	3	12·66	+	1062	o	
6330	10·93	3	-	268	9	4	11·16	+	006	c	
6331	11·16	4	-	220	30	3	11·37	+	042	o	
†6332	8·52	11	-	537	33	3	9·62	-	195	c	
6334	8·68	1	-	550	24	4	9·01	-	205	c	
6335	10·64	3	-	350	5	2	10·90	-	055	o	
6336	10·34	2	-	367	3	3	10·61	-	068	c	
6338	7·95	0	-	542	9	10	7·82	-	200	c	
6339	9·44	2	-	548	5	4	9·77	-	204	c	
6340	11·08	1	-	235	5	2	11·30	+	031	c	
6341	10·27	1	+	075	14	11	10·37	+	263	c	
6341b	12·92	4	-	033	13	6	4	13·06	-	041	c
‡6341c	(15·15)	17	(+1450)	180	3	2	(14·71)	(+1294)	o		
6342	11·27	1	-	122	20	4	11·44	+	115	o	
6342a	13·40	2	+	1640	25	4	12·92	+	330	o	
6343	10·72	6	-	422	12	5	4	11·01	-	110	c
6344	10·59	...	-	330	...	1	10·84	-	041	c	
6345	10·88	6	-	333	7	3	11·13	-	043	c	
6348	6·59	1	-	795	15	2	7·01	-	389	c	
6349	7·65	2	-	570	8	6	7·99	-	221	c	
6350	10·96	2	-	327	17	3	11·19	-	038	c	
6350a	14·65	3	+	936	28	5	14·43	+	909	c	
6352	10·95	1	-	150	33	2	11·14	+	094	o	
6355	12·37	5	-	022	10	2	12·51	+	042	o	
6360	11·03	0	-	279	5	2	11·26	-	002	o	
6361	10·90	1	-	335	5	2	11·15	-	044	o	
6362	10·16	1	-	436	7	3	10·45	-	120	o	

\* This reading includes the light from two stars.

† This star is near 6329 the light from which may be responsible for some of the apparent scatter in the readings for 6332.

‡ Small deflections and large scatter.

TABLE II (cont.)

CPD No.	<i>b</i> Mean	s.d.	1000 Cpe Mean	s.d.	Obsns <i>r</i>	<i>n</i>	<i>pPg</i>	<i>pCi</i> × 1000	Posn	Sp	HD
6366	11.97	1	+ 773	28	3	3	11.81	+ 787	o		
6368	11.13	9	- 320	18	3	3	11.38	- 933	o		
6370	11.05	1	- 320	19	2	2	11.30	- 933	o		
6371	11.33	3	+ 1200	28	3	3	11.02	+ 1107	o		
- 59°											
6539	11.78	3	- 243	7	3	3	12.00	+ 045	o		
6539a	13.17	6	- 090	8	3	2	13.33	+ 139	o		
6539b	13.31	5	+ 1550	58	3	3	13.87	+ 1369	o		
6539c	12.81	1	- 055	27	3	2	12.96	+ 166	o		
6540	11.71	1	- 095	15	2	1	11.87	+ 136	o		
6541	10.87	1	- 344	9	5	4	11.13	- 050	o		
6541a	12.53	2	- 110	10	3	3	12.70	+ 125	o		
6541b	14.52	...	+ 1340	...	1	1	14.15	+ 1212	o		
6541c	11.63	2	+ 020	7	3	2	11.75	+ 222	o		
6541d	11.94	...	- 408	...	1	1	12.22	- 201	o		
6549	11.66	1	+ 050	20	2	2	11.77	+ 245	o		
6553	10.87	1	- 380	10	3	2	11.14	- 078	c		
6556	11.24	2	- 220	7	4	3	11.45	- 042	o		
6557	8.81	2	- 583	9	3	3	9.16	- 230	c		
6558	10.81	2	- 375	15	2	2	11.08	- 074	c		
6562	9.64	1	- 493	7	3	3	9.95	- 163	o		
6562a	13.70	9	+ 1120	20	2	2	13.42	+ 1047	o		
6562b	12.58	3	+ 160	35	2	2	12.67	+ 289	o		
6562c	13.66	5	+ 140	85	2	2	13.74	+ 312	o		
6563	9.30	1	- 515	9	4	4	9.62	- 179	c		
6568	10.33	3	- 413	9	3	3	10.61	- 103	o		
6575	11.40	1	+ 248	30	3	3	11.44	+ 393	o		
6576	8.17	1	- 285	5	2	2	8.40	- 007	o		
6578	10.12	2	- 395	5	2	2	10.40	- 089	o		
6579	11.69	2	+ 895	45	2	2	11.37	+ 465	o		

The points for the cluster members then fall within a band in the array. Such results are typified by the figures of Binnendijk (8) for the Pleiades. In recent years Eggen (4) has produced a considerable amount of observational data leading him to conclude that the observed bands in such a diagram possess a fine structure. Certain observers do not agree with this result, e.g. Johnson and Morgan (9). The present observations do not lend themselves to provide a precise test of fine structure, mainly because of a lack of independent evidence of which stars are actually members of the cluster. However, as will be shown later, the results may be interpreted either in terms of a fine structure (FS) or of a band (B). In the sequel both methods are dealt with, without any implication that either is correct.

Factors tending to cause a colour-luminosity array to depart from a close regular relationship between the two quantities are :—

- (a) Observational error dispersion of the results.
- (b) Distance between the back and front of the cluster.
- (c) Inclusion of close double stars in the array.
- (d) Existence of localized reddening within the cluster.
- (e) Inclusion of non-cluster stars within the array.
- (f) Existence of the so-called "cosmic dispersion".

(a) *Error dispersion of the observations.*—The standard deviations given in Table II average about  $\pm 0^m.025$  in colour and  $\pm 0^m.03$  in magnitude on the Cpe and *b* scales. The equivalent figures on the *pCi* and *pPg* scales are  $\pm 0^m.02$  and  $\pm 0^m.03$  respectively. These of course refer to the internal consistency of the

observations only, and are presumably due mainly to instrumental behaviour, errors in scale reading, and atmospheric variations. As in the present instance the colour parameter is the more important one in determining departure from a curve, a criterion has been adopted that any result departing more than about  $0^m.025$  in  $C_{pe}$  from a suggested curve, except in a few cases where the s.d. differs greatly from its mean, would be unlikely to belong to that curve. The dispersions of the present results are rather greater than is usual in photoelectric work at Canberra (viz.  $0^m.01$  or better in magnitude), but in order to make the most use of available telescope time, much of the work has been carried out on nights that have not been of the first quality and this has increased the dispersions.

pPg

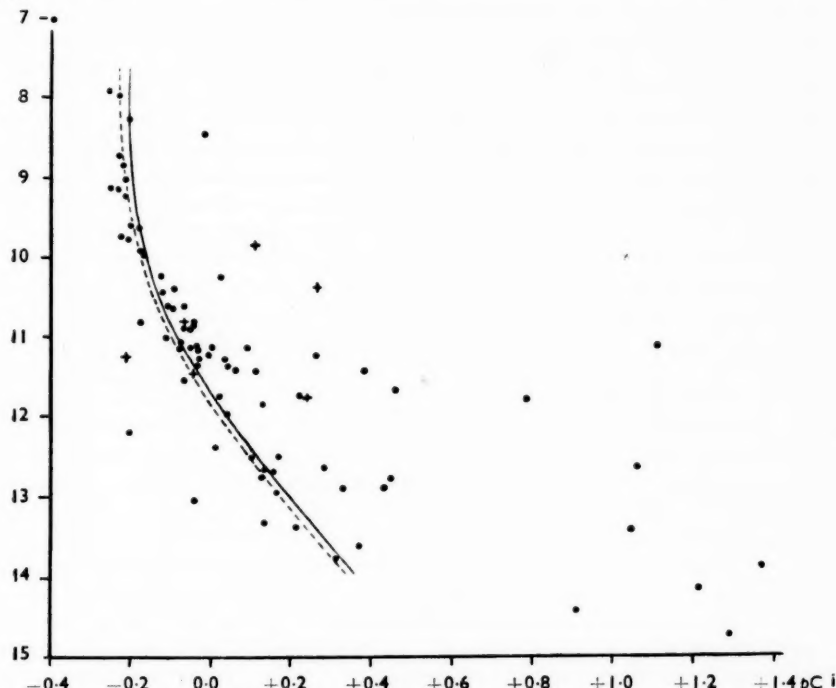


FIG. 2.—Colour-magnitude diagram for NGC 6025. The full curve is taken from Binnendijk's observations for the Pleiades displaced on magnitude scale by  $4^m.6(3)$  units. The broken line shows Binnendijk's curves adjusted by  $0^m.04$  and  $4^m.41$  in colour and magnitude respectively.

(b) *Distance between back and front of the cluster.*—For spherically shaped clusters of relatively small angular diameter  $\theta$ , the apparent magnitude difference between equally luminous stars situated at the nearest and farthest points of the cluster is approximately  $2\theta$  ( $\theta$  in radians) or  $0.0006\theta$  ( $\theta$  in minutes of arc). In the present case  $\theta$  does not exceed  $30'$  and the difference is  $0^m.017$ . This would be quite negligible in the type of diagram found.

(c) *Inclusion of close double stars.*—The observed result for an unresolved binary system is displaced from the result for the brighter component in a colour-magnitude diagram by an amount dependent on the magnitude difference between the components. Thus for zero magnitude difference there is a displacement of

0.75 unit in apparent magnitude without change of colour (if the system is a member of the cluster). Holmberg (10) shows for the Hyades that a maximum colour displacement of  $0^m.05$  occurs when the magnitude difference is  $1^m.5 - 2^m.0$ .

No catalogues have been found to give any specific information of any spectroscopic or other close double stars in the cluster. It is possible that some of the stars later marked as non-members of the cluster might in actual fact be close binary systems belonging to it.

(d) *Existence of reddening in the cluster.*—The results were examined to determine whether any special areas within the cluster were occupied by stars that were systematically redder than might be expected from the general trend of the curve in Fig. 2. No clear evidence of any areas of differential reddening was obtained although it is possible that an area to the south-east of the cluster may be slightly affected in this way.

(e) *Inclusion of non-cluster stars in the array.*—This may be the principal cause of the scatter observed in Fig. 2. Few observations are available which would enable any given star to be positively identified as a cluster member. Mr Wood, Government Astronomer of Sydney Observatory, has kindly made available some unpublished results of proper motions in the cluster region. He considers that the cluster stars have proper motions of something less than one second per century, relative to the stars used as comparisons, and that, at the present stage, it is not possible to identify members positively by their motion. Certain stars of larger proper motion may however be excluded as members of the cluster. In these circumstances the results have been treated statistically with the object of ascertaining whether the probable number of field stars in the central region of the cluster agrees with the number of observations in the same region departing from the system of curves determined by Eggen for the Pleiades. For this purpose star images on an astrographic plate of the region, taken by Wood, were counted. The plate showed stars to about the same magnitude as those measured photometrically in the central region. The number of stars per square of  $10'$  side in regions definitely outside the cluster was  $6.5 \pm 2.8$  (s.d. per single square). It was taken that any square for which the residual was more than twice the s.d., i.e. any square containing more than 12 stars, was definitely within the cluster. The measuring réseau had been adjusted so that the bulk of the cluster was contained in one square which was found to contain 26.5 stars. An adjoining square contained 14.5 stars. It was obvious that both squares were associated with the cluster but a more detailed examination was needed to determine what proportions of the square containing 14.5 stars was covered by cluster stars. Smaller regions of the square were examined and this led to the limits shown in Fig. 1 being adopted as representing the central region of the cluster. A check was obtained by comparing the density of stars over all the area (viz. 130 square minutes) within these limits and density in the 26.5-star square which was clearly a cluster area. The full area of 130 square minutes would be expected to contain 34.5 stars on the 26.5-star basis. The actual number of stars counted on the plate was 32, showing the adopted area to be substantially correct. Further, the maximum number of field stars to be expected in the area, allowing a dispersion of 1.5 times the standard deviation as likely, would be 12.5, a figure which will be referred to later.

*Interpretation in terms of colour-luminosity band (B).*—The colour-magnitude diagram for all the observed stars is shown in Fig. 2, where the results are plotted

in  $pPg$  and  $pCi$  coordinates. The full curve there fitted to the observations is taken from Binnendijk's results for the Pleiades cluster, displaced on the magnitude scale by  $4\cdot6(3)$  units. As the modulus for the Pleiades is  $5\cdot0$ , this is equivalent to assuming a modulus of  $9\cdot16$  for NGC 6025. The colour coordinate has been left unchanged. Although the fit is not very satisfactory the diagram can be used to examine the "cosmic dispersion" of the colour-luminosity relation. For this purpose stars whose colour falls within  $0^m\cdot05$  of the line in Fig. 2 have been regarded as cluster members. This gives a cluster membership of 46 stars, but if the permitted residual is taken as  $0^m\cdot1$  then seven more stars are to be included in the cluster. The s.d. of one of the 46 points from the line amounts to  $\pm 0^m\cdot029$  in colour. As the (internal) s.d. of an observation is  $\pm 0^m\cdot019$  the "cosmic dispersion" is calculated as  $\pm 0^m\cdot021$ . This may be compared with the figure of  $\pm 0^m\cdot059$  given by Holmberg for the case of the Hyades cluster, where the stars have been selected by proper-motion criteria. However, the present figure is dependent largely on the scatter permitted in the selected stars. Its main use is to indicate that the criterion adopted in the present case is not less strict in the mean than that employed in the known case of the Hyades cluster. The 46 stars to be regarded as cluster members by this method are listed in Table III. One of these stars, viz. 296 (i.e. CPD  $-60^\circ$  6296) is reported by Wood as having relatively large proper motion.

TABLE III  
NGC 6025  
*Cluster members by band interpretation*

286c	*319	*344	541a
*286e	*321	345	*553
*294	323	*349	556
296	*325	350	*557
*297	326	*355	*558
*298	*332	360	*562
303	*334	362	*562c
305a	*335	*368	*563
*310	*336	*370	568
311	*338	539	*578
*316	*339	539c	
*317	343	541	

\* Stars marked thus are given as cluster members by both band and fine-structure interpretations.

A more satisfactory fit for the brighter stars is obtained if both the colour and magnitude coordinates are adjusted, by  $0^m\cdot04$  and  $4^m\cdot41$  respectively. This assumes a modulus of  $5^m\cdot0 + 4^m\cdot41 = 9^m\cdot41$  and allows for a discrepancy of  $0^m\cdot04$  in the two colour scales, which might have arisen observationally or have been brought about by the Pleiades being slightly reddened relative to NGC 6025. This adjustment is shown by the dotted line in Fig. 2. Neither curve gives a good representation of the results over the whole range of magnitude.

*Interpretation by fine-structure curves (FS).*—The colour-magnitude array for the central region as defined by star counts, plotted on the  $pPg$  and  $pCi$  scales, is shown in Fig. 3. The curves determined by Eggen were superposed on the points to give the best apparent agreement. This occurred when the modulus for the cluster was taken as  $9^m\cdot53$  and the colour scale was moved so that the

NGC 6025 results were bluer by 0.04 units than Eggen's figures. Examination of this diagram (see also Table IV) shows that, allowing an extension of Eggen's "bright blue dwarf" sequence, as shown by a broken line, twenty-one stars fall in the system, and eleven fall outside its limits. Of these eleven stars it is possible some would be spectroscopic binaries and would, if their components were of appropriate magnitude, account for some of the anomalies. Holmberg mentions that some 10 out of 49 known cluster members of the Hyades are given as spectroscopic binaries. If this proportion is maintained in the present cluster then about 4 of the 11 observed anomalies might be accounted for in this manner. Accordingly the number of field stars to be accounted for would be between 7 and 11, which figures are within the expected maximum of 12.5 derived above. It is therefore concluded that there is nothing in the present results to provide positive evidence against the concept that the actual members of the cluster NGC 6025 would give a colour-luminosity array which could be represented by the curves drawn by Eggen for the Pleiades. Further, certain of the results which fall notably away from the lines in Fig. 3 are from stars which have proper motions thought by Wood to be large enough to show non-membership of the cluster. These stars are as follows :—

$-59^{\circ}$	6549 and 6556
$-60^{\circ}$	6296, 6308, 6327 and 6341

They are to be regarded as non-members of the cluster both by photometric and proper-motion criteria. One star,  $-60^{\circ} 6334$ , belongs photometrically to the cluster but has a relatively large proper motion. The stars filling the gap between the blue dwarf and the bright blue dwarf lines (see Fig. 3) do not show proper motion, but, of course, whilst relatively large proper motion indicates non-membership of the cluster, the converse, that relatively small proper motion indicates membership, is not necessarily true. Finally the bright star  $-60^{\circ} 6348$ , which falls well away from the lines, is noted as having a spectrum which shows the lines  $H\beta$  and  $H\gamma$  in emission, and this may account for its relatively blue colour. Twenty-seven stars, denoted by asterisks in Table III, are given as members both by B and FS criteria. These 27 stars include  $-60^{\circ} 6334$  which is reported by Wood as having a relatively large proper motion.

5. *Distance and dimensions.*—Collinder's catalogue lists a variety of figures for the angular diameter of the cluster, ranging from  $10'$  given by Melotte to a figure of  $19'$  from Raab. The present star-counting results suggest a figure of  $12'$  for the central region, but including the outer stars which fall on the lines in Fig. 2 the cluster may be regarded as extending over an area about  $28'$  in diameter as far as stars down to about the twelfth magnitude are concerned or about  $30'$  to cover the stars listed in Table IV.

Collinder, from an estimate of the integrated magnitude of the cluster, gives a figure of 1020 parsecs for the distance, neglecting absorption. Trumpler's photographic modulus of  $9^{m}.5$  from spectroscopic parallaxes corresponds, for zero absorption, to a distance of 800 parsecs, whilst Mrs Riecke's modulus gives 480 parsecs. The fine-structure interpretation of Fig. 3 suggests a modulus of  $9^{m}.5(3)$ , agreeing excellently with Trumpler's result and corresponding to a distance of 805 parsecs. Adopting the present figures of distance and diameter leads to an estimate of some 6.2 parsecs for the overall dimensions of the cluster, with a possible reduction on account of absorption.

TABLE IV

*NGC 6025 interpreted by fine-structure hypothesis*

CPD No.	Dwarfs	Blue dwarfs	Bright blue dwarfs	Non-members
<b>I. Stars in central field</b>				
(a) Brighter than about 12 <sup>m</sup>				
-59°	6553		×	
	6557		×	
	6558		×	
	6563		×	
-60°	6294		×	
	6297		×	
	6308			
	6310	×		
	6313			×
	6316		×	
	6317		×	
	6319		×	
	6321		×*	
	6322			×†
	6323			×
	6325		×	
	6326			×
	6327			×
	6330		×	
	6332	×		
	6334	×		
	6336		×	
	6338	×*		
	6339	×*		
	6340		×	
	6341			×
	6343			×
	6344		×	
	6345			×
	6348			×
	6349		×	
	6350			×
(b) Stars fainter than 12 <sup>m</sup>				
	6341b			×
	6341c			×
<b>II. Stars outside central field but falling on curves of array</b>				
-59°	6562		×	
	6562c	×		
	6563		×	
	6578		×	
-60°	6286e	×		
	6298		×	
	6320	×		
	6331		×	
	6335			×
	6368		×	
	6370		×	

\* Large s.d. † 1 observation.

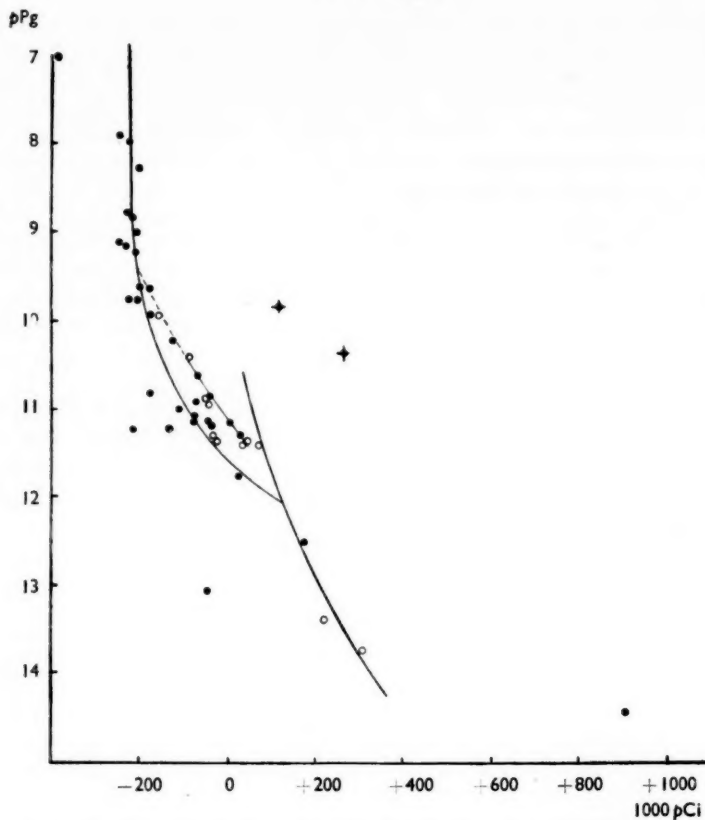


FIG. 3.—Colour-magnitude diagram for the central region of the cluster. The curves are those given by Eggen for the Pleiades, taking the modulus for the cluster as  $9^m\cdot53$  and adjusting the colour scale by the addition of  $0^m\cdot040$  to Eggen's figures.

The following table, which applies to stars brighter than  $12^m$ , for which the observations are relatively complete, summarizes the results of the "fine structure" (FS) and "band" (B) methods of examining the measurements.

TABLE V  
NGC 6025  
Stars brighter than  $12^m$

	FS	B
Angular diameter (minutes)	28	30
Distance (zero absorption) parsecs	805	830
Linear diameter (zero absorption) parsecs	6.5	7.2
Cluster members		
Dwarfs	4	
Blue dwarfs	16	
Bright blue dwarfs	12	
Total stars	32	41
Density (stars per parsec <sup>3</sup> )	0.2	0.2

*Acknowledgments.*—It is a pleasure to acknowledge the help received in discussions with Professor R. v. d. R. Woolley and Professor J. Schilt, as well as the kindness of Mr H. Wood in making available the unpublished results of his observations of the proper motions of stars in the cluster. Mr Wood and Dr de Vaucouleurs have also obtained plates of the region for counting and identification purposes.

Commonwealth Observatory,  
Mount Stromlo,  
Canberra, Australia :  
1953 May 11, revised October 26.

#### References

- (1) R. J. Trumpler, *L.O.B.* 420, 154, 1930.
- (2) P. Collinder, *Ann. Obs. Lund*, No. 2, 1931.
- (3) C. A. Riecke, *Harv. Circ.* No. 397, 1935.
- (4) O. J. Eggen, *Ap. J.*, 111, 349, 1950.
- (5) G. E. Kron, *Ap. J.*, 115, 1, 1952.
- (6) R. v. d. R. Woolley and S. C. Gascoigne, unpublished material.
- (7) R. v. d. R. Woolley, K. Gottlieb and A. Przybylski, *M.N.*, 112, 665, 1952.
- (8) L. Binnendijk, *Ann. Leiden*, XIX, 1946.
- (9) H. L. Johnson and W. W. Morgan, *Ap. J.*, 114, 522, 1951.
- (10) E. Holmberg, *Lund Medd.*, Ser. II, No. 113, 68, 1944.

## A PHOTOGRAPHIC SURVEY OF GALACTIC CLUSTERS NGC 6531, 6546, 6469, 6494, 6544, 7127, 7128

S. N. Svolopoulos

(Communicated by the Director, Norman Lockyer Observatory)

(Received 1953 April 28)

### Summary

The methods applied in this paper have been described in previous communications from the Norman Lockyer Observatory. The distance modulus, based on CI, is used for the recognition of cluster members and the determination of the cluster distance. For the clusters NGC 6531, 6546, 6494 corrections for absorption were obtained, after estimations of the CE. This was not possible for the clusters NGC 6469, 7127, 7128. The clusters NGC 6469 and 7127 are assumed to contain giants. For the NGC 6544 a general description is given.

---

The methods of surveying the galactic clusters, described by G. Alter in previous contributions from the Norman Lockyer Observatory (1), have been applied to seven galactic clusters, with the results given in this paper. The material is arranged as in the communications mentioned.

The clusters of the present paper are located in parts of the sky including striking objects, such as conspicuous nebulae, obscuring matter and tufts of filmy light.

The mean deviations of magnitudes of the NPS on the set of plates of the clusters NGC 6531, 6546 was  $\pm 0^m.12$  on the photographic scale, and  $\pm 0^m.18$  on the photovisual scale. The mean error of the CI is therefore  $\pm 0^m.21$ . The corresponding numbers for the set of plates of the clusters NGC 6469, 6494 were  $\pm 0^m.18$ ,  $\pm 0^m.16$  and  $\pm 0^m.22$  respectively; while for the clusters NGC 7127, 7128 they were  $\pm 0^m.11$ ,  $\pm 0^m.13$  and  $\pm 0^m.17$  respectively. The order of exposure in all cases was: NPS-Cluster.

NGC 6531  
R.A.  $17^h 58^m 6^s$ , Dec.  $-22^\circ 30'$  (1900.0)

This cluster shows a strong concentration in the centre, where, on the Sidmouth plates, the stars are almost indistinguishable. Shapley (2), Raab (3), Trumpler (4), Collinder (5), C. A. Ricke (6), Hayford (7) and Zug (8) have published results of investigations on this cluster.

The star counting gave 109 stars as the total number within a cluster region of  $13.^{\circ}6$  diameter. After correction for background the number of cluster stars is 57. The accompanying figure shows the star densities per square degree within the cluster region after correction for background.

Table I gives the CE of some cluster stars after a comparison of CI computed from the spectral types, published by Zug and in the HD Extension (1949), with the CI found in this investigation.

In Table II the coordinates, the magnitudes and the distance moduli of the stars within the cluster area are shown. The distance modulus  $m - M$  was obtained from the CI corrected for the CE given in Table I. For the other stars, of unknown spectral type, the assumption of a mean CE + 0.43 was made.

The mean distance modulus of the cluster group is 9.34. This value, according to the formula

$$m - M_0 = 5 \log r + a_{pr} \cdot r - 5 \quad (1)$$

(where  $a_{pr} = 0^m.35$  per kiloparsec was assumed) corresponds to a distance  $680 \pm 60$  parsecs.

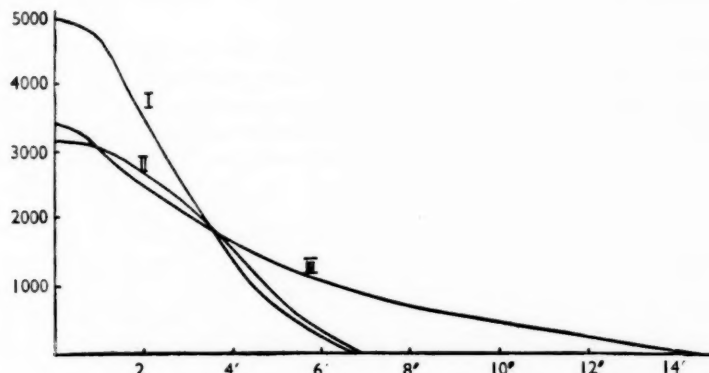


FIG. 1.—Star density per square degree above background density.  
I, NGC 6531. II, NGC 6546. III, NGC 6494.

TABLE I  
Colour excess (NGC 6531)

Star	CE	Star	CE
24	+0.89	47	+0.10
25	0.39	48	0.39
29	0.12	50	0.01
32	0.20	56	1.32
33	0.33	55	0.44
45	1.07	63	1.00

Therefore the cluster diameter is  $d = 13'.6 = 2.7$  parsecs.

The results of previous observations are

	Distance	Diameter
Raab	715 pc	19-20' 4.2 pc
Shapley	570-910	10 2.6
Trumpler	980	12 3.4
Collinder	1590	10 4.6
Rieke	1350	

Of the 57 CI stars of Table II, 44 belong to the cluster and the same relation, when applied to 109 stars obtained by counting, gives a total of 84. We may correct the result in the following way. Out of 15 stars fainter than 12.00, 8 belong to the cluster group and the same relation, when applied to 67 stars fainter

than 12.00, gives 36 cluster stars. When we add the 36 cluster stars, brighter than 12.00, we get 72 cluster stars. Eleven stars of a nearby area of the cluster size are to be found lying in the ( $m - M$ ) cluster range. After applying this background correction, we have 61 as the final number of cluster stars. This number agrees with the one obtained statistically. The dispersion is  $\sigma = \pm 8$ . The magnitude distribution (after correction for background) is given in the following table:

$m_v$	8	9	10	11	12	$> 12.5$
Number of stars	1	4	4	6	18	28

A comparison of the magnitudes and CI of Table II with that given by Zug showed appreciable differences.

TABLE II

Coordinates, magnitudes and distance moduli of 57 stars (NGC 6531)

Zero point=star number 46, unit= $1' \cdot 0$ ,  $X$ =east,  $Y$ =south. Coordinates of the assumed cluster centre  $X = -1' \cdot 6$ ,  $Y = 0 \cdot 0$ 

Star	$X$	$Y$	$m_p$	$m_v$	$m - M$	Star	$X$	$Y$	$m_p$	$m_v$	$m - M$
54	+1.2	+4.2	11.45	10.28	5.4	25	-2.6	+2.6	9.68	9.43	9.5
90	-0.1	+7.6	12.79	11.51	6.3	40	-1.7	-1.5	12.58	11.89	9.5
91	+4.8	+4.5	12.79	11.52	6.3	63	+4.1	-0.9	9.80	8.97	9.6
71	-1.4	-6.3	13.02	11.97	6.4	36	-1.4	+1.1	11.62	11.14	9.7
56	+1.7	+4.8	13.11	11.73	6.4	39	-2.0	-0.7	13.28	12.53	9.7
64	+5.3	-2.0	12.69	11.53	6.6	62	+4.3	-0.4	12.28	11.67	9.8
						26	-3.9	+0.7	12.17	11.59	9.8
18	-6.5	+0.1	12.15	11.23	7.3	9	-6.7	+2.3	12.11	11.54	9.8
87	-7.9	-3.2	12.89	11.87	7.4	45	-0.1	-0.9	9.85	8.88	9.9
59	+2.2	-3.0	13.33	12.23	7.5	16	-8.2	-0.8	9.36	8.28	9.9
58	+1.5	-1.8	12.90	11.94	7.7	32	-3.7	-4.2	8.51	8.54	10.2
99	+6.1	+2.1	13.35	12.32	7.8	70	-2.1	-6.3	10.37	9.55	10.2
35	-1.6	+1.5	11.83	11.03	8.0	33	-1.1	+2.4	9.47	9.34	10.3
6	-3.9	+4.7	12.30	11.46	8.0	49	+0.1	+0.9	11.12	11.56	10.3
65	+0.7	-5.1	11.93	11.14	8.1	28	-5.1	-0.3	12.25	11.55	10.3
50	+0.4	+1.0	13.15	12.23	8.3	31	-4.6	-4.1	12.03	11.56	10.3
44	-0.5	-2.4	12.03	11.33	8.3	47	+0.8	+0.3	9.64	9.74	10.7
42	-2.9	-2.2	11.62	10.83	8.4	22	-2.4	+4.8	12.49	12.02	10.7
10	-8.0	+1.9	9.51	9.52	8.4	37	-2.4	+0.3	11.72	11.40	10.8
57	-0.2	-3.0	12.55	11.73	8.5	29	-4.9	-1.5	10.10	10.15	10.8
73	-4.8	-6.5	12.12	11.39	8.7	48	+1.3	+0.4	11.88	11.55	10.8
72	-1.7	-7.3	12.67	11.88	8.9	24	-2.4	+3.7	9.57	8.95	10.9
53	-0.2	+2.4	13.17	12.34	9.0						
11	-7.4	+1.1	10.92	10.44	9.0	51	+0.4	+1.5	13.14	12.82	12.2
21	-3.3	+3.4	12.98	12.16	9.1	19	-5.8	+1.0	12.75	12.53	13.1
41	-3.0	-1.3	12.42	11.69	9.1	89	-9.0	-4.8	12.14	12.12	15.3
55	+1.8	+3.4	10.05	9.78	9.2	52	+0.4	+2.0	13.15	13.15	16.2
30	-4.5	-2.7	12.83	12.08	9.4	23	-1.9	+4.1	12.07	12.20	16.2
46	0.0	0.0	8.54	8.71	9.4	74	-4.5	-5.3	12.52	12.55	17.1
						84	+2.4	-6.7	13.22	13.25	17.8

## NGC 6546

R.A.  $18^{\text{h}} 01^{\text{m}} 2\text{s}$ , Dec.  $-23^{\circ} 19'$  (1900.0)

This cluster is a large one, but without appreciable concentration. It is mentioned in the catalogues by Trumpler (4) and Collinder (5). The star counting gave 107 stars within a region of  $13' \cdot 6$  diameter. Correction for the

background density results in 50 cluster stars. The accompanying figure gives the star density per square degree within the cluster region.

Table III shows the results of a comparison of the measured CI of 8 stars with the CI computed from the HD Extension (1949). The mean CE is  $+0^m.12$ .

TABLE III  
Colour excess (NGC 6546)

Star	CE	Star	CE
60	-0.07	91	+0.10
61	+0.13	96	-0.19
75	+0.15	100	+0.29
89	+0.01	102	+0.51

In Table IV the distance modulus  $m - M$  is given after the correction for CE given in Table III. For the stars which do not appear in Table III, the assumption of a mean CE  $+0^m.12$  was made. The stars 60 and 89, which are the brightest of the cluster and are also of late spectral types (M2 and K0 respectively), were regarded as giants and the value  $M=0$  was assumed for them.

TABLE IV  
Coordinates, magnitudes and distance moduli of 23 stars (NGC 6546)

Zero point = star 96 = HD 165554. Unit =  $1^{\circ}0$ , X = west, Y = north. Coordinates of the assumed cluster centre  $X = -2^{\circ}7$ ,  $Y = +0^{\circ}5$

Star	X	Y	$m_p$	$m_v$	$m - M$	Star	X	Y	$m_p$	$m_v$	$m - M$
58	-5.8	+5.3	12.41	10.54	2.1	60	+1.1	+3.7	10.95	9.30	9.3
73	-5.9	+1.4	13.00	11.35	3.6	64	-4.2	+3.7	12.19	11.75	9.3
99	-3.4	-0.4	11.81	10.59	4.2	100	-4.0	-0.1	10.96	10.69	9.6
70	-9.1	+2.4	13.40	12.01	4.9	121	-2.2	-3.9	10.84	10.77	9.9
55	-5.0	+7.5	11.84	10.99	6.1	92	+1.7	-0.4	11.59	11.35	10.0
91	+3.0	-1.9	11.40	10.75	6.7	97	-0.9	+0.4	13.04	12.60	10.1
80	+1.3	+1.8	12.69	11.90	6.9	102	-5.5	-0.3	11.74	11.25	10.2
54	+0.3	+6.4	13.11	12.24	7.3	93	+2.0	-1.3	12.58	12.32	10.7
96	0.0	9.96	9.85	7.5		78	-2.2	+2.5	12.78	12.52	11.0
						75	-2.9	+1.3	10.74	10.76	11.4
103	-6.1	-1.7	11.81	11.37	8.9						
90	+3.8	-2.5	12.14	11.67	9.0	61	-2.1	+3.4	11.04	11.15	12.7
89	+3.9	-0.5	10.19	9.11	9.1						

The mean distance modulus of the cluster group is 9.90 corresponding to

$$r = 830 \pm 60 \text{ parsecs} \quad \text{and} \quad d = 13^{\circ}6 = 3.2 \text{ parsecs.}$$

The results of the previous observations are

	Distance	Diameter
Trumpler	3000 pc	13' 11.1 pc
Collinder	1800	12' 6.3

Trumpler's estimate was not a direct one.

Among the 23 CI stars, 13 belong to the cluster and the same relation when applied to 107 stars, obtained by counting, gives a total of 61 stars. This became 59 after correction for background and agrees with the number of cluster stars obtained statistically. The dispersion is  $\sigma = \pm 8$ .

The magnitude distribution (after correction for background) is given in the following table:

$m_v$	9	10	11	12	$>12\cdot5$
Number of stars	2	0	8	1	48

### NGC 6469

R.A.  $17^{\text{h}}46^{\text{m}}9\text{s}$ , Dec.  $-22^{\circ}19'$  (1900·0)

This cluster is fairly irregular and not well detached from the environs. It is mentioned by Shapley, Raab, Trumpler and Collinder in their papers.

Table V gives the coordinates, magnitudes and distance moduli of stars within the cluster region. In the first part of the table the absolute magnitudes were taken from the main sequence. Here appear two ranges in the distance modulus

TABLE VA

*Coordinates, magnitudes and distance moduli of 21 stars (NGC 6469)*

Zero point = star number 1 = HD 162694. Unit =  $1^{\circ}\text{o}$ , X = west, Y = south. Coordinates of the assumed cluster centre  $X = -0\cdot8$ ,  $Y = 3\cdot7$

Star	X	Y	$m_p$	$m_v$	$m-M$	Star	X	Y	$m_p$	$m_v$	$m-M$
40	-4·0	+5·8	12·42	10·81	2·7	25	+2·8	+7·0	12·54	12·18	9·4
24	+3·2	+4·4	12·51	11·20	4·0	28	+4·1	+2·4	12·60	12·26	9·6
9	-5·4	-2·9	12·92	11·50	4·0	42	-0·3	+10·8	13·22	12·80	9·6
4	-4·6	+2·4	12·83	11·90	6·5	36	+0·9	+4·4	12·90	12·66	10·2
8	-2·6	-2·2	12·66	11·78	6·6	6	+2·9	-1·3	12·88	12·60	10·4
35	+1·1	+2·8	12·90	12·00	7·3	5	+1·6	-0·9	12·88	12·63	10·5
27	+6·7	+5·3	13·20	12·40	7·4	7	-0·5	-4·6	12·69	12·56	11·1
52	-4·3	+2·4	13·12	12·41	7·6	39	-2·8	+8·3	12·72	12·70	11·5
37	+0·2	+4·0	12·92	12·30	7·8	3	-3·3	+1·1	12·61	12·70	12·2
						2	-0·4	+0·3	12·65	12·75	12·5
26	+2·9	+7·7	13·10	12·60	8·9						
1	0·0	0·0	10·87	10·73	9·1						

TABLE VB

Star	$m-M$	Star	$m-M$	Star	$m-M$
24	4·0	6	10·4	4	11·9
		5	10·5	35	12·0
26	8·9	40	10·8	3	12·2
1	9·1	7	11·1	37	12·3
25	9·4	39	11·5	27	12·4
28	9·6	9	11·5	52	12·4
42	9·6	8	11·8	2	12·5
36	10·2				

which indicate two cluster formations. The mean distance modulus of the first group is 6·4, its distance  $190 \pm 20$  parsecs; the corresponding values for the second group are, respectively, 10·5,  $1260 \pm 130$  parsecs. But it is not probable that there are two clusters in exactly the same area; so the nearer group is assumed to be a group of giants. This assumption is supported by the fact that in HD Extension two stars appeared with late spectral types; it is corroborated also by Lundmark (5) who maintains that the cluster is a Praesepe cluster superposed on a Pleiades cluster.

Using the giant values of  $M$  for the stars of the first group, the second part of Table V gives the redistribution of  $m - M$ . Star 40 has been included in the giant group as it appears in HDE as a G0 star. The contrary happens with the star 24, which appears as A.

The mean value of  $m - M$  is 11.02, and consequently  $r = 1600 \pm 170$  parsecs,  $d = 12'.4 = 5.8$  parsecs.

In the case of this cluster, where no CE is available, the absorption has not been considered and the distances are computed according to the formula

$$m - M_1 = 5 \log r - 5. \quad (2)$$

The results of previous investigations were

	Distance	Diameter
Shapley	1820-2880 pc	12' 10.1 pc
Raab	...	22-27 ...
Trumpler	2370	15 10.4
Collinder	1110	11 3.6
Lundmark	1560	10 4.5

The surrounding of the cluster by a dark nebula suggests the necessity, in the case of the above distance, of correcting for absorption; but no spectral types are available.

The star counting gave 164 stars within a diameter of 12'.4. The surrounding of the cluster by a dark nebula prevents a true background correction. The number of CI cluster stars is 20. The magnitude distribution in the cluster is the following:

	$m_v$	II	12	13
Number of stars		2	9	9

### NGC 6494

R.A.  $17^{\text{h}} 51^{\text{m}} 0\text{s}$ , Dec.  $-19^{\circ} 0' (1900\cdot0)$

This cluster is a bright, large one. Results of investigations on this cluster have been published by Shapley, Raab, Trumpler, Collinder and Klauder-Lambrecht (9).

The star counting gave the total number of stars in the cluster region as 333, and the cluster members as 149 within a cluster region of 27'.2 diameter. Our figure shows the star density per square degree within the cluster region. The density distribution given agrees quite well with that given by Klauder and Lambrecht.

Table VI gives the coordinates, magnitudes and distance moduli of the stars within the cluster region. The cluster range contains 95 out of 165 CI stars. The mean value of  $m - M$  for the cluster group is 8.34. This, according to the formula (2), corresponds to a distance of 470 parsecs.

Correction for absorption can be estimated for the 17 cluster stars for which the spectral types are available from HD Extension (1949). Table VII gives both  $m - M_0$  and CE. The average  $m - M$  is 9.63 and the distance, according to formula (1), is 770 parsecs. The mean CE is +0.52. No assumption can be made for the CE of the other stars. First, because the number of cluster stars with known CE is relatively too small and no investigation of the value of CE in the other stars is possible. Second, it is not possible to apply mean CE as the cluster covers quite

TABLE VI

Coordinates, magnitudes and distance moduli of 165 stars (NGC 6494)

Zero point=star number 152=HD 163426. Unit=1°, X=west, Y=south. Coordinates of the assumed cluster centre X=-0°1, Y=-2°4

Star	X	Y	$m_p$	$m_v$	$m-M$	Star	X	Y	$m_p$	$m_v$	$m-M$
133	-5°3	-4°2	10°76	10°17	1°3	150	-1°8	+0°8	12°51	11°66	6°6
200	-1°2	-2°9	11°49	9°81	1°4	172	+12°3	-4°6	11°82	11°17	6°6
158	+7°0	+1°3	9°73	8°53	1°7	63	+8°6	+8°3	11°37	10°71	6°7
244	+10°4	-10°9	10°84	9°48	2°2	211	-0°3	-8°8	13°46	12°45	6°7
54	+4°3	+8°0	12°48	10°85	2°8	145	-5°4	-1°0	13°21	12°27	6°9
92	+1°4	+5°8	11°50	10°20	3°0	210	-0°1	-8°3	11°93	11°36	7°2
219	-4°5	-8°7	11°81	10°57	3°2	100	-4°2	+6°7	10°10	9°76	7°2
226	-3°3	-11°8	12°03	10°64	3°2	206	+2°7	-5°7	10°70	10°32	7°2
94	+0°8	+4°6	12°27	10°86	3°4	107	-9°0	+4°4	12°71	12°00	7°2
159	+8°7	+1°2	12°94	11°35	3°5	128	-11°1	-3°0	13°30	12°45	7°2
220	-5°3	-8°2	12°25	10°88	3°6	176	+11°6	-6°8	13°10	12°25	7°2
108	-9°8	+5°0	12°81	11°34	3°7	207	+2°9	-8°3	10°27	9°94	7°3
227	-2°6	-11°1	12°46	11°12	3°8	51	-0°5	+7°7	12°89	12°15	7°3
193	+1°7	-2°5	12°00	10°79	3°8	56	+6°7	+7°3	12°77	12°05	7°3
148	-2°9	-1°2	12°56	11°21	3°9	140	-9°2	-0°4	13°75	12°80	7°3
151	-1°2	+0°1	12°36	11°06	3°9	225	-6°3	-12°0	11°91	11°37	7°4
110	-11°1	+6°2	13°72	12°11	4°0	165	+6°6	-1°1	12°40	11°79	7°4
192	+2°1	-3°0	12°89	11°53	4°2	202	-0°9	+3°6	12°71	12°05	7°4
62	+8°6	+9°4	12°71	11°43	4°3	55	+6°5	+7°7	10°90	10°51	7°5
208	+1°6	-8°4	12°22	11°10	4°6	85	+6°2	+6°7	13°11	12°40	7°6
105	-7°7	+3°5	13°37	12°30	4°7	185	+5°2	-5°4	12°88	12°22	7°6
216	-3°2	-5°7	11°41	10°44	4°8	113	-12°3	+2°6	13°41	12°65	7°8
129	-8°8	-9°6	13°50	12°18	5°0	141	-8°3	-0°3	13°45	12°69	7°8
81	+6°5	+3°8	12°01	10°98	5°1	233	+5°2	-14°1	12°21	11°69	7°8
198	+0°4	-2°5	12°70	11°67	5°1	157	+5°9	+1°4	13°80	13°00	8°0
229	+0°7	-12°4	12°02	10°80	5°2	222	-9°0	-8°5	12°57	12°04	8°0
149	-2°5	+0°4	11°21	10°33	5°2	104	-7°4	+2°2	13°43	12°76	8°1
203	0°0	-5°0	11°36	10°49	5°3	218	-3°5	-7°9	12°66	12°13	8°1
228	-2°2	-9°2	13°34	12°13	5°3	52	+0°7	-7°6	13°46	12°81	8°2
123	-10°1	-5°9	13°34	12°14	5°3	127	-9°7	+4°9	13°59	12°90	8°2
131	-7°7	-4°4	13°27	12°07	5°3	147	-3°3	+1°5	13°21	12°64	8°3
217	-2°9	-6°9	11°38	10°52	5°4	241	+6°2	-7°2	14°05	13°29	8°3
173	+13°7	-4°8	13°91	12°68	5°7	82	+5°3	+3°7	11°66	10°43	8°4
205	+1°3	-6°3	11°57	10°76	5°7	90	+0°5	+7°1	14°16	13°36	8°4
231	+4°2	-12°5	12°43	11°45	5°9	201	+0°3	-3°8	11°69	11°32	8°4
246	+15°8	-15°6				13°51	12°91	8°5			
168	+10°9	-3°0	10°79	10°24	6°1	130	-7°3	-5°9	11°21	10°91	8°5
191	+2°6	-3°7	10°63	10°10	6°1	53	+2°2	+8°1	14°11	13°40	8°6
154	-0°1	+2°6	11°91	11°12	6°1	103	-5°8	+2°0	10°71	10°35	8°6
161	+5°3	-0°1	11°33	10°69	6°1	194	+1°5	-1°9	11°30	10°17	8°7
164	+4°3	-1°7	11°66	10°94	6°1	243	+12°1	-9°2	13°80	13°22	8°9
163	+4°8	-1°2	11°61	10°90	6°1	74	+12°7	+1°8	13°72	13°16	9°0
177	+11°3	-7°2	13°65	12°54	6°1	83	+4°7	+4°4	13°20	12°70	9°0
152	0°0	0°0	10°40	9°89	6°1	224	-7°8	-12°4	11°84	11°52	9°0
187	+3°5	-4°2	11°60	10°92	6°2	236	+4°2	-9°6	13°45	12°94	9°1
122	-10°7	-6°9	9°97	9°54	6°2	242	+10°5	-9°2	14°08	13°52	9°3
153	+1°0	+0°4	11°03	10°45	6°2	49	-2°2	+9°6	13°14	12°72	9°5
138	-7°1	-1°1	13°01	12°02	6°3	124	-10°2	-5°2	11°08	10°95	9°5
212	-1°2	-7°6	10°35	9°90	6°4	84	+5°5	+5°4	12°95	12°57	9°6
155	+1°1	+2°5	12°32	11°48	6°4	169	+12°7	-2°0	13°76	13°28	9°6
91	+2°0	+6°0	11°88	11°16	6°4	204	+0°3	-5°8	11°40	11°30	9°9
125	-9°1	-5°0	12°48	11°62	6°4	247	+14°8	-15°6	12°79	12°46	9°9
106	-7°9	+4°0	13°31	12°30	6°5	86	+5°7	+6°8	14°10	13°62	10°0
183	+7°0	-6°6	12°26	11°46	6°5	162	+5°6	-0°7	13°40	13°02	10°0
143	-6°1	+0°4	11°69	11°06	6°6	64	+9°6	+8°1	13°05	12°72	10°1

TABLE VI (Continued)

Coordinates, magnitudes and distance moduli of 165 stars (NGC 6494)

Zero point=star number 152=HD 163426. Unit=1°, X=west, Y=south. Coordinates of the assumed cluster centre X=-0°1, Y=-2°4

Star	X	Y	$m_p$	$m_v$	$m-M$	Star	X	Y	$m_p$	$m_v$	$m-M$
178	+ 10°8	- 6°7	13°75	13°33	10°1	237	+ 4°8	- 9°6	12°55	12°76	11°7
184	+ 6°6	- 5°4	12°09	11°89	10°1	160	+ 7°1	+ 0°2	13°20	13°13	11°7
57	+ 7°0	+ 6°8	12°40	12°16	10°2	215	- 2°3	- 5°0	13°53	13°37	11°8
139	- 9°4	- 1°0	13°15	12°96	10°2	209	+ 0°6	- 8°1	12°27	12°35	11°8
114	- 11°9	- 1°0	13°68	13°29	10°3	88	+ 4°3	+ 6°7	12°95	12°96	11°8
188	+ 3°3	- 2°4	13°15	12°83	10°3	179	+ 9°6	- 5°8	13°35	13°52	11°8
121	- 12°6	- 7°0	11°65	11°63	10°4	181	+ 7°5	- 3°2	13°27	13°19	11°8
156	+ 3°1	+ 2°5	12°73	12°48	10°4	196	- 1°8	- 1°3	10°39	10°61	11°9
245	+ 10°6	- 12°2	12°57	12°37	10°6	50	- 1°6	+ 8°1	12°76	12°82	12°0
180	+ 9°0	- 3°4	12°65	12°46	10°7	77	+ 10°9	+ 6°5	13°71	13°59	12°1
80	+ 7°9	+ 4°0	13°59	13°27	10°8	240	+ 7°4	- 7°5	13°62	13°62	12°6
195	+ 0°1	- 1°4	13°06	12°82	10°8	186	+ 5°2	- 4°2	12°99	13°08	12°6
134	- 6°5	- 3°4	12°35	12°29	11°0	213	- 2°4	- 6°3	12°20	12°32	12°6
142	- 7°6	- 0°3	13°20	12°96	11°0	199	- 0°4	- 2°6	12°54	12°68	12°7
238	+ 5°8	- 9°1	13°30	13°10	11°0	60	+ 6°9	+ 8°6	13°39	13°56	13°0
87	+ 4°8	+ 7°1	14°03	13°70	11°1	135	- 5°8	- 3°1	13°86	14°08	13°0
101	- 3°4	+ 3°0	13°55	13°28	11°1	276	- 5°8	- 14°9	13°16	13°29	13°3
230	- 0°1	- 12°8	12°47	12°46	11°1	59	+ 7°7	+ 8°0	12°72	12°89	13°5
170	+ 9°9	- 3°5	12°27	12°28	11°2	182	+ 6°9	- 3°7	12°40	12°58	13°5
93	+ 2°9	+ 4°8	12°56	12°50	11°2	197	- 1°1	- 1°6	12°27	12°48	13°7
235	+ 6°9	- 10°4	12°77	12°69	11°3	136	- 5°5	- 3°1	13°83	13°95	13°8
166	+ 6°7	- 1°8	13°00	12°87	11°6	221	- 6°1	- 8°3	12°77	12°98	14°1
102	- 4°8	+ 2°6	12°99	12°90	11°6	89	+ 2°2	+ 7°9	12°20	12°52	15°3
95	- 1°9	+ 4°0	13°16	13°03	11°6	272	- 4°4	- 13°5	12°57	12°88	15°6
47	- 2°6	+ 10°9	12°96	12°91	11°6	190	+ 3°5	- 1°4	12°94	13°24	15°7
214	- 1°0	- 5°8	13°59	13°39	11°6	167	+ 10°0	- 1°9	12°73	13°05	15°9
78	+ 9°5	+ 6°8	12°99	12°90	11°6	322	- 10°0	- 1°5	13°20	13°49	15°9
96	- 2°4	+ 5°3	13°18	13°09	11°7	239	+ 6°4	- 8°4	12°84	13°23	16°4

TABLE VII  
Distance modulus and colour excess (NGC 6494)

Star	$m-M$	CE	Star	$m-M$	CE
122	8·1	+0·33	124	9·7	+0·06
100	8·5	+0·41	55	9·9	+0·47
152	8·8	+0·53	130	10·0	+0·35
168	9·1	+0·57	163	10·0	+0·76
82	9·3	+0·25	164	10·0	+0·77
153	9·4	+0·60	125	10·5	+0·88
103	9·5	+0·41	225	10·5	+0·59
63	9·6	+0·68	233	11·1	+0·60
161	9·6	+0·66			

a big area in which sudden changes of absorption are obvious even at a first glance at the area. This is also borne out by Klauder's and Lambrecht's investigation of the density distribution.

Therefore we get from Tables VI and VII respectively:

$$r = 470 \pm 40 \text{ parsecs}, \quad d = 27' \cdot 2 = 3 \cdot 7 \text{ parsecs}$$

and (corrected for absorption)

$$r = 770 \pm 50 \text{ parsecs}, \quad d = 27' \cdot 2 = 6 \cdot 1 \text{ parsecs}.$$

The results of previous investigations were

	Distance	Diameter	
Shapley	870-1380 pc	25'	10.0 pc
Raab	400	43-51	5.5
Trumpler	660	27	5.9
Collinder	957	25	7.0

The CI method gives a different result for the star number from the statistical method. Among the 165 CI stars, 95 belong to the cluster modulus range, and the same relation, when applied to the 333 stars obtained by counting, gives, after correction, 169 cluster stars. This number is different from the number 149 obtained statistically. The dispersion is  $\sigma = \pm 13$ . The difference is due to deviations in CI. As the stars in the area of this particular cluster appear in chains, some fainter stars located in the haloes of bright stars appear brighter than they are. The modulus range, and hence the star number, depends on a statistical behaviour, so that a few faint stars having larger deviations are not included within the right range of  $m - M$  in Table VI.

The magnitude distribution in this cluster, after correction for background, is in the following table :

Number of stars	$m_v$	10	11	12	13	$> 13.5$
		12	17	24	20	96
NGC 6544						

R.A.  $18^{\text{h}} 01^{\text{m}} 2$ , Dec.  $-25^{\circ} 01'$  (1900.0)

This cluster is a very faint object mentioned in Shapley's catalogue of open clusters, but, according to Collinder (5), it "seems to be a globular cluster or anagalactic nebula". NGC 6544 appears on Sidmouth plates as a very compact conglomeration, not resolved, of very faint stars. The unresolved central part is of about  $1.5'$  diameter. Around that there are about seven stars in a diameter of about  $2.7'$ .

#### NGC 7127

R.A.  $21^{\text{h}} 40^{\text{m}} 5$ , Dec.  $+54^{\circ} 09'$  (1900.0)

This cluster is a small and poor one, mentioned in Shapley's catalogue. It is located in the middle of a small area, extremely poor in stars. On account of its particular situation the star counting was not done in the usual way, but a comparison of the cluster's region with some neighbouring regions of the same size was made. Within a diameter  $2.8'$  of the cluster's region there are 15 stars. After the correction the number of cluster stars is 8.

Table VIII gives the distribution of  $m - M$  and it is given in two parts, of which the first shows the stars separated in two ranges, and the second is a rearrangement of the first, treating the first group of stars as giants (as was done in the case of NGC 6469). In this table we see that the giants fit well into the dwarf range.

Table VIII shows that the mean distance modulus is 10.28 in case A and 10.55 in case B corresponding to

Case A  $r = 1120 \pm 120$  pc,  $d = 2.8 = 1.0$  pc.

Case B  $r = 1300 \pm 120$  pc,  $d = 2.8 = 1.1$  pc.

Since spectral types are not available it is not possible to suggest a correction for the interstellar absorption.

The data in Shapley's catalogue are

$$r = 1820-2880 \text{ parsecs}, \quad d = 1' \cdot 0 = 0 \cdot 8 \text{ parsecs}.$$

The number of cluster stars is 10 (among them 3 giants), against 8 obtained by counting.

The magnitude distribution is given in the following table :

Number of stars	$m_p$	I0	II	I2	I3	I4	I5
	I	I	5	I	I	I	I

TABLE VIII

*Coordinates, magnitudes and distance moduli of 15 stars (NGC 7127)*

Zero point=star 13. Unit= $1' \cdot 0$ , X=east, Y=north. Coordinates of the assumed cluster centre  
 $X = -0 \cdot 5$ ,  $Y = +0 \cdot 4$

A Normal distribution						B Giants included	
Star	X	Y	$m_p$	$m_v$	$m-M$	Star	$m-M$
14	+0.5	+0.7	12.26	11.53	6.6	7	9.2
13	0.0	0.0	10.49	10.06	6.8	11	9.4
9	-0.5	+0.5	12.75	11.92	6.8	15	9.7
7	-0.7	+1.1	12.27	11.92	9.2	13	10.1
11	-0.3	+1.0	13.95	13.41	9.4	10	10.1
15	+0.6	-0.6	12.54	12.22	9.7	3	10.7
10	-0.5	-0.9	11.51	11.47	10.1	1	11.4
3	-1.2	+0.5	12.42	12.28	10.7	12	11.5
1	-1.5	+0.5	13.88	14.20	11.4	14	11.5
12	-0.3	+1.6	14.12	14.56	11.5	9	11.9
2	-1.2	+1.5	13.19	13.34	13.6	2	13.6
6	-0.9	+1.4	13.69	13.84	14.1	6	14.1
8	-0.5	+1.8	13.26	13.47	14.6	8	14.6
4	-1.1	-0.3	14.13	14.35	15.7	4	15.7
5	-1.1	-0.8	14.22	14.50	16.5	5	16.5

## NGC 7128

R.A.  $21^{\text{h}}40^{\text{m}}.7$ , Dec.  $+53^{\circ}15'$  (1900.0)

This cluster is a small one mentioned in the catalogues of Shapley, Trumpler and Collinder. It is located within a small area of low star density, like the previous cluster. So the star counting and the correction for background were done in the same way as with NGC 7127. Within a diameter  $3' \cdot 1$  of the cluster's region there are 16 stars. After correction the number of cluster stars is 9. In Table IX we find the mean distance modulus of the cluster group (without correction for absorption) to be 10.99, corresponding to

$$r = 1570 \pm 170 \text{ parsecs}, \quad d = 3' \cdot 1 = 1.5 \text{ parsecs}.$$

The results of the previous investigations were

	Distance	Diameter
Shapley	1820-2880 pc	$2' \cdot 1 \cdot 7$ pc
Trumpler	3650	$3 \cdot 2 \cdot 3 \cdot 5$
Collinder	6670	$2 \cdot 3 \cdot 5 \cdot 3$

Trumpler's distance was not measured but computed.

The number of cluster stars after reduction is 9, coinciding with the number obtained by counting.

The magnitude distribution is given in the following table:

Number of stars	$m_p$	12	13	$>13\cdot5$
	1	2	6	

TABLE IX

*Coordinates, magnitudes and distance moduli of 14 stars (NGC 7128)*

Zero point=star 15. Unit= $1'\cdot0$ ,  $X$ =east,  $Y$ =north. Coordinates of the assumed cluster centre  
 $X=-0\cdot8$ ,  $Y=+0\cdot6$

Star	$X$	$Y$	$m_p$	$m_v$	$m-M$	Star	$X$	$Y$	$m_p$	$m_v$	$m-M$
15	0·0	0·0	11·33	9·94	2·5	14	-0·2	+0·5	12·34	12·37	11·3
7	-1·3	+0·5	11·89	10·37	2·7	8	-1·2	+0·9	13·96	13·83	12·3
11	-0·9	-0·1	12·61	11·14	3·5	6	-1·4	-0·2	13·64	13·64	12·4
12	-0·6	+1·0	12·88	12·52	9·7	13	-0·4	+1·2	13·42	13·60	14·3
4	-1·5	-0·4	14·19	13·66	9·7	16	+0·3	-0·3	13·73	13·95	15·3
10	-1·0	+1·3	12·8	12·58	10·6	5	-1·4	+1·5	13·35	13·70	16·9
1	-2·0	+1·3	13·30	13·70	10·7						
3	-1·5	+1·9	13·55	13·86	11·2						

The plates used in this investigation were taken by Dr G. Alter when he was in Sidmouth, between the years 1939 and 1944, and I am also indebted to him for his papers which proved most helpful to me. I am grateful to Professor F. J. M. Stratton and the I.A.U. for the grant which enabled me to carry out my work at the Norman Lockyer Observatory. I should like also to express my thanks to Mr D. L. Edwards, Director of the Norman Lockyer Observatory, and to Mr D. R. Barber for their interest and helpful discussions throughout the course of my work at the Norman Lockyer Observatory.

*Norman Lockyer Observatory,*

*Sidmouth :*

1953 April 23.

#### References

- (1) G. Alter, *M.N.*, **100**, 387, 1940; *M.N.*, **101**, 89, 1941; *M.N.*, **101**, 298, 1941; *M.N.*, **103**, 10, 1943; *M.N.*, **104**, 179, 1944.
- (2) H. Shapley, *Star Clusters*, Harv. Obs. Mon., No. 2, 1930.
- (3) S. Raab, *Lund Medd.*, Ser. II, 28, 1922.
- (4) R. J. Trumpler, *L.O.B.*, **14**, 170, 1930.
- (5) P. Collinder, *Lund Annals*, II, 1931.
- (6) C. A. Ricke, *H.C.*, 397, 1935.
- (7) P. Hayford, *L.O.B.*, **16**, 53, 1932.
- (8) R. S. Zug, *L.O.B.*, **18**, 89, 1937.
- (9) H. Klauder and H. Siedentopf, *A.N.*, **268**, 197, 1939.

## SOME REMARKS ON THE INTERPRETATION OF APSIDAL-MOTION CONSTANTS IN CLOSE BINARY SYSTEMS

Zdeněk Kopal

(Received 1953 October 26)

### Summary

The aim of the present paper has been to establish explicit formulae for the computation of the constants  $k_j$  of apsidal motions in close binary systems, invoked by the  $j$ -th harmonic distortion of their components of arbitrary structure. If the degree of central condensation of such components is high, and their (equilibrium) density distribution  $\rho(a)$  remains *analytic* at the surface  $a=a_1$ , it is shown that

$$k_j = \frac{j+1-\eta_j(a)}{2j+2\eta_j(a_1)},$$

where the quantity  $\eta_j(a_1)$  is expressible by a series on the right-hand side of equation (14) within the domain of its convergence (the existence of the latter defining the "stars of high condensation").

If the density distribution characterizing our stars is such that not all derivatives of  $\rho(a)$  are finite on the surface, it is shown that the values of  $k_j$  may be effectively approximated by means of the equation

$$(2j+1)a_1^{2j+1}k_j = 3(j+2) \int_0^{a_1} Da^{2j} da,$$

where  $D \equiv \rho/\bar{\rho}$ ,  $\bar{\rho}(a)$  denoting the mean density interior to  $a$ . The derivation of this formula reveals that the error of this representation of  $k_j$  should diminish with increasing value of  $j$  as well as with increasing degree of central condensation.

A numerical application to the polytropic family of models discloses that, if the ratio of the central to the mean density of our configuration exceeds (say) one hundred, the above approximate formula should furnish the values of  $k_2$  correctly within the limits of errors affecting their empirical determination in most practical cases, while the question of errors of our approximate values of  $k_3$  or  $k_4$  will scarcely ever arise.

---

Ever since Russell's pioneer work on the subject (1) it has been generally recognized that the observed rate of apsidal advance in close binary systems exhibiting eccentric orbits represents a royal road to certain empirical information concerning the internal structure of the constituent components. In more precise terms, the rate of apsidal advance arising from  $j$ -th harmonic distortion of either component is known to be proportional (to the first order in small quantities) to the constant

$$k_j = \frac{j+1-\eta_j(a_1)}{2j+2\eta_j(a_1)}, \quad (1)$$

where  $\eta_j(a_1)$  denotes the surface ( $a = a_1$ ) value of a particular solution of Radau's differential equation

$$a \frac{d\eta}{da} + \eta(\eta - 1) + 6D(\eta + 1) = j(j + 1), \quad (2)$$

satisfying the initial condition

$$\eta_j(0) = j - 2, \quad (3)$$

where  $D = \rho/\bar{\rho}$ ,  $\rho(a)$  denoting the density of the respective undistorted star at a distance  $a$  from its centre, while  $\bar{\rho}(a)$  stands for the mean density inside a volume of radius  $a$ . The  $j$ -th harmonic distortion of figure of the respective components due to its own axial rotation and to the tidal effect of its mate—which causes the apsidal advance—can, in turn, be shown (2) to be proportional to

$$\Delta_j = 2k_j + 1 = \frac{2j+1}{j+\eta_j(a_1)}. \quad (4)$$

The values of  $k_j$  (or  $\Delta_j$ ) in specific eclipsing systems can be established by an approximate analysis of the observational data (3); and their interpretation represents so far the only available empirical check of the theories of the internal structure of main-sequence stars.

The foregoing definition of the constant  $k_j$  should enable us to predict the rate of apsidal advance in close binary systems caused by mutual distortion of their components—at the price of a numerical integration of equation (2)—provided that the equilibrium density distribution  $\rho(a)$  of the distorted bodies is *a priori* known. It throws, however, very little light on the following converse question of considerable astrophysical interest: namely, *what is the exact amount of information an empirical knowledge of  $k_j$  entitles us to draw concerning the internal constitution of the respective stars?* This question will be the subject of our present discussion.

If we regard this problem from a completely general point of view, any attempt at a comprehensive answer encounters serious difficulties. In special cases, however, our problem can be solved in a closed form. Thus, if the function  $D(a)$  in (2) is set equal to zero (which would correspond to an infinite density concentration), equation (2) can be solved to yield

$$\eta_j(a) = j + 1, \quad (5)$$

which, in turn, leads to the well-known results of  $k_j = 0$  and  $\Delta_j = 1$ . Moreover—and this is a fact of salient importance—numerical integrations of (2) have revealed that, for models of high central condensation, the values of  $k_j$ —though finite—approach zero rapidly; and the values of  $\Delta_j$  tend asymptotically to one. Since the density concentrations of actual stars are very likely high, the whole astrophysical interest is largely confined to this particular case.

The point of departure of the present investigation will, therefore, be a search for the reason why the values of  $k_j$  as defined by equation (1) diminish so rapidly with increasing degree of central condensation. In doing so we shall be led to construct new asymptotic relations between  $k_j$  and  $\rho(a)$ , which will not only enable us to compute the values of  $k_j$  for centrally condensed stars in a more expeditious manner (i.e. by simple quadratures rather than by way of numerical integration of a differential equation), but will also render the dependence of  $k_j$  on  $\rho(a)$  much more transparent than it was in our original formulation of the problem.

In order to do so, let us depart from Radau's equation (2) which is quadratic in the dependent variable. One way of removing this non-linearity is to replace  $\eta(a)$  by a new variable  $y(a)$ , defined by

$$\eta = \frac{a dy}{y da} - 3 \frac{\rho}{\bar{\rho}}, \quad (6)$$

which transforms (2) in

$$\frac{d^2y}{da^2} = \left\{ \frac{j(j+1)}{a^2} + g(a) \right\} y, \quad (7)$$

where we have abbreviated

$$g(a) = \frac{a^2(d\rho/da)}{\int_0^a \rho a^2 da} = \frac{3}{a\rho} \frac{d\rho}{da}. \quad (8)$$

In order to solve this equation, let us set

$$y(a) = a^{j+1} \exp \int u(a) da, \quad (9)$$

where  $u(a)$  denotes a new variable defined by a non-homogeneous differential equation

$$\frac{du}{da} + u^2 + \frac{K}{a} u = g(a) \quad (10)$$

of the Riccati type, where we have abbreviated

$$K = 2(j+1). \quad (11)$$

Suppose that we assume now a solution of (10) to exist in the form

$$u(a) = \sum_{i=0}^{\infty} \frac{u_i(a)}{K^{i+1}} \quad (12)$$

of a series in descending powers of  $K$ , an insertion of (12) in (10) and the fact that the ensuing series must vanish identically determines the successive values of  $u_i(a)$  as:

$$\left. \begin{aligned} u_0 &= ag, \\ u_1 &= -au_0', \\ u_2 &= -a\{u_1' + u_0^2\}, \\ &\vdots \\ u_i &= -a \left\{ u_{i-1}' + \sum_{k=1}^{i-1} u_k u_{i-k} \right\}, \end{aligned} \right\} \quad (13)$$

in terms of the function  $g(a)$  depending on the structure of the respective configuration, and of its successive derivatives. If we insert now (12) in (9), differentiate the latter logarithmically and insert in (6), we find that, on the surface,

$$\eta_j(a_1) = j+1 + \sum_{i=0}^{\infty} \frac{u_i(a_1)}{2^{i+1}(j+1)^{i+1}}. \quad (14)$$

For stellar configurations of high central condensation, the quantity  $g(a)$  as well as its derivatives are likely to be very small for  $a=a_1$ , and tend in fact to zero as the condensation becomes infinite. Moreover, the quantity  $K$  whose powers constitute the denominators of successive terms on the right-hand side of (14) is numerically equal to 6, 8 and 10 for the second, third and fourth

spherical harmonic distortion, respectively—a fact which should assist the convergence of our expansion. This is why, for centrally condensed configurations,  $\eta_j(a_1)$  departs so little from its limiting value of  $j+1$ —the less so, the greater  $j$ —and, consequently, why the constants  $k_j$  are numerically as small as was heuristically established by previous investigators.\*

An application of the foregoing equation (14) to the actual calculation of  $k_j$  is, however, inseparably connected with the problem of convergence of a sequence of the values of  $|u_i(a_1)|$ . Whether or not such values—small as they are—diminish actually with increasing  $i$  so as to render the infinite series on the right-hand side of (14) convergent depends, of course, on the particular properties of the respective stellar models, and cannot be answered *a priori* in full generality. For some models this convergence may indeed be so rapid that the series on the right-hand side of (14) may be terminated after a very few terms. Other models may, however, possess such special features as to make a solution of (10) of the form (12) actually non-existent. This is, for instance, true of the well-known polytropic family of models whose successive density derivatives at the surface are either zero or infinite.† In the face of such a situation the need evidently arises for broadening the basis of our analytical approach to the problem at issue so as to encompass even such recalcitrant cases.

In order to do so, let us return to Radau's equation (2) and inquire as to the possibility of constructing such solutions of it, which, in addition to fulfilling the initial condition (3), is required to assume at the surface ( $a=a_1$ ) a specific value  $\eta(a_1)=\lambda$  (say). If we revert from  $\eta(a)$  to the variable  $y(a)$  introduced by the transformation (6), this is tantamount to a search for characteristic solutions of the following linear boundary-value problem:

$$L[y] = g(a)y, \quad (15.0)$$

$$y(0) = 0, \quad y'(a_1) = \lambda y(a_1), \quad (15.1)$$

where

$$L \equiv \frac{d^2}{da^2} - \frac{j(j+1)}{a^2}, \quad (16)$$

and  $\lambda$  is a prescribed parameter.

The operator  $L$  is evidently self-adjoint. Its Green's function appropriate for the given boundary conditions will, therefore, be symmetrical and of the form

$$G(a, \xi) = -\frac{1}{2j+1} \{ \xi^{-j} + C_j \xi^{j+1} \} a^{j+1} \quad (\xi \geq a), \quad (17)$$

in which we have abbreviated

$$a_1^{2j+1} C_j = \frac{j+a_1 \lambda}{j-a_1 \lambda + 1}, \quad (18)$$

which, by (1), can be seen to reduce to

$$C_j^{-1} = 2a_1^{2j+1} k_j.$$

\* For a recent comprehensive summary of numerical determination of apsidal-motion constants for different stellar models, *cf.*, e.g., L. Motz, *Ap. J.*, 115, 562, 1952.

† As is well known, for complete polytropes  $\rho = \rho_c y^n$ , where  $y$  denotes the Emden function corresponding to a polytropic index  $n$ . In consequence, the  $k$ -th derivative of  $\rho$  will contain a term multiplied for  $y^{(n-k)}$ ; and as  $y$  vanishes on the surface  $y^{(n-k)}(a_1)$  will become zero or infinite depending on whether  $n \geq k$ .

With the aid of the foregoing Green's function the differential boundary-value problem may be rewritten in the form of the following integral equation, revealing that

$$(2j+1)y(a) = -a^{j+1}C_j \int_0^{a_1} g(\xi)y(\xi)\xi^{j+1} d\xi \\ - a^{-j} \int_0^a g(\xi)y(\xi)\xi^{j+1} d\xi \\ - a^{j+1} \int_a^{a_1} g(\xi)y(\xi)\xi^{j+1} d\xi. \quad (19)$$

Now we have already seen that, for configurations of high central condensation,  $k_j$  is apt to become a very small quantity. If so, however, then the constant  $C_j$  (being inversely proportional to  $k_j$ ) must necessarily be large. The three integrals on the right-hand side of (19) are all quantities of the same order of magnitude; but only the first one is multiplied by  $C_j$ . Therefore, to a first approximation, equation (19) should be essentially equivalent to

$$(2j+1)y(\xi) = -a^{j+1}C_j \int_0^{a_1} g(\xi)y(\xi)\xi^{j+1} d\xi; \quad (20)$$

but since the limits of the integral on the right-hand side are now constant, the solution of this equation is clearly of the form

$$y(a) = Aa^{j+1}, \quad (21)$$

where  $A$  is a constant. Since, however, equation (20) is homogeneous in the dependent variable, its validity requires that the value of  $C_j$  involved in it be, not arbitrary, but given by the equation

$$C_j^{-1} = 2a_1^{2j+1}k_j = -\frac{3}{2j+1} \int_0^{a_1} \frac{1}{\bar{\rho}} \frac{d\rho}{da} \xi^{2j+1} d\xi, \quad (22)$$

which thus expresses the desired parameter  $k_j$  in terms of a simple quadrature of the ratio  $\rho'/\bar{\rho}$ .

It may be noted that the integral on the right-hand side admits of the foregoing simplification. Since the mean density  $\bar{\rho}(a)$  inside a sphere of radius  $a$  is defined by

$$\bar{\rho} = \frac{3}{a^3} \int_0^a \rho a^2 da, \quad (23)$$

so that

$$\frac{a}{3} \frac{d\bar{\rho}}{da} = \rho - \bar{\rho}, \quad (24)$$

a resort to partial integration reveals that

$$\int_0^{a_1} \frac{1}{\bar{\rho}} \frac{d\rho}{da} a^{2j+1} da = 3 \int_0^{a_1} D^2 a^{2j} da - 2(j+2) \int_0^{a_1} Da^{2j} da. \quad (25)$$

For centrally condensed configurations  $D \ll 1$  and, therefore,  $D^2 \ll D$ . In such cases, the first integral on the right-hand side of the foregoing equation is likely to be very small in comparison with the second and may, therefore, be neglected.

Doing so we arrive at last at the final result of this investigation in the form

$$(2j+1)a_1^{2j+1}k_j = 3(j+2) \int_0^{a_1} Da^{2j} da, \quad (26)$$

expressing the apsidal-motion constants  $k_j$  of centrally condensed configurations in terms of a quadrature of the ratio  $D = \rho/\bar{\rho}$ , weighted by  $a^{2j}$ . It transpires, therefore, that for such configurations the values of  $k_j$  are primarily determined by the behaviour of the ratio  $D$  throughout the interval  $0 \leq a \leq a_1$ , with the contribution of the outer parts of stellar interiors becoming relatively the more important the higher the value of  $j$ .

It is interesting, in this connection, to recall that Motz (4) has recently examined a suggestion (credited to Russell) that the apsidal-motion constant  $k_2$  is determined essentially by the radius of gyration  $H$  of our configuration which is known to be defined by

$$H^2 = \frac{8\pi}{3M} \int_0^{a_1} \rho a^4 da, \quad (27)$$

where  $M$  denotes the total mass of the configuration. On the basis of a series of numerical integrations Motz has established the existence of an empirical relation between  $k_2$  and  $H/a_1$  which appeared to be quasi-linear in their logarithms; but some models deviated conspicuously from it. The outcome of our investigation throws some more general light on the question of the dependence of  $k_j$  on the density distribution of the respective models; and discloses, in particular, that, to a first approximation,  $k_j$  should be proportional to an integral of  $(\rho/\bar{\rho})a^{2j}$ —rather than of  $\rho a^{2j}$ —taken between the limits  $(0, a_1)$ .

In order to test the performance of our approximate formula (26) in a practical case, we set out to approximate with its aid the apsidal-motion constants  $k_j$ , for  $j=2, 3, 4$ , appropriate for the polytropic gas spheres characterized by the index  $n=3$  and 4. In this case equation (26) assumes the particular form

$$(2j+1)x_1^{2j+1}k_j = (j+2) \int_0^{x_1} U x^{2j} dx, \quad (28)$$

where  $x_1$  stands for the first zero of the corresponding Emden function  $y(x)$  and

$$U = -\frac{xy^n}{y'} = 3D \quad (29)$$

denotes a function which has been tabulated by Comrie and Sadler (5).

The outcome of our computation is summarized in the following table, in which the constants  $k_j$  approximated with the aid of (28) are compared with those

	$k_j$	
	$n=3$	$n=4$
$j=2$	0.01207 (0.0144)	0.001100 (0.00119*)
$j=3$	0.003524 (0.00368)	0.0002319 (0.000235)
$j=4$	0.001387 (0.00140)	0.0000653 (0.00007)

\* See footnote on p. 775.

(in parentheses) obtained by Chandrasekhar (6) on the basis of numerical integration of a differential equation equivalent to Radau's.\* Considering the simplicity of (26), the degree of approximation attained with its aid appears to be satisfactory for all practical purposes (for one can very seldom establish the observed value of  $k_j$  within an error of less than 5-10 per cent), and exhibits a marked improvement with increasing values of both  $j$  and  $n$ —i.e. precisely in such cases when a numerical integration of Radau's equation becomes most laborious.

*Department of Astronomy,  
University of Manchester:  
1953 October 26.*

#### References

- (1) Russell, H. N., *M.N.*, **88**, 642, 1928.
- (2) Sterne, T. E., *M.N.*, **99**, 451, 1939.
- (3) Sterne, T. E., *M.N.*, **99**, 662, 1939; or Kopal, Z., *Harv. Obs. Circ.*, No. 443, 1941.
- (4) Motz, L., *Ap. J.*, **115**, 562, 1952.
- (5) Comrie, L. J. and Sadler, D. H., *British Assoc. Mathematical Tables*, Vol. 2 (Emden Functions), London, 1932.
- (6) Chandrasekhar, S., *M.N.*, **93**, 449, 1933.

\* For  $n=4$  and  $j=2$  Chandrasekhar (*M.N.*, **93**, 449, 1933; Table VI) gave  $\Delta_2=1.00267$ , corresponding to  $k_2=0.00134$ . This value appears, however, to be appreciably in error; for a repeated numerical integration retaining additional decimal figures led to  $k_2=0.001194$  as given above for the purpose of comparison. Any further increase in precision of this result would be possible only if additional decimals were given in the British Association Tables of the *U*-function.

It may be added that, inasmuch as Chandrasekhar's value of  $\Delta_2$  for  $n=3.5$  (*cf.* S. Chandrasekhar, *M.N.*, **93**, 574, 1933; revised in *Ap. J.*, **95**, 579, 1942) was based on interpolation between the corresponding values for  $n=1$ , 1.5, 2, 3 and 4, the present revision of the quantity  $\Delta_2$  for  $n=4$  should alter also the interpolate for  $n=3.5$  (as quoted, for instance, by Motz).

## PHOTOELECTRIC OBSERVATIONS OF OCCULTATIONS AT THE CAPE OBSERVATORY

*A. W. J. Cousins and R. Guelke*

(Communicated by H.M. Astronomer)

(Received 1953 December 1)\*

### *Summary*

A simple apparatus for observing occultations photoelectrically is described. The curves obtained for the occultations of Antares on 1950 May 4, 1951 July 15, 1952 April 13 and 1953 March 8 are given, reduced to a standard form in which the ordinates represent percentages of the unobstructed starlight, and the abscissae angular measure across the star.

*Introduction.*—In 1949 Professor R. O. Redman and Dr A. D. Thackeray called the attention of Dr Stoy to the series of occultations of Antares, then about to begin, and suggested that they should be observed in an attempt to determine the diameter of the star. It was doubtful whether a refractor of 24 inches aperture would be large enough to give useful results but the necessary subsidiary apparatus was designed and built in time for the first occultation on 1950 May 4. The observation made on that occasion has been described elsewhere (1). Its value is considerably impaired by the presence of a parasitic 50-cycle ripple on the trace. Observations free from this defect were obtained on 1951 July 15, 1952 April 13 and 1953 March 8. It was not possible to observe the other occultations of this series because of cloud.

The photometer is of simple construction. A metal plate with a series of interchangeable diaphragms replaces the usual plateholder on the 24-inch Victoria Telescope. A photomultiplier tube and amplifier are enclosed in a metal box which is hinged to the telescope so that it can be swung aside while the cross-wires of the guiding telescope are being adjusted to correspond accurately with the centre of the diaphragm. The R.C.A. 931-A photomultiplier tube has its own light-tight housing within the box and is provided with a shutter and a Fabry lens. A voltage divider for the multiplier is mounted on the tube socket.

The amplifier circuit is illustrated in Fig. 1. The sensitivity control in the anode circuit of the multiplier is variable in steps from 20 megohms downwards. A potentiometer provides grid bias for balancing the moonlight and dark current from the multiplier tube. No other controls are necessary.

The photometer was originally operated entirely from batteries, but these have been largely replaced by a mains-operated power pack with regulated output voltages. A 6-volt storage battery still provides current for the amplifier heater and an H.T. battery is connected between the output cable and the Y-plates of the cathode ray oscilloscope used as a recorder. The purpose of this latter battery is to centre the spot on the oscilloscope screen. It has been found best to use a comparatively low voltage, between 70 and 80 volts per stage, on the multiplier tube.

\* Received in original form 1952 December 1.

Three twin beam oscilloscopes have been tried, and in every case it has been found necessary to connect the output from the amplifier tube directly to the Y-plates of the cathode ray tube to avoid mains interference. Even this is not always effective, and, as has already been remarked, there was considerable interference on the trace of 1950 May 4. These instruments allow a timing wave and clock pulses to be recorded as well as the star trace, and this feature has led to the routine use of the instrument for timing ordinary occultations (2, 3).

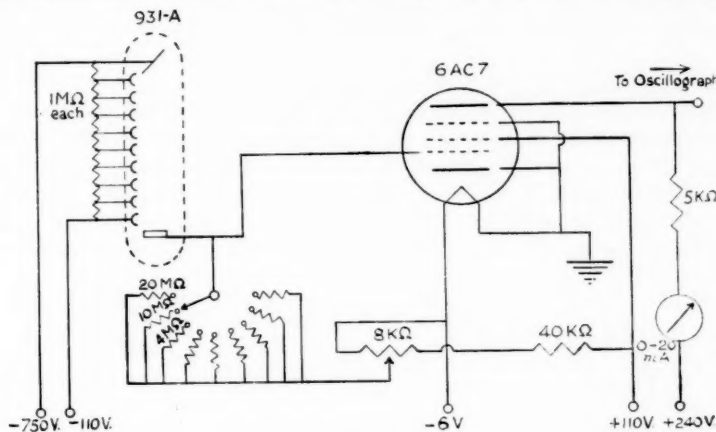


FIG. 1.

Most of the light reaching the photomultiplier tube is scattered moonlight. Only when the moon is very young or the star unusually bright is the starlight of comparable intensity. The unwanted light can be reduced by using a smaller diaphragm, but the size cannot be reduced too far or vignetting of the image will aggravate the already troublesome seeing "noise". At the Cape it has seemed best to use a comparatively large diaphragm. For the reappearance of 1950 May 4 a diaphragm with an aperture of 2 mm was used. For subsequent occultations the aperture was 1 mm (corresponding to 30") in diameter. With a reflecting telescope and good seeing, smaller sizes could undoubtedly be used.

If the objective were perfectly clean, the scattered light would be mainly from the sky, but in the case of the Victoria Telescope much the greater portion originates in the tarnished surfaces of the comparatively old objective. Any variation in the moonlight due to clouds or haze has an immediate effect on the intensity of this scattered light. A milliammeter in series with the amplifier valve enables the observer to see what is happening and to make the necessary adjustments to prevent saturation.

It is possible to check the sensitivity by moving the telescope slightly and "occulting" the star by the edge of the diaphragm. Such a check also serves to verify the centring of the star.

The regular (8-inch) guiding telescope serves admirably for disappearances: for reappearances guiding presents something of a problem. This was solved temporarily for the reappearances of Antares by fitting a small telescope that could be inclined sufficiently to guide on a nearby bright star (e.g.  $\sigma$  or  $\tau$  Sco) that was itself not occulted.

*The Antares observations.*—The circumstances of the four occultations observed at the Cape were as follows:

Date	Type	Age of Moon	G.M.T.	P.A.	Angle between normal to limb and Moon's motion	Rate (/sec)
1950 May 4	RD	16·7 <sup>d</sup>	2 21·0	267	14	0·414
1951 July 15	DD	11·4	16 42·7	43	68	0·181
1952 April 13	RD	19·1	22 16·9	301	12	0·459
1953 March 8	RD	22·0	01 56·2	235	52	0·233

The records obtained on the second and later occasions are shown in Plate 11. A record of an occultation of A Scorpii ( $4^m\cdot8$  B3), a star of presumably negligible diameter, is given for comparison. The timing trace consists of a ripple at either 50 or 100 cycles per second punctuated once a second by a signal from the standard clock. In the reductions allowance was made for the fact that the time and star traces are not quite vertically above each other on the film and that the camera drive was not always uniform. The response of the equipment was not linear

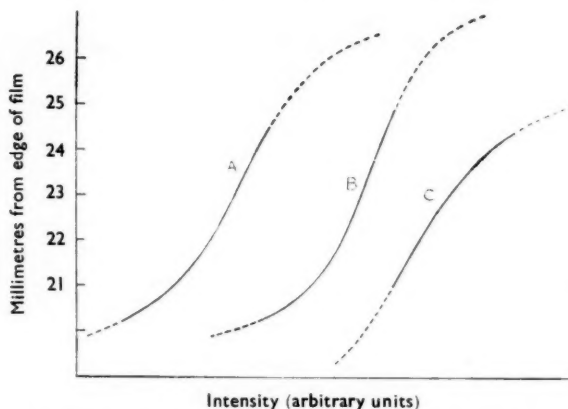


FIG. 2.—Calibration curves : A, 1951 July 15; B, 1952 April 13; C, 1953 March 8.  
(Thick portions actually employed in reductions.)

and the necessary correction was determined by the following method. The light of the moonlit sky was used to provide a source of constant intensity and a rotating sector was run in front of the diaphragm to produce a rapid alternation of light and darkness on the sensitive surface of the photomultiplier tube. The bias was then adjusted so that this constant signal was recorded at different heights on the oscilloscope screen, the amplitude of the approximately square wave so produced being a measure of the sensitivity of the apparatus at that particular height. From these results it is possible to deduce a curve of deflection against incident intensity. The non-linearity is almost entirely due to the amplifier. The results are shown in Fig. 2. It is possible that some portions of these curves may be in error by one or two tenths of a millimetre.

No corrections have been applied to the measures of the trace of the occultation of 1950 May 4 which were made on the original film with a long screw measuring machine. No calibration is available but as the deflection was small and not too

near the saturation point, it is believed that any distortion due to non-linearity of response will be unimportant.

The observed curves reduced to a standard form of representation in which the ordinates represent percentages of unobstructed starlight, and the abscissae angular measure across the star, are illustrated in Fig. 3.

The overall time constant of the apparatus was about one millisecond. The speed of response is therefore adequate to avoid distortion from this cause. The trace of A Scorpii (Plate 11) confirms this.

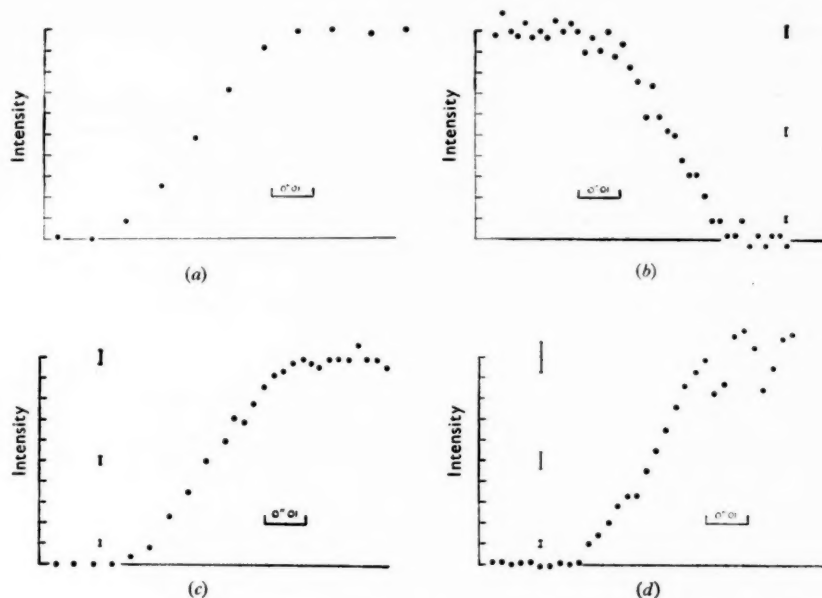


FIG. 3

(a) Occultation of Antares, 1950 May 4. (b) Occultation of Antares, 1951 July 15.  
(c) Occultation of Antares, 1952 April 13. (d) Occultation of Antares, 1953 March 8.

The short vertical lines indicate the standard error of a plotted point of the corresponding intensity.

The most serious cause of distortion of the curves is the seeing. Seeing noise is directly proportional to the amount of starlight. It is therefore most conspicuous when the star is clear of the Moon and is absent when the star is occulted. Variations in the scattered light are normally too slow to produce distortion. Shot noise merely broadens the trace.

The seeing noise has been determined by measuring the trace from the unocculted star at intervals of 0.01 second and computing the r.m.s. variations over periods of 0.1 second. Slower variations have little effect in distorting the curve. Peaks occasionally reach, but rarely exceed, twice the r.m.s. value. The uncertainty due to known causes and expressed as the standard error of a plotted point is indicated by short vertical lines in the figures. No satisfactory criterion is available for the occultation of 1950 May 4.

The effective diameters deduced from the curves on the assumption of a uniformly illuminated circular star disk and a smooth occulting edge are as follows:

1950 May 4	0"·045
1951 July 15	0"·035
1952 April 13	0"·045
1953 March 8	0"·040

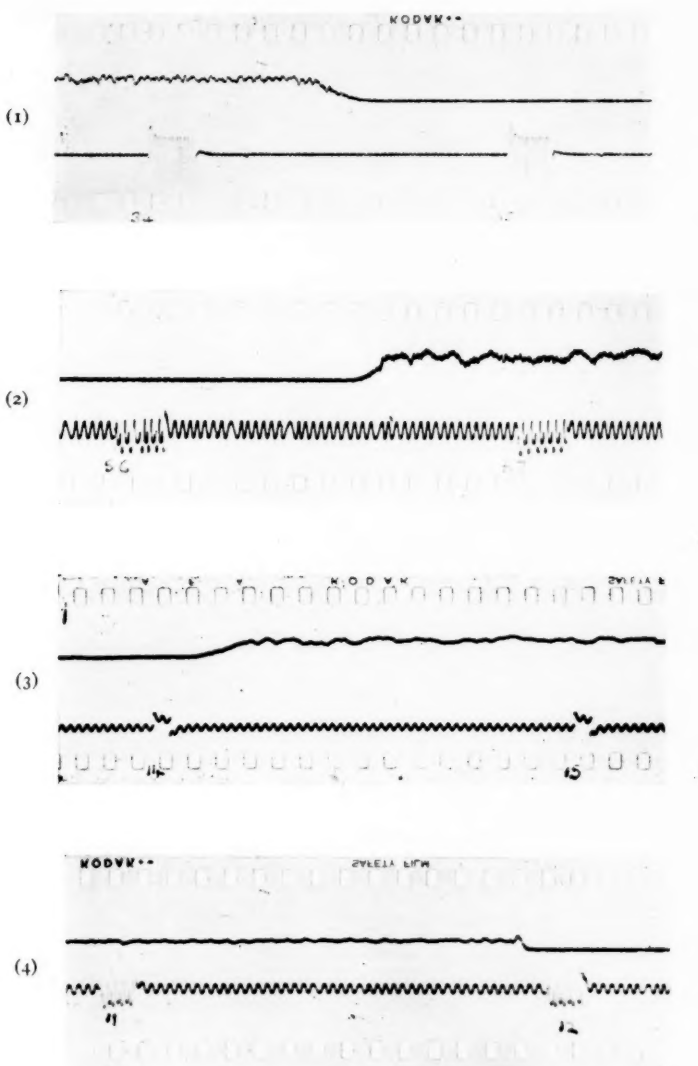
The thanks of the authors are due to Dr R. H. Stoy for his continued interest in the observations and for his help in carrying them out, to Mr B. Offen who constructed the mechanical parts of the photometer and to Dr David S. Evans for helpful discussions.

*Royal Observatory,  
Cape of Good Hope:  
1953 November 20.*

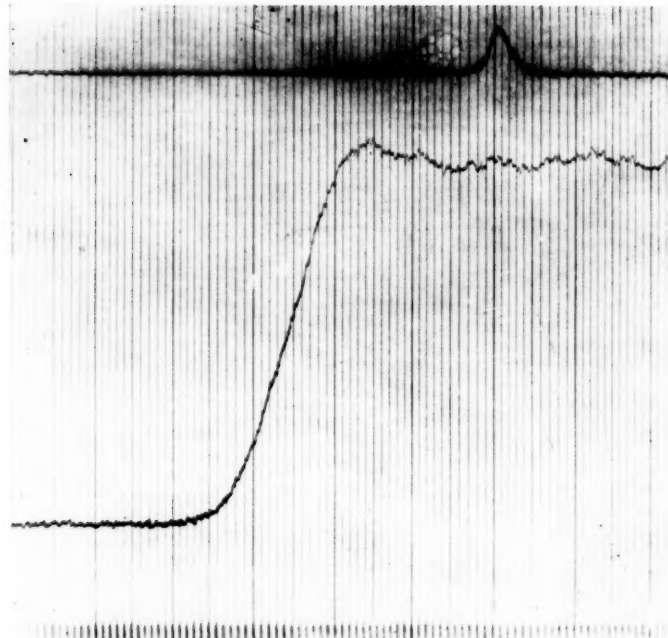
*Dept. of Electrical Engineering,  
University of Cape Town.*

#### *References*

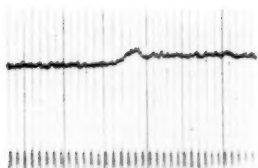
- (1) A. W. J. Cousins and R. Guelke, *Mon. Not. Astron. Soc. S.A.*, IX, 36, 1950.
- (2) A. W. J. Cousins and R. Guelke, *Mon. Not. Astron. Soc. S.A.*, IX, 56, 1950.
- (3) See e.g. "Timing of Occultations", David S. Evans, *The Observatory*, 71, 155, 1951.

*Occultation traces observed at the Cape*

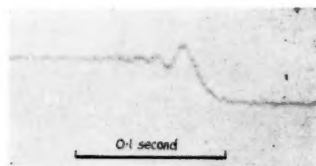
- (1) Antares, 1951 July 15. D.D.
- (2) Antares, 1952 April 13. R.D.
- (3) Antares, 1953 March 8. R.D.
- (4) A Sco, 1951 September 7. D.D.



(1)



(2)



(3)

*Occultations of Antares as observed at Pretoria.*

- (1) Antares, 1952 April 13. Top line, 1 second pulses; centre line, occultation trace; bottom line, 100 c/sec timing trace.
- (2) Antares B, 1952 April 13. Same scale as (1).
- (3) Antares B, 1953 March 8.

## OBSERVATIONS OF OCCULTATIONS OF ANTARES WITH THE RADCLIFFE REFLECTOR

David S. Evans\*, J. C. R. Heydenrych† and J. D. N. van Wyk†

(Communicated by H.M. Astronomer at the Cape)

(Received 1953 December 21)

### Summary

The occultation of Antares on 1952 April 13 was observed photoelectrically and traces for both components were obtained. At the occultation of 1953 March 8 only the trace for the companion was obtained.

A special prediction of the circumstances of the occultation of Antares on 1952 April 13 was kindly supplied by H.M. Nautical Almanac Office. These were:

Disappearance: 21<sup>h</sup> 21<sup>m</sup> 07<sup>s</sup> (U.T.) at P.A. 52°.4.

Reappearance: 21<sup>h</sup> 57<sup>m</sup> 34<sup>s</sup> (U.T.) at P.A. 349°.2.

Age of Moon: 19.1 days.

Time interval between passages of terminator and dark limb: 4 min.

Star 116 B Sco, 9' from dark limb in P.A. 68° at moment of reappearance.

The reappearance was observed using the star 116 B Sco (HD 148760) as a guide star.

The photocell used was an E.M.I. tube type 5060 placed at the Newtonian focus of the Radcliffe reflector. A diaphragm was placed in the focal plane and the cone of rays was allowed to expand so as to form a circular patch on the cathode. The tube was operated at 100 volts per stage and the maximum collector current drawn was just under 70 micro-amperes. These figures are both far below the ordinary safe operating limits. The dynode supply had a stability of better than one part per thousand for periods of up to 10 minutes, with a ripple of less than 10 millivolts. The signal was brought to the amplifier by a coaxial cable of low capacity, about 12 micro-micro-farads per foot. The amplifier circuit with built-in vacuum tube voltmeter is shown in Fig. 1.

A Hathaway Type S8-D.B. oscillograph was used for recording. Three galvanometers recording on bromide paper 10 inches wide driven at 10 inches per second were used. One recorded the signal output from the photomultiplier tube and amplifier: one carried a series of one second pips from a Muirhead phonic Motor Clock driven from a 1000 c/s tuning fork oscillator: the third recorded a sinusoidal voltage of 100 c/s from a Hewlett Packard Audio Oscillator. The internal time marker of the Hathaway recorder is inaccurate and the marks were used only for convenience in measuring the trace.

The galvanometer used for recording the occultation was of the moving coil type with a d.c. sensitivity of 6.4 cm/millampere/metre and a natural frequency of 580 c/s. The sensitivity in the recorder was 2.3 cm/millampere. For the

\* Royal Observatory, Cape of Good Hope.

† National Physical Laboratory, S.A. Council for Scientific and Industrial Research.

occultation the amplifier was adjusted for a bias of  $-5.0$  volts on each tube and 125 volts on the anode of the photomultiplier tube. The d.c. supply voltage on the amplifier was 320 volts and the plate current from each tube 21.5 milliamperes. The coarse sensitivity control was set in the 200 K ( $R_5$ ) position. Under these conditions the d.c. response was found to be linear up to 15 milliamperes into the galvanometer. At minimum gain the current gain was found to be 0.65 milliamperes/volt. The theoretical analysis of the circuit yielded the figure of 0.67 milliamperes/volt.

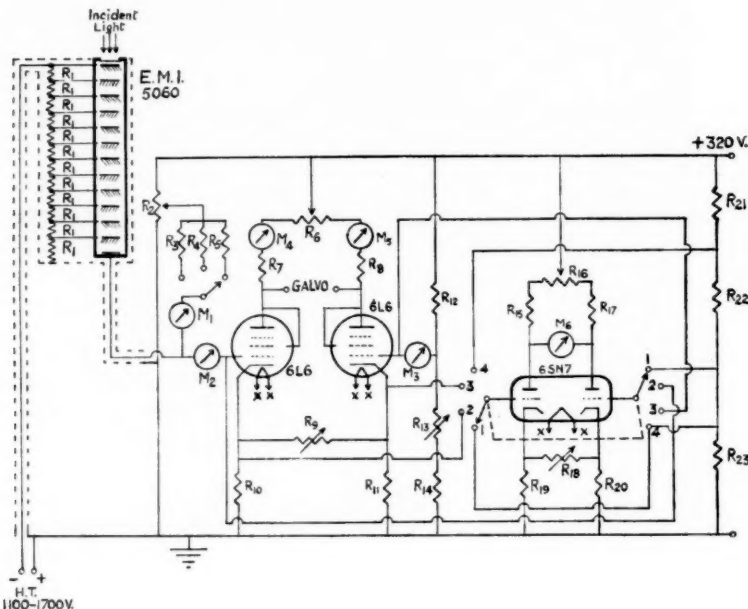


FIG. 1.

**Resistors**

$R_1 = 50\text{ K}\Omega$ ;  $R_2 = 100\text{ K}\Omega$ , wire-wound potentiometer;  $R_3 = 10\text{ K}\Omega$  wire-wound;  $R_4 = 50\text{ K}\Omega$  wire-wound;  $R_5 = 200\text{ K}\Omega$  wire-wound;  $R_6 = 1\text{ K}\Omega$  wire-wound potentiometer, pre-set;  $R_7 = R_8 = 5\text{ K}\Omega$  wire-wound;  $R_9 = 1\text{ K}\Omega$  wire-wound potentiometer;  $R_{10} = R_{11} = 5.5\text{ K}\Omega$  wire-wound;  $R_{12} = 200\text{ K}\Omega$  wire-wound;  $R_{13} = 50\text{ K}\Omega$  wire-wound potentiometer;  $R_{14} = 75\text{ K}\Omega$  wire-wound;  $R_{15} = R_{12} = 10\text{ K}\Omega$  selected;  $R_{16} = 2\text{ K}\Omega$  potentiometer;  $R_{18} = 2\text{ K}\Omega$  potentiometer, pre-set;  $R_{19} = R_{20} = 12\text{ K}\Omega$ ;  $R_{21} = 215\text{ K}\Omega$ ;  $R_{22} = 5\text{ K}\Omega$ ;  $R_{23} = 100\text{ K}\Omega$ .

**Meters**

$M_1$ : 0-100  $\mu A$ ;  $M_2$ ,  $M_3$ : microammeters, not used;  $M_4$ ,  $M_5$ : 0-50 mA;  $M_6$ : 0-5 mA.

**Supply**

XX: 6-volt filament supply.

Minimum gain was used during the occultation. For the same settings the linearity test curve of Fig. 2(a) was obtained. The frequency response curve for the whole installation is shown in Fig. 2(b).

At the occultation everything went smoothly. Antares was about 3 hours east of the meridian at about  $45^\circ$  altitude. The seeing was poor. The sky was partly cloudy, but the phenomenon took place in a gap in the clouds. There may have been a little haze or high cirrus over the position at the time, but if so, it was very thin.

The trace shows both components. At this occultation the track of the star relative to the lunar limb made an angle of  $58^{\circ}4$  to the normal at the point of emergence. The rate of advance of the limb parallel to itself was taken as  $0''\cdot241$ /second. The effective wave-length of response for the equipment as a whole on the blue companion was estimated as approximately  $4000\text{ \AA}$ . The measures of the trace for the companion are compared with the theoretical

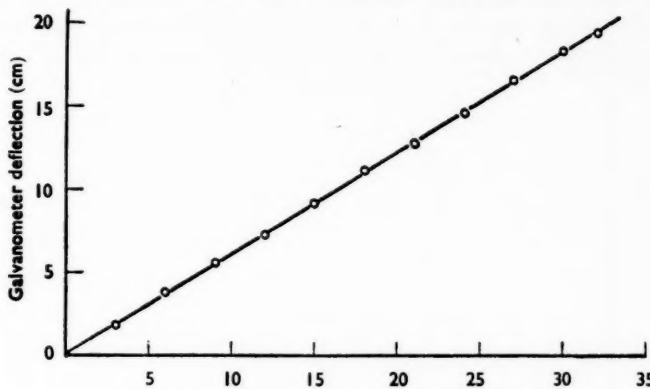


FIG. 2 (a).—Voltage increment on signal grid of amplifier.  
(Unit =  $0\cdot42$  volts.)

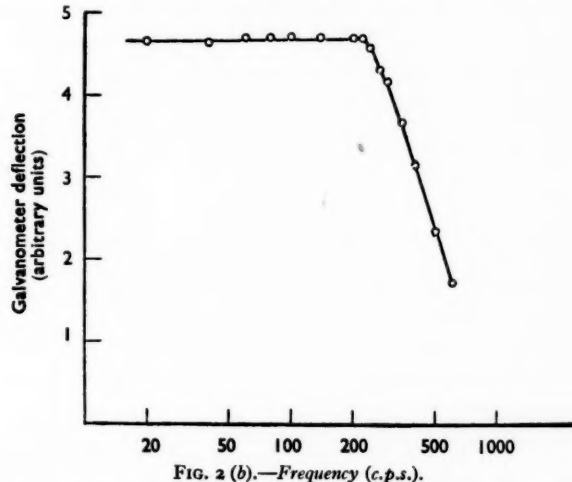


FIG. 2 (b).—Frequency (c.p.s.).

diffraction pattern for a point source at this wave-length in Fig. 3. The interval between the times of reappearance of the two components was  $3^{\circ}59$ . This result, together with the corresponding intervals for the 1953 observations at the Cape and at the Union Observatory, gives a separation between the components of  $3''\cdot16$  and a position angle of  $274^{\circ}38'$ . The residuals are:—

Pretoria, 1952	$0\cdot022$ .
Cape, 1953	$0\cdot036$ .
Johannesburg, 1953	$0\cdot025$ .

Curvature of the limb was neglected and the residuals are the residuals in time converted to angle at the rate of advance of the lunar limb parallel to itself appropriate to each occultation.

The measures of the trace for the primary component are shown in Fig. 4. Seeing fluctuations up to 7·5 per cent (3·75 per cent on either side of the mean) are observed to affect the unobscured light of the star. Seeing fluctuation amplitudes are proportional to intensity. Hence if the figure of 7·5 per cent be taken as the maximum for the unobscured light, the corresponding maximum displacements due to seeing at smaller deflection can readily be computed.

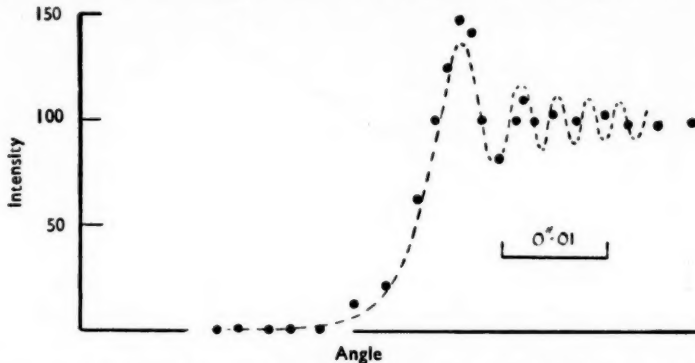


FIG. 3.—Measured points compared with the theoretical diffraction pattern for a point source.

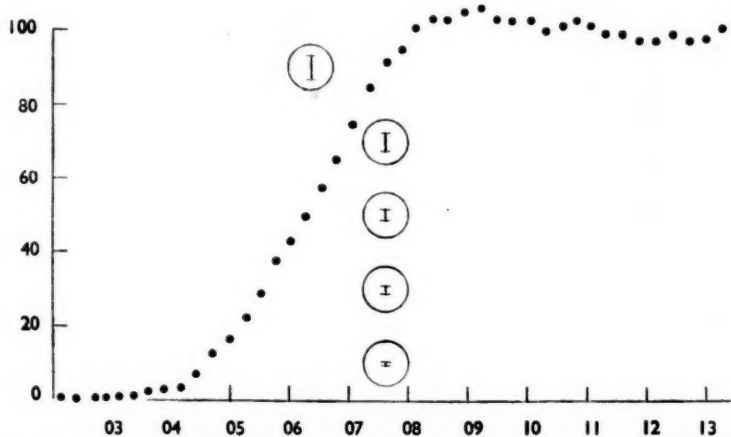


FIG. 4.—The vertical lines enclosed in the circles show the maximum possible displacement due to seeing at the given level.

These values are shown by the lengths of the vertical lines within the circles in Fig. 4. It will be noticed that, even if at each level the observed points are displaced by these amounts, the curve corresponding to the passage of a straight edge over a uniform circular disk cannot be produced. The best fit to the "straight-line" part of the curve gives a diameter of 0'·042. This curve should be compared with that obtained at the Cape on the same occasion.

At the occultation of 1953 March 8 apparatus which was largely identical with that used on the previous occasion was employed. Owing to an unfortunate accident only the trace for the companion was obtained. The measures are compared with the theoretical diffraction pattern in Fig. 5. The traces are all reproduced in Plate 12.

At this point it may be convenient to make a comment on the trace obtained with the Radcliffe reflector at the occultation of 1950 June.\* It is now suspected that, between the last check on this point and the occultation itself, the build-up of lunar background light may have produced a slight saturation effect. The degree of saturation can only have been slight, however, for the equipment

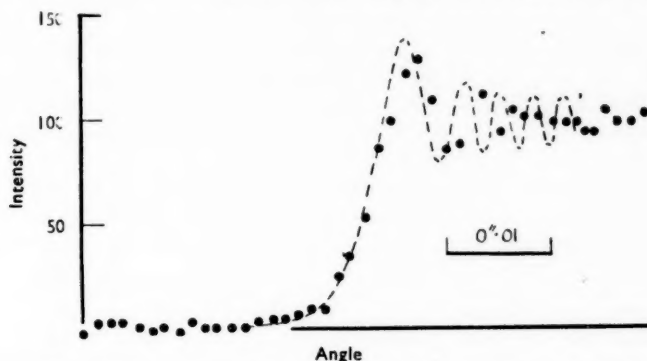


FIG. 5.—Measured points compared with the theoretical diffraction pattern for a point source.

responded with a deflection not noticeably different from that produced by the star on test runs. This will have affected the upper part (shoulder) of the curve obtained, but the deviations from the standard form of curve appropriate to the passage of a straight edge over a uniform disk still remain at the lower part (toe) of the curve.

Our thanks are due to the Director and Staff of the Radcliffe Observatory for the facilities and assistance during the observations, and to the S.A. Council for Scientific and Industrial Research, Pretoria, for permission for some of us to participate in this investigation. We are also indebted to the other members of the Electrotechnology Sub-division of the National Physical Laboratory for their invaluable assistance both before and at the time of the observations.

*Royal Observatory,  
Cape of Good Hope:  
1953 November 30.*

*National Physical Laboratory,  
Pretoria.*

\* M.N., **III**, 64, 1951.

MEAN AREAS AND HELIOGRAPHIC LATITUDES OF  
SUNSPOTS IN THE YEAR 1949

*Royal Observatory, Greenwich*

(Communicated by the Astronomer Royal)

(Received 1953 October 26)

The following results are in continuation of those given in *M.N.*, 113, 262, 1953, and are derived from the measurement at Herstmonceux of photographs taken at the Royal Observatories of Greenwich and the Cape and at the Kodak-kanal Observatory, India. From May 2, the Greenwich photographs were all taken at the new site at Herstmonceux Castle.

Table I gives the mean daily areas of umbrae, whole spots and faculae for each synodic rotation of the Sun included in the year 1949; the means for the year as a whole are included in Table II, which summarizes the yearly values since the last sunspot minimum of 1944.

TABLE I  
Mean Daily Areas

No. of Rotation 1948-49	Rotation Commenced U.T.	Days Photo- graphed	Projected*			Corrected for Foreshortening†		
			Umbræ	Whole Spots	Faculae	Umbræ	Whole Spots	Faculae
1275	Dec. 30.63	27	490	3006	1726	363	2228	2072
1276	Jan. 26.97	28	837	4839	2220	592	3485	2678
1277	Feb. 23.31	27	809	4877	2141	603	3667	2622
1278	Mar. 22.63	27	422	2355	1793	341	1930	2277
1279	Apr. 18.91	27	389	2083	2077	280	1520	2504
1280	May 16.14	27	291	1573	2134	220	1221	2650
1281	June 12.35	28	382	2070	2435	286	1558	2972
1282	July 9.55	27	477	2926	2177	343	2107	2646
1283	Aug. 5.76	27	500	3014	2107	373	2242	2527
1284	Sept. 2.00	27	537	3160	2300	392	2288	2736
1285	Sept. 29.27	28	444	2674	2182	310	1887	2606
1286	Oct. 26.56	27	407	2653	2242	302	2001	2723
1287	Nov. 22.86	27	365	2311	2214	273	1739	2665

\* Expressed in millionths of the Sun's disk.

† Expressed in millionths of the Sun's hemisphere.

Table III gives for each rotation in the year 1949 the mean daily area of the whole spots (corrected for foreshortening) and the mean heliographic latitude of the spotted areas for both northern and southern hemispheres.

The mean heliographic latitudes of the entire spotted area and the mean distance from the equator of all spots are also tabulated. The mean values for the year 1949 are included in Table IV.

TABLE II

## Mean daily areas

Year	No. of Days		Projected*			Corrected for Foreshortening†		
	Photo-graphed	Without Spots	Umbrae	Whole Spots	Faculae	Umbrae	Whole Spots	Faculae
1944	366	157	30	160	284	23	126	344
1945	365	14	102	560	774	78	429	940
1946	365	0	389	2381	1794	291	1817	2188
1947	365	0	558	3559	2326	405	2637	2894
1948	366	0	419	2618	1849	314	1977	2331
1949	365	0	485	2873	2140	356	2129	2597

\* Expressed in millionths of the Sun's disk.

† Expressed in millionths of the Sun's hemisphere.

TABLE III

No. of Rotation	Rotation Commenced U.T. 1948-49	Spots North of the Equator			Spots South of the Equator			Mean Distance from Equator of all Spots
		Mean Daily Area	Mean Helio- graphic Latitude	Mean Daily Area	Mean Helio- graphic Latitude	Mean Latitude of Entire Spotted Area		
1275	Dec. 30.63	1312	19.96	916	11.86	+6.88	16.63	
1276	Jan. 26.97	1258	14.57	2226	10.87	-1.68	12.21	
1277	Feb. 23.31	2328	13.22	1338	11.95	+4.03	12.76	
1278	Mar. 22.63	1215	13.28	715	15.33	+2.69	14.04	
1279	Apr. 18.91	808	13.25	712	14.21	+0.39	13.70	
1280	May 16.14	812	10.98	409	9.93	+3.98	10.63	
1281	June 12.35	709	10.32	849	10.31	-0.92	10.31	
1282	July 9.55	768	15.04	1338	15.26	-4.21	15.18	
1283	Aug. 5.76	1702	13.39	540	14.11	+6.77	13.57	
1284	Sept. 2.00	605	12.39	1683	13.13	-6.38	12.94	
1285	Sept. 29.27	1344	13.46	543	13.06	+5.83	13.34	
1286	Oct. 26.56	1314	16.74	688	8.18	+8.18	13.80	
1287	Nov. 22.86	1128	16.93	611	9.90	+7.50	14.46	

TABLE IV

Year	Days Photographed	Spots North of the Equator			Spots South of the Equator			Mean Distance from Equator of all Spots
		Mean Daily Area	Mean Helio- graphic Latitude	Mean Daily Area	Mean Helio- graphic Latitude	Mean Latitude of Entire Spotted Area		
1944	366	42	19.00	83	22.81	-8.70	21.53	
1944	366	{ Old Cycle New Cycle	7	4.17	6	7.61	-1.14	5.72
			35	22.18	77	24.02	-9.63	23.45
1945	365	121	20.13	309	20.26	-8.92	20.22	
1946	365	1127	20.74	690	18.79	+5.73	20.00	
1947	365	992	16.58	1645	17.86	-4.91	17.38	
1948	366	936	14.92	1041	13.53	-0.06	14.19	
1949	365	1178	14.30	951	12.14	+2.49	13.33	

Tables II and IV are in continuation of similar tables in *Monthly Notices*: for the years 1874 to 1888, 49, 381, 1889; 1889 to 1902, 63, 465, 1903; 1901 to 1914, 76, 402, 1916; 1913 to 1924, 85, 1007, 1925; 1923 to 1933, 94, 870, 1934; and 1933 to 1945, 110, 501, 1950.

The rotations in Tables I and III are numbered in continuation of Carrington's series.

The chief features of the record for the year 1949 are as follows:—

(1) The high values for the mean daily area of sunspots and of faculae—respectively 2120 and 2597 millionths of the Sun's hemisphere—exceed the corresponding values for 1948, and indicate a prolongation of maximum conditions from the notable peak of 1947.

Inspection of the run of mean daily areas of sunspots for each synodic rotation of 1949, given in Table I, shows very high values for Rotations 1276 and 1277, i.e. about 10 months after a similar peak in 1948, which in turn came about 12 months after the great peak of the cycle in 1947. The high level maintained by faculae throughout 1949 is also seen from Table I.

A short survey of the sunspots for 1949 has been published in *Monthly Notices*, 110, 169, 1950. The largest group of the year, with a mean area for its disk passage of 2213 millionths of the Sun's hemisphere, crossed the central meridian on January 22 in latitude 23° N.

(2) On no day in 1949 were sunspots and faculae absent from the Sun's disk.

(3) The mean weighted latitude of all spots was 13°.3, i.e. 4° nearer the equator than for the maximum year 1947 (Table IV). The northern hemisphere had the larger mean area (1178 millionths as against 951 millionths for the southern hemisphere), the average latitude of the latter being 2° nearer the equator than the former.

(4) The number and distribution, northern and southern hemisphere, of spot groups of (a) two days or longer; (b) one day only, are as follows:—

	(a)	(b)
Northern spots	284	69
Southern spots	229	41
Total	513	110

The range in latitude for the longer-lived spots was from 0° to 35°. The latitudes of the one-day spots ranged from 0° to 32°.

An appended table gives the mean daily areas of sunspots and faculae (corrected for foreshortening and expressed in millionths of the Sun's hemisphere) for each calendar month of 1949.

#### *Monthly Mean Daily Areas of Sunspots and Faculae*

1949

Month	Spots	Faculae	Month	Spots	Faculae
Jan.	2240	2206	July	1752	2825
Feb.	3640	2691	Aug.	2265	2436
Mar.	3277	2493	Sept.	2185	2806
Apr.	1882	2453	Oct.	1815	2622
May	1217	2437	Nov.	2313	2744
June	1606	2858	Dec.	1486	2616

*Royal Greenwich Observatory,  
Herstmonceux Castle, Sussex :  
1953 October 24.*

## THE EFFECT OF WINDS AND BODILY TIDES ON THE ANNUAL VARIATION IN THE LENGTH OF DAY\*

*Yale Mintz and Walter Munk*

### *Summary*

The effect of winds is to vary the length of day by 0·7 milliseconds between February and August. The bodily tides result largely in a semi-annual variation of 0·4 ms. The combined effect of winds and tides is not far out of line with astronomical measurements since 1950. The fluid core of the Earth hardly participates in these variations in angular velocity and there is a half-year slippage of 23 metres between core and mantle at the equator. Eventually the astronomical measurements may provide a basis for determining the Love number  $h$ .

\* The full text of this paper is published in *M.N., Geophys. Suppl.*, 6, No. 9, 1954.

## ERRATA

*M.N.*, 103, No. 3, 1943:George Alter, *Galactic Absorption and Star Distribution*.

P. 164, line 8 from bottom,

$$\text{for} \quad B' = \frac{b}{\log e} \frac{\partial b}{\partial r_0},$$

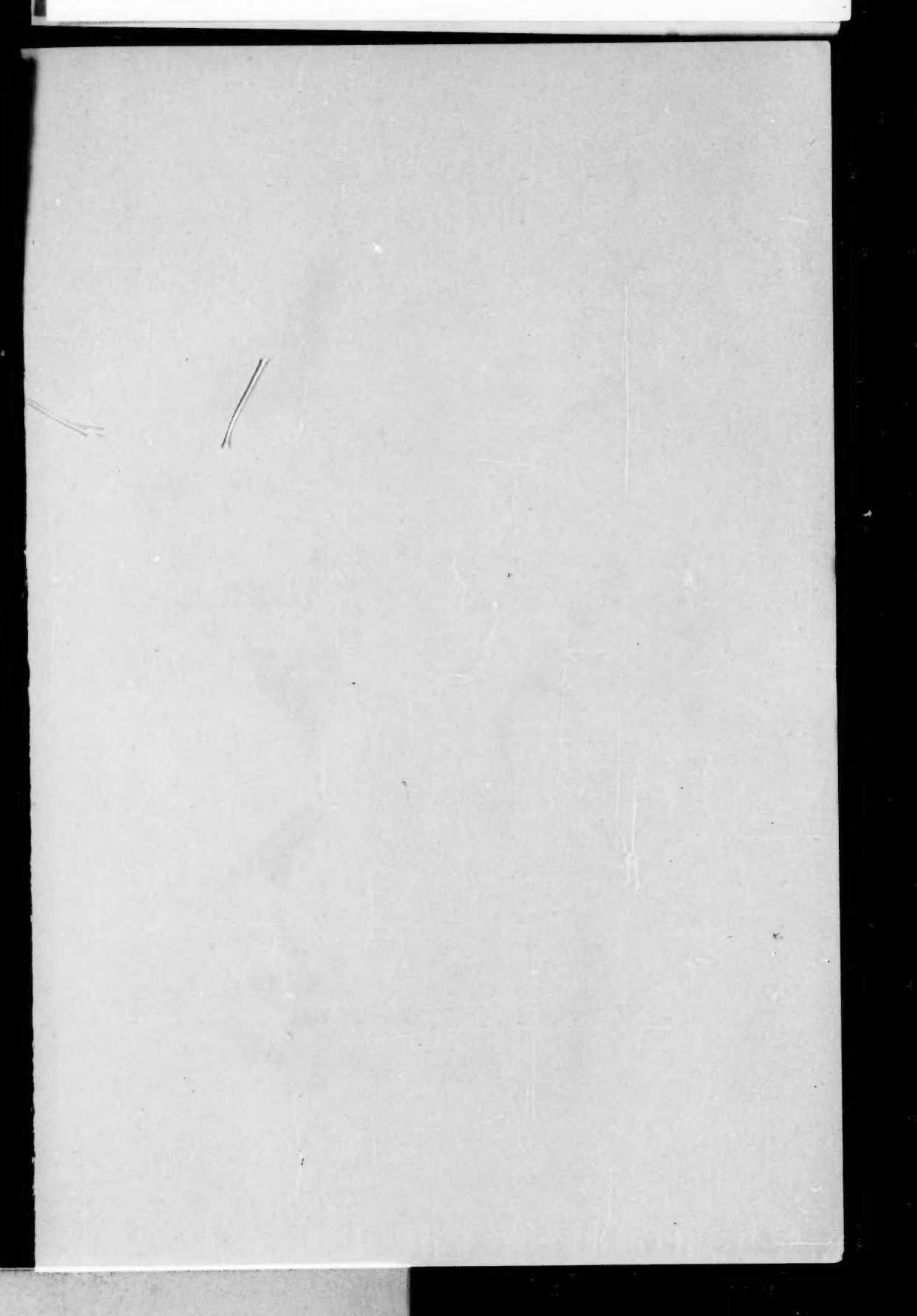
$$\text{read} \quad B' = \frac{1}{\log e} \frac{\partial b}{\partial r_0}.$$

P. 165, line 2,

$$\text{for} \quad G = e^{\frac{3}{5 \log e}} [a_{pv} r_0 - 12(1 - e^{-\frac{1}{2}a_s r_0})],$$

$$\text{read} \quad G = \exp \left\{ \frac{3}{5 \log e} [a_{pv} r_0 - 12(1 - e^{-\frac{1}{2}a_s r_0})] \right\}.$$

*M.N.*, 113, No. 3, 1953:*Obituary Notices*, L. J. Comrie.P. 298, l. 17 from bottom, *for Pukekoke* *read Pukekohe*.P. 296, l. 20 from bottom, *for ten million* *read two million*.*M.N.*, 113, No. 5, 1953:R. Wilson, *The ionized helium series originating from the fifth quantum level*.P. 560, line 16, *for m=n^{-1} (\Sigma \Delta / F)* *read m=n^{-1} \Sigma (\Delta / F)*.



## CONTENTS

	PAGE
<b>Meeting of 1953 November 13 :</b>	
Fellows elected ... ... ... ... ... ... ... ...	655
Junior Members elected ... ... ... ... ... ...	655
Presents announced ... ... ... ... ... ...	655
Presentation of the Gold Medal ... ... ... ...	656
<b>Meeting of 1953 December 11 :</b>	
Fellows elected ... ... ... ... ... ...	656
Junior Members elected ... ... ... ... ...	657
Presents announced ... ... ... ... ...	657
<b>E. P. Hubble, The law of red-shifts (George Darwin Lecture)</b> ... ... ...	658
<b>S. Chandrasekhar, Problems of stability in hydrodynamics and hydromagnetics (George Darwin Lecture)</b> ... ... ...	667
<b>J. W. Dungey, The motion of magnetic fields</b> ... ... ...	679
<b>A. Przybylski, The maximum effect of convection in stellar atmospheres on the observed properties of stellar spectra. I</b> ... ... ...	683
<b>P. A. Sweet and A. E. Roy, The structure of rotating stars. I</b> ... ...	701
<b>L. Mestel, Rotation and stellar evolution</b> ... ... ...	716
<b>A. R. Hogg, Photometry of the galactic cluster NGC 6025</b> ... ...	746
<b>S. N. Svolopoulos, A photographic survey of galactic clusters NGC 6531, 6546, 6469, 6544, 7127, 7128</b> ... ...	758
<b>Zdeněk Kopal, Some remarks on the interpretation of apsidal-motion constants in close binary systems</b> ... ... ...	769
<b>A. W. J. Cousins and R. Guelke, Photoelectric observations of occultations at the Cape Observatory</b> ... ...	776
<b>David S. Evans, J. C. R. Heydenrych and J. D. N. van Wyk, Observations of occultations of Antares with the Radcliffe reflector</b> ... ...	781
<b>Royal Observatory, Greenwich, Mean areas and heliographic latitudes of sunspots in the year 1949</b> ... ...	786
<b>Summary of paper published in the <i>Geophysical Supplement</i>:</b>	
<b>Yale Mintz and Walter Munk, The effect of winds and bodily tides on the annual variation in the length of day</b> ... ...	789
<b>Errata</b> ... ... ...	790